

Inaugural dissertation
for
obtaining the doctoral degree
of the
Combined Faculty of Mathematics, Engineering and Natural Sciences
of the
Ruprecht - Karls - University
Heidelberg

Presented by
Julia Denise Peterson, M.Sc
Born in Ann Arbor, MI, USA
Oral examination: 27 March, 2023

**Developments Toward an iPSC-Derived
T-Cell Immunotherapy
Using S/MAR DNA Vectors**
A Focus on Hematopoietic Stem and Progenitor Cells

Referees

Prof. Dr. Ralf Bartenschlager
Dr. Richard P. Harbottle



Quote

“A human being is a part of the whole called by us universe, a part limited in time and space. He experiences himself, his thoughts and feeling as something separated from the rest, a kind of optical delusion of his consciousness. This delusion is a kind of prison for us, restricting us to our personal desires and to affection for a few persons nearest to us. Our task must be to free ourselves from this prison by widening our circle of compassion to embrace all living creatures and the whole of nature in its beauty.”

— Albert Einstein

“Peace can only come as a natural consequence of universal enlightenment...” “The scientific man does not aim at an immediate result. He does not expect that his advanced ideas will be readily taken up. His work is like that of the planter—for the future. His duty is to lay the foundation for those who are to come, and point the way.”

— Nikola Tesla



Acknowledgements

I give a warm thanks to my parents, the only two people whom I've known my entire life. Thank you for not only providing the opportunities, since childhood, for me to grow into the person I am today, but also for supporting my academic choices and personal journey. My journey to another continent—Europe—initially proved to be emotionally difficult, as it would be for most parents. Though, we found our strongest place of acceptance and unattachment—the ultimate form of unconditional love. Thank you for accepting the choices I've made to follow my heart, my values, and myself. Your unattached acceptance, support, and unconditional love means more than the world to me.

The only person whos known me their entire life, my sister Natalie, we will always have that special bond as sisters. Thank you for housing me and picking me up from the airport. Supporting me with these little things has made a difference and means a lot to me.

Cosmo, my baby parrolet, words cannot express my love for you. I wish I could have you in Europe.

Toros Tasgins, thank you for your support on the project. I really appreciate your passion and dedication to it. You obtained fantastic results that were invaluable for this thesis.

Alicia Roig-Merino and Manuela Urban, thank you for the strong foundation on urinary-derived iPSCs that led to the development of my project.

Richard, thank you for accepting me into your lab and financially supporting me. Thank you for the opportunity to grow into an independent scientist.

Anna Hartley, Aga Sekretny, and Francesco Baccianti, thank you for your support on viral vector production. Michael Bonadonna, thank you for your support on bone marrow transplantations. Carlo Amato and Giada Peron, thank you for teaching me LaTeX.

I thank all of my friends for their support. It is lovely to have a community of people who understand the PhD lifestyle. Shout outs to “the original pumpkins”.

I must give a deep thanks to the people I've meant along my life journey who acted as a life lesson and pointed me in the direction of personal growth. I give a deep thanks to Thais Gibson who was my guide on this journey and helped me reach a healthier and more mature mental space.

Finally, I pay my respects to the mice used during this study. Nothing is in vain; you will support and save many lives.



Abstract

Randomly integrating viral vectors pose a genotoxic risk when used as a genetic modification tool. Our lab has developed a non-integrating DNA vector (S/MAR DNA vector) that persists episomally in cells and provides long-term transgene expression similarly to integrating viral vectors. In this project, I show a proof of concept of developing an off-the-shelf iPSC-derived T-cell immunotherapy using S/MAR DNA vectors. I developed an S/MAR DNA vector that is optimal for T-cells as well as iPSC genetic modification. I created a platform to screen vector features in mouse hematopoietic stem and progenitor cells. I indicate that iPSC lines that were genetically modified using S/MAR DNA vectors can differentiate into hematopoietic stem and progenitor-like cells, and I compared it with an iPSC line genetically modified using a lentiviral vector. Finally, this report shows that iPSC lines expressing a CAR can differentiate into phenotypic T-cells.

The personalization of gene and cell therapies is expensive. They may become more affordable and accessible to patients when iPSCs are used to generate allogeneic cell therapies. Exploiting iPSCs could reduce the cost, offer a healthier cell source, provide a quicker treatment option, and offer a more standardized therapy to patients. The data described in this report suggest the possibility of generating iPSC-derived T-cell immunotherapies utilizing S/MAR DNA vectors.



Zusammenfassung

Zufällig integrierende virale Vektoren stellen ein genotoxisches Risiko dar, wenn sie als Instrument zur genetischen Veränderung eingesetzt werden. Unser Labor hat einen nicht integrierenden DNA-Vektor (S/MAR-DNA-Vektor) entwickelt, der episomal in Zellen verbleibt und eine langfristige Transgenexpression ähnlich wie ein integrierender viraler Vektor ermöglicht. In diesem Projekt zeige ich einen Machbarkeitsnachweis für die Entwicklung einer "off-the-shelf" iPSC-abgeleiteten T-Zell-Immuntherapie mit S/MAR-DNA-Vektoren. Ich habe einen S/MAR-DNA-Vektor entwickelt, der optimal für die genetische Veränderung von sowohl T-Zellen als auch iPSCs ist. Ich habe eine Plattform geschaffen, um Vektoreigenschaften in hämatopoetischen Stamm- und Vorläuferzellen der Maus zu prüfen. Ich zeige, dass eine iPSC-Linie, die mit S/MAR-DNA-Vektoren genetisch modifiziert wurden, zu hämatopoetische Stamm- und Vorläuferzellen entwickeln können, und ich habe sie mit einer iPSC-Linie verglichen, die mit einem lentiviralen Vektor genetisch modifiziert wurde. Schließlich zeigt dieser Bericht, dass eine iPSC-Linie, die mit ein CAR modifiziert wurden, zu phänotypische T-Zellen entwickeln können.

Die Personalisierung von Gen- und Zelltherapien hat sie kostspielig gemacht. Sie können erschwinglicher und zugänglicher für Patienten werden, wenn iPSCs verwendet werden, um allogener Zelltherapien zu produzieren. Die Nutzung von iPSCs könnte die Kosten senken, eine gesündere Zellquelle bieten, eine schnellere Behandlungsoption für Patienten bieten und die Entwicklung von einer standardisierteren Therapie ermöglichen. Die in diesem Bericht beschriebenen Daten deuten auf die Möglichkeit hin, iPSC-abgeleitete T-Zell-Immuntherapien unter Verwendung von S/MAR-DNA-Vektoren zu erzeugen.



Contents

Acknowledgements	VII
Abstract	IX
Zusammenfassung	XI
List of Figures	XIX
List of Tables	XXIII
Abbreviations	XXV
1 Historical Content	1
1.1 Historical Content for Gene and Cell Therapy	1
1.2 Historical Content for the Treatment of Cancer	4
1.3 Pluripotent Stem Cell Gene Therapy	8
1.4 Modes of Genetic Modification	11
1.4.1 Viral Vectors	11
1.4.1.1 AAV	12
1.4.1.2 Gamma-Retroviral Vector	13
1.4.1.3 Lentiviral Vector	15
1.4.2 Gene Editing Technologies	16
1.4.2.1 CRISPR/Cas9	17
1.4.2.2 TALENs and ZFNs	18
1.4.3 Transposons	19
1.4.4 S/MAR DNA Vectors	20
2 My Project's Vision	23
2.1 The Plan	23
2.2 The Benefits of an Allogeneic iPSC-Derived T-Cell Immunotherapy	24
2.2.1 Predicted to Reduce Costs of Cell Therapy	24
2.2.2 An Off-The-Shelf Therapy for Patients	27
2.2.2.1 HLA Homozygous iPSC Banks	27
2.2.2.2 Mass Production	28
2.2.3 Derived From a Healthier Cell	28
2.2.4 Standardized Therapy That Could Follow a Centralized Model	28
2.3 The Benefits of Using S/MAR DNA Vectors	29
2.4 Project Aims That Were Achieved	31



Results	33
3 Vector Features Most Suitable for T-Cell and U-iPSC Genetic Modification	35
3.1 T-Cells and Human U-iPSCs Can Maintain S/MAR DNA Vectors	36
3.1.1 Jurkat76 Can Retain S/MAR DNA Vectors	37
3.1.2 Human U-iPSCs Can Retain S/MAR DNA Vectors	39
3.1.3 Section Discussion	39
3.2 Screening Transgenes	39
3.2.1 dTomato Expression is Negligibly Correlated With Cell Viability . . .	39
3.2.2 T-Cells Expressing Anti-CEA CAR and Anti-MART-1 TCR Efficiently Target and Kill Cancer Cells	41
3.2.3 Section Discussion	42
3.3 Screening S/MARs	42
3.3.1 Comparing S/MARs in Human U-iPSCs	42
3.3.2 Comparing S/MARs in Jurkat76	44
3.3.3 Cytokine Secretion Upon Cellular Entry of DNA Vectors Containing Unique S/MARs	45
3.3.4 Section Discussion	45
3.4 Screening Promoters	46
3.4.1 Comparing Promoters in Human U-iPSCs	47
3.4.2 Comparing Promoters in Jurkat76	48
3.4.3 Cytokine Secretion Upon Cellular Entry of DNA Vectors Containing Unique Promoters	49
3.4.4 Section Discussion	50
3.5 Screening Production Backbones	51
3.6 Conclusion	51
3.7 Future Aims	52
4 A Protocol to Expand Mouse HSPCs to High Cell Yields	53
4.1 The Expansion of Mouse HSPCs	53
4.1.1 Mouse HSPCs Proliferate in Yamazaki Medium	53
4.1.2 Mouse HSPCs Depleted of Mature Hematopoietic Cells Expand in Yamazaki Medium	55
4.1.3 Mouse HSPCs Expand Following MHEP	56
4.1.4 MHEP-Expanded Mouse HSPCs Engraft in Mice	58
4.1.5 Section Discussion	59
4.2 The Genetic Modification of Mouse HSPCs	60
4.2.1 S/MAR DNA Vectors Can be Introduced Into Mouse HSPCs	60
4.2.2 DNA Triggers Increased Secretion of IFN-Beta from Mouse HSPCs . .	62
4.2.3 Inhibitors Reduce IFN-Beta Secretion, but Lead to no Improvements in Viability nor Transfection Efficiency	63
4.2.4 AAVs Containing S/MARs Can Modify Mouse HSPCs and Improves Expression Persistence	64
4.2.5 Section Discussion	65



4.3	Conclusion	65
4.4	Future Aims	65
5	Yielding HSPCs from S/MAR DNA Vector-Modified U-iPSCs	67
5.1	Urinary Stem Cells Can be Reprogrammed Into iPSCs	67
5.1.1	Section Discussion	68
5.2	U-iPSCs are Genetically Modified With the Latest S/MAR DNA Vector . . .	68
5.2.1	Section Discussion	72
5.3	Modified Lines Remain Phenotypically Similar to Non-Modified U-iPSCs . .	73
5.3.1	Section Discussion	73
5.4	U-iPSC Lines Can Differentiate Into HSP-Like Cells	74
5.4.1	Section Discussion	76
5.5	U-iPSC Lines Can Differentiate Into HSP-Like Cells Primed for the Lymphoid Lineage	77
5.5.1	Section Discussion	81
5.6	Conclusion	82
5.7	Future Aims	82
6	Yielding Anti-CEA CAR T-Cells From S/MAR DNA Vector-Modified U- iPSCs	83
6.1	U-iPSCs Can be Engineered to Express Anti-CEA CAR	84
6.2	Anti-CEA iPSC-Derived CD34+ Cells Can Differentiate Into Phenotypic T-Cells	85
6.3	Discussion	85
6.4	Conclusion	86
6.5	Future Aims	86
7	Conclusion	89
8	Methods	91
8.1	Human Cell Culture	91
8.1.1	Jurkat76 Cell Line	91
8.1.1.1	Thawing Jurkat76	91
8.1.1.2	Routine Maintenance of Jurkat76	91
8.1.1.3	Transfection of Jurkat76	92
8.1.1.4	Flow Cytometry Analysis of Jurkat76	93
8.1.1.5	Using FACS to Collect a Specific Jurkat76 Population	93
8.1.2	Primary Human T-Cells	93
8.1.2.1	Collecting and Expanding T-Cells From a Human Buffy Coat	93
8.1.2.2	Thawing Primary Human PBMCs	94
8.1.2.3	Transfection of Primary Human T-Cells	94
8.1.2.4	Flow Cytometry Analysis of Primary T-Cells	95
8.1.2.5	General Maintenance of Primary Human T-Cells	96
8.1.3	Immortalized Normal Human Dermal Fibroblasts (iNHDFs)	96
8.1.3.1	Thawing iNHDFs	96
8.1.3.2	Routine Maintenance of iNHDFs	96



8.1.3.3	Transfection of iNHDFs	96
8.1.3.4	Supernatant Collection for ELISA: iNHDFs	97
8.1.4	HEK293T Cell Line	98
8.1.4.1	Thawing HEK293T	98
8.1.4.2	Routine Maintenance of HEK293T	98
8.1.5	Human Induced Pluripotent Stem Cells (iPSCs)	98
8.1.5.1	Generating Human iPSCs From Urinary-Derived Cells	98
8.1.5.2	Thawing Human iPSCs	98
8.1.5.3	Routine Maintenance of Human iPSCs	99
8.1.5.4	Validating iPSC Phenotype: AP Staining	99
8.1.5.5	Validating iPSC Phenotype: IF Staining	100
8.1.5.6	Transfection of iPSCs	101
8.1.5.7	Lentiviral Vector Transduction of iPSCs	102
8.1.5.8	Developing Vector-Maintained iPSC Lines	102
8.1.5.9	Flow Cytometry Analysis of iPSCs	102
8.1.6	Differentiation: iPSCs Into HSPCs	103
8.1.6.1	Method 1	103
8.1.6.2	Method 2	104
8.1.6.3	Validating iPSC-Derived HSPC Phenotype Using FACS	105
8.1.6.4	Validating iPSC-Derived HSPC Functionality Using MethoCult	105
8.1.7	Differentiation: iPSC-Derived HSPCs Into T-Cells	107
8.1.7.1	Method 2: A Continuation From Section 8.1.6.2	107
8.1.7.2	Validating iPSC-Derived T-Cell Phenotype Using FACS	108
8.2	Mouse Cell Culture	109
8.2.1	Mouse HSPCs	109
8.2.1.1	Extracting Bone Marrow Cells From Mouse Femurs and Tibias	109
8.2.1.2	Culturing Mouse Bone Marrow Cells Depleted of Mature Hematopoietic Cells	110
8.2.1.3	Culturing Mouse Bone Marrow Cells Enriched With Rare HSPC Populations	111
8.2.1.4	Gentle Medium Changes for Mouse HSPCs	112
8.2.1.5	Transfecting Mouse HSPCs	112
8.2.1.6	Transducing Mouse HSPCs Using AAVs	114
8.2.1.7	Flow Cytometry Analysis of Mouse HSPCs	114
8.2.1.8	FLOWMAP Code	114
8.3	Cell Culture: Routine Procedures	115
8.3.1	Cell Counting	115
8.3.2	Preparing FBS Aliquots	115
8.3.3	Microplasma Testing	115
8.3.4	Cell Line Validation	116
8.3.5	Dead Cell Removal	116
8.3.6	Cell Cryopreservation	116
8.3.7	ELISA Legendplex	116



8.3.8	ELISA InvivoGen	117
8.3.9	Absolute Count Beads	117
8.4	Plasmids	117
8.4.1	DNA Vectors With a Bacterial Backbone	117
8.4.2	DNA Vectors With an RNA-out R6K Backbone	119
8.4.3	Plasmid: Routine Procedures	120
8.4.3.1	DNA Precipitation	120
8.4.3.2	Quality Control: Restriction Digest Test	120
8.4.3.3	Quality Control: Sanger Sequencing	120
8.4.3.4	Glycerol Stocks	120
8.5	Viral Vector Production	120
8.5.1	Lentiviral Vector Production	120
8.5.2	AAV Vector Production	122
8.6	Mouse Bone Marrow Transplantations	125
8.6.1	Preparing Recipient Mice for Transplantations	125
8.6.2	Preparing Donor Cells for Primary Engraftment	125
8.6.2.1	Preparing Bone Marrow Protection Cells (Ly5.1)	125
8.6.2.2	Preparing Expanded HSPCs (Ly5.2) With Bone Marrow Protection Cells	125
8.6.3	Preparing Donor Cells for Secondary Engraftment	126
8.6.4	Performing Bone Marrow Transplantations	126
8.6.5	Peripheral Blood FACS Analysis	126
8.6.6	Bone Marrow FACS Analysis	127
A	Materials	129
A.1	Cells	129
A.1.1	Human Cells	129
A.1.2	Murine Cells	129
A.1.3	Bacteria	129
A.2	Mammalian Cell Culture	130
A.2.1	Plasticware	130
A.2.2	Cell Culture Components	131
A.2.3	Cell Medium Composition	137
A.2.4	Transfection/Transduction Reagents	138
A.3	Mammalian Cell Analysis	139
A.3.1	Plasticware	139
A.3.2	Kits	139
A.3.3	Commercial Reagents	139
A.3.4	Prepared Solutions	140
A.3.5	Pre-Defined Chemical Reagents	140
A.3.6	FACS	141
A.3.6.1	FACS Beads	141
A.3.6.2	FACS Antibodies	141
A.3.7	IF Staining Antibodies	143



A.3.7.1	Primary IF Antibodies	143
A.3.7.2	Secondary IF Antibodies	143
A.4	Virus Production	144
A.4.1	Plasticware	144
A.4.2	Commercial Solutions	144
A.4.3	Prepared Solutions	145
A.5	Bacterial Cell Culture	146
A.5.1	Plasticware and Glassware	146
A.5.2	Commercial Culture Components	146
A.5.3	Prepared Culture Compositions	146
A.6	Plasmid Production	147
A.6.1	Kits	147
A.6.2	Commercial Solutions	147
A.6.3	Pre-Defined Chemical Reagents	147
A.7	Cloning Primers	148
A.8	Vectors	151
A.8.1	DNA Vectors	151
A.8.2	Viral Vectors	151
A.9	Mice	152
A.9.1	Mouse Lines	152
A.9.2	Materials for Mouse Handling	152
A.10	Equipment	153
A.11	Software	154
B	Supplemental Results	155
B.1	Chapter 3	155
B.2	Chapter 4	158
B.3	Chapter 5	162
B.4	Chapter 6	162
	References	163



List of Figures

1.1	Structural depiction of a TCR and CAR.	7
1.2	Schematic representation of ESC and iPSC development and differentiation.	10
1.3	Differences between a wild-type AAV and an AAV viral vector.	13
1.4	Schematic representation of a gamma-retroviral vector provirus.	15
1.5	Schematic representation of a SIN lentiviral vector provirus.	16
1.6	Classic gene-editing systems mechanism of action.	19
1.7	The mode of action of a transposon.	20
1.8	Schematic representation of how S/MAR DNA vectors work.	21
1.9	The evolution of our lab's S/MAR DNA vectors.	22
2.1	Steps to create an U-iPSC-derived T-cell immunotherapy.	24
2.2	The process of manufacturing and distributing autologous and allogeneic T-cell immunotherapy.	26
2.3	Comparing the COG for autologous and allogeneic cell therapies.	27
2.4	Description of the manufacturing process of an AAV vector.	30
2.5	A description of this project's aims.	31
3.1	Schematic representation of the features screened within human U-iPSCs and T-cells using S/MAR DNA vectors.	36
3.2	Jurkat76 cells retain S/MAR DNA vectors at various percentages that are dependent on vector features.	37
3.3	Jurkat76 cells expressing dTomato 24 and 33 days post-modification retain transgene expression for 1 month.	38
3.4	Modified U-iPSC lines retain S/MAR DNA vector transgene expression.	39
3.5	Negligible correlation between cell viability and dTomato expression in human primary T-cells is present.	40
3.6	Negligible correlation between cell viability and dTomato expression in human U-iPSCs is present.	40
3.7	T-cells expressing anti-CEA CAR and anti-MART-1 TCR display targeted killing of cancer cells.	41
3.8	Transfection efficiencies and cell viabilities comparing S/MARs within S/MAR DNA vector-modified human U-iPSCs.	43
3.9	S/MAR-4 has the highest proportion of cells stably retaining transgene expression after 128 days in culture.	44
3.10	S/MAR-4 induced the lowest production of IFN β , relative to the other S/MARs tested.	45



3.11	Comparing transfection efficiencies and cell viabilities of human U-iPSCs modified with S/MAR DNA vectors containing unique promoters.	47
3.12	Promoter sEF1 has the highest proportion of cells stably retaining transgene expression after 128 days in culture.	48
3.13	Promoters CAG and sEF1 induced IFN β production least, relative to the other promoters tested.	49
4.1	Cell populations enriched for mouse HSCs produce higher cell counts within Ham's F-12 medium conditions and remain more enriched for LSK CD150+ cells.	54
4.2	Cell populations depleted of only mature hematopoietic cells expand to millions of cells and retain a high enrichment of HSC-like cells in Ham's F-12 medium conditions.	56
4.3	Data pertaining to the MHEP protocol.	57
4.4	MHEP-expanded mHSPCs can successfully engraft in mice.	58
4.5	dTomato expression from mHSPCs modified with an S/MAR DNA vector is lost by 9 days post-modification.	60
4.6	Opt 8 with 36 $\mu\text{g}/\text{mL}$ is the most effective method for the genetic modification of mHSPCs.	61
4.7	IFN- β is secreted upon cellular entry of DNA.	62
4.8	DNA sensing pathway antagonists reduce IFN β secretion from modified mHSPCs but lead to no significant improvements in viability nor transfection efficiency.	63
4.9	mHSPCs can be genetically modified using AAV viral vectors, and they extend transgene expression persistence.	64
5.1	Schematic representation of urinary stem cell reprogramming.	68
5.2	Schematic representation of S/MAR DNA vector and lentiviral vector genome used for U-iPSC modification.	69
5.3	Transfection and transduction of human iPSCs using vectors containing S/MARs.	70
5.4	U-iPSC lines stably expressing dTomato were generated using S/MAR DNA vectors and lentiviral vectors.	71
5.5	Microscope images of established U-iPSCs lines taken at 200x magnification assessing alkaline phosphatase expression and the expression of various pluripotency markers.	73
5.6	Approximately half of iPSC derived CD45+ cells are primed for the myeloid lineage following method 1.	74
5.7	S/MAR DNA vector-modified U-iPSCs can differentiate into HSPC-like cells.	75
5.8	U-iPSC lines could produce hematopoietic progenitor cells in CFU.	75
5.9	FACS plots displaying the enrichment of HSPC-like cells within our differentiated iPSC population following method 2.	78
5.10	Alterations in dTomato expression were observed after iPSCs were differentiated into HSPCs following method 2.	79
5.11	The majority of iPSC-derived CD45+ HSPCs produced following method 2 are CD33-.	80



5.12 U-iPSC-derived CD34+ cells differentiate into phenotypic T-cells following method 2.	80
6.1 iPSCs can be engineered to express anti-CEA CAR.	84
6.2 Anti-CEA CAR-expressing iPSCs can differentiate into phenotypic T-cells from iPSC-derived CD34+ cells.	87
B.1 Establishing S/MAR DNA vectors in primary human T-cells.	155
B.2 Calibration curves used for Invivogen IFN-beta ELISA.	156
B.3 Calculating the concentration of endotoxins present in S/MAR DNA Vectors.	157
B.4 FACS gating scheme used to collect various mouse HSPC populations.	158
B.5 FACS gating used to calculate BM composition.	159
B.6 Representative flow cytometry gating scheme for sample analysis of expanded mHSPCs.	159
B.7 The genetic modification of mHSPCs using lipofection.	160
B.8 Pre-screening of MaxCyte GT electroporation protocols for mouse HSPCs.	160
B.9 Calibration curves for Legendplex analysis.	161
B.10 The effects of DNA sensing pathway inhibitors on mHSPC viability.	161
B.11 Assessing the T-cell phenotype of CD34+ suspension cells that underwent T-cell differentiation.	162
B.12 Assessing the phenotype of iPSC lines that underwent HSPC differentiation.	162



List of Tables

1.1	Approved gene and cell therapies in the EU.	4
1.2	Properties of TCRs and CARs.	8
1.3	Viral vectors used to genetically modify cells.	11
2.1	Cost of approved gene and cell therapies in 2017.	25
3.1	S/MAR DNA vector establishment rates in human U-iPSCs: Comparing S/MARs	43
3.2	S/MAR DNA vector establishment rates in human U-iPSCs: Comparing promoters	48
4.1	Medium composition of supplemented Ham's F-12 medium for mHSC expansion.	54
4.2	Predicted cell counts after expanding HSPC populations for 14 days.	55
4.3	Combined percentages resulting from each MaxCyte GTx protocol.	61
8.1	Primary antibodies used for IF staining of iPSCs.	100
8.2	Secondary antibodies used for IF staining of iPSCs.	101
8.3	FACS antibodies used to assess iPSCs phenotype.	103
8.4	Composition of the medium used for method 2 HSPC differentiation.	104
8.5	FACS antibodies used for the FACS analysis of iPSCs-derived HSPCs.	106
8.6	FACS compensation beads used to phenotype iPSCs-derived HSPCs.	106
8.7	Aliquots prepared of method 2 T-cell differentiation medium.	107
8.8	Composition of the medium used for method 2 T-cell differentiation.	108
8.9	FACS antibodies used to assess the phenotype of iPSCs-derived T-cells.	109
8.10	FACS antibodies used to assess the phenotype of mHSPCs.	112
8.11	FACS compensation bead used to phenotype mHSPCs.	112
8.12	Cell cryopreservation medium.	116
8.13	The required reagents to PCR amplify a ligation insert.	118
8.14	PCR cycle settings to amplify a ligation insert.	118
8.15	The required reagents to digest a backbone.	118
8.16	Cell counts used for mouse bone marrow engraftments.	125
8.17	FACS antibodies used to phenotype mouse peripheral blood cells after engraftment.	126
8.18	FACS antibodies used to phenotype mouse bone marrow cells after engraftment.	128
8.19	FACS compensation beads used to phenotype mouse cells after engraftment.	128



Abbreviations

- AAV** adeno-associated viral vector. 2, 11, 12, 13, 64, 65
- ADA** adenosine deaminase deficiency. 2
- ADA-SCID** severe combined immunodeficiency due to adenosine deaminase deficiency. 2, 25
- APOE** apolipoprotein gene cluster. 22, 35
- bp** base pairs. 17, 21, 36, 49
- CAG** CMV early enhancer/chicken beta actin. 35, 36, 37, 46, 47, 48, 50
- CAR** chimeric antigen receptor. 6, 7, 23, 26, 28, 35, 36, 41, 42, 51, 82, 83, 84, 86, 87, 89
- CEA** chimeric carcinoembryonic antigen. 35, 36, 41, 42, 51, 84, 85, 86, 87, 89
- CFU** colony-forming unit. 74, 75, 76
- CI** chimeric intron. 35, 36, 47, 48, 49, 50, 51, 85
- CMV** cytomegalovirus. 14, 35, 46
- COG** cost of goods. 26, 28
- CRISPR/Cas9** clustered regularly interspaced short palindromic repeats and CRISPR-associated protein 9. 11, 16, 17, 18, 19
- crRNA** crispr RNA. 17
- CTLA-4** cytotoxic T lymphocyte-associated protein-4. 5
- dsDNA** double-stranded DNA. 12, 13
- EBNA** Epstein-Barr nuclear antigen. 8, 24, 67, 68
- EMA** European Medicines Agency. 5, 7, 24
- ESC** Embryonic stem cells. 8, 22, 27, 81
- FACS** fluorescence-activated cell sorting. 37, 53, 57, 60, 64, 70, 71, 72, 74, 75, 78, 80, 81, 84, 87
- FDA** United States Food and Drug Administration. 1, 5, 6, 7, 8
- GM-CSF** granulocyte-macrophage colony-stimulating factor. 5



gRNA single guide RNA. 17

GvHD graft vs. host disease. 27

HDR homologous-directed repair. 17, 18

HIV immunodeficiency virus. 69

HIV-1 immunodeficiency virus type one. 15, 19

HLA human leukocyte antigen. 1, 23, 26, 27, 28, 42

HR homologous recombination. 17

HSC hematopoietic stem cell. 18, 53, 54, 58, 59, 75, 76, 77, 78, 81

HSPC hematopoietic stem and progenitor cell. 1, 2, 14, 21, 23, 28, 31, 35, 46, 52, 53, 55, 56, 57, 58, 59, 60, 62, 63, 64, 65, 67, 74, 75, 76, 77, 78, 79, 80, 81, 82, 83, 85, 89

HvGD host vs. graft disease. 27

IF immunofluorescence. 68, 73, 84

IFN interferon. 21, 22, 35, 41, 42, 45, 46, 49, 50, 51, 62, 63, 65

IL-2 interleukin-2. 6

iNHDF immortalized normal human dermal fibroblast. 42, 45, 46, 49, 50

iPSC induced pluripotent stem cell. 8, 9, 11, 22, 23, 24, 26, 27, 28, 29, 31, 39, 67, 68, 69, 70, 72, 73, 74, 76, 77, 78, 79, 81, 82, 83, 84, 85, 86, 87, 89

ITR inverted terminal repeats. 12

kb kilobase. 12, 13, 15

LDL low-density lipoprotein. 15

LMO2 LIM only protein 2. 2, 3, 14

LPLD lipoprotein lipase deficiency. 2

LSK Lin⁻ Sca-1⁺ c-kit⁺. 53, 55, 56, 60, 61, 64

LTR long terminal repeat. 14, 16, 69

MART-1 melanoma antigen recognized by T-cells 1. 6, 35, 36, 41, 42, 51

MECOM ecotropic virus integration site 1 protein homolog. 2

MFI mean fluorescent intensity. 39, 40, 47, 69, 71, 77, 81, 82

MHC major histocompatibility complex. 6, 7, 27

MHEP mouse HSPC expansion protocol. 56, 57, 58, 59, 65



- MOI** multiplicity of infection. 12, 64
- NHEJ** non-homologous end-joining. 17, 18
- PAM** protospacer adjacent motif. 17
- PBRsAs** performance-based risk-sharing arrangements. 26
- PD-1** programmed cell death protein 1. 5
- ROCK** Y27632, inhibitor of Rho-associated kinase. 63
- S/MAR** scaffold/matrix attachment region. 11, 20, 21, 22, 23, 24, 29, 31, 35, 36, 37, 39, 41, 42, 43, 44, 45, 46, 47, 49, 50, 51, 52, 60, 61, 62, 64, 65, 67, 68, 69, 70, 71, 72, 73, 74, 77, 78, 81, 82, 84, 85, 86, 89
- SB** sleeping beauty. 20
- SCID** severe combined immunodeficiency. 3, 18, 22
- sEF1** short elongation factor 1. 35, 36, 46, 47, 48, 49, 50, 51, 68, 69, 85, 89
- SIN** self-inactivating. 3, 14, 15, 16
- ssDNA** single-stranded DNA. 12, 18
- ssRNA** single-stranded RNA. 13, 15
- TALEN** transcription activator-like effector nucleases. 11, 16, 18, 19
- TCR** T-cell receptor. 6, 7, 23, 26, 28, 35, 36, 41, 42, 51
- TIL** tumor-infiltrating lymphocytes. 6
- TIRs** terminal inverted repeats. 19, 20
- TLR** toll-like receptor. 63, 65
- tracrRNA** trans-activating crisper RNA. 17
- U-iPSC** urinary-derived iPSCs. XIX, 23, 24, 31, 35, 36, 39, 41, 42, 45, 46, 47, 50, 51, 52, 67, 68, 70, 71, 73, 74, 75, 79, 80, 81, 82, 89
- USC** urinary stem cells. 67, 68
- VSV-G** vesicular stomatitis virus. 15
- ZFN** zinc finger nuclease. 11, 16, 18, 19



Chapter 1

Historical Content

1.1 Historical Content for Gene and Cell Therapy

Many are familiar with the concept of small-molecule drugs for medicinal applications. A new era has emerged, in which patients are no longer primarily treated with chemistry-based drugs. A shift to biology-based therapies, including gene and cell therapies, has occurred [174].

In 1957, Dr. E. Donnall Thomas performed the first reported bone marrow transplantation, which involved replacing a patient's bone marrow cells with donor bone marrow [309]. Bone marrow transplantations can be considered among the first implemented cell therapies. Cell therapy is a treatment given to a patient that is composed of a cell population derived from a donor (allogeneic) or the patient (autologous). The initial bone marrow transplantations performed by Dr. Thomas had negligible success [30]. With his colleagues, Dr. Thomas continued to develop bone marrow transplantations further [30]. The first United States Food and Drug Administration (FDA) approved hematopoietic stem and progenitor cell (HSPC) bank was HEMACORD in 2011 [134, 227], and, as of today, 8 HSPC banks have been approved by the FDA for bone marrow transplantations [313].

Allogeneic cell therapies require finding an human leukocyte antigen (HLA) matched donor, which can be difficult [9]. Treating patients with autologous cells, removes the need of finding a matched donor, and ensures a full HLA match. They entail the *ex vivo* expansion and manipulation of extracted patient cells that are reintroduced into the patient [157].

Autologous cell therapies have been used for various applications, such as generating skin substitutes for wound healing [157]. Many times, they require alternations to a malfunctioning gene. Additionally, costs related to *ex vivo* culture commonly increase the price of autologous cell therapies [157].

In the 1960s, the concept of genetically fixing a malfunctioned gene was first described; this is called gene therapy [102]. This opened the door to personalized therapies that utilize a patient's cells. In 1988 the first gene therapy clinical trial, for Gaucher disease, commenced [222]. During this time, most gene therapies had no therapeutic benefits, and some even lead to adverse effects [7, 149]. Scientists have continued to develop gene and cell therapies, which have led to great advancements in recent years.

The first approved gene therapy in the EU appeared in 2012; it is named Glybera (alipogene tiparvovec) [7, 241, 180, 314]. Patients treated with Glybera received a minimum of 10 vials



via intramuscular injection [241, 314]. As one vial costs 100,000 euros, a treatment with Glybera was at least 1 million euros [241, 210]. Glybera treated lipoprotein lipase deficiency (LPLD) [314]. Patients with LPLD harbor a genetic defect in the gene expressing lipoprotein lipase; this ultimately leads to fat buildup in the body, and when left untreated leads to a terminal illness through pancreatitis [241]. Glybera is composed of an adeno-associated viral vector (AAV) carrying the wild-type cDNA sequence for lipoprotein lipase [241, 107]. Glybera delivers the corrected LPL gene sequence into patients resulting in functional lipoprotein lipase. Eight subjects were enrolled in the EU clinical trials for Glybera. All subjects had previously suffered from severe episodes of pancreatitis and were diagnosed with LPLD. Over the first 12 weeks post-dosing, subjects displayed a reduction in their median triglyceride levels [314]. Two out of eight patients met acute primary endpoint criteria [314]. Unfortunately, all subjects exhibited triglyceride levels around or above their starting baseline three years post-dose [314]. Inflammation at the injection site was also observed [314]. Glybera is no longer approved for usage in the EU [93].

In 2016, The first market authorized *ex vivo* gene therapy in the EU appeared: Strimvelis [94]. Strimvelis treats a rare immunodeficiency disease called severe combined immunodeficiency due to adenosine deaminase deficiency (ADA-SCID) [180]. With this disease, patients are unable to produce T-cells, B-cells, or NK-cells, which means their adaptive immune system is essentially absent, and patients can easily get sick from microbial infections [312]. Strimvelis is an *ex vivo* gene therapy composed of HSPC extracted from a patient that are genetically altered *ex vivo* using a gammaretroviral vector containing the wild-type functional cDNA sequence of adenosine deaminase deficiency (ADA) [236]. These cells are reintroduced into the patient with the hopes of a successful engraftment and treatment [236]. 22 patients have been treated with Strimvelis—some patients have been treated too recently to collect reliable efficacy and safety data [236]. 18 of these patients were enrolled in the integrated population of the EU clinical trials and have a 100% survival rate [236]. 14 of the 17 subjects with publicly available data displayed survival without PEG-ADA-enzyme replacement therapy intervention for greater than or equal to three months post-therapy; three patients required intervention [236]. Patient's severe infection rates dropped each year post-therapy, with having the lowest rate of severe infection during the four to eight year follow-up period [236]. The presence of CD3+ cells (T-cells), CD19+ cells (B-cells), and CD56+ CD16+ (NK-cells) steadily remained above baseline values from one to eight years post-therapy [236]. Additionally, the presence of antibodies against various diseases was detected in the majority of patients after halting intravenous immunoglobulin therapy, and a number of subjects contained long-lived antibodies [236]. All 18 subjects reported adverse effects, with the majority being labeled as grade one or two infection and infestation, skin and subcutaneous tissue disorders, and blood and lymphatic system disorders [236]. ADA-SCID patients treated with a cell therapy similar to Strimvelis were reported to contain cell clones with vector integration near the ecotropic virus integration site 1 protein homolog (MECOM) or LIM only protein 2 (LMO2) loci [312, 282]. Though, there were no reports of leukoproliferation in patients treated with Strimvelis [312]. In October 2020, one patient was diagnosed with a T-cell leukemia (lymphoma) and its relationship to the therapy (possibility of genotoxic concerns) is currently being investigated [241, 312, 98].



Concerns surrounding viral vector genotoxicity were significantly highlighted in the French X-linked severe combined immunodeficiency (SCID) clinical trial in the early 2000s when four of the initial seven infants treated with genetically altered cells developed leukemia [241, 123]. It was reported that vector integration into the LMO2 locus (a proto-oncogene) was responsible for this onset of uncontrolled clonal expansion (leukemia) [124]. Genotoxicity issues were also highlighted in trials for Wiskott-Aldrich syndrome[41] and X-linked chronic granulomatous disease [294]. Genotoxicity is a massive concern with gene therapies, and the scientific community is investigating novel vector designs associated with lower genotoxic risks [171].

The latest generation of lentiviral vectors (3rd generation) is one of the safest integrating viral vectors; it contains a self-inactivating (SIN) feature [241, 124]. Many gene therapy clinical trials are currently underway using SIN lentiviral vectors. Other genetic modification tools that are reported to have lower genotoxic risks have also been explored (see chapter 1.4 for further information). Safety is still a massive aspect of gene and cell therapy, and many trials require long-term patient observation before market approval. Another arising issue of gene and cell therapies is their cost (see section 2.2.1 for further information).

Current clinical trials for gene therapies, include treatment options for epilepsy [315], severe hemophilia A [95], metachromatic leukodystrophy [236], Artemis-deficient SCID [316], Leber's Hereditary Optic Neuropathy [333], and many more. Thousands of trials for gene therapies have been registered, and include greater than 300 phase-three studies [180]. 14 gene therapies have (or had) market authorization in the EU (Table 1.1) [247].¹

¹Table 1.1 contains products with a valid EU marketing authorization. Some products may not be available on the market.



Table 1.1: Approved gene and cell therapies in the EU [247].

Name	Market Authorization Holder	License Number	License Date
Abecma	Celgene Europe B.V., NL	EU/1/21/1539	18.08.21
Breyanzi	Bristol Meyers Squibb Pharma EEIG, IR	EU/1/22/1631	04.04.22
Carvykti	Janssen Cilag International BV, Belgien	EU/1/22/1648	25.05.22
Glybera	uniQure biopharma B.V., Niederlande	EU/1/12/791/001	25.10.12
Imlygic	Amgen Europe B.V.	EU/1/15/1064	16.12.15
Kymriah	Novartis Europharm Ltd., IRL	EU/1/18/1297	23.08.18
Libmeldy	Orchard Therapeutics (Netherlands) B.V., NL	EU/1/20/1493	17.12.20
Luxturna	Novartis Europharm Limited	EU/1/18/1331	22.11.18
Roctavian	BioMarin International Limited, Ireland	EU/1/22/1668	24.08.22
Strimvelis	Orchard Therapeutics B.V., NL	EU/1/16/1097	26.05.16
Tecartus	Kite Pharma EU B.V., NL	EU/1/20/1492	14.12.20
Upstaza	PTC Therapeutics International Limited, Ireland	EU/1/22/1653	18.07.22
Yescarta	Kite Pharma EU B.V., NL	EU/1/18/1299	23.08.18
Zolgensma	Novartis Europharm Limited, Dublin	EU/1/20/1443	18.05.202

1.2 Historical Content for the Treatment of Cancer

The first reported attempt for the treatment of cancer was in 1891 when Dr. William B. Coley treated a patient’s sarcoma by erysipelas inoculation at the Memorial Hospital in New York [311]. He generated a cocktail of filtered bacteria and bacterial lysates, which was called the “Coley Toxins” [190]. The first patient to receive the “Coley Toxins” was a 21-year-old suffering from a considerable tumor. The treatment was implied to be a success as the patient had complete remission, and later, at the age of 47, passed away due to a heart attack [69]. Thousands of patients administered the “Coley Toxins” were reported by various doctors to be successfully treated [190]. Many practitioners were also suspicious of the reported results [190]. In 1909, Paul Ehrlich developed the theory of cancer immunosurveillance, which stated that immune systems normally suppress tumor cell formation; this theory was also met with skepticism [89]. A shift toward radiation therapy for the treatment of cancer arose as practitioners, such as Allen Pusey, reported successful treatment using it [260]. Radiation



therapy was also more accepted within the medical community [190]. In the 1940s, the FDA approved the first chemotherapy, nitrogen mustard (mechlorethamine) [311, 197, 196]. The immune system and its relationship to cancer was still met with skepticism evidenced by Osias Stutman reporting in 1974 that the immune system does not protect against cancer [302], and Richmond T. Prehn and Joan M. Main stating in 1957 that “as a result of apparent failure during the past half-century, it is current consensus that immune mechanisms probably will be of little use in the control of this disease” [311, 256]. Countless researchers found supporting evidence for the theory of cancer immunosurveillance [117, 211, 120, 322, 163], such as Michael J. Berendt and Robert J. North who reported in 1978 that tumor regression after endotoxin treatment is contingent on T-cell-mediated immunity [24]. The basic principles of the “Coley Toxins” and Ehrlich’s theory of cancer immunosurveillance are now understood—the immune system can effectively treat and prevent certain cancers [281, 290, 289]. In the late 1900s, a shift towards immune-related therapies for the treatment of cancer began. During this time, the FDA approved the first immunotherapies, including TICE BCG and Rituxan [208, 239, 202, 109].

Various types of cancers that were considered fatal, such as metastatic melanoma, are being treated due to innovations in immunotherapies [176, 175, 15, 205, 181, 182]. Approved immunotherapies include targeted inhibitors, such as inhibitors against BRAF/MEK; immune checkpoint blockades, such as cytotoxic T lymphocyte-associated protein-4 (CTLA-4) and programmed cell death protein 1 (PD-1) inhibitors; oncolytic viruses, such as T-VEC; and T-cell immunotherapies [176]. Immune checkpoint blockades were discovered after Tasuku Honjo and colleagues showed in 1999 that mice knocked-out for PD-1 develop autoimmune syndromes [231, 230]. In 2008, the first clinical trial for an immune checkpoint blockade was commenced [99, 311]. These therapies, ipilimumab and tremelimumab, consisted of a monoclonal antibody that induced CTLA-4 blockade, which was used to treat patients with malignant melanoma [99, 311]. In 2011, ipilimumab (Yervoy) was approved by the FDA and European Medicines Agency (EMA), and is reported as the first agent from a phase three clinical trial to extend the life of advanced melanoma patients [139, 45, 44]. Other approved immune checkpoint blockades include PD-1 inhibitors Keytruda and Opdivo [198, 47, 46, 43], and there are numerous immune checkpoint blockades currently in clinical trials [39]. Oncolytic viruses are viruses that were naturally selected or artificially designed to target cancer cells [23]. They hijack the host cell’s replication machinery and lysis the cell in the process, releasing newborn viral particles and cancer antigens [16], which also promotes an endogenous inflammatory response against the cancer [23]. The first approved oncolytic virus was Imlygic (Talimogene laherparepvec) in combination with granulocyte-macrophage colony-stimulating factor (GM-CSF), which was approved by the EMA in 2015 for treating melanoma [7, 241, 180, 10]. The eight initially approved immunotherapies (BRAF inhibitors Vemurafenib, Dabrafenib, Trametinib, and Cobimetinib; anti-CTLA-4 antibodies Ipilimumab, Pembrolizumab, and Nivolumab; and the modified oncolytic herpes virus Talimogene laherparepvec) show a durable clinical response in patients and the majority of them extend a patient’s life [176]. Many combination therapies are utilized, merging radiation, surgery, chemotherapy, molecular targeted therapies, and/or immunotherapies [311, 176, 43, 42].

In 1982, it was reported that lymphoid cells expanded in interleukin-2 (IL-2) could effectively treat subcutaneous FBL3 lymphomas in mice [87]. In 2002, two studies indicated for the first time that clonally selected patient T-cells expanded *in vitro* could cause tumor regression in patients suffering from advanced melanoma [336, 84]. The first study utilized tumor-infiltrating lymphocytes (TIL) [84], while the second study utilized melanoma antigen recognized by T-cells 1 (MART-1) and gp-100 specific CD8 T-cells [336]. These studies were a part of many that paved the way toward clinically approved T-cell immunotherapies. T-cell immunotherapy has become increasingly popular, as shown by its market growth between 2012 and 2019. The non-existent global market revenue of chimeric antigen receptor (CAR) T-cell immunotherapy in 2012 grew to 700 million dollars in 2019 [218].

As mentioned above, one type of adaptive T-cell immunotherapy includes TILs. TILs are lymphocytes extracted from a patient's tumor and expanded *ex vivo*, then reintroduced into the patient [270, 220]. Shortly after Rosenberg demonstrated the anti-tumor effects of murine TILs in 1987 [293], Rosenberg and colleagues treated the first melanoma patients using IL-2 and autologous TILs [270]. Within this preliminary study, 9 out of 15 patients were reported to have tumor regressions [270]. Rosenberg and colleagues made various genetic modifications to TILs to improve tumor lysis and tracking capability [268, 269]. They have submitted various IND applications [271, 272, 273, 274]. To this date, no TIL therapies have been FDA-approved for the treatment of cancer. The inability of TILs to persist within patients has been reported as a major limitation of them [265].

T-cell receptor (TCR) T-cell immunotherapy is another type of adaptive T-cell immunotherapy. A TCR T-cell therapy is composed of patient T-cells that are genetically engineered *ex vivo* to express a TCR that targets a specific tumor antigen presented at the surface of a cancer cell by major histocompatibility complex (MHC) class one. TCR T-cell immunotherapies do not require the *ex vivo* expansion of tumor-specific clones, which was commonly done previously [209, 279]. Rosenberg and colleagues indicated in 1999 that human T-cells could be genetically engineered to express a TCR, and that these cells had anti-tumor reactivity *in vitro* [68]. The National Institutes of Health Clinical Center—with Steven Rosenberg as the principal investigator—submitted the first TCR T-cell immunotherapy for FDA approval in 2004 [224, 225]. In 2006, Steven Rosenberg and colleagues showed T-cells expressing anti-MART-1 TCR led to tumor regressions in melanoma patients, and patients sustained high levels of circulating T-cells 1-year post-infusion [209]. Adverse reactions to anti-MART-1 TCR T-cells have been reported, such as severe dermatitis, uveitis, vitiligo, and hearing loss, due to “on-target off-tumor” effects [121]. Literature also reports that cancer cells can avoid immunosurveillance by downregulating MHC class one expression, which is a problem for TCR T-cell immunotherapy efficacy [136].

CAR T-cell immunotherapy is another class of adaptive T-cell immunotherapy. A CAR is a synthetic protein consisting of a single chain variable fragment of a monoclonal antibody, TCR signaling domains, and, sometimes, a costimulatory domain (Figure.1.1) [153]. CARs bind to an antigen present on the surface of a cancer cell, such as a carbohydrate, lipid, or protein, and do not require the presentation of the antigen via MHC class one [86, 40]. In 1989, Zelig Eshbar and colleagues show that T-cells genetically modified to express a CAR

recognize and kill cancer cells [118]. In 2008, it was shown that a CAR T-cell immunotherapy induced a clinical response in three out of seven patients with B-cell lymphomas [310]. Literature further reports that clinical responses to CAR T-cell treatment last up to one year, induce *in vivo* expansion of the cell therapy, and are associated with long-term functional persistence [255, 156]. Such improvements have led to the first FDA and EMA approved T-cell immunotherapies, Kymriah[232, 233] and Yescarta™ [159, 160]. To date, five CAR therapies have been approved by the FDA and EMA since 2017 [233, 160, 56, 154, 161]. A main concern of CAR T-cell immunotherapy is cytokine release syndrome, which has been reported in several patients [172].

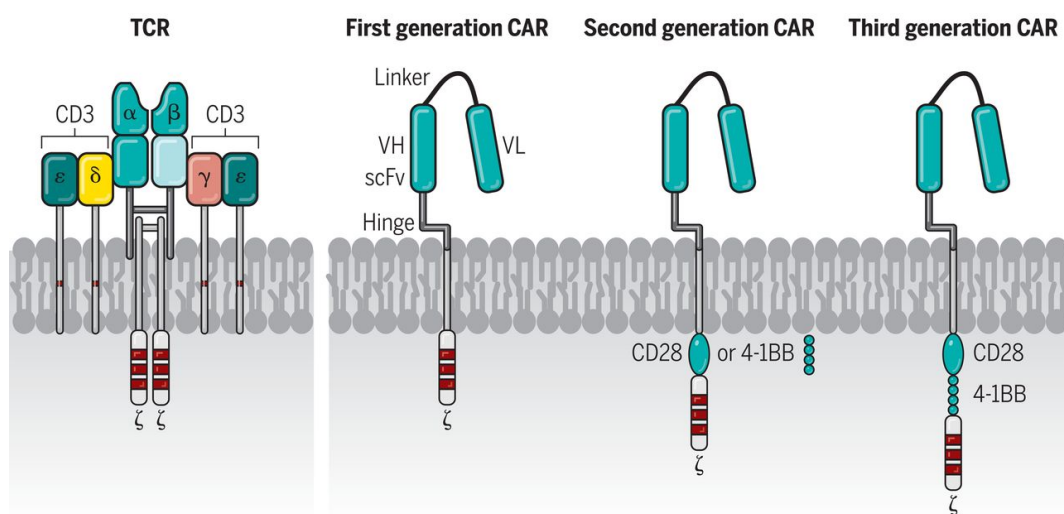


Figure 1.1: Structural depiction of a TCR and CAR. On the left is a graphical representation of a TCR. It is composed of various subunits. Three generations of CARs are depicted on the right. Newer generations implement co-stimulatory domain(s). The image is obtained from [153].

CARs and TCRs have advantages and disadvantages. TCRs utilize endogenous T-cell signaling pathways [185, 63], and TCRs mediate T-cell activation at lower antigen densities relative to CARs as TCRs amplify the signal through additional cell surface proteins. (Table.1.2) [128, 304, 141, 258]. This makes TCR T-cells more sensitive, but also more prone to “on-target off-tumor” interactions [128]. Though, TCRs lower affinity range helps to lessen “on-target off-tumor” interactions [128, 140]. CARs are not dependent on antigen presentation via MHC class one, unlike TCRs, and a range of surface molecules can be targeted [86, 40]. CAR T-cells can also kill cancer cells faster (serial killing) relative to TCR T-cells, which have a slower onset but longer duration due to the structure of the receptor and mode of activation [337].

Researchers have investigated novel ideas to improve T-cell immunotherapies. Such ideas include implementing a suicide gene (in case the therapy goes awry) [337], tracking systems (to locate the immunotherapies distribution) [250], and cytokine expression upon T-cell activation (to promote immune system engagement) [67]. In general, scientists continue to explore the vast possibilities immunotherapy has to offer.



Table 1.2: Properties of TCRs and CARs [128].

Receptor Property	TCR	CAR
Number of subunits in receptor complex	10	1
Coreceptor, co-stimulator involvement	Yes (CD4, CD8, CD28, etc.)	None known
Typical range of affinities for antigen	$10^4 - 10^6 M^{-1}$	$10^6 - 10^9 M^{-1}$
Number of surface receptors per T cell	50,000	>50,000 but varies
Minimum number of antigens required on target cells	1	>100

1.3 Pluripotent Stem Cell Gene Therapy

Embryonic stem cells (ESC) are cells present in an embryo that can differentiate into any human cell type (Figure.1.2) [259]. Researchers have extracted ESCs from embryos and have used them for various research applications [177]. This has provoked great controversies as embryos are damaged during this process [327, 79].

An induced pluripotent stem cell (iPSC) is a cell with the capacity to also differentiate into any human cell type [305]. Unlike ESCs, iPSCs develop from mature cells, such as fibroblasts or blood cells, that are reprogrammed into ESC-like cells (Figure.1.2) [305]. iPSCs have provoked less controversy relative to ESCs as the collection of iPSCs does not require the manipulation of embryos [327, 79]. iPSCs are readily available to researchers who lack access to ESCs or who work in countries where work with ESCs is banned [188, 8, 187]. The method of reprogramming a mature cell into an iPSC was developed by Shinya Yamanaka in 2007 [305]. He was later recognized for this achievement with the 2012 Nobel Prize in Physiology or Medicine [70]. Literature reports reprogramming can be achieved using non-integrating technologies, such as EBNA-based plasmids [267] and mRNA [14], which have lower genotoxic risks relative to the initially used gammaretroviral vectors [305]. iPSCs injected into mouse embryos have been reported to produce chimeric animals [215], and iPSCs have been shown to differentiate into germ cells [305, 245, 142]. These characteristics make iPSCs controversial as germline editing is a possibility with them [186]. The usage of iPSCs to produce somatic cell gene therapies is less controversial and benefits the community.

To date, there are no iPSC-based cell therapies with market authorization in the EU or USA [313, 247]. Seven iPSC-based cell therapies are in FDA clinical trials [22, 132, 221, 165, 133, 108, 96]. These include treatments for refractory age-related macular degeneration, by injecting iPSC-derived retinal pigment epithelium (RPE) into a patient's retinal space [22, 221]; for severe ischemic cardiomyopathy or heart-failure, using iPSC-derived cardiomyocytes [132, 165, 133, 108]; and for advance solid tumors, using iPSC-derived NK cells (FT500) [96]. The majority of iPSC-related clinical trials collect cells from a donor and use them for pre-clinical applications, such as disease models [151, 317, 61, 316, 280, 206] and pre-clinical investigations of potential iPSCs-derived cell therapies [223, 183]. Researchers have used iPSCs as a disease model to understand Ataxia-Telangiectasia [151], intellectual disabilities



[317, 316], Inborn Errors of Metabolism [61], and cardiovascular phenotypes [280, 206]. Trials using iPSCs as a cell-based therapy to treat patients are recent. The seven mentioned above commenced between February 2019 and October 2022 with five of them in phase one and two of them in phase two: iPSC-derived RPE/PGLA and iPSC-derived cardiomyocytes (BioVAT-HF) [22, 132, 221, 165, 133, 108, 96].

iPSCs can be used for vast purposes, and their novelty has recently been noticed. In 2022, various companies, such as Fujifilm Cellular Dynamics, Inc., Century Therapeutics, and Bristol Myers Squibb have amplified their commitment to iPSC-based therapies and/or iPSC banking [50, 105]. Researchers also continue to explore the vast possibilities of iPSCs [162, 137, 321]. In the future, I believe iPSC-derived cell therapies will be more prevalent within clinical trials and could be the answer to more affordable prices for gene and cell therapies (See section 2.2).

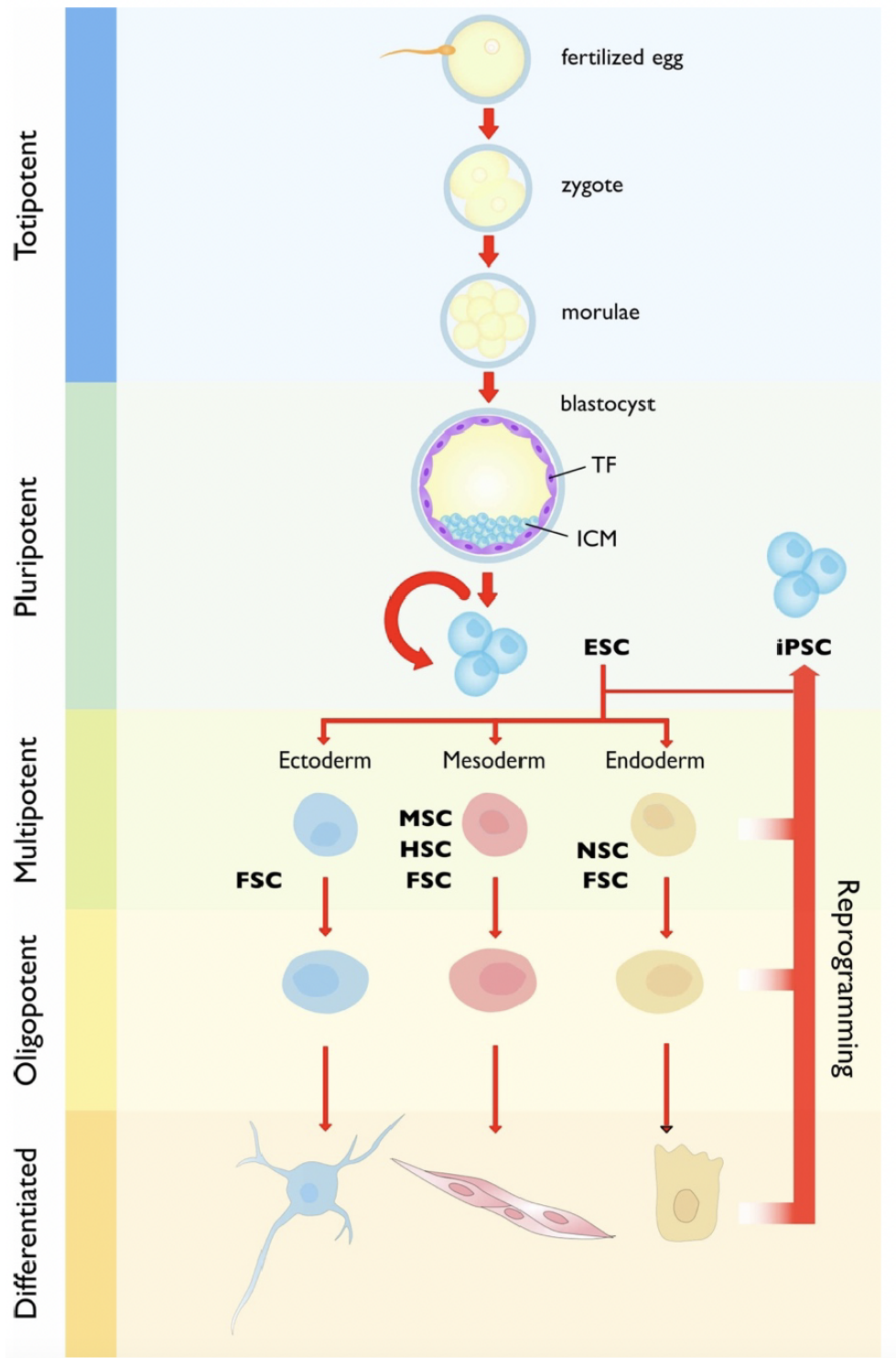


Figure 1.2: Schematic representation of ESC and iPSC development and differentiation. ESCs and iPSCs are classified as pluripotent cells. ESCs are derived from embryos while iPSCs are derived from somatic cells. ESCs and iPSCs both can differentiate into any human cell type. The image is obtained from [267, 100].



1.4 Modes of Genetic Modification

There are various ways to genetically modify cells. To choose an appropriate vector format, one should consider the size of the transgene, the overall size of the total DNA, the required duration of treatment, the cell type to be genetically modified, the way the vector will be delivered to the patient (*ex vivo*, *in vivo*, or *in situ*), potential immune responses, and costs [7, 241]. Within this section, I will highlight seven classical approaches to genetically modify cells: AAV, gamma-retroviral vector, and lentiviral vector transduction; clustered regularly interspaced short palindromic repeats and CRISPR-associated protein 9 (CRISPR/Cas9), transcription activator-like effector nucleases (TALEN), and zinc finger nuclease (ZFN) gene editing; and transposons. I have also provided a summary on scaffold/matrix attachment region (S/MAR) DNA vectors as the data shown in this report assess the application of S/MAR DNA vectors for iPSC-derived immunotherapies. The benefits of using an S/MAR DNA vector are described in section 2.3.

1.4.1 Viral Vectors

AAVs, gamma-retroviral vectors, and lentiviral vectors are three of the most prevalently used viral vectors for gene therapies (Table.1.3) [112, 173]. Adenoviral vectors have also been widely utilized [112]. Clinical applications of them can be complicated as patients commonly contain pre-existing immunity against them [66, 72]. Literature reports adenoviral vectors evoke strong immune responses within patients [66, 72]. This makes adenoviral vectors a propitious vaccine vehicle or oncolytic virus [173], rather than a tool for gene and cell therapies. AAVs, gamma-retroviral vectors, and herpes simplex virus were among the first reported gene therapy tools used [222, 314, 103]. Viral vectors have been reported to alter cellular gene expression and functionality [254, 242]. They have also been associated with genotoxic risks [242]. Researchers have developed vast modifications to viral vectors to make them safer [241].

Table 1.3: Viral vectors used to genetically modify cells [180].

Vector	Transfection capacity	Integration	Restrictions
Adenovirus	< 7.5 kb	None	Causes immune response, short-term expression
AAV	< 4.5 kb	Low	Causes immune response
Herpesvirus	> 30 kb	None	May cause immune response
Retrovirus	< 8 kb	High	Risk of insertional mutagenesis. Just infects dividing cells
Lentivirus	8–10 kb	High	Risk of insertional mutagenesis



1.4.1.1 AAV

AAV vectors are classically considered a safer viral vector relative to integrating viral vectors [62]. They are a non-enveloped virus a part of the parvovirus family that packages single-stranded DNA (ssDNA) [170]. They deliver their ssDNA genome into the cell host, which is then converted into dsDNA and forms various shapes including circular monomers and circular concatemer [88, 191]. AAVs can transduce dividing and non-dividing cells [323, 51]. AAV DNA predominately persists episomally within the host [88, 216, 323]. This gives them a lower genotoxic risk, but only provides transient gene expression as episomal vectors are lost during cell division [88, 216]. If a long-term persistent expression of the delivered transgene is desired, AAVs should only be used within cell types that do not habitually divide, such as neurons, retinal pigment epithelium cells, and mature cardiac muscle cells. Low frequency integrations have been reported [200], and clonal expansions related to them have been shown in dogs and mice [228, 189, 76]. No clonal expansions related to AAV integration have yet been reported in humans [189]. AAVs are reported to have a small packaging size; they support a maximum genome size of <4.5 kb [180]. AAVs classically require a higher titer as a high multiplicity of infection (MOI) is generally required to successfully modify cells [64]. Additionally, as AAV infections are common in childhood, many people have pre-existing AAV immunity (particularly to AAV serotype 2) [170]. When an AAV vector gene therapy is delivered to a patient with such immunity, the patient's immune system might neutralize it [171]. Though, this neutralization can be prevented using immunosuppressants or different viral serotypes [171, 226, 35].

A benefit of AAVs is the numerously available serotypes [171]. A serotype can improve the transduction efficacy (tropism) for one's intended cell type [171]. There are at least 12 AAV serotypes discovered for primates (including humans) [303]. With the advent of genetic engineering, new forms of AAVs have been generated. A commonly used method is called pseudotyping; this uses the capsid proteins from one serotype to package the expression cassette and inverted terminal repeats (ITR)s from another serotype [49]. Pseudotyped AAVs improve and expand the viral tropism. Capsids composed of capsid proteins from various serotypes (hybrid capsids) also have been generated and show improved viral tropism [49]. Additional AAV variants, such as self-complementary AAVs and "increased packaging" AAVs, have been generated to increase the speed of transgene expression and increase the packaging size of AAVs, respectively [83, 192].

AAV vectors are commonly generated using a rep/cap plasmid, helper plasmid, and transfer plasmid (Figure.1.3) [1]. The rep/cap plasmid expresses the capsid protein as well as proteins needed for AAV replication [1]. The helper plasmid contains genes that mediate AAV replication [1]. The transfer plasmid contains the AAV genome, which is the DNA that will be inserted into the host (provirus) [1]. Keeping replication and capsid proteins separate from the transfer plasmid produces viruses that are replication-incompetent (viral vectors) [246]. When a host is treated with a viral vector, viruses cannot be produced. AAV production requires several days and is quite labor-intensive compared to other gene modification tools. The process first requires the production of the three plasmids, which are then introduced into HEK293T. Three days post-genetic modification, HEK293T cells are collected, and the

viral vectors produced within them are extracted and purified using an iodixanol or cesium chloride gradient. Further steps might be necessary to replace the solvent viral vectors are present in, which depends on the sensitivity of the cell type used. Then, the viral vectors are titered. (See section 8.5.2 for a further description of an AAV production method).

Approved gene therapies using AAVs include Glybera, Luxturna, and Zolgenma [313, 247]. Many AAV gene therapies are in clinical trials, including treatments for macular degeneration [6]. One downfall of an AAV is its expensive clinically relevant production costs [53].

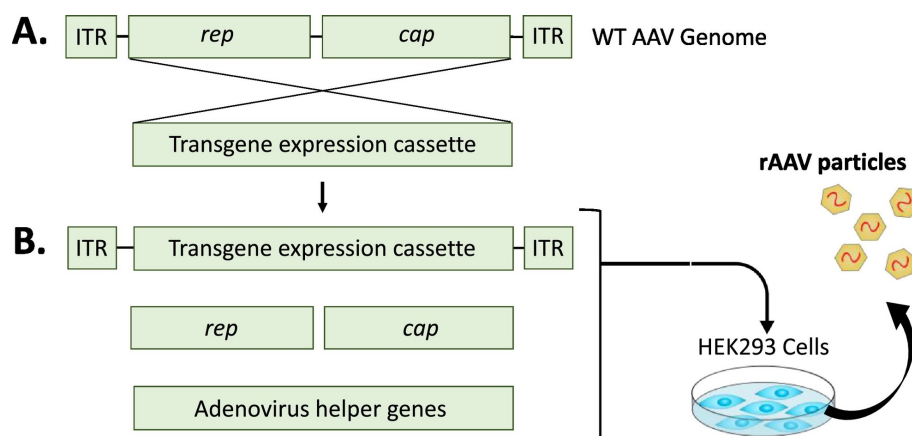


Figure 1.3: Differences between a wild-type AAV and an AAV viral vector. A) Schematic representation of an AAV genome. A wild-type AAV genome contains *rep* and *cap* protein sequences flanked by ITRs. To create an AAV viral vector, *rep* and *cap* are replaced with a transgene of interest. B) Schematic representation of AAV viral vector production. Three plasmids are commonly utilized to produce a viral vector packaged with the transgene flanked by ITRs. Plasmids are used so *rep*, *cap*, and AAV helper proteins are present for virus assembly. As these protein sequences are not incorporated into the provirus, the AAV becomes replication-incompetent. The image is obtained from [229].

1.4.1.2 Gamma-Retroviral Vector

Gamma-retroviral vectors are enveloped viral vectors that package two copies of single-stranded RNA (ssRNA), viral reverse transcriptase, and viral integrase (Figure.1.4) [2, 184, 213]. Gamma-retroviral vectors can package up to 8 kb of RNA—almost double the capacity of AAVs [180]. They are replication-incompetent derivatives of the Moloney Murine Leukemia Virus or Murine Stem Cell Virus (MSCV) genomes [17]. Upon cellular entry, a gamma-retroviral vector releases its packaged material into the cytosol [213, 90]. The RNA is reverse transcribed into dsDNA aided by the viral reverse transcriptase [213]. This viral DNA is shuttled in association with microtubules toward the host nucleus [90]. Once cells pass M phase (the nucleus is degraded), the viral integrase incorporates the viral DNA into the host's genome [213, 90]. Gamma-retroviral vectors semi-randomly integrate into the host's genome [98, 2]. They are reported to have preferred integration sites in transcriptional start sites [241, 242]. So, unlike AAVs, the gamma-retroviral provirus persists in dividing and differentiating cells as it becomes part of the host's genome. Gamma-retroviral vectors have a vast array of possibilities for pseudotyping, which increases their range of tropism [288]. Viral envelope glycoproteins used to pseudotype gamma-retroviral vectors include capsid proteins from



lyssaviruses, arenaviruses, hepadnaviridae, flaviviridae, paramyxoviridae, baculovirus, filoviruses, and alphaviruses [288]. Gamma-retroviral vectors have a vast history of genotoxicity concerns [241, 123, 294, 21]. Gamma-retroviral vectors have been reported to have one of their integration sites near the proto-oncogene LMO2 [124]. As described in section 1.1, this has caused devastating adverse side effects, such as the development of cancer in many patients treated with such gene therapies. Another downfall of gamma-retroviral vectors is that they can only enter mitotically active cells [180].

One concern during viral vector production is the development of replication-competent viruses [283]. A gamma-retrovirus requires the genetic code and expression of gag/pol and env to be replication-competent [283]. Gamma-retroviral vectors do not contain gag/pol and env gene sequences, rendering them replication-incompetent [283]. By placing gag/pol and env on separate plasmids from the transgene flanked by the LTRs, replication-incompetent viral vectors can be produced [283]. Multiple recombination events must occur for a replication-competent viruses to be created following this method [283].

Gamma-retroviral vectors are not classified by generations [3]. However, it is possible to create a SIN gamma-retroviral vector [3, 167]. It has been reported that SIN viral vectors significantly lower the risk of insertional mutagenesis within the host as sequences associated with proto-oncogene activation have been removed [241, 124, 213, 339, 199]. SIN viral vectors have a removal of the enhancer/promoter region within the 3' U3 of the LTR. Since the 3' U3 is used to generate both LTRs within the integrated provirus, this alternation results in the absence of this region in the 5' and 3' U3 (Figure.1.4) [98, 213]. The removed 5' U3 can be replaced with a heterologous promoter, such as the cytomegalovirus (CMV) promoter, (this is sometimes performed to improve vector production) and a synthetic promoter or endogenous human promoter is located upstream of the transgene (this is required for the expression of the transgene within the host) [312, 282, 213]. SIN viral vectors have also been modified to include an insulator within the remaining U3 region [241, 213]. Though, this has been associated with a drop in viral titer [320].

In the early 1990s, gamma-retroviral vectors were the first viral vectors used for HSPC gene therapy [98]. Strimvelis, the first *ex vivo* gene therapy given market authorization in the EU, utilizes a gamma-retroviral vector [222, 7]. Many clinical trials during this time utilized them [238]. As described in section 1.1, numerous patients treated with these cell therapies developed leukemias related to gamma-retroviral integration near a proto-oncogene [241, 123, 41, 294]. Data initially indicated that Strimvelis did not have these cancer related adverse effects. In 2020, one patient treated with Strimvelis was reported to have developed a leukemia [237]. Yescarta, one of the first approved T-cell immunotherapies utilizes a SIN gamma-retroviral vector [159]. Though, more applications of *ex vivo* gene therapies recently use lentiviral vectors as they are reported to be safer [98].

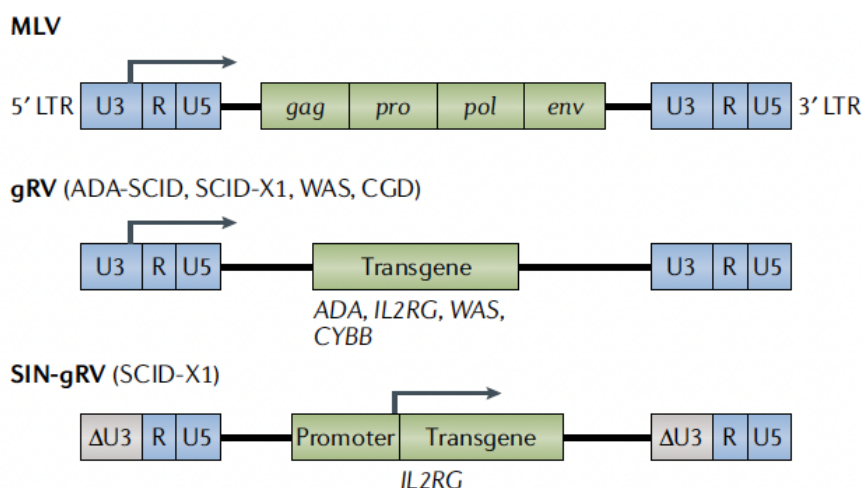


Figure 1.4: Schematic representation of a gamma-retroviral vector provirus. MLV represents a wild-type gamma-retroviral vector genome. gRV displays the provirus of a classic gamma-retroviral vector. SIN-gRV depicts the provirus of a SIN gamma-retroviral vector. The image is obtained from [98].

1.4.1.3 Lentiviral Vector

Lentiviral vectors are derived from the same virus family as gamma-retroviral vectors (retrovirus family) [5]. They are also envelope viruses packaging two copies of ssRNA, viral reverse transcriptase, and viral integrase, and they also semi-randomly integrate into the host's genome [213]. The difference between gamma-retroviral vectors and lentiviral vectors is that lentiviral vectors are based off the genome of the immunodeficiency virus type one (HIV-1) [5]. Unlike, gamma-retroviral vectors, lentiviral vectors can infect both dividing and non-dividing cells and has a genome capacity ranging between 8-10 kb [180, 213]. It has also been reported that lentiviral vectors have preferred integration sites in transcriptional units [241, 242, 213]. This characteristic renders lentiviral vectors safer than gammaretroviral vectors as gammaretroviral vectors integrate near transcriptional start sites, which may result in the transcriptional activation of a proto-oncogene [241, 98]. So far, no patient has been reported to contain insertional mutagenesis from a lentiviral vector after a cell therapy treatment [98].

Similar to gamma-retroviral vectors, lentiviral vectors can be pseudotyped to improve tropism [288]. The classical HIV-1 envelope protein, which binds CD4, can be replaced with envelope proteins from other viruses, such as the vesicular stomatitis virus (VSV-G) [213]. VSV-G is a commonly used lentiviral vector pseudotype [288]; it binds to receptors of the LDL-receptor family. As the LDL receptor is found in a vast array of cell types, using it expands lentiviral tropism [213]. Transduction efficiency using lentiviral vectors can be low [131]. However, it can be improved when using cationic polymers, such as polybrene [126].

There are three generations of lentiviral vectors [4]. The second and third generations are commonly used for viral vector production in the lab. For clinical applications, the third-generation is primarily used (Figure.1.5). The third-generation is the safest lentiviral vector as a SIN viral vector is used and production is performed using four vectors (less

chance of recombination events leading to replication-competent viruses) [241, 124]. Both second and third generations utilize a synthetic promoter or endogenous human promoter located upstream of the transgene [4]. Producing a second-generation lentiviral vector requires three plasmids: a packaging plasmid, an envelope plasmid, and a transfer plasmid. The packaging plasmid consists of the capsid (*gag*), non-structural enzymatic proteins (*pol*), *rev*, and *tat* gene sequences [213, 4]. The envelope plasmid contains the gene sequence for the envelope protein [213, 4]. The transfer plasmid contains a promoter and transgene of interest flanked between LTRs, which will be the provirus [4]. Third-generation production method utilizes four plasmids: the packaging plasmid, the regulatory plasmid, the envelope plasmid, and the transfer plasmid [85]. The third-generation packaging system separates the second generation packaging plasmid into two plasmids: the packaging plasmid (a plasmid contains *gag* and *pol*) and a regulatory plasmid (a plasmid containing the *rev* gene sequence) [4]. The *tat* gene is absent in this generation [4]. The titer of third-generation lentiviral vectors is generally lower than second-generation lentiviral vectors [106].

Skysona, Zynteglo, and Kymriah are a few cell therapies approved that utilized lentiviral vectors [233, 31, 32]. A lentiviral vector with safer features have been associated with lower viral titers [106]. This could lead to higher production costs as more reagents would be required to produce the required titer.

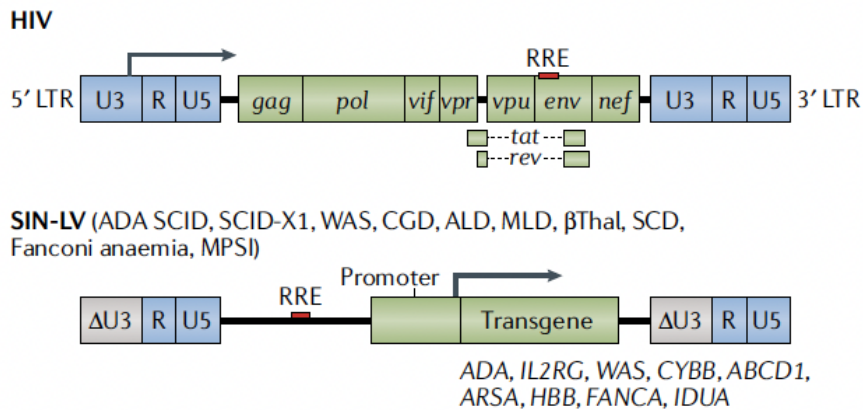


Figure 1.5: Schematic representation of a SIN lentiviral vector provirus. HIV represents a wild-type lentiviral vector genome. SIN-LV depicts the provirus of a SIN lentiviral vector. The image is obtained from [98].

1.4.2 Gene Editing Technologies

While viral vectors semi-randomly integrate into the genome, gene editing technologies edit a specific area of the genome [98]. If there is a disruption in a gene's sequence, gene editing technologies can correct it within its natural cassette [241]. cDNA can be inserted into its natural gene cassette allowing its natural promoter and enhancer sequences to drive its expression. Gene editing technologies can modify, delete, or correct precise areas of the genome [98]. Three of the most common gene editing technologies include CRISPR/Cas9, TALENs, and ZFN [241].



1.4.2.1 CRISPR/Cas9

CRISPR-Cas is an anti-viral mechanism some bacteria species possess [178, 20]. When the genome of an unfamiliar bacteriophage is present inside a bacterium, the CRISPR-Cas machinery scans this bacteriophage genome for areas of high binding affinity. Once it finds a specific sequence (approximately 30 bp), it is replicated and inserted into the CRISPR cassette. CRISPR contains a small piece of various viral genomes that are separated by spacer DNA [20]. This sequence is transcribed and this transcribed mRNA is cut at the spacer junctions, producing small pieces of RNA (crispr RNA (crRNA)) that, in association with the Cas-9 protein and trans-activating crispr RNA (tracrRNA), target and cut the recognized foreign DNA [20, 82].² When a bacterium is infected with the same bacteriophage, the respective crRNA/tracrRNA/Cas-9 complex adheres to the foreign sequence and clips it [178, 20]. CRISPR is essentially a bacteria's immune system.

This system has been revolutionized for gene therapy applications and is called CRISPR/Cas9. CRISPR/Cas9 was discovered in 2012 [150]. It consists of two main parts: a single guide RNA (gRNA) and Cas-9 protein (Figure.1.6) [82]. The same concept used for bacterial immunity—targeted DNA cutting—also applies to classical CRISPR/Cas9 gene therapy applications. The gRNA is essentially a crRNA and tracrRNA combined by a tetraloop [150, 284]. The gRNA specifies the target site and forms a stem loop structure that interacts with the Cas-9 protein [150]. This gRNA Cas-9 complex targets the area of the genome it recognizes and forms a double-stranded break there [150]. This creates room for DNA to be inserted via homologous-directed repair (HDR) (corrections) or an opportunity for the gene to be deactivated via non-homologous end-joining (NHEJ) (disruptions or deletions) [241, 98]. The cassette DNA is delivered to the host, and the transgene, which is flanked by homologous DNA sequences of the host's genomic cut site, inserts between the cut fragments via HDR [263, 78, 71]. The gene editing corrections are dependent on DNA repair pathways utilizing HDR, specifically homologous recombination (HR), which competes with NHEJ; this can ultimately affect the gene editing efficiency [219]. The S phase has been shown to stimulate HR repair [241]. Therefore, methods that push cells into the S phase have been implemented during genetic modification [241].

Off-target cleavage (Indels) using CRISPR/Cas9 do commonly occur. It has been reported that CRISPR/Cas9 can tolerate up to five mismatched base pairs for an off-target cleavage to occur [284, 104]. Various modifications to the CRISPR/Cas9 system have been performed to improve its accuracy and efficiency, such as using Cas-9 variants (some from other bacterial strains and others with synthetic alterations) or configurations to the gRNA [284, 81, 179]. This has been shown to increase the number of available PAMs, and improve target site specificity [179, 253]. *In situ* screenings have been developed, and help researchers determine appropriate PAMs and potential off-target cleave sites, so suitable modifications can be made to their system to reduce off-target effects [253].

Prime editing is a system recently developed that mediates targeted insertions, deletions, and base-to-base conversions without creating double-stranded breaks, nor needing donor DNA [12]. It's composed of a catalytically impaired Cas9 protein that is fused to an engineered

²S. pyogenes Cas9 Biology of the type II-A CRISPR-Cas system.



reverse transcriptase, and a prime editing guide RNA (pegRNA) [13]. A pegRNA specifies the target site and encodes the anticipated edit [13]. It has been reported that all 12 base edit conversions can be made using prime editing [13]. Prime editing has also displayed fewer by-products related to HDR and significantly lower off-target edits relative to CRISPR/Cas9 [13].

Base editing consists of a catalytically impaired Cas nuclease fused to a nucleobase deaminase enzyme (enzyme that functions on ssDNA) and, periodically, a DNA glycosylase [264]. Base editing is similar to prime editing as it does not require double-stranded breaks, nor donor DNA. However, only the four transition mutations are possible with base editing: C→T, G→A, A→G, and T→C [13].

Currently, there are no approved gene and/or cell therapies utilizing CRISPR/Cas9 [313, 247]. The clinical usage of CRISPR/Cas9 is heavily being investigated, and there are numerous clinical trials underway using this genetic modification system. Applications include T-cell immunotherapies [143, 334, 55] and hematopoietic stem cell (HSC) monogenic cell therapies [328, 325, 29]. Preclinical studies have shown that CRISPR/Cas9 or ZFN could be used to genetically correct SCID-X1 [278, 248]. A current limitation of CRISPR/Cas9, and genetic modification technologies in general, is off-target effects. Though, on-target accuracy is improving, and off-target edits are reported to be lower using CRISPR/Cas9 relative to other gene editing technologies, such as TALENs and ZFNs [74].

1.4.2.2 TALENs and ZFNs

ZFNs were discovered in 1985 by Miller, McLachlan, and Klug [201]. There are various types of zinc fingers, but a classical ZFN consists of a protein complex chelated to a zinc ion [244]. Each ZFN generally recognizes three nucleic acids (an amino acid code) [244]. For gene editing, a ZFN chain is created by combining ZFNs [244]. At one end of the ZFN chain, a nonspecific FOKI nuclease is present [244]. If two ZFN chains are designed appropriately, the FOKI enzyme will heterodimerize and cleave the DNA precisely within the spacer DNA (Figure.1.6) [244]. If gene correction is desired, template DNA can be delivered to the cell, similar to CRISPR/Cas9, and inserted between the cut site via HDR [98]. When there is a lack of template DNA present, the cut site will classically repair via NHEJ, and renders the gene inactive [98]. Many off-targets have been reported when using ZFNs [74]. TALENs, a system also based on FOKI, are reported to have less off-target edits relative to ZFNs [74]. ZFNs are also reported to be more difficult to design, produce, and validate relative to TALENs [82].

TALEN proteins were first reported in 2009 by Jens Boch [34, 25]. TALENs are composed of a chain of DNA-binding domains (Figure.1.6) [152]. These DNA-binding domains are derived from transcription activator like effectors (TALEs), which are proteins secreted by the bacteria *Xanthomonas* [152]. Each DNA-binding domain is specific for one nucleic acid, which makes TALENs more adaptable to design relative to ZFNs [82, 33]. On one end of the TALEN, a nonspecific FOKI nuclease domain is present [152]. When TALENs are designed appropriately, FOKI will dimerize and form a cut within the spacer sequence between the two TALEN monomers (Figure.1.6) [152].

ZFNs designed to disrupt the gene sequence for the chemokine receptor 5 (CCR5)—a co-receptor for HIV-1—have entered phase one and two clinical trials for the treatment of HIV/AIDS [152, 249, 318, 276]. Additionally, Collectis S.A has submitted clinical trials for T-cell immunotherapies utilizing TALENs [59, 58, 57]. Engineered nucleases face three main challenges for their clinical approval: gene-editing efficiency, gene editing accuracy, and their delivery [7].

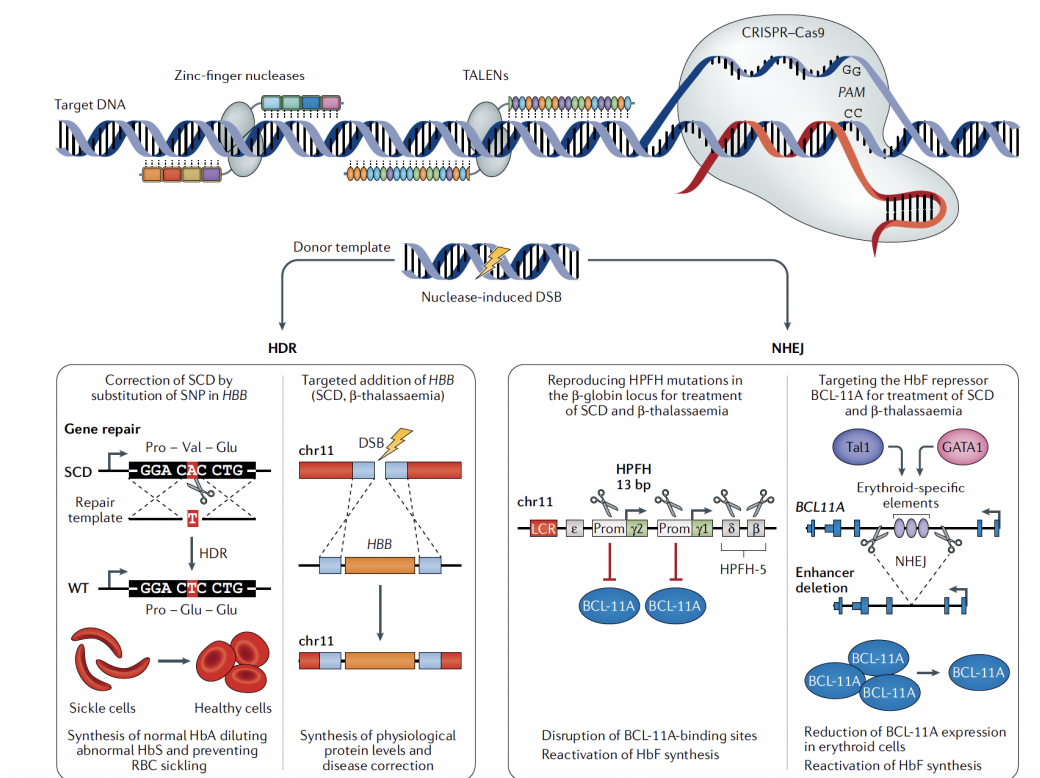


Figure 1.6: Classic gene-editing systems mechanism of action. When using genome editing systems, such as ZFNs, TALENs, and CRISPR/Cas9, genomic DNA can be altered by introducing foreign DNA via HDR or knocking out a gene via NHEJ. A single nucleotide or a DNA fragment can be inserted via HDR to treat a patient. A gene can be knocked-out to create disease models or to treat a patient. The image is obtained from [98].

1.4.3 Transposons

Barbara McClintock discovered transposable elements and was recognized for this discovery with the 1983 Nobel Prize in Physiology or Medicine [19]. A transposon system, used for gene and cell therapy, consists of transposase enzymes and a gene of interest flanked by terminal inverted repeats (TIRs) (Figure.1.7) [158]. The genetic sequence for the transposase enzyme is incorporated into a plasmid that is delivered to the cell along with a plasmid containing the gene of interest flanked by TIRs [158]. Once in the nucleus, transposase enzymes are transcribed and translated. These produced enzymes excise the gene of interest at the TIRs and this sequence is incorporated into the genome at compatible loci [158]. Transposons can jump between different sites [193]. PiggyBac transposons are reported to be remobilized by the human PGD5 transposase; this increases their genotoxic risk [158, 135]. The most

common transposon is derived from ancestral salmon DNA; it is called sleeping beauty (SB) [146]. SB transposons have a lower genotoxic risk relative to other transposon systems as they cannot remobilize human transposons, and no human protein has been reported to remobilize DNA inserted by SB transposons [158]. SB transposons display lower variations in their integration site profile relative to integrating viral vectors [113]. Researchers also aim to further improve SB integration specificity [166]. SB transposons have a lower production cost as plasmids are commonly only required [158]. A disadvantage of SB transposons is that directed integration is not possible, such as with gene editing tools. Additionally, the human genome may contain sequences similar to SB TIRs that SB transposases could associate with, which may result in unwanted genomic manipulations [110]. Delivering SB transposases already bound to the gene of interest flanked by TIRs could reduce this risk [110].

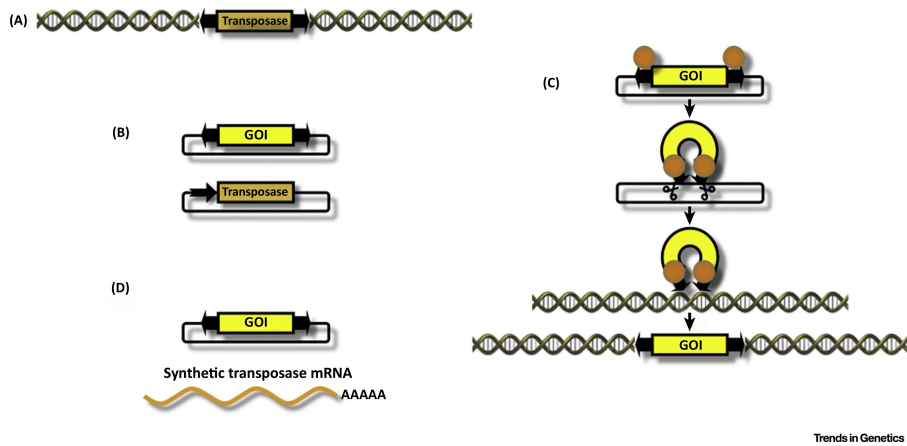


Figure 1.7: The mode of action of a transposon. A) The sequence for transposase elements are found in the genome of living creatures. B) Transposase and DNA flanked by TIRs can be used to genetically modify genomic DNA. This system is called a transposon. C) A gene of interest is inserted into genomic DNA at specific sites by the transposase proteins. D) The transposase can be inserted into the host as mRNA or template DNA (Figure.1.7A) that is transcribed into mRNA, and subsequently translated into protein. The image is obtained from [158].

1.4.4 S/MAR DNA Vectors

The usage of plasmids for gene therapy was proposed in the 1990s [171]. They have a minimal risk of integration into the genome. Though, plasmids have been used sparsely due to their short half-life, particularly in dividing cells [171].

DNA vectors containing an S/MAR may be an alternative option to other gene-modifying technologies. They are circular pieces of DNA that are retained episomally in a cell, and have persistent transgene expression (similar to a genome integration technology) due to a special sequence of DNA present in the vector: the S/MAR [18, 147]. S/MAR DNA elements are found in mammalian origins of replication; they anchor the genome to the nuclear matrix, promote replication, and regulate gene expression [207, 65, 80]. Vectors containing S/MAR DNA elements are indicated to associate with the nuclear matrix in regions near genome attachment sites and replicate due to an association with subunits of an origin of replication complex (Figure.1.8) [148, 18, 147, 277]. Episomal vectors containing the S/MAR region

associated with the human *IFN β* gene show mitotic stability in various cell types [127, 122], including mouse HSPCs [324]. The first reported S/MAR vector, pEPI vector, was indicated to stably express its transgene (GFP) and be mitotically stable without selection [122]. However, it contains numerous CpG motifs [122], and further research indicates poor establishment efficiency with and without selection [37, 266]. Scientists have modified S/MAR-based vectors since, creating more sophisticated vectors.

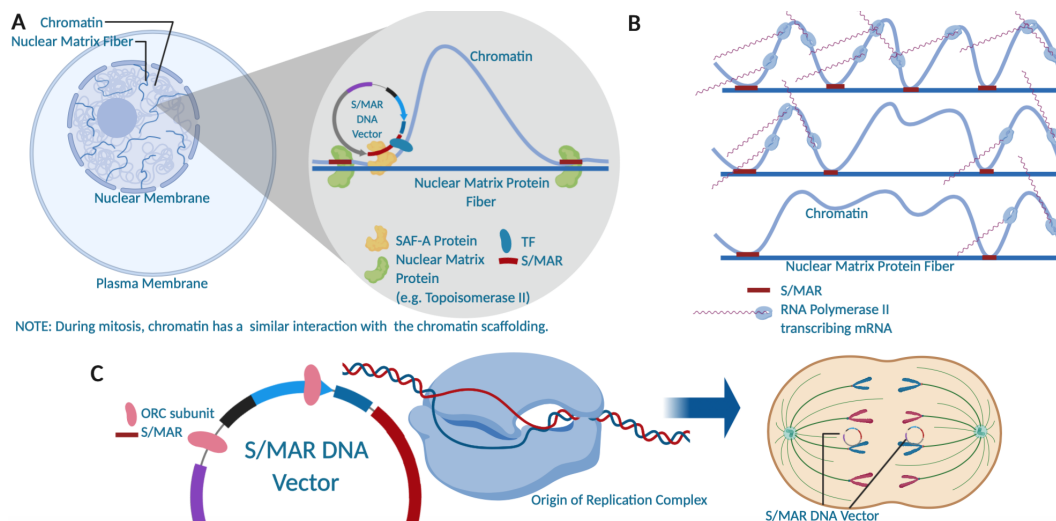


Figure 1.8: Schematic representation of how S/MAR DNA vectors work. A) Model displaying S/MAR vector's association to the chromatin and nuclear matrix through interactions with transcription factors and the SAF-A protein [148, 18, 147]. B) Model displaying active transcription in areas of the genome where S/MAR regions are associated with the nuclear scaffold C) Proposed model of how S/MAR vectors replicate in *Saccharomyces cerevisiae*. Subunits a part of the origin of replication complex (ORC), such as Orc2p and Mcm2p, associate with S/MAR vectors before S-Phase, and S/MAR DNA vectors replicate at the same rate as the cellular genome [277].

Our lab continues to modify S/MAR-based vectors in an effort to improve transfection efficiency, establishment, and transgene expression in various cell types (Figure.1.9). In pEPI, Kanamycin/G418 acts as the bacteria backbone with an adjunctive eukaryotic selection marker (neomycin) [127]. Colleagues have substituted this feature for a classic kanamycin bacterial backbone and placed a eukaryotic selection marker, puromycin, following the transgene [37]. This minimized the size of the bacterial backbone and provided more consistent maintenance of transgene expression as the selection marker was present near the transgene rather than the bacterial backbone, which is a feature prone to silencing. By doing this, our lab was able to improve the efficiency of vector establishment [36]. As methylation—silencing—of bacterial backbones is common in eukaryotic cells, an insulator was placed in front of the promoter to protect the features located between it and the S/MAR, which also acts as an insulator, from methylation [37]. Colleagues from my lab further reduced the size of the bacterial backbone by replacing the kanamycin bacterial backbone (1725 bp) with a nano-sized bacteria backbone called NTXTM RNA-out (458 bp) [37]. NTXTM RNA-out lacks immunogenic CpG regions. Cells modified with S/MAR vectors containing NTX RNA-out have fewer differentially expressed genes relative to cells modified with S/MAR vectors containing a kanamycin bacterial backbone [267]. Colleagues from my



lab substituted the original S/MAR, that was derived from the IFN β gene region for an S/MAR sequence from the apolipoprotein gene cluster (APOL) gene region, which decreased the vector's size [37]. Lab members also show improved establishment efficiency and transfection efficiency in T-cells using this vector [36]. Additionally, colleagues have flanked the S/MAR fragment with splice site signals and this improved establishment efficiency, transfection efficiency, and increased expression of the transgene protein [37].

As these vectors have evolved, our lab has differentiated S/MAR modified mouse and human ESCs and iPSCs into various cell types while still maintaining the vector [266]. Additionally, they have demonstrated that a pancreatic cancer cell line (BX2C-3) could be genetically modified using S/MAR DNA vectors and transgene expression persisted in the line after it was engrafted into SCID mice [38]. Our lab is continuously improving S/MAR DNA vectors and aims to use them for various biological applications.

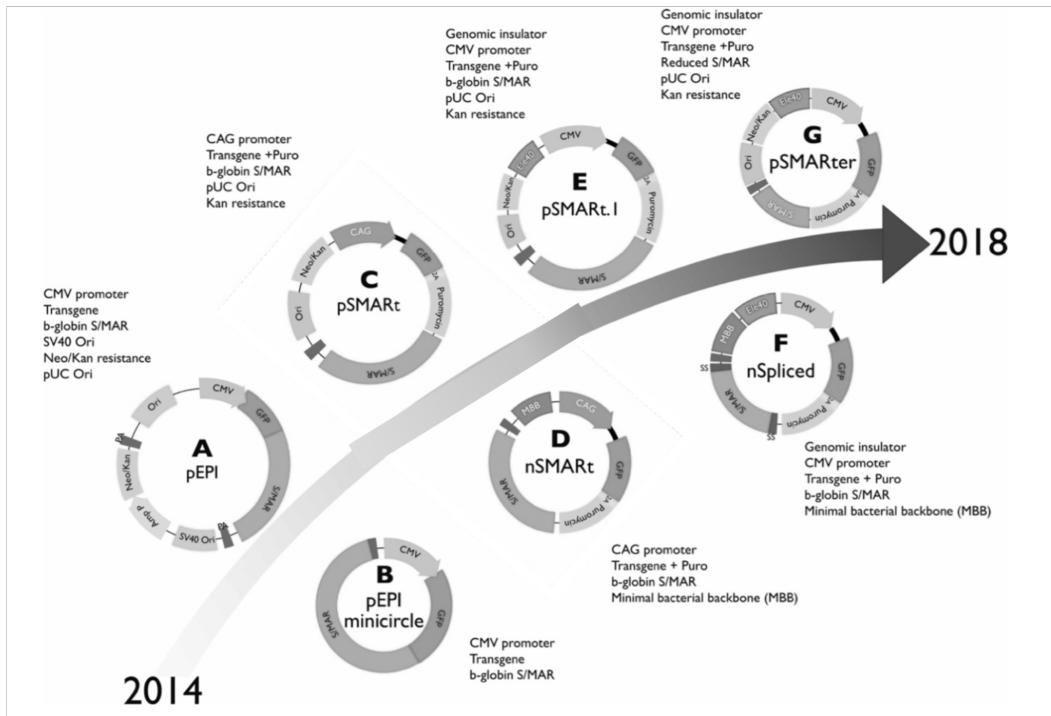


Figure 1.9: The evolution of our lab's S/MAR DNA vectors. nSpliced was developed through modifications to the bacterial backbone, selection marker, and S/MAR sequence of pEPI. Additionally, an insulator was incorporated. The image is obtained from [266].



Chapter 2

My Project's Vision

2.1 The Plan

I propose that a novel T-cell immunotherapy can be created by genetically modifying urinary-derived iPSCs (U-iPSC) using S/MAR DNA vectors, and differentiating them into T-cells. The aim is to create an iPSC-derived T-cell expressing a CAR or TCR. Before T-cell differentiation, iPSCs must first differentiate into HSPCs. This report is primarily focused on that step.

Our lab has shown that urinary-derived cells can be reprogrammed into iPSCs [319]. As urinary-derived cells are collected non-invasively, this could lead to a wider variety of banked HLA types due to increased donor participation. The benefits of an iPSC-derived T-cell over a classic T-cell immunotherapy are highlighted in the following sections (section 2.2). The proposed steps to create an U-iPSC-derived T-cell immunotherapy (proof of concept) are highlighted in Figure.2.1.

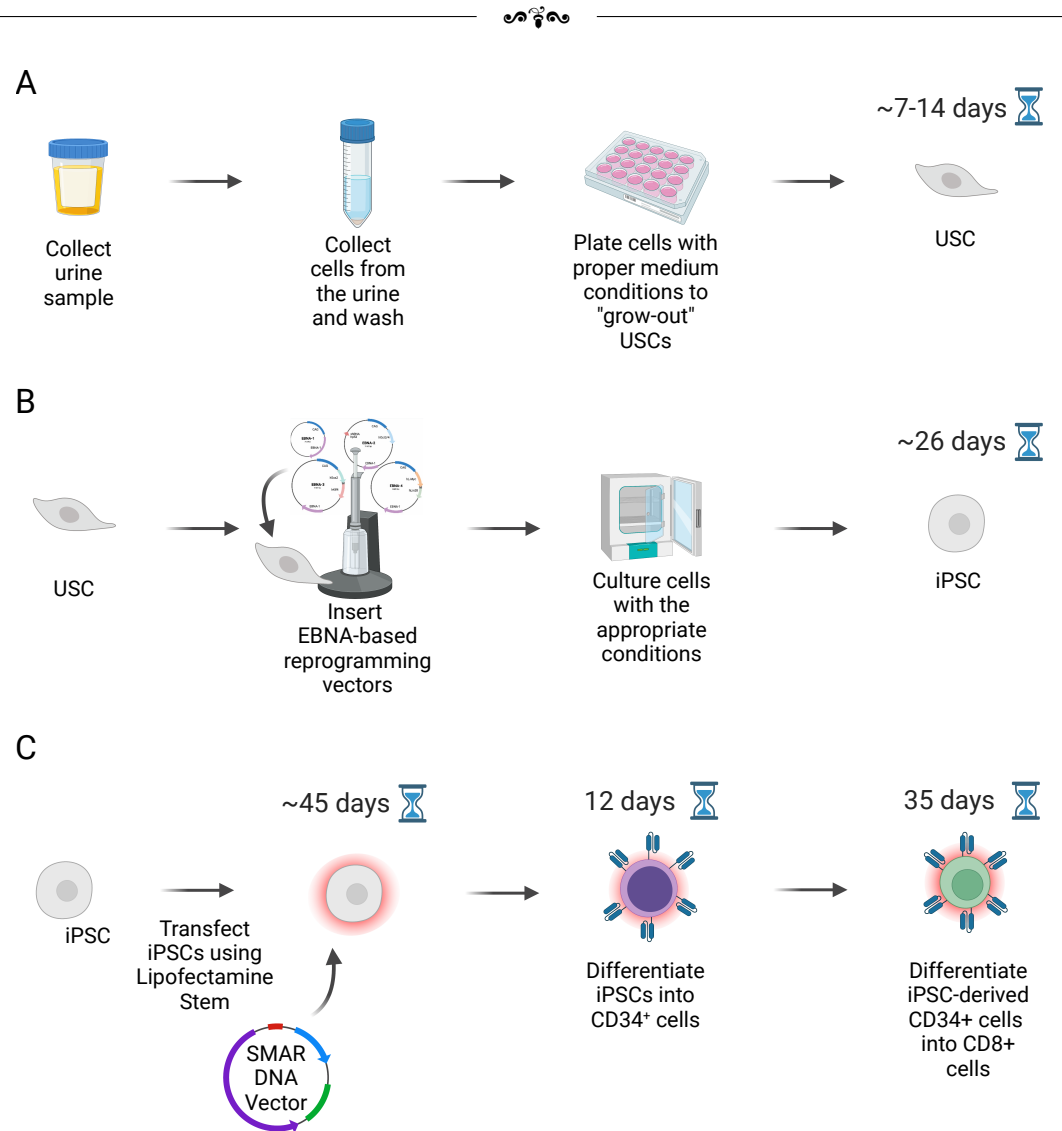


Figure 2.1: Steps to create an U-iPSC-derived T-cell immunotherapy. A) Cells are collected from donor urine samples, and the urinary stem cells (USCs) are expanded. B) EBNA-based reprogramming vectors are then inserted into the USCs, leading to the development of iPSCs. C) The generated U-iPSCs are transfected with S/MAR DNA vectors. Then, they are differentiated into CD34⁺ cells, and subsequently into T-cells.

2.2 The Benefits of an Allogeneic iPSC-Derived T-Cell Immunotherapy

2.2.1 Predicted to Reduce Costs of Cell Therapy

The accumulation of high expenses in drug development, high expenses in manufacturing, and small markets have led to an evolving problem with the price of gene and cell therapies [7]. As gene and cell therapy is considered a one-time treatment, pharmaceutical companies lack the opportunity to lower the product's price and recover costs from a consistent stream of revenue, eventually making a profit [155]. EMA-approved cell and gene therapies in 2021



ranged from 28,000€ per year to 1,575,000€ flat-cost (Table.2.1¹) [180]. This range exceeds the price of many alternative state-of-the-art therapies [241], and is likely to impede gene and cell therapy access to non-affluent patients and impoverished patients in nations that might greatly benefit from such therapies—sickle cell anemia occurs mainly in African populations [7]. Nevertheless, in 2012, investors' interest in gene and cell therapies emerged; venture capital companies supported gene and cell therapy start-ups [155]. Some pharmaceutical companies had acquired gene and cell therapy companies [155]. The return on investment for certain gene and cell therapies has been minimal, and has required some companies to reevaluate these departments. In 2018, GSK reviewed its rare diseases unit to improve returns within its business [138]. This resulted in GSK selling its rare disease portfolio to Orchard therapeutics [119]. Stimvelis was included in that portfolio, a gene and cell therapy priced at 594,000€ in 2018 [241, 138]. This therapy was used to treat 16 patients since its approval in 2016 [119]. Another example is Glybera™. It was marketed at 1,000,000\$ in 2015 within the EU [210] and was used to treat one patient in 2016 [155]. In 2017, UniQure decide to discontinue its market authorization [155]. By reducing the cost and increasing the output of gene and cell therapies, its economic value is predicted to rebalance, resulting in more production and consumption [171].

Table 2.1: Cost of approved gene and cell therapies in 2017 [241].

Name (Brand Name)	Vendor	Indication	Approval Region	Price (k€)
Onasemnogene abeparvovec (ZOLGENSMA®)	Novartis	Spinal muscular atrophy	2019 (USA)	2.125
Betibeglogene autotemcel (ZYNTEGLO®)	bluebird bio	Transfusion dependent b-thalassemia	2019 (EU)	1.575
Voretigene neparvovec (LUXTURN A®)	Spark Therapeutics	Leber's congenital amaurosis	2017 (USA)	850
Alipogene tiparvovec (GLYBERA®)	UniQure	Lipoprotein lipase deficiency	2012 (EU*)	1.000
STRIMVELIS®	Orchard Therapeutics	ADA-SCID	2016 (EU)	594
Tisagenlecleucel (KYMRIAH®)	Novartis	B acute lymphoblastic leukemia	2017 (USA)	475
Axicabtagene ciloleucel (YESCARTA®)	Kite Pharma	Type of non-Hodgkin lymphoma	2017 (USA)	373
Talimogene laherparepvec (IMLYGIC®)	Amgen Inc	Melanoma	2015 (USA and EU)	65

Various governments have considered solutions to support patients with the cost of gene and cell therapies. Some states contemplated implementing a subscription, in which governments pay a fee to pharmaceutical manufacturers who provide patients unlimited access to gene and

¹k€: thousands of euros



cell therapy for a set period [7]. Another idea is performance-based risk-sharing arrangements (PBRsAs), in which the full cost of the therapy is charged within the contract, but refunds are earned if agreed-upon therapeutic targets are not reached for the treated patient [7, 155]. PBRsAs have been and are being used for Luxturna (Spark Therapeutics) and Zolgensma (Novartis) [7]. Current payment strategies may not be sustainable with the increasing presence of gene and cell therapies in the market [7]. Additionally, “pay for outcome” strategies have been shown to not entice greater usage of gene and cell therapies, such as Strimvelis [155]. Thus, it is important for all parties involved—payers, manufacturers and key stakeholders—to explore new approaches [125]. Finding new ways to reduce the cost, provide coverage, or create stable medical insurance structures for gene and cell therapies is crucial for creating an affordable sustainable framework for patients and pharmaceutical companies [155, 125].

One part of the solution could also be reducing gene and cell therapy’s personalization. It is predicted that this would lead to a reduction in the cost of goods (COG) (Figure.2.3) [129]. Allogeneic products, such as an off-the-shelf allogeneic iPSC-derived T-cell immunotherapy could reduce the personalization of T-cell immunotherapies as it’s a product that would be produced in mass, aliquoted, and used by numerous patients (Figure.2.2). Personalization would still be present to a degree that allows the selection of an appropriate HLA donor and an appropriate CAR or TCR. Though, it would be greatly reduced, and subsequently would be predicted to reduce COG.

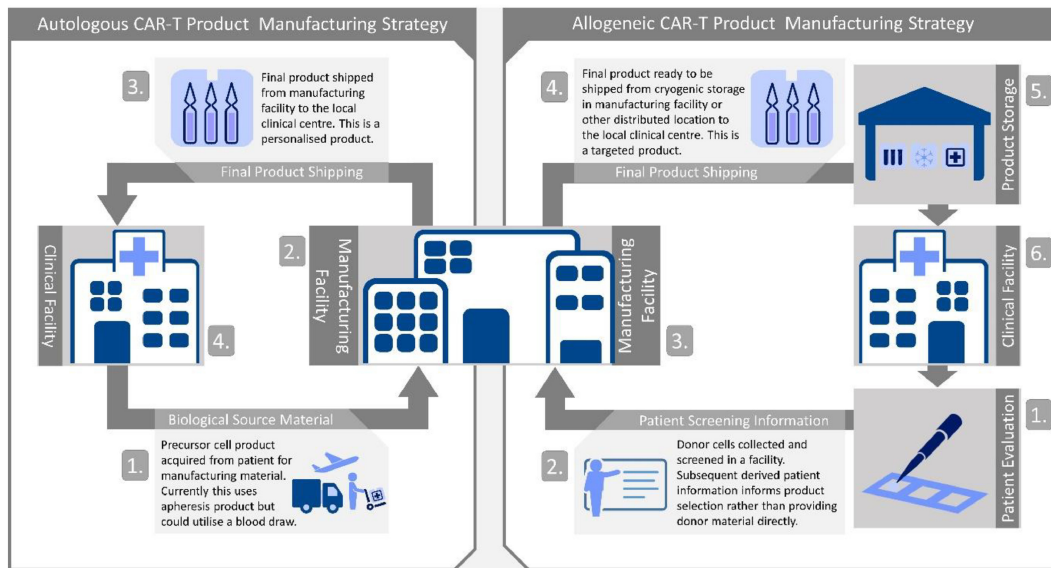


Figure 2.2: The process of manufacturing and distributing autologous and allogeneic T-cell immunotherapy. The left figure depicts the process of manufacturing a classic autologous T-cell immunotherapy. The right depicts the process of manufacturing and distributing an allogeneic T-cell immunotherapy. The image is obtained from [129].

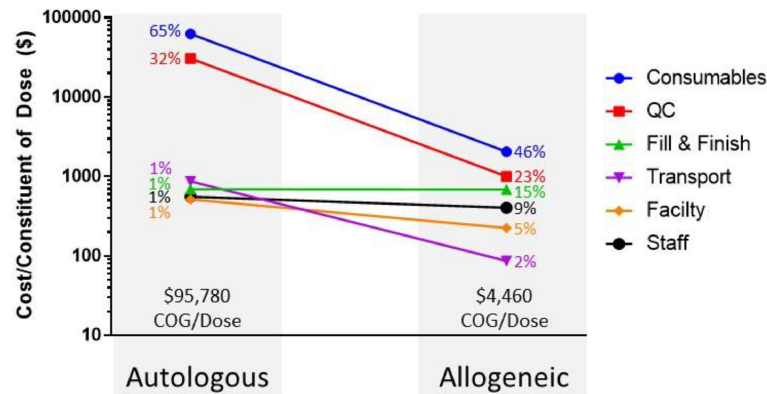


Figure 2.3: Comparing the COG for autologous and allogeneic cell therapies. The average COG per dose of a cell therapy is predicted to drop from 95,780\$ to 4,460\$ when comparing an autologous cell therapy to an allogeneic cell therapy, respectively. The image is obtained from [129].

2.2.2 An Off-The-Shelf Therapy for Patients

2.2.2.1 HLA Homozygous iPSC Banks

The HLA complex is a set of proteins that produce human MHCs [73, 97]. These complexes are expressed on the surface of a cell and play an important role in the immune system [97]. The immune system uses MHCs to determine if a cell is endogenous [97]. If a patient is given an organ transplant and HLA types are 0% matched, host and donor immune cells will recognize this and attack as a protection mechanism. This is called host vs. graft disease (HvGD) and graft vs. host disease (GvHD) [97].

One benefit of current autologous T-cell therapies is that HvGD and GvHD are negligible issues as the patient's cells are utilized. There are at least 2,158 HLA haplotypes reported within the global population [115]. Due to the large selection of HLA haplotypes and the inability of publicly donated organs to meet it, it is often difficult for patients requiring an allogeneic therapy to find a fully matched HLA donor [111]. Half-matched donors have been approved for various transplantations [111], and it has been reported that matching HLA-A, -B, and -DR is most important and reduces the risk of allograft rejection [168, 308, 235]. The personalization of autologous T-cell therapies is beneficial to prevent such adverse effects (HvGD and GvHD). However, it has resulted in unaffordable treatment costs, as discussed in section 2.2.1. Finding a balance is imperative.

With this project, I propose to create iPSC-derived T-cells using an HLA homozygous iPSC bank. A cell with a homozygous HLA haplotype contains fewer HLA isoforms relative to a heterozygous HLA haplotype. Thus, they match with a larger set of patients. It's reported that 10 ESC lines composed of homozygous haplotypes could provide at least an HLA-A, -B, and -DR match for 38% of the UK population [307]. It has also been estimated that 50 HLA homozygous donors could be used as HLA-matched donors for 90.3% of the Japanese population—based on the 24,000 individuals representing the Japanese population in this study [217]. Since iPSCs can be extensively expanded, such banks would be considered sustainable [169]. It's reported that more systems for the storage and manufacturing of cell

banks will be created [171]. California's stem cell agency is creating an iPSC repository from thousands of patients [52]. The non-profit European Bank for induced Pluripotent Stem Cells (EBiSC) has centralized 895 iPSC lines that are available to researchers [101]. The Center for International Blood and Marrow Transplant Research has attempted to create an iPSC bank that largely represents the HLA haplotypes of the US population [60]. Unfortunately, only 19 participants were recruited, and this study was terminated due to slow accrual [60]. Though, it shows the growing interest in such banks.

HLA homozygous iPSC lines could be genetically modified to express a TCR or CAR, then differentiated into T-cells that are aliquoted and cryopreserved. These aliquots could serve as a quick off-the-shelf therapy for patients. As cells are generated in bulk and produced from a set of donors, and used to treat numerous patients, the COG is predicted to drop (see section 2.2.1).

2.2.2.2 Mass Production

Another benefit of using iPSC-derived T-cells over a classic T-cell immunotherapy is the mass number of cells that can be generated. This is especially beneficial for pediatric patients, in which adequate cell counts are commonly unattainable for cell therapy [77].

2.2.3 Derived From a Healthier Cell

Sometimes with autologous cell therapies, a suboptimal quantity and/or quality of cells is collected [275]. This is commonly the case for patients with sickle cell disease, in which HSPCs mobilize poorly [241]. The usage of granulocyte colony-stimulating factor (G-CSF) for mobilization is not recommended in such patients [241]. Another example is the treatment of cancer patients with autologous T-cell immunotherapy. Variations in cell quality and quantity are common between patients [275]. iPSC-derived cells from healthy donors could provide a more consistent and reliable cell source.

The genetic modification of cells is associated with various genotoxic risks (see section 1.4.1). Genomic safe harbors have been defined, and cell therapies with provirus integration into these sites are suggested to be safer [114]. By using iPSCs, particular clones that fulfill these requirements could be selected, expanded, and utilized [243].

2.2.4 Standardized Therapy That Could Follow a Centralized Model

There are two models proposed for the manufacturing of gene and cell therapies: the centralized and decentralized model [241]. The centralized model has the patient's cells locally collected, then shipped to a centralized facility where genetic modification takes place. These genetically modified cells are cryopreserved and shipped back to the original destination [241]. Following a centralized model better guarantees a product is created in a controlled and standardized manner. A centralized model has widely been used for gene and cell therapies. It is associated with high manufacturing costs related to supplemental materials, labor, and transportation/logistics [130]. This model is intended for therapies with an extended shelf life and a low degree of personalization [241, 292], which does not fit the



classic definition of autologous cell therapy. The decentralized model has the whole manufacturing process occur at the local destination, where the patient's cells are collected [241]. A decentralized model provides greater flexibility to a patient's needs [241], and removes costs associated with transportation/logistics to a centralized facility. Following a centralized model, transportation is 1% of the total production costs of an autologous T-cell therapy, which is quite minimal (Figure.2.3) [129]. So, the biggest benefit gene and cell therapies get by shifting to a decentralized model is the flexibility that it provides to personalized cell therapies, which is highly desirable [241, 130]. A difficulty with the decentralized model is the ability to create a standardized product in a decentralized manner as well as the complexity of therapy reimbursement as the ownership is dispersed [241, 130]. A decentralized model would most likely require an additional set of skilled employees [241], and may rely on a model similar to franchise operations [130]. This could lead to higher costs for drug production; the business model, risks, and costs would have to be compared. The decentralized model fits well with current gene and cell therapies because of their high degree of personalization. By un-personalizing gene and cell therapies, the centralized model could more easily be followed, which is a model comfortable and familiar to regulatory agencies, policy makers and stakeholders [241]. Reducing cell therapy personalization is possible using iPSCs, as described in the above sections.

2.3 The Benefits of Using S/MAR DNA Vectors

There is a safety concern when using genome-integrating technologies (section 1.4). S/MAR DNA vectors persist episomally—they do not integrate into the genome [36], which may appease classic safety concerns. S/MAR DNA vector-modified cells and non-modified cells have a closer relationship in mRNA expression relative to lentiviral vector-modified cells, which suggests less alterations to cell functionality when using them [36]. Antibody neutralization, which is common when using certain viral vectors [155], is a minimal concern when using plasmids. Many technologies are limited by their packaging size. This is not the case for S/MAR DNA vectors, which essentially have unlimited capacity. Non-viral vectors may solve manufacturing shortfalls associated with viral vectors [155]. S/MAR DNA vectors have low production costs as plasmids are only required (Figure.2.4). Scalability of upstream processes related to viral vector production is necessary to lower its production costs [54].

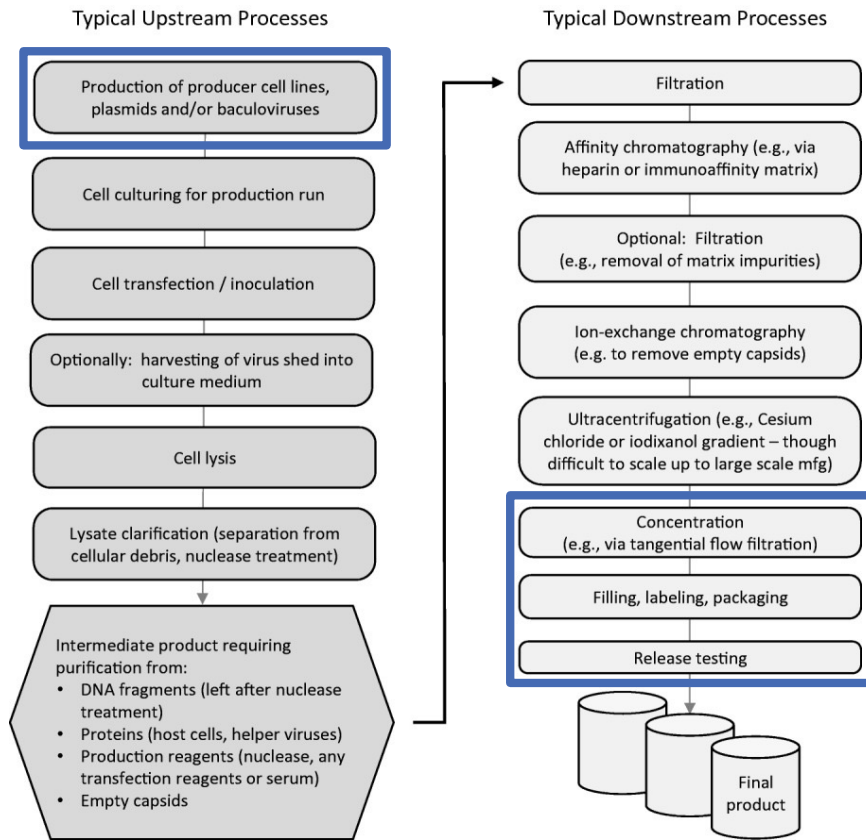


Figure 2.4: Description of the manufacturing process of an AAV vector. This figure summarizes the required steps to produce an AAV. The purple boxes indicate the steps required to produce an S/MAR DNA vector. S/MAR DNA vectors are quicker and cheaper to produce relative to viral vectors in general. It should be noted that vector purification and quality control of S/MAR DNA vectors are also required. The image is obtained from [155].



2.4 Project Aims That Were Achieved

I have created a clean S/MAR DNA vector with simple cloning capabilities. It consists of negligible unnecessary DNA sequences and single restriction enzyme cut sites between each vector feature. I have screened vector features in human T-cells and U-iPSCs to determine optimal vector features for creating an iPSC-derived T-cell (Chapter 3). I improved a current HSPC model to screen S/MAR DNA vectors (Chapter 4). I show that S/MAR DNA vector-modified human U-iPSCs can differentiate into HSPCs primed for the myeloid lineage or the lymphoid lineage, and how that compares to lentiviral vector-modified U-iPSCs (Chapter 5). Additionally, I have preliminary data indicating that HSPCs primed for the lymphoid lineage can differentiate into phenotypic T-cells (section 5.5 and Chapter 6).

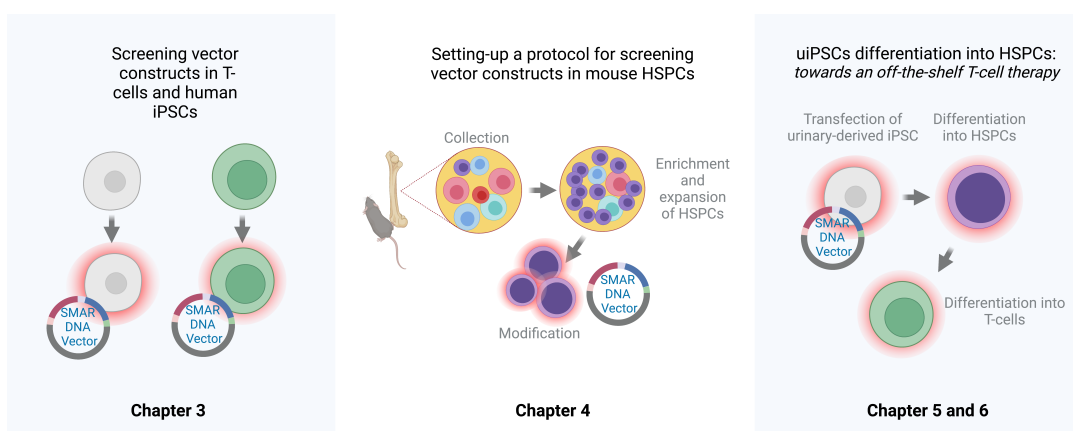


Figure 2.5: A description of this project's aims.

Results



Chapter 3

Vector Features Most Suitable for T-Cell and U-iPSC Genetic Modification

The purpose of this chapter is to find suitable vector features that are least immunogenic for cells, and that provide consistent transgene expression. I assessed vector features within U-iPSCs and T-cells as the aim of this project is to develop an U-iPSC-derived T-cell immunotherapy. Screening vector features in HSPCs would also be useful as an U-iPSC must differentiate into an HSPC before the production of a T-cell. At the time, our lab lacked access to affordable healthy human HSPC samples. Recently, a standardized protocol for the expansion of mouse HSPCs became available. I have made developments towards a model for screening vector features within mouse HSPCs, which is described in chapter 4. This chapter (chapter 3) contains a summary of the features I found to be optimal in human U-iPSCs and T-cells.

Four features of a classic S/MAR DNA vector were assessed: the S/MAR, the promoter, the transgene, and the production backbone (Figure.3.1). An S/MAR DNA vector is circular DNA that persists episomally in human cells. It contains a unique DNA sequence called S/MAR, which associates with cellular scaffolding and hijacks replication proteins, allowing cells to retain these vectors long-term (see section 1.4.4 for a further description of S/MAR DNA vectors) [207, 147, 148, 18, 277]. There are several types of S/MARs. Within these studies, I screened four different versions: S/MAR-1 through S/MAR-4. S/MARs are ranked by length. S/MAR-1 has the longest sequence and S/MAR-4 has the shortest. The S/MAR sequence was shortened, but the functional core AT content/ratio was maintained. S/MAR-1 is derived from the human *IFN β* gene region while S/MAR-2 through S/MAR-4 are derived from the *APOE* gene region. I screened three promoters¹: the CMV early enhancer/chicken β actin (CAG), short elongation factor 1 (sEF1), and sEF1+a chimeric intron (CI). Three transgenes were assessed: dTomato, anti-chimeric carcinoembryonic antigen (CEA) CAR, and anti-MART-1 TCR. Two versions of production backbones were also assessed: a classical ampicillin bacterial backbone and an NTX RNA-out R6K. Vectors that were compared all contained the exact same DNA sequences except for the feature it represented.²

¹The promoter drives the expression of the transgene.

²Slight differences in the DNA sequence were noticed between vectors with different production backbones.

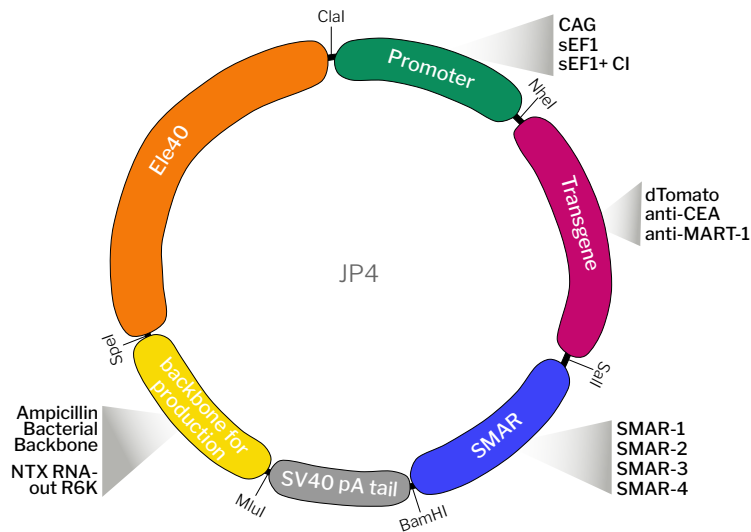


Figure 3.1: Schematic representation of the features screened within human U-iPSCs and T-cells using S/MAR DNA vectors. All vectors contained the insulator element40 (Ele40) and SV40 poly-A tail (poly-A). Three promoters were screened: CAG, sEF1, and sEF1+ a CI. Four S/MARs were compared: S/MAR-1, S/MAR-2, S/MAR-3, and S/MAR-4. Two production backbones were assessed: a classical ampicillin bacterial backbone and the NTX RNA-out R6K developed by Nature Technologies. The transgenes dTomato, anti-CEA CAR, and anti-MART-1 TCR were assessed for their functionality.

3.1 T-Cells and Human U-iPSCs Can Maintain S/MAR DNA Vectors

It's crucial to determine that both human T-cells and U-iPSCs can maintain S/MAR DNA vectors. To get a preliminary indication that this is possible, cells were genetically modified and kept in culture without selection. The percentage of cells maintaining expression during this time frame was then assessed. Data here support that S/MAR DNA vectors can be stably maintained in both human T-cells and human U-iPSCs, and data indicate that cell type (not vector feature) determines the length of time it takes until cells retaining the vector long-term can be identified—culture time for transiently expressing cells to loss transgene expression. Preliminary data suggest it takes 12-28 days for an U-iPSC line to establish our S/MAR DNA vectors. T-cell establishment data indicate that some vector features are more difficult to establish relative to their respective counterparts, also shown in Appendix B.1 Figure.B.1.

This was related to the insertion of the NTX RNA-out R6K backbone. Restriction digest cut sites indicated in Figure.1.1 are based on an S/MAR with an ampicillin bacterial backbone. For vectors containing the NTX production backbone, the cut site between Element40 and the promoter is BspHI, which cuts at the last 10 bp of Element40.



3.1.1 Jurkat76 Can Retain S/MAR DNA Vectors

Data here show that Jurkat76 cells retain S/MAR DNA vectors (Figure.3.2). Vector features alter the percentage of cells retaining the vector long-term. S/MAR-1 and CAG established in the highest percentage of cells, 3% and 1.4% on average respectively. Jurkat76 cells stably retaining vectors appear approximately 24 days post-modification. dTomato+ cells were collected via fluorescence-activated cell sorting (FACS) on days 15, 24, and 33 post-modification and kept in culture for 1 month (Figure.3.3). Cells collected on days 24 and 33 retained transgene expression over this one month while cells collected on day 15 had a significant drop in the percentage of cells retaining transgene expression. These data support that Jurkat76 cells with transient transgene expression are lost between 21- and 24-days post-modification.

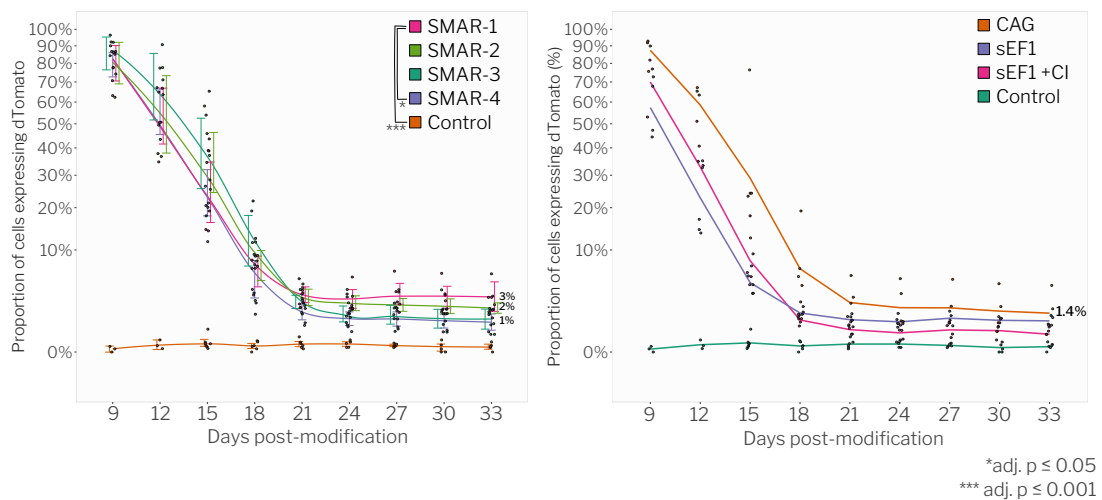


Figure 3.2: Jurkat76 cells retain S/MAR DNA vectors at various percentages that are dependent on vector features. S/MAR-1 and promoter CAG were shown to establish in the highest proportion of cells relative to their respective counterparts. $1(10)^6$ Jurkat76 cells were electroporated using an SE cell line 4D-nucleofector kit (Lonza) with pulse code CL120. Three days post-electroporation, 10,000 alive cells expressing dTomato were sorted into a well of a 96-well plate. The proportion of cells expressing dTomato was then monitored every three days. Data were collected from 5 independent experiments. Error bars represent an 80% confidence interval. Statistical analysis was performed using Tukey one-way ANOVA for data collected on day 33.

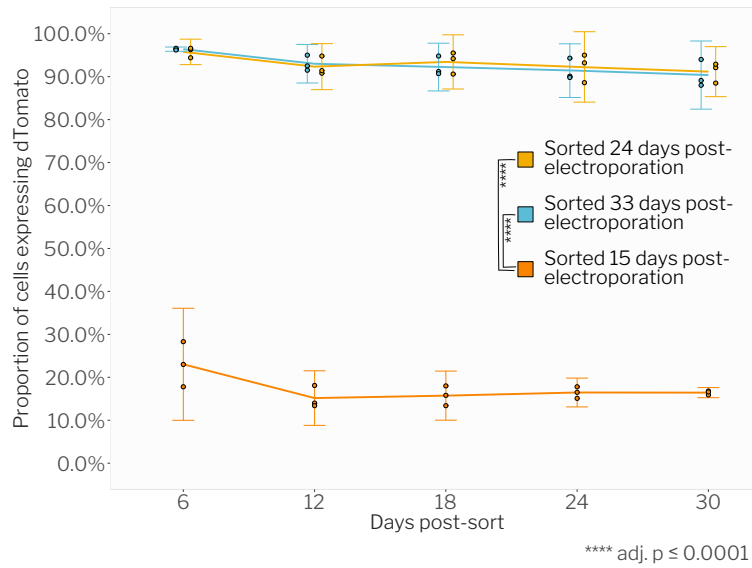


Figure 3.3: Jurkat76 cells expressing dTomato 24 and 33 days post-modification retain transgene expression for 1 month. $1(10)^6$ Jurkat76 cells were electroporated using an SE cell line 4D-nucleofector kit (Lonza) with pulse code CL120. 15, 24, and 33 days post-electroporation, 10,000 alive cells expressing dTomato were sorted into a well of a 96-well plate. The proportion of cells expressing dTomato was then monitored every six days for one month. Data were collected from 3 independent experiments. Error bars represent an 95% confidence interval. Statistical analysis was performed using Tukey one-way ANOVA for data collected on day 30.



3.1.2 Human U-iPSCs Can Retain S/MAR DNA Vectors

Human U-iPSCs can maintain S/MAR DNA vectors long-term, and stably expressing U-iPSC lines appear 12-28 days post-modification [319].

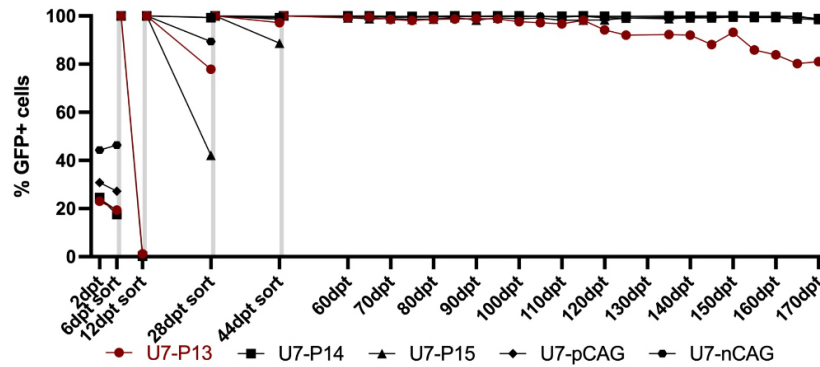


Figure 3.4: Modified U-iPSC lines retain S/MAR DNA vector transgene expression. U-iPSC lines were generated via passive selection. Sortings took place on days 6, 12, 28, and 44 post-modification. The percentage of cells still expressing transgene was monitored for 4 months after the final sort. This image is obtained from Manuela Urban [319].

3.1.3 Section Discussion

From the data obtained in this section, it was determined that S/MAR DNA vectors can be used to produce stable transgene expression in human U-iPSCs and T-cells. Vector establishment rates were quite low, ranging from 0.0002% (Table.3.2) to 3% (Figure.3.2) depending on the cell type and vector used. It is important to assess the episomal status of the S/MAR vector within these modified cells. Attempts to assess this were made with a great degree of difficulty. Thus, these data are absent within this report. Integration analysis is significantly important, and data about it must be collected.

3.2 Screening Transgenes

3.2.1 dTomato Expression is Negligibly Correlated With Cell Viability

I conducted proof of concept studies that require a reporter gene. It's reported that the expression of some fluorescent proteins, such as GFP, makes certain cell types prone to death and can alter the functionality of T-cells [164, 11]. As human iPSCs and primary human T-cells, in general, can be sensitive cell types, I assessed the effects of dTomato expression on cellular viability within human T-cells and U-iPSCs (Figure.3.5 and Figure.3.6). Four S/MAR NTX RNA-out R6K vectors containing dTomato (all with variations at the S/MAR) and three to seven S/MAR bacterial backbone vectors containing dTomato (all with variations at the promoter) were screened. Data indicate negligible correlations between cellular viability and the percentage of dTomato+ cells, as well as between cellular viability and the geometric mean fluorescent intensity (MFI) of dTomato expression in both T-cells and U-iPSCs.

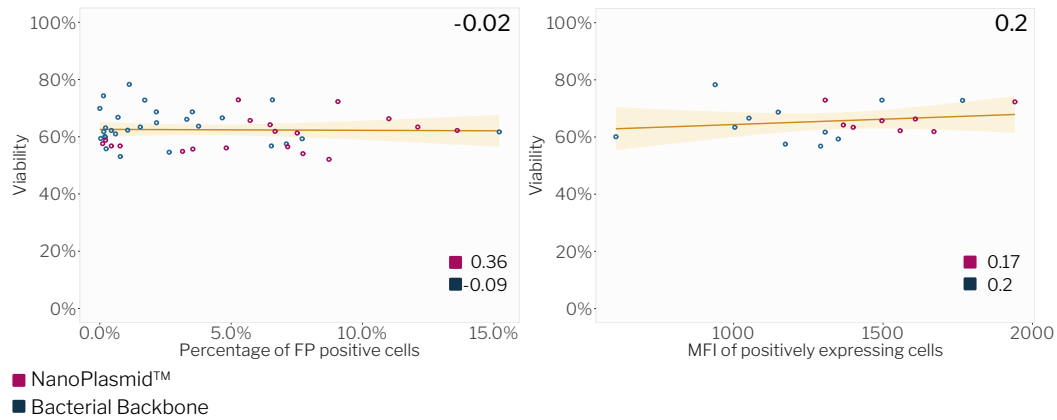


Figure 3.5: Negligible correlation between cell viability and dTomato expression in human primary T-cells is present. CD3 T-cells were enriched from PBMCs using Pan T-Cell Isolation Kit. Three days later $2(10)^6$ cells were electroporated with $2 \mu\text{g}$ of DNA using a P3 primary cell 4D-nucleofector kit (Lonza) with pulse code FI115. 3 days post-modification, 20,000 alive cells expressing dTomato were sorted into the well of a 96-well plate. 6 days post-sort (9 days post-modification), dTomato+ cells and viability were assessed using flow cytometry (graph on the left). The relationship between viability and geometric MFI of dTomato expression in dTomato+ cells is shown in the graph on the right. Correlations were calculated via R using the Pearson method. Data for the figure on the left are derived from ≥ 4 donors, and 2 independent experiments comparing ≤ 11 different vectors. Data for the figure on the right are derived from 2 donors, and 1 independent experiment comparing ≤ 11 different vectors.

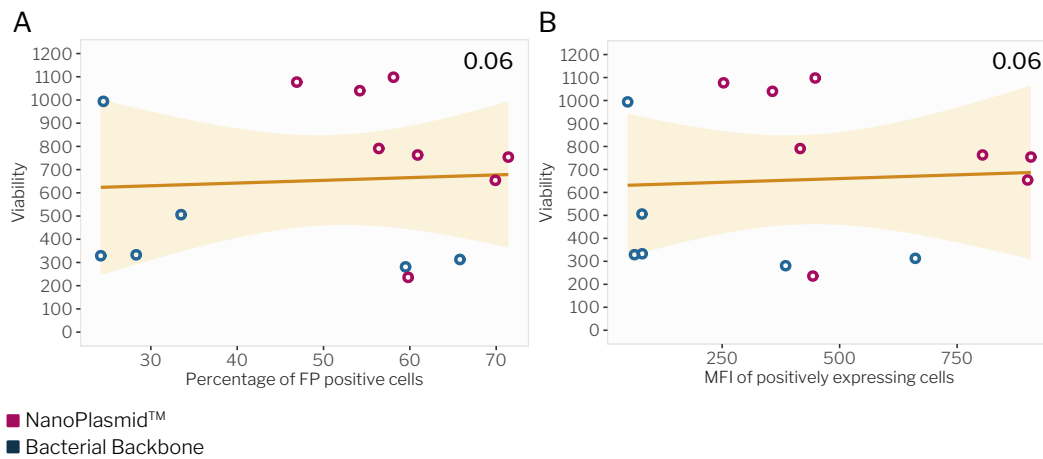


Figure 3.6: Negligible correlation between cell viability and dTomato expression in human U-iPSCs is present. $4(10)^5$ cells were seeded into a 24-well plate. On the following day, 600 ng of DNA was delivered using Lipofectamine Stem. 3 days post-modification, dTomato+ cells and viability were assessed using flow cytometry (graph on the left). The relationship between cell viability and geometric MFI of dTomato expression in dTomato+ cells is shown in the graph on the right. Correlations were calculated via R using the Pearson method. Data were derived from 2 replicates comparing ≤ 7 different vectors.



3.2.2 T-Cells Expressing Anti-CEA CAR and Anti-MART-1 TCR Efficiently Target and Kill Cancer Cells

The final aim of this project is to create an U-iPSC-derived T-cell expressing a CAR or TCR. It was assessed whether anti-CEA CAR or anti-MART-1 TCR within an S/MAR DNA vector provides targeted killing capabilities to primary human T-cells. Data show a significant difference in killing between CAR or TCR-modified T-cells relative to control T-cells, as shown in Figure.3.7. This suggests targeted killing is present when T-cells are modified to express anti-CEA CAR or anti-MART-1 TCR. A significantly higher concentration of interferon ($\text{IFN}\gamma$) was present in the supernatant of samples containing CAR or TCR-modified T-cells, relative to the other control samples. This suggests more activation of CAR and TCR T-cells relative to non-modified cells.

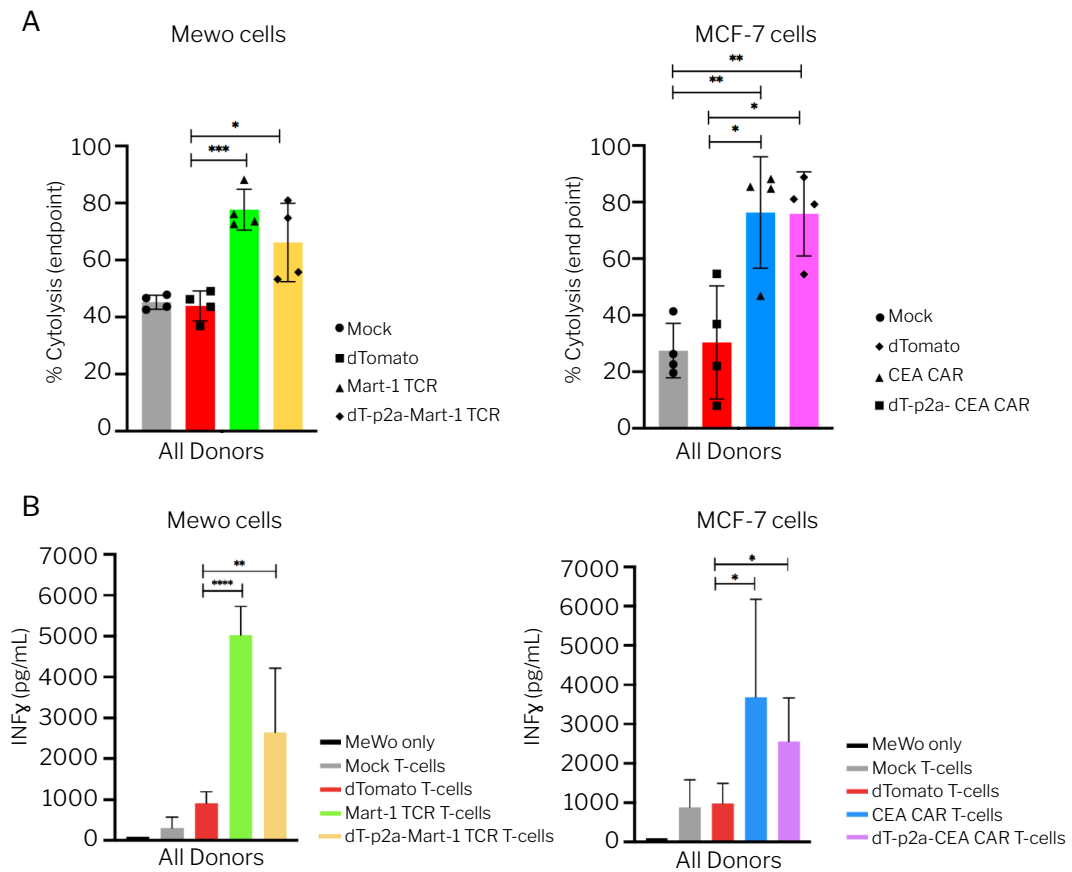


Figure 3.7: T-cells expressing anti-CEA CAR and anti-MART-1 TCR display targeted killing of cancer cells. Human primary T-cells were modified to express anti-CEA or MART-1 specific receptors using S/MAR DNA vectors. Anti-MART-1 or anti-CEA T-cells were co-cultured with the human melanoma cell line (MeWo) or breast adenocarcinoma cell line (MCF-7), respectively, in an xCELLigence plate at a 1:1 effector/target ratio. A) Graphs depict the percentage of cytolysis. Cytolysis was calculated by normalizing the end point cell index by the cell index at a standard initial time point. B) Displays the concentration of $\text{IFN}\gamma$ (pg/ml) in the supernatant 48 hours after T-cells were added. An unpaired parametric two-tailed T-test was performed (GP: 0.0332(*), 0.0021(**), 0.0002(***), <0.0001(****)). Data were collected from 4 donors, and two independent experiments. Data were obtained from Toros Tasgins.

3.2.3 Section Discussion

Within human primary T-cells and U-iPSCs, dTomato is a suitable reporter gene that has a negligible negative correlation with cell viability. Studies directly assessing the effects of dTomato expression on cellular functionality would be interesting as alternations in T-cell functionality have been reported with GFP expression. No differences in the killing capability between non-modified T-cells and dTomato modified T-cells is indicated. No differences in the killing capability between CAR/TCR modified T-cells and CAR-dTomato/TCR-dTomato T-cells is indicated (Figure.3.7). This provides a preliminary indication that T-cell killing is not significantly altered by dTomato expression or S/MAR DNA vector modification.

Off-target killing is indicated from the large cytolysis percentage associated with non-modified and dTomato only T-cells, which is common for *in vitro* killing assays as HLA types are not commonly matched. Nevertheless, T-cells modified with S/MAR DNA vectors containing anti-CEA CAR or anti-MART-1 TCR display a significant targeted killing capacity. I would like to determine the killing capacity of U-iPSC-derived T-cells modified with anti-CEA CAR or anti-MART-1 TCR.

3.3 Screening S/MARs

Here I compare four S/MARs for their maintenance in human U-iPSCs and Jurkat76 cells as well as their immunogenicity, upon cellular entry, in immortalized normal human dermal fibroblast (iNHDF)s. S/MAR DNA vector establishment rates in human U-iPSCs were calculated. I also assessed the long-term transgene expression in T-cells for a preliminary indication of possible transgene persistence within U-iPSC-derived T-cells. I obtained an indication for the immunogenicity against different S/MAR sequences by comparing IFN β secretion upon S/MAR DNA vector cellular entry. Long-term transgene expression in human U-iPSCs is important as I aim for an off-the-shelf therapy that could be continuously expanded and used by multiple patients (for more details see section 2.1). These data are lacking within this section and are crucial to determine the most optimal features to use in human U-iPSCs.

3.3.1 Comparing S/MARs in Human U-iPSCs

Similarities in transfection efficiency using different S/MARs in human U-iPSCs were noticed, ranging between 50-65% (Figure.3.8). I noticed a trend in their corresponding mean cell viability. The smaller the S/MAR sequence—S/MAR sequences become gradually smaller toward S/MAR-4—the higher the cell viability. I found S/MAR-1 and S/MAR-2 have the highest establishment rates (0.056% and 0.04%) relative to S/MAR-3 and S/MAR-4 (0.0006% and 0.0007%)(Table.3.1), which is a similar tendency found in Jurkat76. Additional data points must be collected before any conclusions as two replicates were used for this study, and no statistics were performed. Long-term maintenance of S/MAR DNA vectors in human U-iPSCs is crucial to assess and is a future aim.

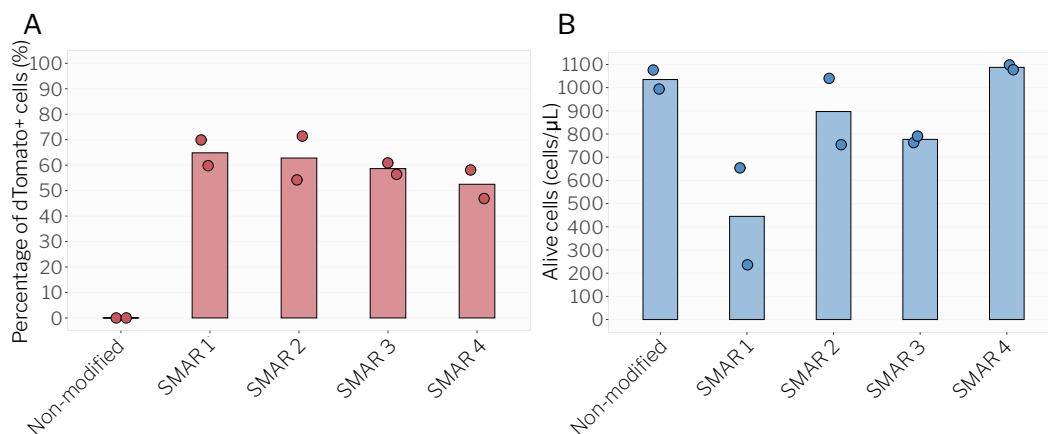


Figure 3.8: Transfection efficiencies and cell viabilities comparing S/MARs within S/MAR DNA vector-modified human U-iPSCs. $4(10)^5$ cells were seeded into a 24-well plate. The following day, 600 ng of DNA was delivered using Lipofectamine Stem. A) Bar graphs depicting S/MAR vector transfection efficiency 3 days post-modification. B) Bar graphs depicting cell viabilities corresponding with S/MAR vector transfection efficiency 3 days post-modification. Data contains two replicates.

Table 3.1: S/MAR DNA vector establishment rates in human U-iPSCs: Comparing S/MARs

	Establishment Rates (%)
Non-modified	0.0000%
S/MAR-1	0.0555%
S/MAR-2	0.0392%
S/MAR-3	0.0006%
S/MAR-4	0.0007%

3.3.2 Comparing S/MARs in Jurkat76

After 128 days within Jurkat67 cells, at least 80% of cells were still expressing dTomato for all cell lines established with S/MAR DNA vectors (Figure.3.9). A significant reduction in the percentage of cells expressing dTomato was shown for S/MAR-1 and S/MAR-3 between days 4 and 128. No significant reduction in the percentage of cells expressing dTomato was present for S/MAR-4 between days 4 and 128. No statistical analysis was performed for S/MAR-2 as only 2 replicates were present.

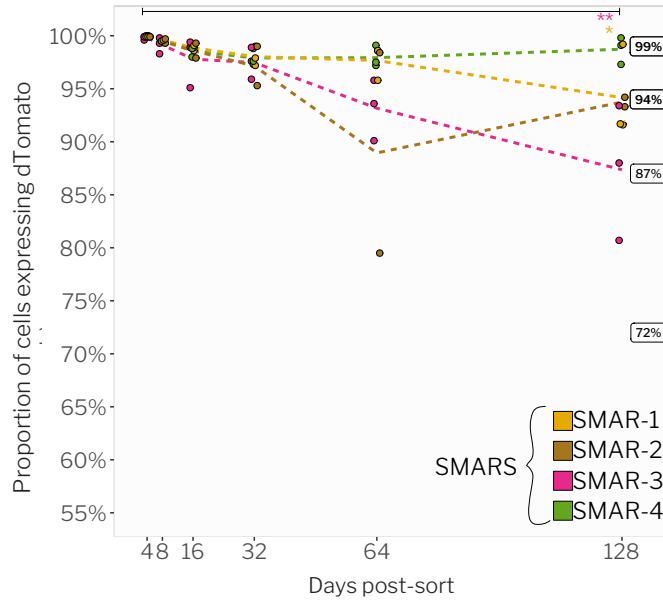


Figure 3.9: S/MAR-4 has the highest proportion of cells stably retaining transgene expression after 128 days in culture. Alive dTomato+ Jurkat76 cells were sorted consecutively 1,3,5, and 7 weeks after electroporation. The proportion of cells remaining dTomato+ was monitored for 128 days after the final sort that was performed on week 7. Image contains data from 3 independent experiments. Statistical analysis was performed using Tukey one-way ANOVA for all samples except S/MAR-2 as only two replicates are present. Adjusted p-value ≤ 0.05 (*). Adjusted p-value ≤ 0.01 (**).



3.3.3 Cytokine Secretion Upon Cellular Entry of DNA Vectors Containing Unique S/MARs

Every vector induced significant amounts of IFN β secretion within 48 hours relative to untreated MEFs (Figure.3.10). S/MAR-4 had the lowest median concentration of IFN β compared to the other S/MARs, but no significant difference was found between S/MAR DNA vector treated groups. Calibration curves for this test can be found in Figure.B.2.

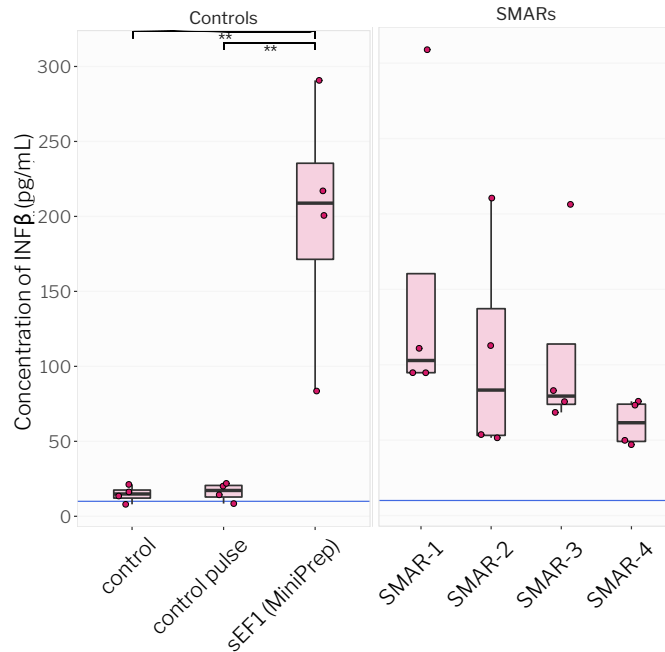


Figure 3.10: S/MAR-4 induced the lowest production of IFN β , relative to the other S/MARs tested. $2(10)^5$ iNHDFs were electroporated with 1 μ g of DNA using a P2 primary cell 4D-nucleofector kit (Lonza) with pulse code DT130. Medium was collected 48 hours post-electroporation and stored at -20°C . IFN β ELISA was conducted using a LumiKineTM Xpress hIFN- μ 2.0 kit. Data contains four independent cultures. Data is depicted in boxplots. Statistical analysis was performed using Tukey one-way ANOVA. ** adjusted p-value ≤ 0.01 .

3.3.4 Section Discussion

S/MAR-4 is considered the most optimal S/MAR for our intended application as it induces the lowest secretion of IFN β upon cellular entry and was shown in Jurkat76 to be stably maintained for 128 days post-establishment. S/MAR-1 and 2 establish in a higher percentage of cells relative to the other S/MARs—this is shown in human U-iPSCs and Jurkat76. Though, long-term persistence and immunogenicity were considered more important variables as transgene expression must persist through the differentiation process (a process that lasts a couple of months) and strong immunogenicity may alter cellular functionality, which may affect the differentiation process.

A positive trend was present between S/MAR length and IFN β production in iNHDFs (Figure.3.10), and a negative trend was present between S/MAR length and cell viability in U-iPSCs (Figure.3.8B). Though no significant difference was present, the existence of these



trends in two separate experiments utilizing different models is noteworthy and worthy of further investigation.

The IFN β screening was performed in iNHDFs as fibroblasts provide a stronger immune response upon DNA entry. With this model, I could more easily compare vector features. A screening in primary T-cells and Jurkat76 was attempted. However, the response was below the detection limit. Cytokine release was screened in mouse HSPCs using S/MAR DNA vectors (section 4.2.2). Of the cytokines compared, this study indicates IFN β is induced the strongest upon DNA vector entry.

DNA vectors are produced using bacteria. So, trace levels of endotoxins may be present in DNA samples. sEF1 (miniprep), contains DNA extracted without the removal of endotoxins, which acts as a positive control to assess the influence endotoxins have on this test. Sample sEF1 (miniprep) has the same DNA sequence as sample sEF1. As sample sEF1 had endotoxins removed, sample sEF1 and sEF1 (miniprep) can be compared to assess the influence of endotoxins on this test. These findings are summarized in Figure.3.10.

Additionally, I calculated endotoxin levels within vectors produced in-house and externally, a difference was noticed between these groups (Appendix.B.3).³ It's beneficial to screen endotoxin levels within each DNA sample, to ensure the reliability of this test. Nevertheless, S/MAR DNA vectors containing unique S/MARs or promoters were produced from the same entity to prevent alternations due to extraneous variables associated with vector production.

Long-term persistence of vectors was assessed using the Jurkat76 cell line. Primary T-cells are a closer model to our intended cell type: U-iPSC-derived T-cell. However, primary T-cells remain alive *in vitro* for approximately 21 days post-modification (Appendix.B.1), which is not optimal for long-term studies. U-iPSC-derived T-cells were also not utilized as genetically modified U-iPSC lines must be established (max. 1.5 months), then differentiated into T-cells (between 1-2 months). This is not efficient for a rapid screening. The purpose of this study is to reduce the number of vectors screened in U-iPSC-derived T-cells. Additionally, an established U-iPSC-derived T-cell differentiation protocol was not available within our lab. Our lab is still working to establish it. As previously mentioned, it is important to assess long-term transgene expression in human U-iPSCs. This experiment was attempted and prematurely terminated due to complications with the medium, which lead to cell death.

3.4 Screening Promoters

In this section, a similar comparison as described in section 3.3 was performed utilizing S/MAR DNA vectors with unique promoters. Some promoters, particularly CMV and CAG, have been associated with a loss of transgene expression *in vitro* and *in vivo* [329, 338, 335]. Due to this, I assessed long-term transgene expression. I also compared the establishment rates in U-iPSC lines using different promoters, and I obtained an indication of the immunogenicity against different promoters by comparing IFN β secretion upon S/MAR DNA vector cellular entry.

³No statistics were calculated within test B.3 as only one replicate was used.



3.4.1 Comparing Promoters in Human U-iPSCs

S/MAR DNA vectors containing the CAG promoter have the highest transfection efficiency (63%)(Figure.3.11). Vectors containing sEF1 and sEF1+CI have transfection efficiencies of 29% and 26%, respectively. The corresponding cell viability was highest for sEF1 (750 cells/ μ L) and lowest for sEF1+CI and CAG (331 cells/ μ L and 297 cells/ μ L). There were slight differences in the MFI of dTomato expressing cells, in which CAG had a stronger MFI (geometric mean: 2335) relative to sEF1+CI (geometric mean: 1140) and sEF1 (geometric mean: 564). I found a larger percentage of U-iPSCs establish vectors with CAG relative to sEF1 and sEF1+CI. This pattern was also shown in the Jurkat76 cell line (Figure.3.2). I found U-iPSCs modified with S/MAR DNA vectors containing the sEF1+CI promoter lost transgene expression, while expression persisted in a subset of cells modified with vectors containing sEF1 or CAG (Table.3.2). Additional data points must be collected before any conclusion as only two replicates were used for this study.

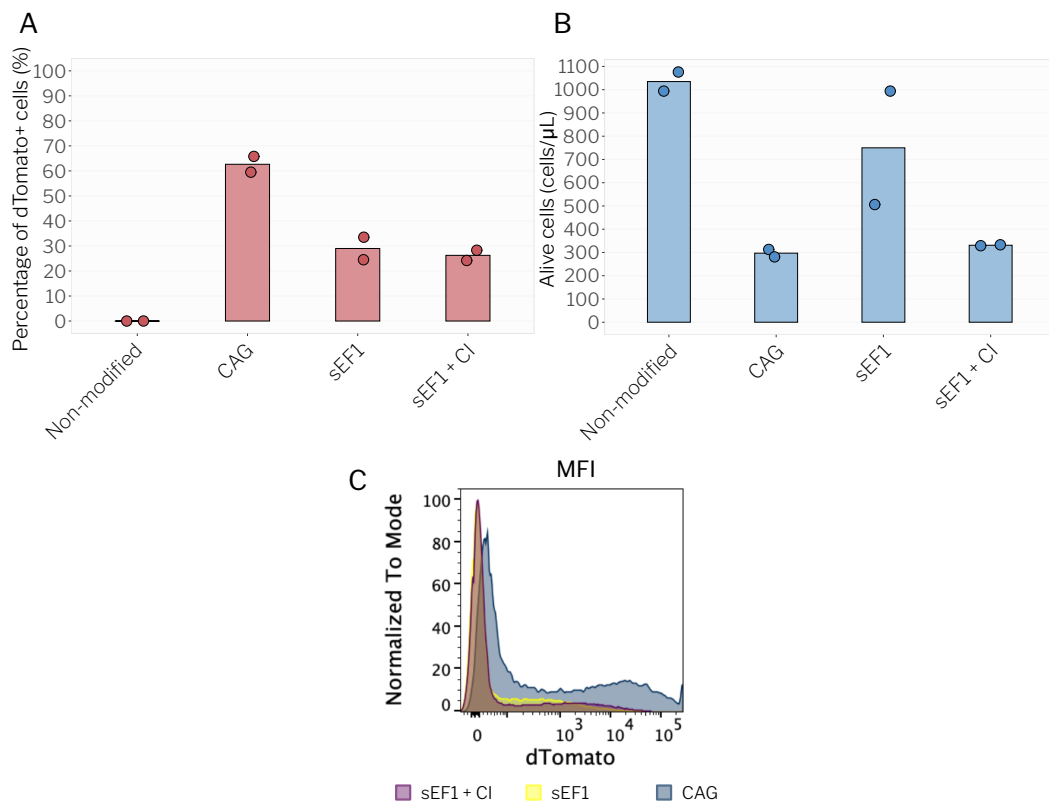


Figure 3.11: Comparing transfection efficiencies and cell viabilities of human U-iPSCs modified with S/MAR DNA vectors containing unique promoters. $4(10)^5$ cells were seeded into a 24-well plate. The following day, 600 ng of DNA was delivered using Lipofectamine Stem. A) Bar graphs depicting S/MAR vector transfection efficiency 3 days post-modification. B) Bar graphs depicting cell viabilities 3 days post-modification. C) Histogram displaying the fluorescence intensity of dTomato expression; values were normalized by mode. Data contains two replicates.



Table 3.2: S/MAR DNA vector establishment rates in human U-iPSCs: Comparing promoters

Establishment Rates (%)	
Non-modified	0.0000%
CAG	0.0185%
sEF1	0.0002%
sEF1+CI	0.0000%

3.4.2 Comparing Promoters in Jurkat76

Jurkat76 cells modified with vectors containing sEF1 or sEF1+CI retained expression in 99% and 89% of cells, respectively, 128 days post-modification (Figure.3.12). A gradual decline in the percentage of Jurkat76 cells expressing dTomato was shown for the CAG promoter, which had 72% of cells expressing dTomato 128 days post-modification. The data indicate large variations in the percentage of cells retaining dTomato expression for samples associated with the sEF1+CI or CAG promoter (StD: 16.46 and 18.6) while samples modified with the sEF1 promoter had the smallest variation (StD: 0.6).

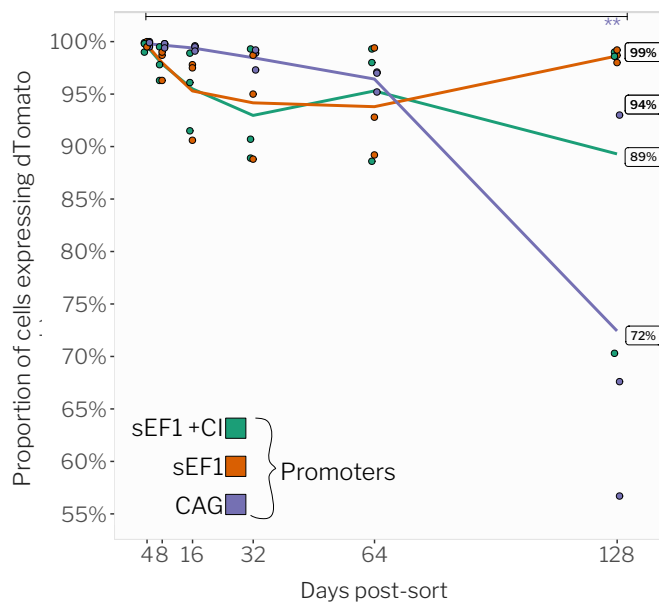


Figure 3.12: Promoter sEF1 has the highest proportion of cells stably retaining transgene expression after 128 days in culture. Alive dTomato+ Jurkat76 cells were sorted consecutively 1, 3, 5, and 7 weeks after electroporation. The proportion of cells remaining dTomato+ was monitored for 128 days after the final sort that was performed on week 7. Image contains data from 3 independent experiments. Statistical analysis was performed using Tukey one-way ANOVA. Adjusted p-value ≤ 0.05 (*). Adjusted p-value ≤ 0.01 (**).



3.4.3 Cytokine Secretion Upon Cellular Entry of DNA Vectors Containing Unique Promoters

S/MAR DNA vectors induce iNHDFs to secrete significant amounts of $\text{IFN}\beta$, 3 to 12 folds higher compared to the pulsed non-modified control (Figure.3.13). This was also shown in section 3.3.3, which screened S/MARs. I saw an increased presence of $\text{IFN}\beta$ in the supernatant of cells modified with vectors containing a CI relative to cells modified with vectors lacking a CI. These data suggest that the addition of a CI leads to stronger activation of pathways upstream of $\text{IFN}\beta$. The promoter sEF1 was associated with the lowest concentration of $\text{IFN}\beta$ in the supernatant of modified cells (66 pg/mL). A positive control called “sEF1 miniprep” was used to compare the effects of endotoxins on $\text{IFN}\beta$ secretion. The only difference between sample sEF1 miniprep and sEF1 is that endotoxins were removed from sEF1. Comparing these samples, the removal of endotoxins reduced $\text{IFN}\beta$ production by 2-fold.

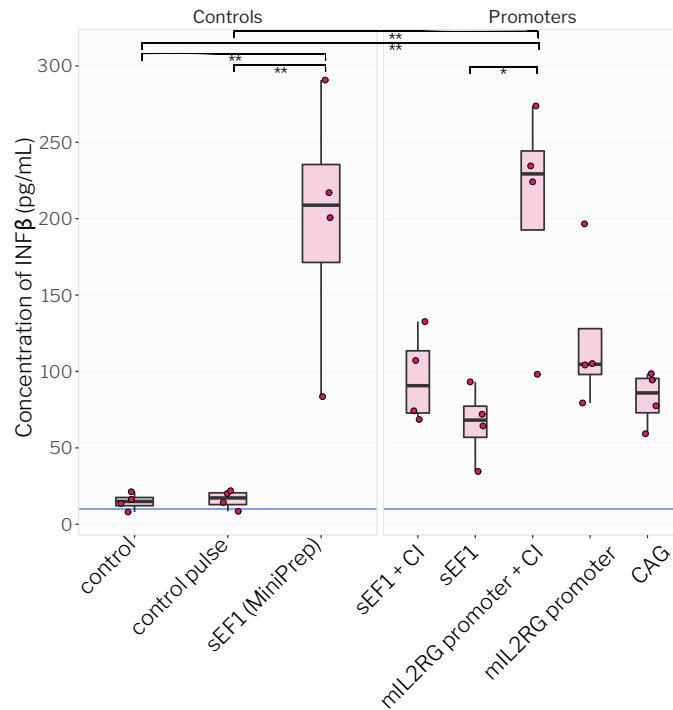


Figure 3.13: Promoters CAG and sEF1 induced $\text{IFN}\beta$ production least, relative to the other promoters tested. $2(10)^5$ iNHDFs were electroporated with $1 \mu\text{g}$ of DNA using a P2 primary cell 4D-nucleofector kit (Lonza) with pulse code DT130. Medium was collected 48 hours post-electroporation and stored at -20°C . $\text{IFN}\beta$ ELISA was conducted using a LumiKine™ Xpress hIFN- β 2.0 kit. Data contains four independent experiments. Data is depicted in boxplots. Statistical analysis was performed using Tukey one-way ANOVA. *adjusted p-value ≤ 0.05 . **adjusted p-value ≤ 0.01 . ***adjusted p-value ≤ 0.001 . mL2RG promoter, 500 bp of the mouse IL2RG promoter. CI, chimeric intron.

3.4.4 Section Discussion

Based on these screenings, sEF1 is considered the most suitable promoter for our intended application. Data indicate that cells could establish vectors containing this promoter in both T-cells (section 3.1.1) and U-iPSCs (Table.3.2), and transgene expression persisted for months with small variations between replicates (Figure.3.12)—suggesting a high reproducibility. sEF1 was associated with the lowest concentration of IFN β in the supernatant of modified cells, relative to the other promoters screened (sEF1+CI and CAG). CAG was associated with the highest cellular establishment and with one of the lowest concentrations of IFN β . Though, steady declines in transgene expression were found in cell lines established with vectors containing CAG over 128 days (Figure.3.12). dTomato expression was lost in iPSCs modified with vectors containing sEF1+CI within two weeks; an established line could not be generated (Table.3.2). sEF1+CI was also associated with high levels of IFN β secretion, relative to the other promoters assessed.

Data on the expression persistence in established U-iPSCs is missing, these data are crucial for determining a promoter most appropriate for U-iPSCs modification. I also lack data on integrational analysis, which is crucial to ensure S/MAR DNA vectors are remaining episomal.

It is well known that transfection efficiency is negatively correlated to cell viability. This was displayed with CAG having the highest transfection efficiency and the lowest cell viability while sEF1 has one of the lowest transfection efficiencies and the highest cell viability (Figure.3.11). Interestingly, sEF1 and sEF1+CI had similar transfection efficiencies though their corresponding cell viabilities were different (750 cells/ μ L compared to 331 cells/ μ L). This indicates that the CI (or an extraneous variable related to it) is affecting cell viability. Additionally, in Figure.3.13, the addition of a CI led to an increase in IFN β production; this was present in two treatment groups when a CI was added to their promoter.

Endotoxins are associated with IFN β secretion and are inevitably present at trace levels within DNA samples due to production. Endotoxin's disruption to data collected in Figure.3.10 and 3.13 was assessed. iNHDFs modified with a vector containing endotoxins (sEF1 MiniPrep) had a 2-fold increase in IFN β secretion relative to a vector lacking endotoxins (sEF1). A 3-fold increase in IFN β secretion was present for iNHDFs modified with vectors lacking endotoxins (sEF1) relative to non-modified pulsed samples. This suggests that DNA is a greater factor for IFN β secretion rather than trace levels of endotoxins. As endotoxins are indicated to have some influence on IFN β production, vectors containing unique promoters and S/MARs were produced from the same entity to prevent alterations due to extraneous variables associated with vector production. The concentration of endotoxins presents in DNA samples was assessed in Appendix. B.3. See paragraph 4 of section 3.3.4 for a further description of endotoxin's influence.

For details about why iNHDFs were used as a model for the IFN β screening, and why Jurkat76 was used as a model for assessing the long-term persistence of transgene expression, see paragraph 3 of section 3.3.4, and paragraph 5 of section 3.3.4, respectively.



3.5 Screening Production Backbones

For backbone comparisons, S/MAR-3 and sEF1+CI can be compared. Features between S/MAR-3 and sEF1+CI are the same, except S/MAR-3 contains the NTX RNA-out R6K (NB) production backbone while sEF1+CI contains a classical bacterial backbone (BB).⁴ Of the two replicates performed, an U-iPSC line was not established using sEF1+CI (BB) vectors (Table.3.2) while U-iPSC lines were established using vector S/MAR-3 (NB) (Table.3.1). Transfection efficiency and the corresponding viability were higher when using the S/MAR-3 (NB) vector (59% transfection efficiency and 777 cells/ μ L)(Figure.3.8) relative to sEF1+CI (BB) (26% transfection efficiency and 331 cells/ μ L) (Figure.3.11). Both had similar long-term retention in established Jurkat76s (89% and 87% after 128 days)(Figures.3.9 and 3.12). sEF1+CI (BB) had a slightly higher concentration of IFN β present in the supernatant after transfection relative to S/MAR-3 (NB) (Figure.3.13 and 3.10). Therefore, NTX RNA-out R6K was considered the most optimal production backbone.

3.6 Conclusion

T-cells and human iPSCs can retain S/MAR DNA vectors, suggested by the stable maintenance of transgene expression in Figure.3.2 and 3.4. Certain vector features influence establishment success (Table.3.1 and 3.2). dTomato is considered a suitable reporter gene as cell viability did not correlate with dTomato expression (Section.3.2.1). Anti-CEA CAR and anti-MART-1 TCR S/MAR DNA vectors are suitable for assessing the functionality of an U-iPSC-derived T-cell as both vectors lead to the targeted killing of human T-cells (Section 3.2.2). S/MAR-4 is considered the most optimal S/MAR as U-iPSCs can establish vectors containing this feature, this feature is associated with the lowest median concentration of IFN β and long-term transgene expression in established Jurkat76 lines (section 3.3). sEF1 is considered the most optimal promoter as U-iPSCs can establish vectors containing this feature and this feature is associated with long-term transgene expression in established Jurkat76 lines (section 3.4). The NTX RNA-out R6K is considered the most optimal production backbone as a higher percentage of cells establish vectors containing this feature relative to an ampicillin bacterial backbone, and its usage results in a higher transfection efficiency and associated viability (section.3.5).

⁴Other small differences are present between these vectors (see footnote in the beginning of section 3), which might affect the results obtained.



3.7 Future Aims

Future aims pertaining to the screening of vector features include:

- Screening additional vector features, such as the PGK or WASP promoter, and collecting additional replicates for U-iPSC screenings.
- Improving the percentage of human U-iPSCs establishing S/MAR DNA vectors.
- Assessing the long-term persistence of vector features in established human U-iPSC lines.
- Assessing how differentiation into T-cells affect transgene expression using various vector features.
- Screening vector features in HSPCs.
- Performing an integration analysis that compares vector features in established lines.



Chapter 4

A Protocol to Expand Mouse HSPCs to High Cell Yields

Researchers have access to human HSPCs exclusively through a clinic or costly orders of commercial cord blood, bone marrow, or G-CSF-mobilized peripheral HSPCs [251]. Recently, Yamazaki reported that Ham’s F-12 medium supplemented with various reagents supports the growth of mouse HSPCs for up to 8 weeks—these medium conditions will be called “Yamazaki medium” within this report [330, 331]. This permits researchers to conduct novel HSPC-based mouse experiments, which may appeal to the numerous researchers lacking access to human HSPCs [251]. This method—initiating cultures from Lin⁻ Sca-1⁺ c-kit⁺ (LSK) CD34⁻ CD150⁺—led to modest cell yields despite expansion for 1-month. This makes it unsuitable for electroporation-based vector screenings, which require millions of cells [251]. I built upon this method and generated a cost-effective mouse HSPC expansion protocol for pre-clinical investigations requiring high cell yields [251]. This chapter describes that process.

4.1 The Expansion of Mouse HSPCs

Within this section, I describe the development of a protocol for expanding mouse HSPCs to millions of cells in 10 days. This section highlights Yamazaki medium’s ability to support the expansion of HSCs and describes my expansion protocol that builds upon Yamazaki and Wilkinson’s discovery.

4.1.1 Mouse HSPCs Proliferate in Yamazaki Medium

HSPCs with various enrichments of HSCs (Appendix.B.4) were collected into Yamazaki medium (Table.4.1); their expansion rate was assessed (Figure.4.1). Populations more enriched for HSCs expanded more quickly. This is displayed in Figure.4.1A comparing LSK cells (21x), LSK CD150⁺ (101x), LSK CD150⁺ CD48⁻ (141x), and LSK CD150⁺ CD34⁻ (185x) as well as LSK (21x), LSK CD48⁻ (121x), and LSK CD48⁻ CD150⁺ (141x). Marker expression data in Figure.4.1 indicate cells that are derived from more enriched HSC populations remain more enriched for HSCs.¹ Marker expression data was organized into FLOWMAPs (Figure.4.1B). Assessing the distribution of cells within population 3—the population most enriched for HSC-like cells (Lineage⁻, c-Kit⁺, Sca-1⁺, and

¹Example FACS gating plot in Appendix.B.6

CD150+)(Figure.4.1C)— a higher prevalence of cells are derived from parent cell types more enriched for HSCs (Figure.4.1D). I predicted total cells after a 14-day expansion (Table.4.2) by multiplying expansion rates and bone marrow cell counts.² Total cells range between 83,767 and 591,968, which is not optimal for an electroporation—one sample requires a minimum of 300,000 cells. Less enriched populations of HSCs delivered the highest cell counts. I attempted to improve this protocol considering these findings.

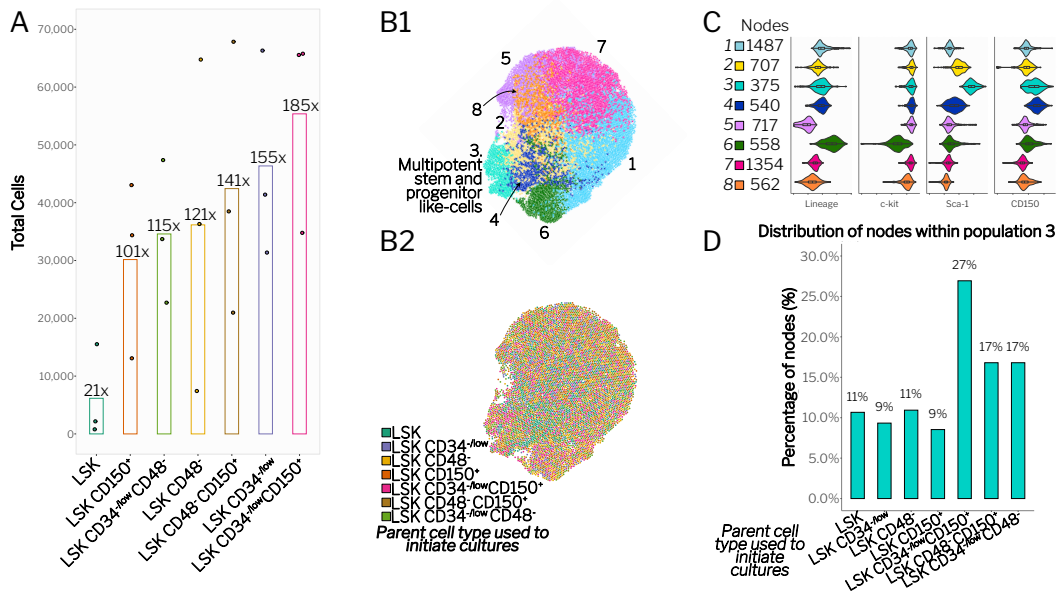


Figure 4.1: Cell populations enriched for mouse HSCs produce higher cell counts within Ham's F-12 medium conditions and remain more enriched for LSK CD150+ cells. 300 cells from each parent population were cultured for 14 days in a fibronectin-coated plate. A) Cell counts were calculated on day 14 using CountBright™ Beads and normalized by the number of cells used to initiate each culture. n=3 independent experiments. B) Dimensionality reduction comparing lineage, c-kit, sca-1, and CD150 expression from cells originating from each parent cell type. The graphs were generated using FLOW-MAP (random subsampling, 300 nodes with no clusters, min=2, max=8, distance metric= manhattan). Communities were predicted using Louvain Modularity community detection algorithm. C) Displays the intensity of marker expression within each predicted population from B1. D) Displays the percentage of parent-cell-type-derived cells present in population 3.

Table 4.1: Medium composition of supplemented Ham's F-12 medium for mHSC expansion.

	Total Volume (μL)
Ham's F-12 Medium	1,900
HEPES (1 M)	200
ITS -X (100X)	200
PVA (10%)	200
Penicillin-Streptomycin-Glutamine (100X)	200
TPO (100 μg/mL)	2
SCF(10 μg/mL)	2

²FACS gating plots used to calculate bone marrow cell counts are found in Appendix.B.5.

**Table 4.2:** Predicted cell counts after expanding HSPC populations for 14 days.

Parent cell type used to initiate cultures	Average count of cells collected from the BM of one mouse	Expansion rate (from 1A)	Predicted cell count after a 14-day expansion
LSK	$1.88(10)^4$	21	393,881
LSK CD34-	$3.82(10)^3$	155	591,968
LSK CD48-	$3.82(10)^3$	121	462,117
LSK CD150+	$1.10(10)^3$	101	111,434
LSK CD150+ CD48-	$5.94(10)^2$	141	83,767
LSK CD34- CD48-	$2.04(10)^3$	115	234,241
LSK CD34- CD150+	$5.94(10)^2$	185	109,907

4.1.2 Mouse HSPCs Depleted of Mature Hematopoietic Cells Expand in Yamazaki Medium

Lineage- bone marrow cells were cultured in Yamazaki medium to calculate total predicted cell counts after a 14-day expansion. Similar methods as described in section 4.1.1. were followed. Data indicate an expansion rate of 41x (Figure.4.2A), which was low compared to the expansion rates calculated in Figure.4.1A. Nevertheless, predicted cell counts after 14 days were approximately $7(10)^7$ per a mouse (Figure.4.2B). Data imply that Yamazaki medium conditions are selective for the growth of HSPCs. This was shown in Figure.4.2C and D, in which bone marrow cells slightly depleted of mature hematopoietic cells (not all) were cultured in Yamazaki medium conditions over 7 days. Populations expressing markers indicative of an HSPC became more prevalent over these 7 days (Figure.4.2C). This was especially evident assessing c-kit expression, in which two populations were always present (low c-kit and high c-kit populations), and the high c-kit population became more prevalent over these 7 days. Data also indicate a drop in cell viability between days 1 and 3, and a recovery of this cell viability between days 3 and 7 (Figure.4.2D), which suggests population enrichment due to the death of cells whose growth is not supported by these medium conditions.

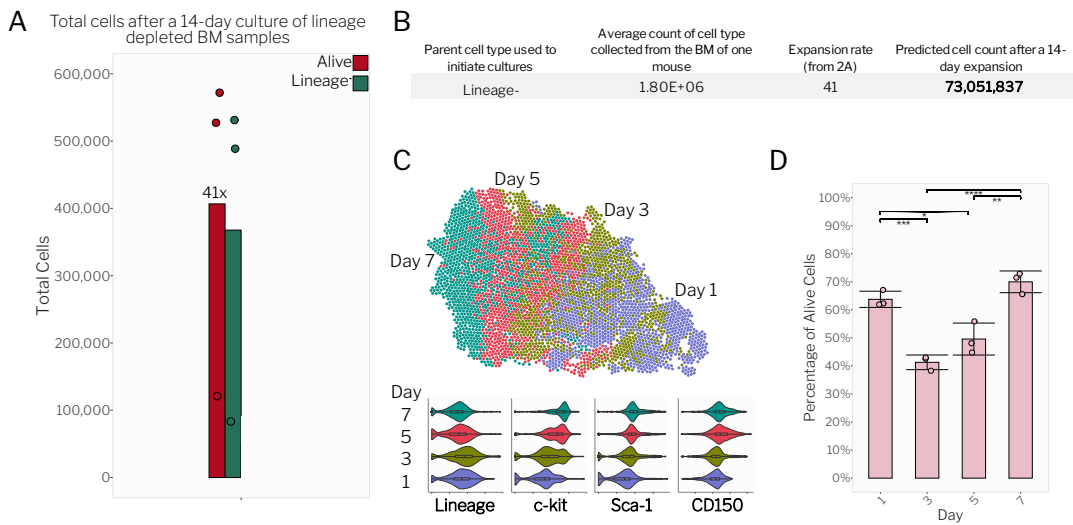


Figure 4.2: Cell populations depleted of only mature hematopoietic cells expand to millions of cells and retain a high enrichment of HSC-like cells in Ham's F-12 medium conditions. 10,000 Lineage- cells were cultured for 14 days in a fibronectin-coated plate. A) Cell counts were calculated on day 14 using CountBright™ Beads and normalized by the number of cells used to initiate each culture. n=3 independent experiments. B) Predicted cell counts after a 14-day expansion of the indicated parent cell type per one mouse. Calculations were made by multiplying the expansion rates in 4.1A or 4.2A by the average number of parent cells present in the bone marrow of one mouse. C) Dimensionality reduction comparing lineage, c-kit, sca-1, and CD150 expression in bone marrow cells kept in Ham's F-12 medium conditions over 7 days. The graph was generated using FLOW-MAP (random subsampling, 600 nodes with 300 clusters, min=2, max=5, distance metric= manhattan, mode= single). Communities were predicted using Louvain Modularity community detection algorithm. D) Bone marrow cells were harvested and cultured in Ham's F-12 medium conditions, and the percentage of viable cells was followed for 7 days. Statistical analysis was performed using Tukey one-way ANOVA. *adjusted p-value ≤ 0.05 . **adjusted p-value ≤ 0.01 . ***adjusted p-value ≤ 0.001 . ****adjusted p-value ≤ 0.0001 .

4.1.3 Mouse HSPCs Expand Following MHEP

I developed a protocol for the expansion of mouse HSPCs based on the Yamazaki expansion protocol, which is named mouse HSPC expansion protocol (MHEP) within this report. The purpose of MHEP is to create mass cell numbers for screening vector features via electroporation (Figure.4.3A). The method initiates cultures from a lineage-depleted population and is based on a 10-day expansion. I found cultures maintain an average viability of 86% with 28% LSK-like cells after 8 days (Figure.4.3D) [251]. I predicted approximately $7(10)^7$ average total cells per mouse after a 14-day expansion could be produced (Figure.4.2) [251], but explicit data indicate approximately $3(10)^6$ average total cells per mouse after a 10-day expansion are produced with a doubling rate of 2.8 days (Figure.4.3C). Differentiation was evident between days 0 and 4 due to the presence of cell aggregates (Figure.4.3B). After day-4 lineage depletion, negligible cell aggregates were present and remained that way for up to 14 days.

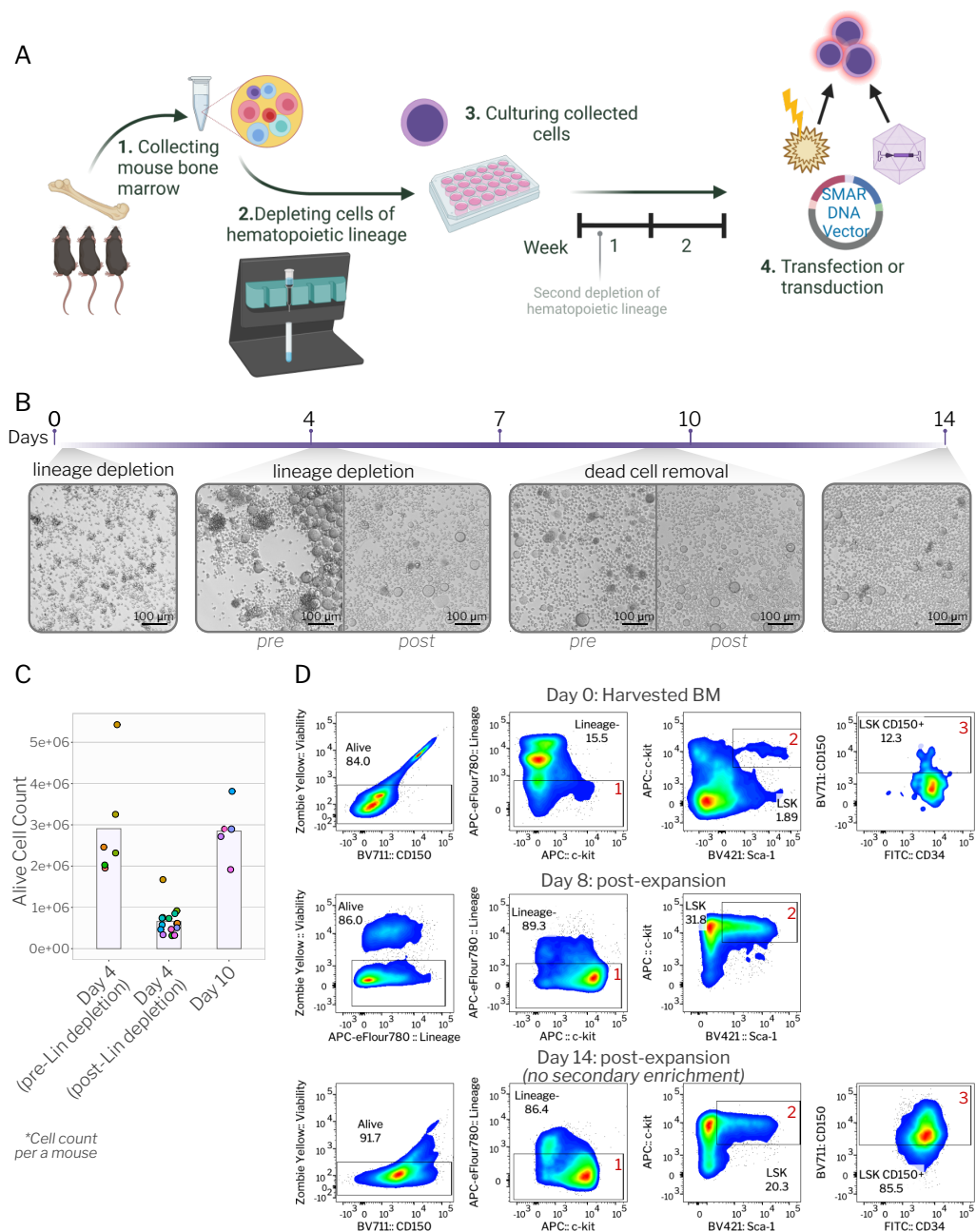


Figure 4.3: Data pertaining to the MHEP protocol. A) Schematic representation of the MHEP protocol. Cells are extracted from the bone marrow of mice. Blood stem and progenitor cells are collected and maintained in culture for 10 days. B) Microscope images of cultures at meaningful time points during the expansion protocol. C) Total cell counts calculated at meaningful time points during the expansion protocol using a Luna™ cell counter. D) FACS plots displaying HSPC-like enrichment on days 0 and 8 following this expansion protocol, and day 14 following this protocol without a secondary enrichment of progenitor cells.



4.1.4 MHEP-Expanded Mouse HSPCs Engraft in Mice

Mouse HSPCs expanded following MHEP were assessed for their HSPC functionality. This was determined by performing primary and secondary engraftments in mice. During the primary engraftment, peripheral blood was collected and analyzed 2 and 4 months post-injection. Data in Figure.4.4A show the percentage of CD45.2 cells present within the B-cell, T-cell, myeloid cell, and monocyte population when engrafting 20,000 expanded mouse HSPCs (CD45.2+) along with 100,000 radio-protective cells (CD45.1+). Data here indicate successful engraftment in all donors—a successful reconstitution was considered $\geq 0.1\%$ of CD45.2+ cells. Bone marrow from primary recipients was harvested 4 months post-injection and the Lin- c-kit+ CD34- CD135- (LK CD34- CD135-) population was analyzed (Figure.4.4B). Various numbers of engrafted cells were compared in Figure.4.4B—200; 2,000; and 20,000 MHEP expanded mHSPCs along with 100,000 radio-protective cells (CD45.1+). These data provide a preliminary indication of HSC enrichment within MHEP cultures (Figure.4.4C), which suggests a preliminary estimate of 1 out of 927 cells as HSC 4 months post-primary engraftment. Secondary engraftment was performed using primary engrafted recipients that were injected with 20,000 MHEP expanded mHSPCs. 4-months post-injection, the peripheral blood of recipients from the secondary engraftment was assessed (Figure.4.4D). Data indicate 2 out of 3 donors had $\geq 0.1\%$ of peripheral blood cells marked as CD45.2+.

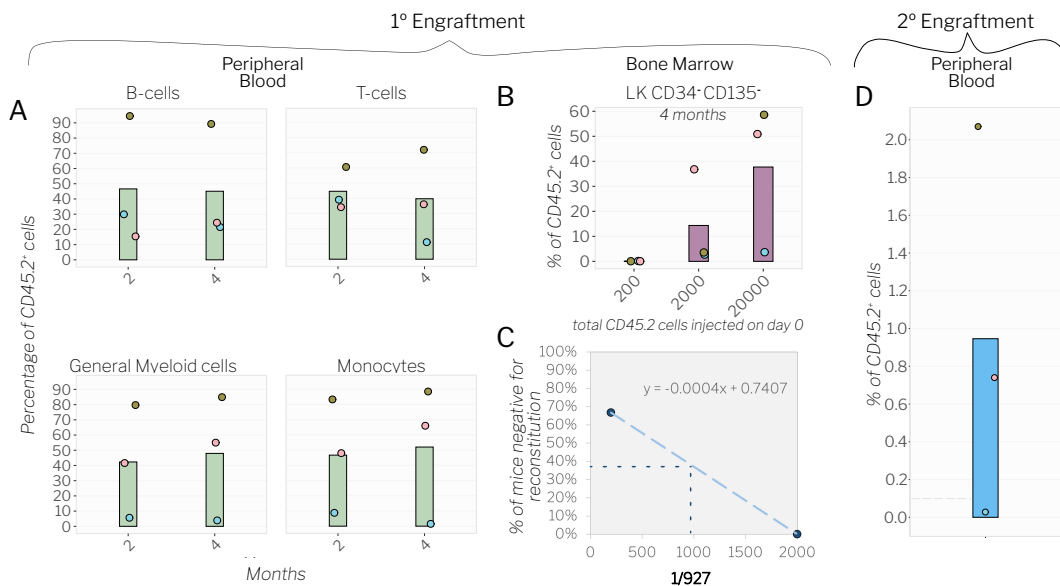


Figure 4.4: MHEP-expanded mHSPCs can successfully engraft in mice. Lineage- cells from C57BL/6 mice (CD45.2+) were expanded for 10 days and 200, 2000, or 20,000 cells were engrafted along with 100,000 radio-protective cells into CD45.1+ mice. Engraftment success was assessed at 2 months and 4 months post-enugraftment by collecting peripheral blood. A) Depicts the percentage of CD45.2+ cells present within the indicated cell population from the peripheral blood of mice engrafted with expanded cells. B) Depicts the percentage of CD45.2+ cells present within the LK CD34- CD135- cell population present in the bone marrow of mice 4 months post-enugraftment. C) Preliminary data calculating the frequency of HSCs (competitive repopulating units) within the expanded cells. A successful reconstitution was considered $\leq 0.1\%$ of CD45.2+ cells. D) Bar graph depicting the percentage of CD45.2+ cells 4 months post-injection in the peripheral blood of secondary recipients engrafted with the bone marrow of primary recipients associated with 20,000 MHEP expanded mHSPCs.



4.1.5 Section Discussion

In Figure.4.1, cells remained in culture for 14 days within a 96-well fibronectin-coated plate. Total cells were collected on day 14, no cell culture splits were performed. Gentle full medium changes may have resulted in a minor loss of cells—even when being extremely mindful. To consider this, medium changes were performed on all samples at the same time to prevent variations in cell count. Marker expression (cell phenotype) was examined during this study. Thus, I assessed the enrichment of HSPC-like cells within each culture. For a stronger confirmation that cells were HSPC, a functional assay, such as mouse transplantation, is necessary and was performed.

Predicted cell counts calculated in Table.4.2 are an estimate based on the expansion rates calculated in Figure.4.1 and the average cell counts found in the bone marrow (Appendix.B.5). Predictions were used at this stage to gain a better understanding of interesting cell populations for HSPC expansion. Actual cell counts are more reliable and were calculated after following MHEP. I calculated approximately $3(10)^6$ cells per mouse after a 10-day expansion with a doubling rate of 2.8 days. This value is much lower than our predicted value of $7.3(10)^7$ cells per mouse after a 14-day expansion [251].

In Figure.4.2C violin plots indicating the expression intensity for Lineage markers, C-kit, Sca-1, and CD150 were assessed over 7 days to determine the capacity of the medium to enrich the HSPC population. Day 0 was not included in this assessment as an overall shift in marker expression was noticed relative to days 1 through 7; *ex vivo* culturing has been shown to shift marker expression. The purpose of this assessment is to compare populations emerging, rather than shifts in expression. A great example of this was displayed with C-kit expression, in which consistently two populations are present, and the high c-kit expressing population increased over these 7 days.

Although medium conditions supported the growth of HSPC-like cells (Figure.4.1), cell aggregates were noticed when higher cell densities were seeded for expansion (Figure.4.3). The secretion of cytokines from cells could lead to this differentiation, which is more significant when cells are plated at higher cell densities. During MHEP, a second enrichment of HSPCs was performed on day 4 to remove cells that had differentiated into mature hematopoietic cells. After this second enrichment, cultures remained enriched and visibility appeared like progenitors cells (no cell aggregates). Day 4 was chosen to perform the secondary enrichment as cell viability began to increase between days 3-5 (Figure.4.2).

The mouse engraftment shown in Figure.4.4 was a preliminary experiment conducted using four conditions with three replicates (Conditions: 0 MHEP cells, 200 MHEP cells, 2000 MHEP cells, and 20000 MHEP cells). Additional donors and conditions would be required to obtain a more accurate prediction of HSC frequency (Figure.4.4C) as only two data points are present, which were each calculated from 3 donors.

4.2 The Genetic Modification of Mouse HSPCs

Genetically modifying mouse HSPCs using non-viral DNA systems has proven to be extremely difficult, shown by the lack of publications on this specific topic and collected data in Appendix.B.7 [251]. I have made improvements in the delivery of non-viral DNA vectors into mouse HSPCs using electroporation [251]. Work is still ongoing to optimize the stable modification of mouse HSPCs using S/MAR DNA vectors [251]. However, in general, the screening of gene therapy vector constructs in mouse HSPCs is made possible by these findings [251].

4.2.1 S/MAR DNA Vectors Can be Introduced Into Mouse HSPCs

Using the MaxCyte GTx™, transfection efficiency was assessed by comparing three pulse codes and three DNA concentrations utilizing S/MAR DNA vectors (Figure.4.6). Pulse codes and DNA concentrations were selected based on a preliminary experiment displayed in Appendix.B.8, which shows a decline in cell viability when DNA concentrations are ≥ 50 $\mu\text{g}/\text{mL}$. These data also suggest Opt5, Opt7, and Opt8 to be the most efficient pulse codes. Cell viability was strongly impacted by the concentration of DNA. This was displayed in Figure.4.6 for all pulse codes. Using Opt5 led to a 5% decrease in cell viability and a 30% drop in cell viability resulted from electroporation with 9 $\mu\text{g}/\text{mL}$ of DNA. Of the protocols screened in Table.4.3, Opt8 with 36 $\mu\text{g}/\text{mL}$ of DNA and Opt5 with 36 $\mu\text{g}/\text{mL}$ of DNA had the highest percentage of viable dTomato+ cells within the total cell population, 2.8% and 2.9% respectively. I determined pulse code Opt8 with 36 $\mu\text{g}/\text{mL}$ of DNA to be the most efficient method as it resulted in the highest percentage of viable LSK dTomato+ cells, 1.2% (Table.4.3). This protocol was associated with an average transfection efficiency of 46.4% within the LSK population along with an average viability of 9% [251]. I attempted to establish a stable expressing line using Opt8 with 36 $\mu\text{g}/\text{mL}$ of DNA. Unfortunately, transgene expression was lost within 9 days post-electroporation (Figure.4.5). I proposed stable maintenance of S/MAR DNA vectors could be achieved by lessening the impact DNA has upon entering mouse HSPCs, which was implied by the low post-electroporation viability [251]. This assessment is explained further in sections 4.2.2 and 4.2.3.

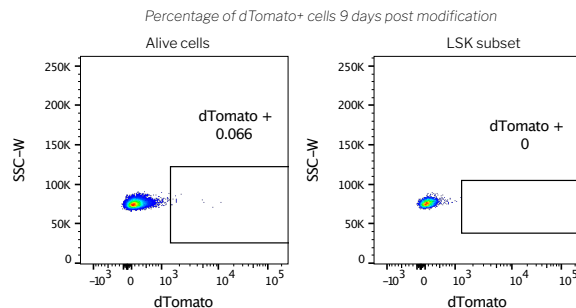


Figure 4.5: dTomato expression from mHSPCs modified with an S/MAR DNA vector is lost by 9 days post-modification. FACS plots of dTomato expression in mHSPCs 9 days after S/MAR DNA vector were introduced into cells. The FACS plot on the left and right show lost dTomato expression within the alive cell and LSK cell subset, respectively.

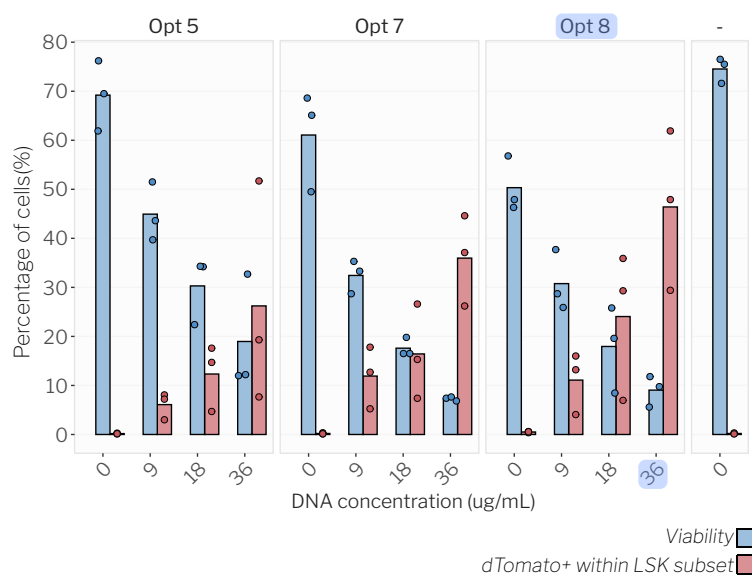


Figure 4.6: Opt 8 with 36 $\mu\text{g}/\text{mL}$ is the most effective method for the genetic modification of mHSPCs. Three electroporation protocols (Opt 5, 7, and 8) along with three S/MAR DNA vector concentrations (9, 18, and 36 $\mu\text{g}/\text{mL}$) were compared using the MaxCyte GTx™. Viability (blue) and transfection efficiency (red) were evaluated 24 hours post-pulse. Blue highlighter indicates the protocol I determined as most efficient.

Table 4.3: Combined percentages resulting from each MaxCyte GTx protocol.

Pulse Code	DNA Conc. ($\mu\text{g}/\text{mL}$)	% of viable LSK dTomato+ cells in total population	% of viable dTomato+ cells in total population
Opt 8	36	1.2	2.8
Opt 5	36	0.9	2.9
Opt 8	18	0.9	2.6
Opt 5	18	0.9	2.2
Opt 7	36	0.7	1.8
Opt 7	18	0.7	1.7
Opt 8	9	0.6	1.8
Opt 7	9	0.6	2.0
Opt 5	9	0.5	1.6
Opt 8	0	0.0	0.3
Opt 7	0	0.0	0.1
-	0	0.0	0.3
Opt 5	0	0.0	0.2

4.2.2 DNA Triggers Increased Secretion of IFN-Beta from Mouse HSPCs

To understand why mouse HSPC cell viability is negatively impacted upon DNA entry, the concentration of IFN β , IFN α , IL-6, IL-1 β , IFN γ , and TNF α was examined in the supernatant of transfected samples (Figure.4.7).³ I found high levels of IFN β present in the supernatant of samples treated with DNA.⁴ Pulsed control and non-pulsed control had a closer relationship, relative to DNA-treated samples, when comparing IFN β concentration. This suggests that DNA is responsible for its secretion. IFN β is classically associated with the cGAS-STING pathway [285]. The c-GAS-STING pathway might be involved in DNA's cellular immunogenicity.

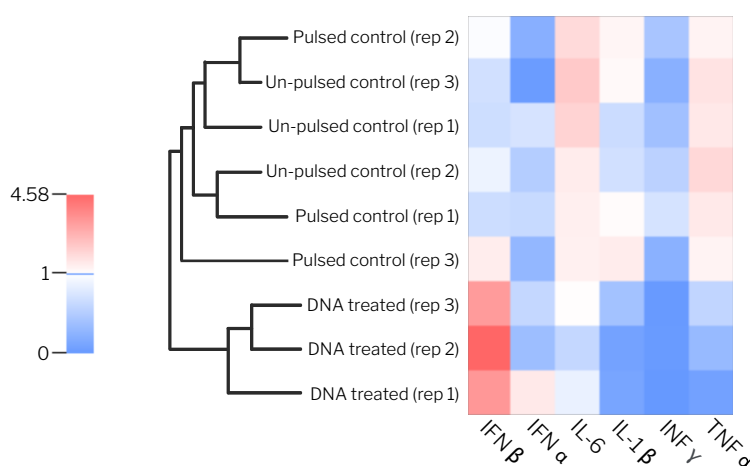


Figure 4.7: IFN- β is secreted upon cellular entry of DNA. Cluster heatmap comparing the concentrations of various cytokines (associated with DNA sensing pathways) in the supernatant 24 hours post-modification. Non-modified mHSPCs, mHSPCs pulsed without DNA, and mHSPCs pulsed with 100 $\mu\text{g}/\text{mL}$ of S/MAR DNA vectors were compared. Expression data were clustered using a Hierarchical algorithm with Pearson as the internal distance and Average as the external distance.

³Calibration curves for calculating cytokine concentration for Figure.4.7 are present in Appendix.B.9

⁴Adjusted p-value of 0.37 for treated samples vs. pulsed control. Adjusted p-value of 0.37 for treated samples vs. non-pulsed control. Adjusted p-value of 1 for pulsed control vs. un-pulsed control.



4.2.3 Inhibitors Reduce IFN-Beta Secretion, but Lead to no Improvements in Viability nor Transfection Efficiency

LEGENDplex analysis revealed IFN β release upon DNA vectors entering mouse HSPCs (Figure.4.7). Attempting to mitigate this, cells were treated with DNA sensing pathway inhibitors pre- and post-electroporation. Inhibitor 1 is an antagonist for the mouse STING protein (cGAS-STING pathway), inhibitor 2 is an antagonist for toll-like receptor (TLR) 7/8/9 (TLRs pathway), and inhibitor 3 is an antagonist for Caspase-1 (AIM2 pathway). Inhibitor concentrations are based on a pre-screening shown in Appendix.B.10. While inhibitors reduced cellular IFN β secretion, which may prevent alterations to HSPC functionality (Figure.4.8A), there were no significant improvements in viability nor transfection efficiency (Figure.4.8B). Literature describes CHIR99021 and ROCK to support the viability and self-renewal of various cell types [234, 332]. I found no reduction in IFN β when treating cells with CHIR99021 or ROCK. CHIR99021 and ROCK were associated with an average reduction in cell viability post-electroporation (Figure.4.8B). No significant differences were found between treatment groups comparing IFN β concentrations (Figure.4.8A) or transfection efficiencies (Figure.4.8B).

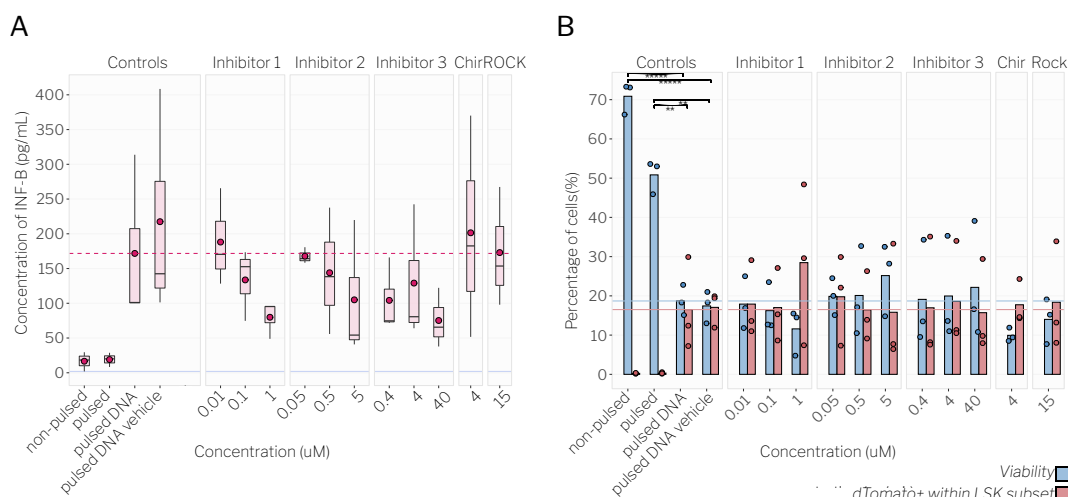


Figure 4.8: DNA sensing pathway antagonists reduce IFN β secretion from modified mHSPCs but lead to no significant improvements in viability nor transfection efficiency. 300,000 mHSPCs were treated with inhibitors for 16 hours before electroporation; inhibitors were added back in 3 hours post-pulse. The supernatant was collected 24 hours post-modification. A) Displays boxplots of IFN β concentration within the supernatant of electroporated cells treated with inhibitors. Pink dots indicate the mean concentration of IFN β within each subset. Data are representative of three independent experiments. B) Displays bar graphs representing mean cell viabilities and transfection efficiencies within each subset 24 hours post-modification. Statistics were calculated using Tukey one-way ANOVA. **adjusted p-value ≤ 0.01 . ****adjusted p-value ≤ 0.00001 .

4.2.4 AAVs Containing S/MARs Can Modify Mouse HSPCs and Improves Expression Persistence

An AAV viral vector delivered our S/MAR DNA construct into mHSPCs. I found improvements in the viability (50%) and transfection efficiency (72% in LSK cells) (Figure.4.9A)—relative to electroporation. Transfection efficiencies were higher in cell types more enriched for HSPCs, 40% in the viable cell population, 72% in the LSK population, and 76.3% in the LSK CD150+ population. Transgene expression persisted for at least 15 days (Figure.4.9B), which is at least 6 days longer than when using electroporation (Figure.4.5).

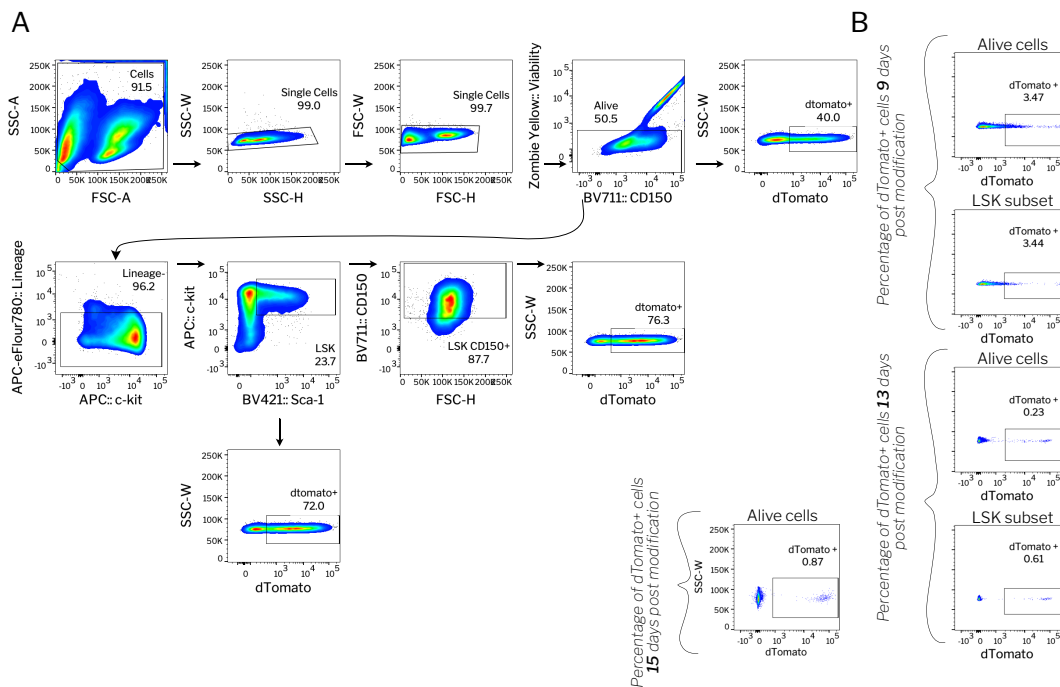


Figure 4.9: mHSPCs can be genetically modified using AAV viral vectors, and they extend transgene expression persistence. $1(10)^5$ cells were treated at an MOI of 10^5 . Transduction efficiency was assessed within the viable cell, lineage-, LSK, and LSK CD150+ cell subsets. A) FACS gating plots assessing the transduction efficiency 48 hours after treatment with AAV viral vectors. B) FACS gating plots assessing the percentage of alive cells and LSK cells expressing dTomato after transduction. The upper plots display the percentage of cells still expressing dTomato 9 days post-modification and the lower plots display the percentage of cells still expressing dTomato 13 and 15 days post-modification.



4.2.5 Section Discussion

Data in Figure.4.6 indicate that transfection efficiency and its associated viability are negatively correlated. To determine the protocol most efficient for the genetic modification of mHSPCs, viability and transfection efficiency both should be considered. Table.4.3 highlights the combined percentage of viable dTomato+ cells within the total population.

In Figure.4.7, $IFN\beta$ is upregulated in DNA-treated samples. Of the three DNA sensing pathways, $IFN\beta$ is classically associated with the cGAS-STING pathway [285]. This preliminary suggests that the c-GAS-STING pathway might be involved with DNA's cellular immunogenicity. An in-depth analysis is required to determine c-GAS-STING's involvement. $IFN\alpha$ is associated with TLR9 activation and the c-GAS STING pathway [212]. $IFN\gamma$ is a type II interferon that is not associated with a DNA sensing pathway. IL-6 is associated with TLR9 and c-GAS STING activation [212]. IL-1 β is indicative of AIM2 activation [212].

In Figure.4.9, the percentage of cells maintaining transgene expression was stable between 13 and 15 days. This could indicate that an established line was generated. Further analysis is required to determine this. Integration analysis is also required to confirm vectors are maintained episomally.

4.3 Conclusion

Mouse HSPC-like cells are supported by Yamazaki medium. Following MHEP, approximately 3 million cells per mouse are generated after a 10-day expansion, and HSPC enrichment is maintained. MHEP expanded cells could engraft in mice and persist for at least 4-months in secondary-engrafted mice. These results support their HSPC functionality. MHEP expanded HSPCs can be genetically modified using S/MAR DNA vectors. Though transgene expression only persists for 9 days and significant amounts of $IFN\beta$ are secreted upon DNA entry. Expression persistence was extended using AAVs, and the episomal maintenance of the vector is necessary to confirm.

4.4 Future Aims

Future aims pertaining to MHEP expanded HSPCs include:

- Assessing the karyotype of MHEP expanded mHSPCs.
- Repeating mouse engraftment using more replicates and conditions.
- Assessing if antagonists improve S/MAR DNA vector persistence within mouse HSPCs.
- Screening vector features in mHSPCs.



Chapter 5

Yielding HSPCs from S/MAR DNA Vector-Modified U-iPSCs

iPSCs have a promising outlook for treating various diseases [252]. Theoretically, they can differentiate into any human cell type and, subsequently, repair functionally defective tissues [252]. iPSCs are generated by reprogramming a differentiated cell, collected from a patient or healthy donor. Non-invasive methods to collect these cells of origin, such as through urine samples, are attractive as donors are imposed to less stress, and these methods are generally more cost-effective compared to classical invasive methods [252]. For their genetic alteration, genome integrating technologies are frequently used as they provide stable transgene expression in mitotically active and differentiating cells [252]. An adverse consequence of using integrating systems is their risk of genotoxicity [252]. I intended to avoid this risk while maintaining the same efficacy as these systems by using S/MAR DNA vectors [252].

In this chapter, I describe a process for generating HSPCs from urinary-derived human iPSCs stably modified with our non-integrating S/MAR DNA vectors—using optimal vector features determined in chapter 3. This acts as an intermediate step in the development of an off-the-shelf T-cell or NK-cell immunotherapy.

5.1 Urinary Stem Cells Can be Reprogrammed Into iPSCs

Within this section, I describe how urinary-derived iPSCs are generated. Cells are collected from urine samples and subsequently plated in the appropriate conditions to support the growth and survival of urinary stem cells (USC). EBNA-based reprogramming vectors are inserted into these USCs and cultured in the appropriate medium conditions to support their transformation toward iPSCs. A schematic representation of this process is displayed in Figure.5.1A. U-iPSCs generated within our lab express alkaline phosphatase as well as pluripotency markers Lin28, Nanog, Tra-1-60, and Oct3/4, which supports their iPSC phenotype (Figure.5.1C). iPSCs were successfully trilineage differentiated—differentiated into cells apart of the mesoderm, endoderm, and ectoderm. This supports their functionality (Figure.5.1B). This U-iPSC line was genetically modified to express a report gene. These data are described in section 5.2.

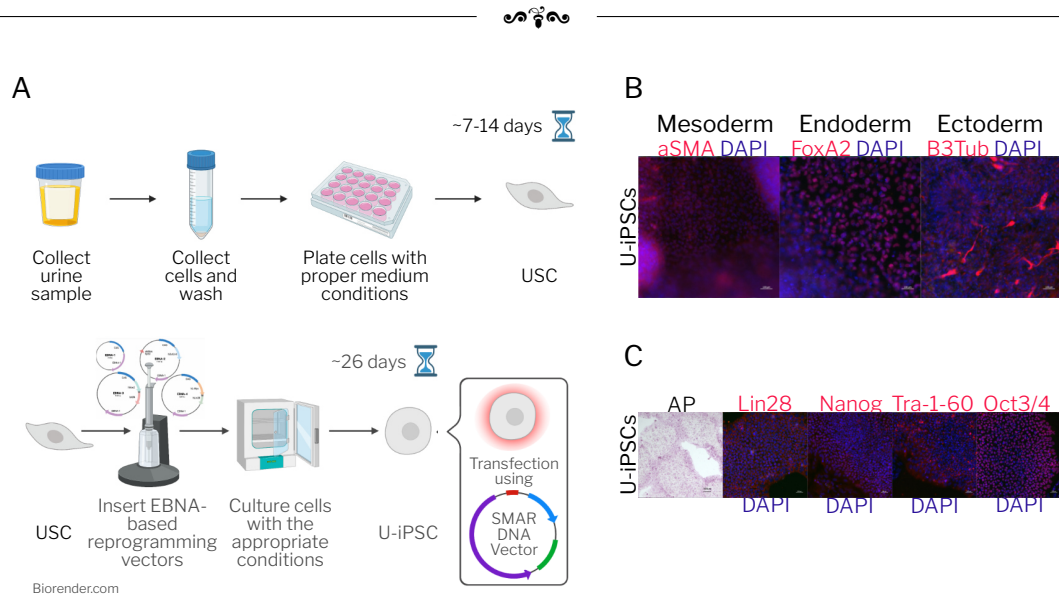


Figure 5.1: Schematic representation of urinary stem cell reprogramming. A) Cells are extracted from urine samples and subsequently plated in the appropriate conditions to support the growth and survival of USCs. After 7-14 days, USCs are transfected with EBNA-based reprogramming vectors and placed in the appropriate medium conditions to support their transformation toward iPSCs. B) IF images of urinary-derived iPSCs (U-iPSCs) that underwent trilineage differentiation. This validates the functionality of our U-iPSCs. Germ layer marker expression (aSMA: mesoderm, FoxA2: endoderm, and B3Tub: Ectoderm) is shown in red; DAPI counterstaining is shown in blue. C) Images of alkaline phosphatase (AP) and pluripotency marker expression in U-iPSCs. This validates the phenotype of our U-iPSCs. Pluripotency markers (Lin28, Nanog, Tra-1-60, and Oct3/4) are shown in red, DAPI counterstaining is shown in blue. Data was obtained from Manuela Urban [319].

5.1.1 Section Discussion

iPSC functionality and phenotype were assessed using trilineage differentiation and immunofluorescence (IF) staining, respectively. This report lacks studies that investigate genetic abnormalities, such as karyotyping. iPSCs lines should be regularly screened for genetic abnormalities to prevent the outgrowth of carcinogenic cells. This is a future aim. Within this report, genetic modification was performed on iPSC lines between passages 11 and 12.

5.2 U-iPSCs are Genetically Modified With the Latest S/MAR DNA Vector

An S/MAR DNA vector containing sEF1 (promoter), dTomato (transgene), S/MAR-4, and NTX RNA-out R6K (production backbone) was used for this proof of concept study (Figure.5.2A), as data suggest these are the most optimal vector features for iPSCs and T-cells (based on results obtained in Chapter 3). A lentiviral vector containing an identical expression cassette was also produced and used as a positive control (Figure.5.2B).

iPSCs modified with this S/MAR DNA vector had an average transfection efficiency of 81% (3 days post-transfection), and iPSCs modified with lentiviral vectors had an average



transfection efficiency of 33% (3-days post-transduction) (Figure.5.3A). At this point, the geometric MFI of S/MAR DNA vector-modified iPSCs was higher relative to lentiviral vector-modified iPSCs (Figure.5.3B), which is also visibly noticeable via microscopy (Figure.5.3C and 5.3D). As the same cell density was seeded before modification, one can visibly compare cell death rates between iPSCs modified with S/MAR DNA vectors and lentiviral vectors (Figure.5.3C and 5.3D). A higher number of viable cells are visibly present after treatment with S/MAR DNA relative to treatment with lentiviral vectors.

Cellular establishment is defined as the point when the subset of cells retaining long-term transgene expression stably persists while cells with transient transgene expression have lost expression. At this point, when cells expressing dTomato are collected, the line should be stably established. Using this S/MAR DNA vector, an establishment rate of 0.026% was obtained, and establishment was supported by the retention of transgene expression 1-month post-sort (Figure.5.4). This establishment percentage was considered decent considering establishment data obtained in sections 3.3.1 and 3.4.1 (0.0555% to 0%). For the lentiviral vector, a 2-week establishment protocol was followed as this is a typical time frame to establish lentiviral vector-modified lines. 1-month post-sort, the percentage of cell remaining dTomato+ dropped to 62%. Fluorescent intensity was also compared, and cells modified using an S/MAR DNA vector had a higher fluorescent intensity, relative to lentiviral vector-modified cells (Figure.5.4C).

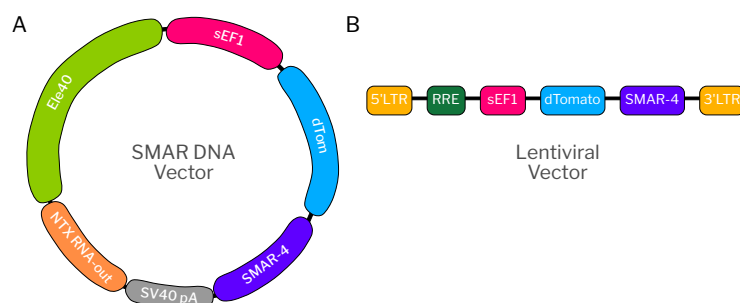


Figure 5.2: Schematic representation of S/MAR DNA vector and lentiviral vector provirus used for U-iPSC modification. A) The S/MAR DNA vector used consists of the insulator element40 (Ele40), short elongation factor 1 (sEF1), dTomato (dTom), our S/MAR4, the SV40 poly-A tail (poly-A), and the NTX RNA-out R6K. B) Lentiviral vectors consist of an identical expression cassette flanked by HIV LTRs.

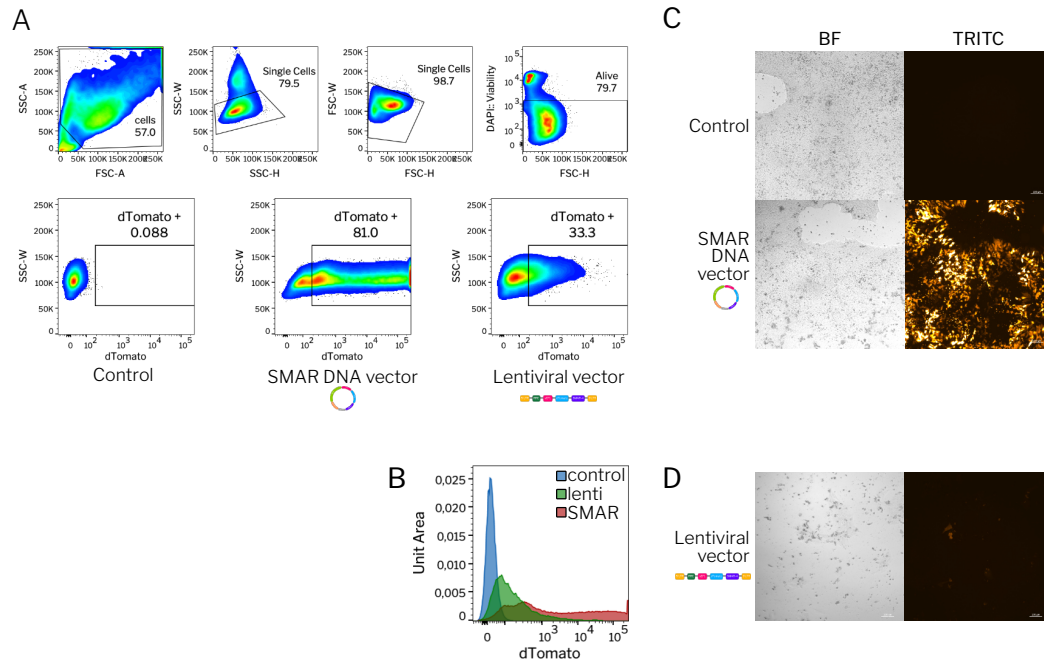


Figure 5.3: Transfection and transduction of human iPSCs using vectors containing S/MARs. $5(10)^4$ iPSCs were seeded. 24 hours later, a full medium change was performed; Lipofectamine STEM/DNA complexes or lentiviral vectors were added to the appropriate wells. For samples containing lentiviral vectors, a full medium change was performed 24 hours after their addition. For samples containing S/MAR DNA vectors, a full medium change was performed 3 days after their addition. A) FACS gating scheme used to assess S/MAR vector transfection efficiency and lentiviral vector transduction efficiency 3 days post-modification. B) Displays the intensity of transgene expression 3 days post-modification. Data were normalized by unit area. C) Microscope images of U-iPSCs transfected with our S/MAR DNA vectors. Images are displayed at 100x and show transgene expression 3 days post-transfection. D) Microscope images of U-iPSCs transduced with a lentiviral vector containing similar features as our S/MAR DNA vector. Images are displayed at 100x and display transgene expression 3 days post-transduction. Data contains two independent experiments with two replicates each.

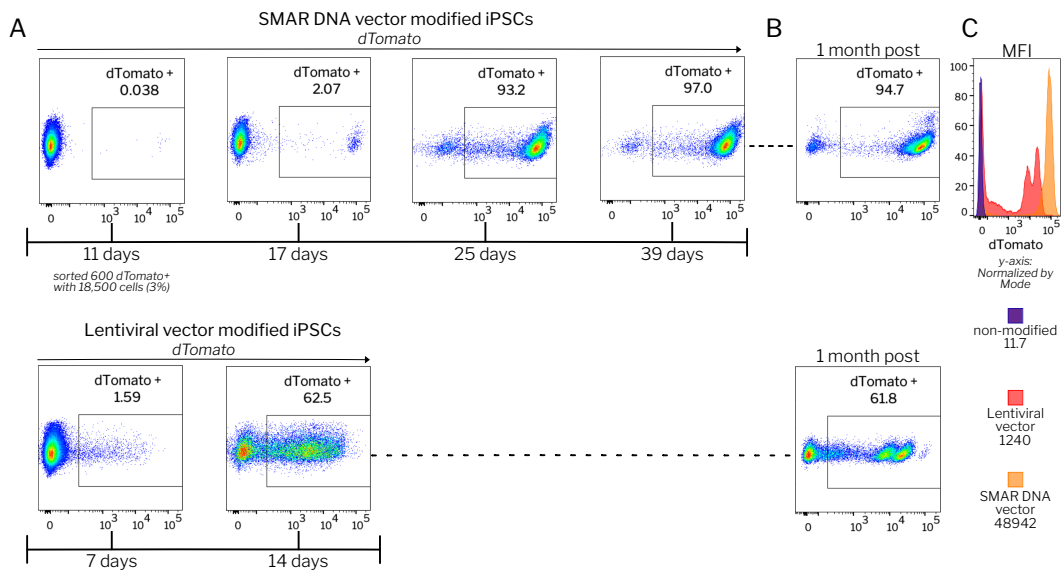


Figure 5.4: U-iPSC lines stably expressing dTomato were generated using S/MAR DNA vectors and lentiviral vectors. A) U-iPSC lines were generated via passive selection. These data show FACS gating plots on the days transgene expressing cells were collected. The top row of FACS plots display the establishment of S/MAR DNA vector-modified U-iPSCs. Sortings took place 11, 17, 25, and 39 days post-modification. The bottom row of FACS plots shows the establishment of lentiviral vector-modified U-iPSCs. Sortings took place 7 and 14 days post-modification, which follows a classic scheme for establishing lentiviral vector-modified cell lines. B) Displays the percentage of cells still expressing dTomato 1-month post the final sort. At this point, 90-100% of cells should express the transgene to consider the line stably established. C) Displays the intensity of transgene expression 1-month post the final sort. Data were normalized by Mode, and geometric MFI is noted. Non-modified cells are represented by the color purple, S/MAR DNA vector-modified cells by orange, and lentiviral vector-modified cells by red.



5.2.1 Section Discussion

One should be mindful of a direct comparison between S/MAR DNA vectors and lentiviral vectors as they are different constructs with different treatment methods. A production backbone is not present in the lentiviral vector provirus as it is an irrelevant feature to incorporate—while it is present in the S/MAR DNA vector. A direct comparison is appropriate for particular questions, such as the general difference in modifying iPSCs using a lentiviral vector with its optimal protocol vs. an S/MAR DNA vector with its optimal protocol. I found S/MAR DNA vectors result in a higher transfection efficiency as well as stronger transgene expression, relative to the lentiviral vector, which may be beneficial for differentiation processes that dampen transgene expression. 1-month post-establishment, lines should maintain dTomato expression in 90-100% of cells. A negligible drop in the percentage of cells retaining transgene expression was present for iPSCs modified using the S/MAR DNA vector while a significant drop was present using the lentiviral vector (Figure.5.4). For future comparisons, the addition of Element40 into the lentiviral vector construct would act as a more precise comparison to the S/MAR DNA vector. It would be interesting to assess the retention of cells maintaining dTomato expression using this lentiviral vector construct.

A second-generation lentiviral vector was generated and used for these experiments. A comparison between S/MAR DNA vectors and a third-generation lentiviral vector would be more clinically relevant and is a future aim.

Microscope images were used to compare the cell viability of iPSCs as they are adherent cells—dead cells are aspirated during medium changes. One could use FACS count beads to obtain absolute cell counts (this was performed in sections 3.4.1 and 3.3.1). In this section, microscope images were used because a difference in cell viability was visually apparent.



5.3 Modified Lines Remain Phenotypically Similar to Non-Modified U-iPSCs

U-iPSC lines stably established with S/MAR DNA vectors were assessed for iPSC phenotypic characteristics (Figure.5.5). For that, I observed the production of alkaline phosphatase as well as the expression of Lin28, Nanog, Tra-1-60, and Oct3/4. No visible differences were present between non-modified U-iPSCs, S/MAR DNA vector-modified U-iPSCs, and lentiviral vector-modified U-iPSCs. A visible difference in dTomato expression was apparent between these lines, as expected.

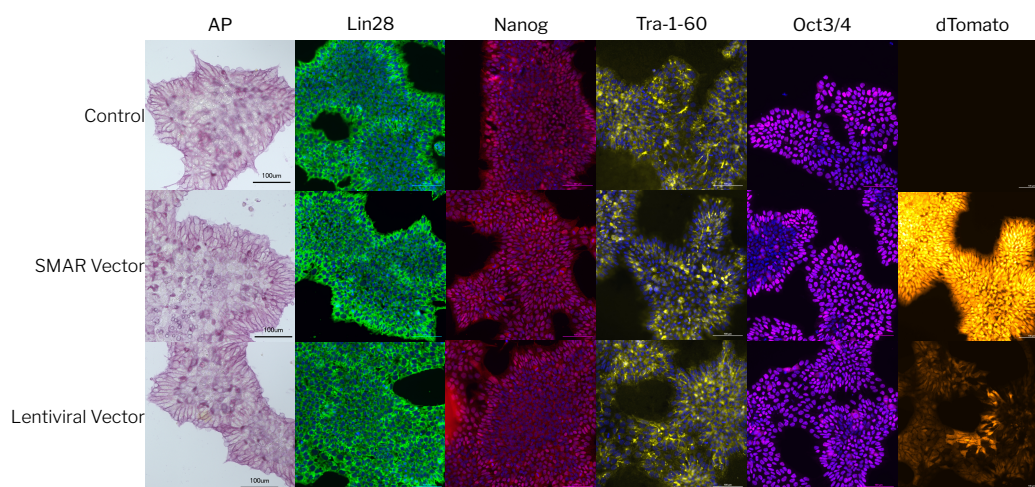


Figure 5.5: Microscope images of established U-iPSCs lines taken at 200x magnification assessing alkaline phosphatase expression and the expression of various pluripotency markers. This validates the phenotype of our modified U-iPSC lines. Lin28 expression is shown in green, Nanog expression is shown in red, Tra-1-60 expression is shown in yellow, and Oct3/4 expression is shown in purple. DAPI counterstaining is shown in blue. dTomato expression is shown in orange.

5.3.1 Section Discussion

The phenotype of U-iPSC lines was assessed using IF of Lin28, Nanog, Tra-1-60, and Oct3/4. Comparing the phenotype of modified U-iPSC lines to non-modified U-iPSC lines is a helpful indicator of iPSC functionality as trilineage differentiation has been performed for the non-modified U-iPSC line (Figure.5.1). A trilineage differentiation is still required to determine the functionality of these modified lines. However, these data provide an helpful indication of it. Vector integration analysis and a screening for genetic abnormalities are lacking, and are a future aim.

5.4 U-iPSC Lines Can Differentiate Into HSP-Like Cells

U-iPSC lines underwent differentiation into HSPCs using the STEMdiff™ Hematopoietic Kit (method 1, described in methods 8.1.6.1). A subset of iPSCs remained in culture so the effects of differentiation on transgene expression could be assessed. Visually, dTomato expression persisted during the differentiation process (Figure.5.7A). Cellular morphologies were representative of HSPC-like cells—single cell suspension. Assessing the phenotype via FACS, marker expression showed 45% of CD43+ CD34+ cells (population 1, Figure.5.7B) were present in all samples, indicating that HSPC-like cells were present. Within population 1, 21% of cells were CD45+ CD90+ for non-modified and S/MAR DNA vector-modified cells while lentiviral vector-modified cells contained 13% CD45+ CD90+ cells within population 1. The percentage of cell expressing dTomato within population 2 was 94% for S/MAR DNA vector-modified cells and 67% for lentiviral vector-modified cells. A minimal drop in the percentage of cells expressing dTomato was observed after differentiation of S/MAR DNA vector-modified iPSCs, from 99% to 94%. Differentiation of lentiviral vector-modified iPSCs into HSPCs led to a larger drop in the percentage of cells expressing dTomato, from 78% to 67%. For both S/MAR DNA vector-modified cells and lentiviral vector-modified cells, a drop in the fluorescence intensity was observed after HSPC differentiation (Figure.5.7B). I also assessed the percentage of CD45+ cells primed for the myeloid lineage, by observing CD33 expression (Figure.5.6). I found 42% of non-modified iPSC-derived CD45+ cells express CD33, 43% of lentiviral vector-modified iPSC-derived CD45+ cells express CD33, and 53% of S/MAR DNA vector-modified iPSC-derived CD45+ cells express CD33. Cells underwent a colony-forming unit (CFU) assay to assess their HSPC functionality (Figure.5.8). I observed various hematopoietic progenitor cells in CFU for S/MAR DNA vector-modified iPSC-derived HSPCs. CFU-E, BFU-E, CFU-GM, and CFU-GEMM were all present. Non-modified and lentiviral vector-modified iPSC-derived HSPCs had many CFU-E colonies and one BFU-E present on average. Non-modified iPSC-derived HSPCs additionally displayed 2 CFU-GM colonies on average.

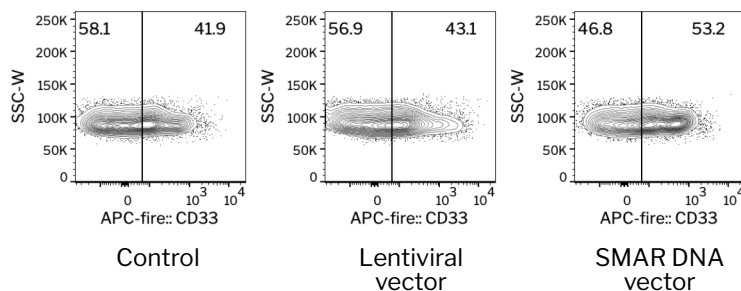


Figure 5.6: Approximately half of iPSC derived CD45+ cells are primed for the myeloid lineage following method 1. iPSCs underwent HSPC differentiation using the STEMdiff™ Hematopoietic Kit. FACS plots display the percentage of CD33+ and CD33- cells within the CD45+ population on day 12.

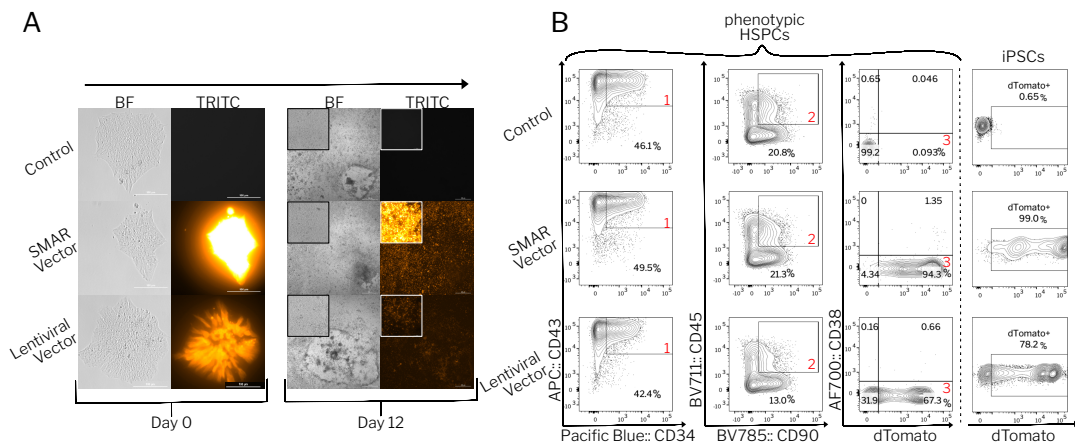


Figure 5.7: S/MAR DNA vector-modified U-iPSCs can differentiate into HSPC-like cells. A) Displays microscope images of U-iPSC lines on day 0 and day 12 of HSPC differentiation. Images were taken at 200x on day 0 and 40x (large images) and 200x (small images) on day 12. dTomato expression is displayed in orange. B) FACS gating plots showing the percentage of cells expressing various HSPC surface markers. Population 1 shows CD43+ CD34+ cells. Population 2 shows CD43+ CD34+ CD90+ CD45+ cells. Population 3 shows CD43+ CD34+ CD90+ CD45+ CD38- dTomato+ cells. Undifferentiated U-iPSCs were cultured in parallel to compare the relative drop in the percentage of cells expressing the transgene after HSPC differentiation. Marker expression within the live cell population is shown here. CD43, embryonic pan-hematopoietic marker; CD45, hematopoietic cells (nucleated); CD34- CD38- CD90+, enriched human HSCs. Data are representative of 2 independent experiments with 2 replicates.

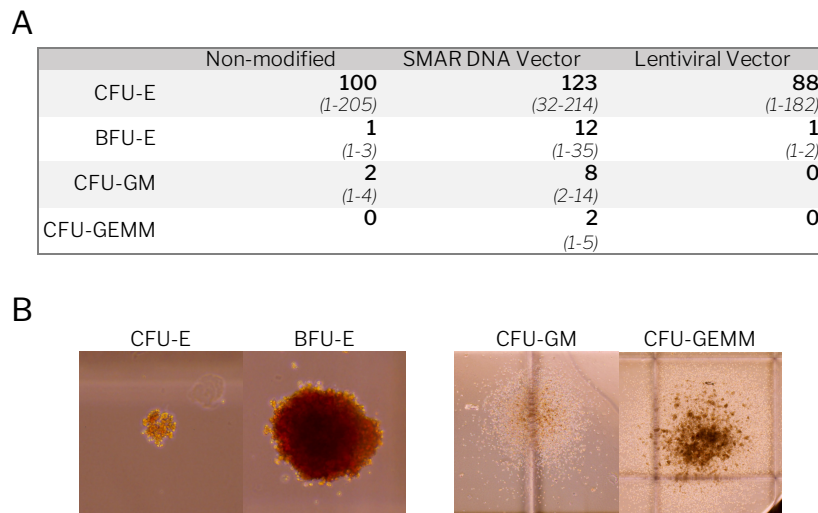


Figure 5.8: U-iPSC lines could produce hematopoietic progenitor cells in CFU. A) Displays HSPC cell colony frequencies produced from U-iPSC derived HSPCs. Data are representative of 2 independent experiments containing 2 replicates each. Mean values \pm 2 standard deviations are displayed. B) Microscope images of a CFU-E, BFU-E, CFU-GM, and CFU-GEMM colony. CFU-E, colony-forming unit-erythroid; BFU-E, burst-forming unit-erythroid; CFU-GM, colony-forming unit-granulocyte, macrophage; CFU-GEMM, colony-forming unit-granulocyte, erythrocyte, macrophage, megakaryocyte.



5.4.1 Section Discussion

The functionality of iPSC-derived HSPCs was supported by their ability to produce CFUs. However, when they underwent T-cell differentiation following method 1, marker expression indicated a poor success rate for T-cell development (Appendix.B.11). This lack of success might be associated to the high expression of CD33 found on CD45+ cells produced following method 1. CD33 is a surface marker for progenitor myeloid cells [287]. T-cells are not a part of the myeloid lineage, they are a part of the lymphoid lineage, which should be CD33-. Approximately half of the HSPCs produced following method 1 are CD33+. Literature reports the expression of CD33 also on HSCs [306]; this study defined an HSC as Lin-CD34+CD38-, which is a population primarily composed of lineage-committed progenitors. It is important to be mindful that CD33 could also be expressed on other hematopoietic populations. In general, CD33 expression gives a good indication of the frequency of myeloid primed progenitor cells. I decided to repeat iPSC differentiation into HSPCs following methods from STEMdiff™ T Cell Kit (method 2). A description of these results is described in section 5.5.

For a discussion on iPSC-derived CD43 expression, see section 5.5.1.

To obtain a better indication of HSPC functionally, a CFU assay was performed (Figure.5.8). CFU assays have a bias for multipotent and lineage-restricted myeloid cells, specifically erythroid (CFU-E and BFU-E) granulocytic and macrophage (CFU-GM) and progenitors apart of both (CFU-GEMM) [297]. This assay primarily supports the growth of hematopoietic progenitor cells with minimal self-renewal [297]. A CFU assay indicates if certain HSPCs are present. A mouse study using a humanized mouse model is arguably the most reliable test to determine the HSC enrichment and function. In Figure.5.7B, HSPC marker expression was assessed. This provides an indication that cells are phenotypically similar to HSPCs. Their HSPC characteristic is also supported by data shown in the CFU assay.

A drop in the percentage of cells expressing dTomato was observed for lentiviral vector-modified iPSC-derived HSPCs following method 1 (Figure.5.7B). As described in section 5.2.1, iPSCs modified using a lentiviral vector containing Element40 might improve cell's retention of dTomato expression. This is a future aim.



5.5 U-iPSC Lines Can Differentiate Into HSP-Like Cells Primed for the Lymphoid Lineage

Established iPSC lines were differentiated into HSPCs following method 2 (methods described in methods 8.1.6.2). Non-modified iPSC-derived HSPCs had a viability of 76.5%, lentiviral vector-modified iPSC-derived HSPCs had a viability of 76.8%, and S/MAR DNA vector-modified iPSC-derived HSPCs have a viability of 52.6%. Approximately 61% of lentiviral vector-modified cells were CD34+, 55% of S/MAR DNA vector-modified cells were CD34+, and 25% of non-modified cells were CD34+ (Figure.5.9). This subpopulation is most important to assess as T-cell differentiation is performed using CD34+ cells. I also examined CD45, CD38, and CD90 expression. The CD38- CD90+ population within the CD34+ CD45+ population is a more enriched population of HSC-like cells. Approximately 9% of non-modified, 6.5% of S/MAR DNA vector-modified, and 5.6% of lentiviral vector-modified iPSC-derived HSPCs were CD34+ CD45+ CD38- CD90+. These data support their HSPC-like phenotype. Their HSPC functionality was supported by non-modified iPSC lines differentiating into phenotypic T-cells (Figure.5.12).

I examined CD33 expression on CD45+ cells to get an indication of the percentage of HSPCs not primed for the myeloid lineage (Figure.5.11). Following method 2, >90% of CD45+ cells on average were CD33- (non-myeloid primed) for each iPSC line used—non-modified iPSCs, 97.5%; lentiviral vector-modified iPSCs, 95.6%; S/MAR DNA vector-modified iPSCs, 90.1%. For a further description of CD33 expression, see section 5.4.1.

dTomato expression was compared in Figure.5.10. There was a drop in the percentage of cells retaining dTomato expression after HSPC differentiation. 99.7% of S/MAR DNA vector-modified iPSCs expressed dTomato while those that underwent HSPC differentiation following method 2 had 60.6% of cells retaining dTomato expression. The lentiviral vector-modified iPSC lines went from 90.7% to 27% dTomato+ cells after HSPC differentiation. Transgene MFI also dropped after HSPC differentiation of dTomato expressing iPSC lines. The intensity of dTomato expression within the formed EBs was visually stronger in S/MAR DNA vector-modified lines relative to lentiviral vector-modified lines (figure.5.10C).

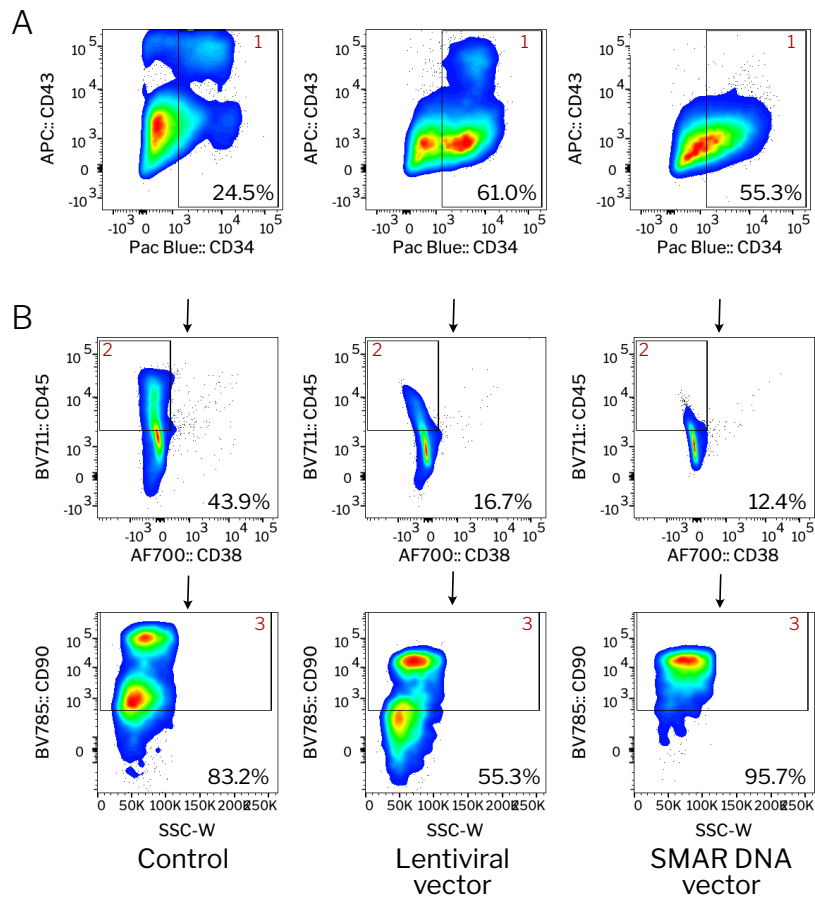


Figure 5.9: FACS plots displaying the enrichment of HSPC-like cells within our differentiated iPSC population following method 2. A) FACS gating plots showing the percentage of CD34+ cells using non-modified iPSCs, lentiviral vector-modified iPSCs, and S/MAR DNA vector-modified iPSCs for HSPC differentiation. Population 1 shows CD34+ cells. B) FACS gating plots showing the percentage of cells expressing various HSPC surface markers. Population 2 shows CD34+ CD45+ CD38- cells. Population 3 shows CD34+ CD45+ CD38- CD90+ cells. HSPCs were created using the STEMdiff™ T Cell Kit (Stem Cell Technologies). Marker expression within the live cell population is shown here. CD43, embryonic pan-hematopoietic marker; CD45, hematopoietic cells (nucleated); CD34- CD38- CD90+, enriched human HSCs. Data is representative of 1 experiment with two replicates.

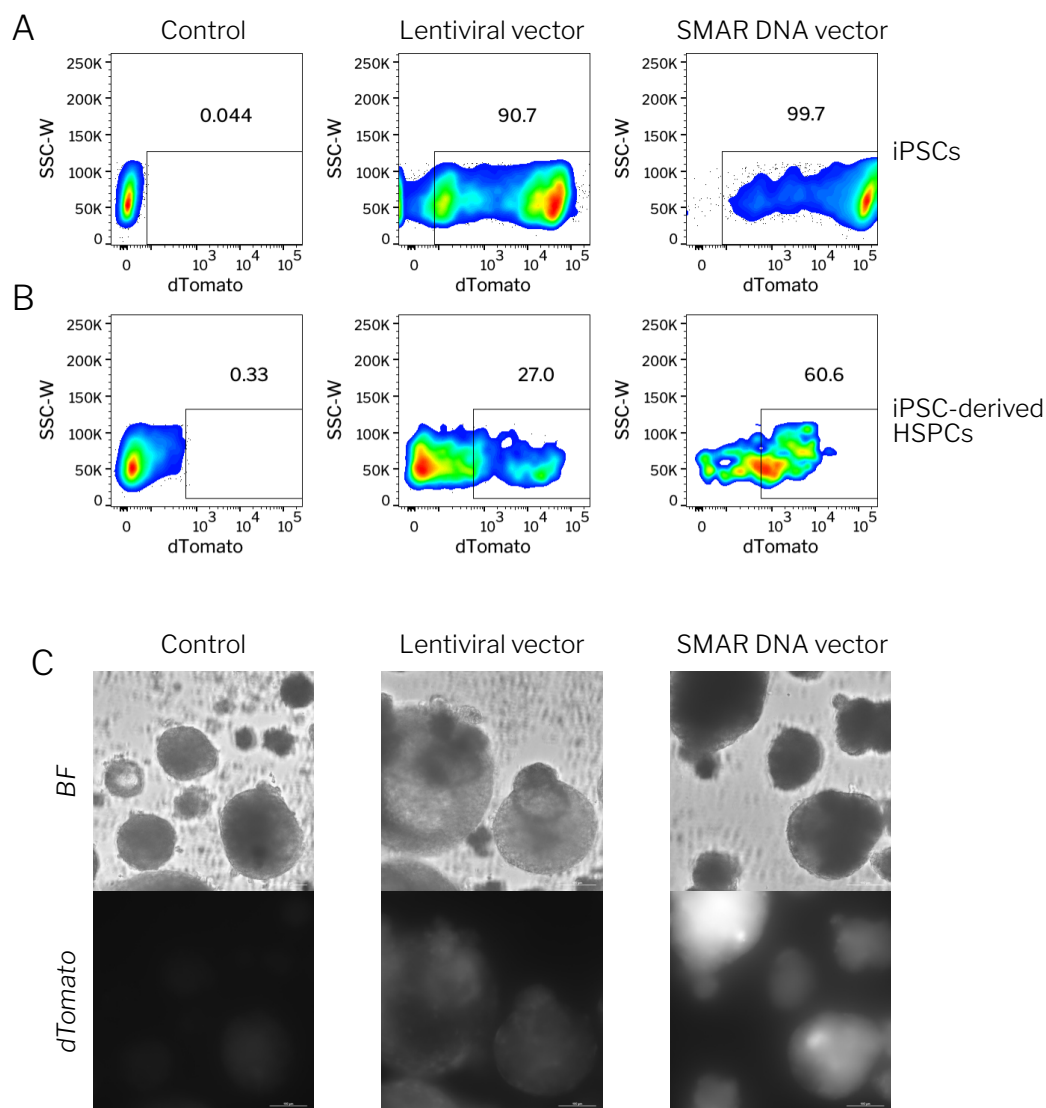


Figure 5.10: Alterations in dTomato expression were observed after iPSCs were differentiated into HSPCs following method 2. A) Shows dTomato expression of iPSCs (that were used for HSPC differentiation). These cells were kept in culture in parallel with HSPC differentiated cells, and dTomato expression was assessed on the final day of HSPC differentiation (day 12). B) Shows dTomato expression on the final day of HSPC differentiation (day 12) C) Displays microscope images of U-iPSC lines on day 12 of HSPC differentiation. Brightfield images are shown above; TRITC channel images are shown below. Images were taken at 200x. Data representative of 1 experiment with two replicates.

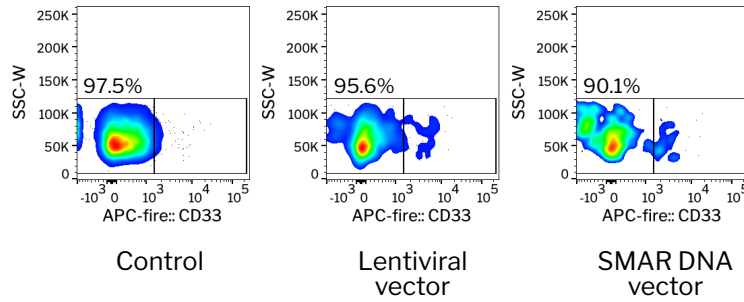


Figure 5.11: The majority of iPSC-derived CD45+ HSPCs produced following method 2 are CD33-. HSPCs were created using the STEMdiff™ T Cell Kit (Stem Cell Technologies). CD33 marker expression within the alive CD45+ cell population is shown here. CD33, transmembrane receptor expressed on cells apart of the myeloid lineage. Data representative of 1 experiment with two replicates.

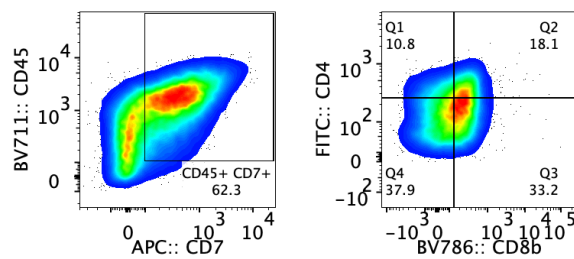


Figure 5.12: U-iPSC-derived CD34+ cells differentiate into phenotypic T-cells following method 2. FACS analysis of U-iPSC-derived CD34+ cells that underwent T-cell differentiation following method 2. CD45, hematopoietic cells (nucleated); CD7, early-stage T-cell marker; CD4, late-stage T-cell marker; CD8, late-stage T-cell marker. Data representative of 1 experiment with two replicates.



5.5.1 Section Discussion

One downfall of using method 2 is the total cell count achieved. Cultures start with 700,000 U-iPSCs and around 10,000 CD34+ cells were produced. Scaling-up for clinical applications might be a problem when utilizing this protocol; it might be beneficial to use another protocol to reach clinically relevant numbers.

In Figure.5.9, CD43 marker expression is displayed, yet the percentage of cells expressing it was not used to calculate the enrichment of HSPCs. CD43 is an important marker that indicates iPSCs/ESCs are differentiating toward hematopoietic cells [326]. The expression of it is also associated with extra-embryonic hematopoietic systems, such as the yolk sac, which is where the first blood cells appear [291, 214]. Yolk sac progenitor blood cells have been reported to successfully produce erythrocytes, megakaryocytes, macrophages, neutrophils, granulocytes, and mast cells, but lack HSC functionality [291, 240, 195, 194, 292]. They are also reported to not generate lymphoid cells and to have a limited capacity for the maintenance of myeloid cells [75]. Unlike yolk sac blood cells, hematopoietic cells apart of the intraembryonic splanchnopleure are shown to produce lymphocytes and multipotent myeloid precursors that contribute to definitive hemopoiesis [75]. *In vitro* differentiation protocols for producing iPSC-derived HSCs indicate the importance of differentiation toward the intra-embryonic blood program (CD43-), rather than the extra-embryonic hematopoietic program (yolk sac-type hematopoiesis) (CD43+) after mesoderm formation has occurred [214]. CD43+ is an early marker indicating iPSCs/ESCs have differentiated toward hematopoietic cells [326]. However, the expression of it after mesoderm formation suggests yolk sac-type hematopoiesis formation, which is unwanted especially for T-cell differentiation [214]. Thus, CD43 was not used to calculate the enrichment of HSPCs in Figure.5.9.

In Figure.5.9, I considered the percentage of CD34+ cells to be the most important, rather than markers for high HSC-like enrichment, such as CD90+ and CD38-. This is because the presence of lymphoid progenitor cells in the CD34+ population might be excluded in more enriched HSC-like populations. It wouldn't be as reliable of a measure for predicting the success of T-cell development.

In Figure.5.10, dTomato expression was assessed in iPSCs undergoing HSPC differentiation. Transgene MFI dropped, as well as the percentage of cells retaining transgene expression. There was a larger drop in transgene retention for lentiviral vector-modified lines relative to S/MAR DNA vector-modified lines. The drop in the percentage of cells retaining transgene expression is a potential problem for the efficacy of a cell therapy. Especially if the retention of transgene expression further drops after T-cell differentiation. As mentioned previously, it would be interesting to assess the retention of dTomato expression with iPSCs modified with a lentiviral vector containing Element40 (Further described in section 5.2.1).

In Figure.5.12, iPSCs-derived T-cells were produced following method 2. FACS analysis supports the phenotype of these T-cells. Cells have undergone, lymphoid progenitor cell expansion and T-cell maturation. At this stage, one would expect a high percentage of CD4+ CD8+ cells, which is the case (approximately 27%).



5.6 Conclusion

Urinary-derived cells are a good cell source for reprogramming (section 5.1) [252]. They can be genetically engineered using S/MAR DNA vectors, and it results in high transfection efficiencies (80%) as well as high MFIs (section 5.2). Stable transgene expressing U-iPSC lines can be created, and their iPSC phenotype remains similar to non-modified U-iPSCs (sections 5.2 and 5.3). Genetically modified U-iPSCs can differentiate into phenotypic and functional HSPCs, and transgene expression persists (section 5.4). Finally, iPSC-derived HSPCs can be differentiated into phenotypic T-cells (section 5.5). In Chapter 6, I describe how iPSCs expressing a CAR can be differentiated into phenotypic T-cells.

5.7 Future Aims

Future aims pertaining to iSPCs and iPSC-derived HSPCs include:

- Further data supporting the functionality of the genetically modified iSPCs via trilineage differentiation.
- Karyotyping and genetic analysis of iSPCs and iPSC-derived HSPCs to assess and screen for oncogenic potential.
- Scaling-up for clinical applications.



Chapter 6

Yielding Anti-CEA CAR T-Cells From S/MAR DNA Vector-Modified U-iPSCs

Within this chapter, iPSCs are genetically modified to express a CAR, and these data preliminarily indicate that such cells can differentiate into phenotypic T-cells. T-cell production is based on method 2 described in method 8.1.7.1. Data on iPSC-derived HSPCs, primed for the lymphoid lineage, are described in section 5.5.



6.1 U-iPSCs Can be Engineered to Express Anti-CEA CAR

Preliminary data indicate a low transfection efficiency (3%) in iPSCs using an S/MAR DNA vector containing anti-CEA CAR as the transgene (Figure.6.1A). Nevertheless, iPSCs expressing anti-CEA were able to be collected, and data indicate a population maintaining up to 50% of anti-CEA expressing iPSCs (Figure.6.1B)—a 100% stably established line was not generated. After the final sort, cells were cryopreserved. Three months later, the anti-CEA iPSC line was thawed and the percentage of cells expressing anti-CEA was assessed (Figure.6.1C). Data indicate a similar percentage of cells expressing anti-CEA prior to cryopreservation (53% relative to 51%). iPSC phenotype was assessed for the presence of AP production and the expression of pluripotency markers Tra-1-60, Nanog, Lin28, and Oct3/4 (Figure.6.1D).

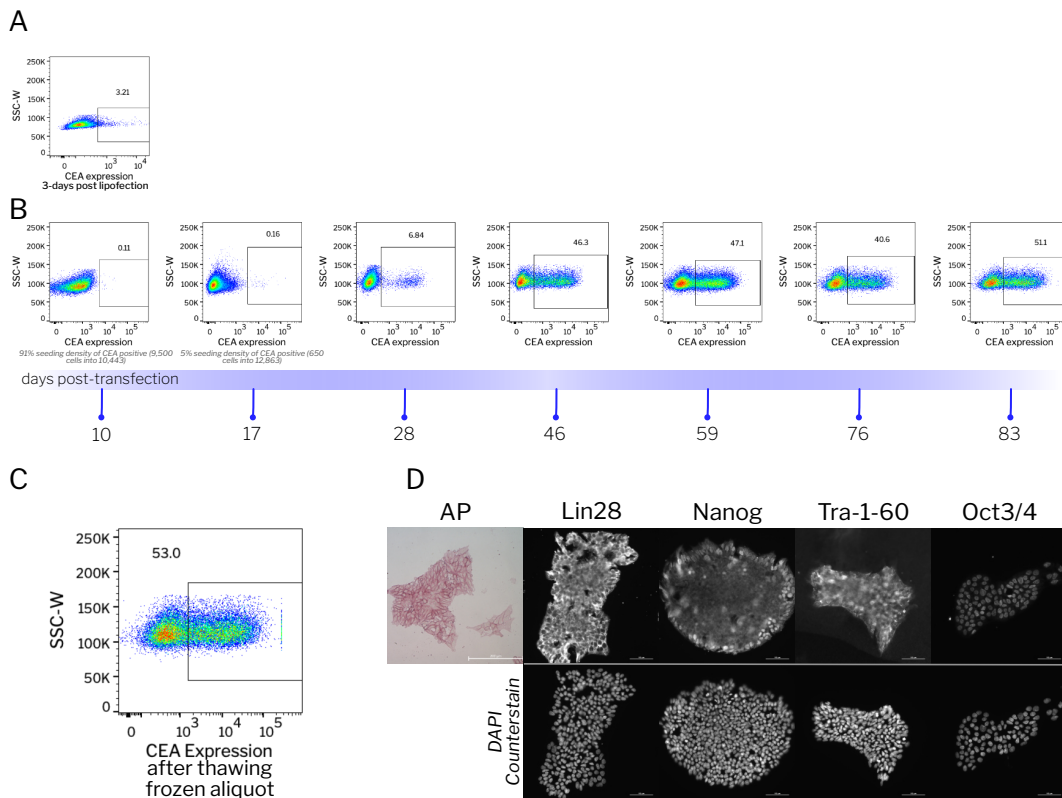


Figure 6.1: iPSCs can be engineered to express anti-CEA CAR. A) Displays FACS plot of anti-CEA expression in iPSCs 3 days post-lipoflection. B) Displays FACS plots of anti-CEA expression in iPSCs while developing the line. The timeline indicates days post-transfection when anti-CEA expressing cells were collected. C) FACS plot displaying anti-CEA expression after thawing cryopreserved cells. D) AP and IF staining of anti-CEA iPSC line. Images are displayed at 200x.



6.2 Anti-CEA iPSC-Derived CD34+ Cells Can Differentiate Into Phenotypic T-Cells

The anti-CEA iPSC line was differentiated in HSPCs (Appendix.B.12). CD34+ cells from these iPSC-derived HSPCs were used for T-cell differentiation following method 2 (Figure.6.2A). Differentiation consisted of two phases: lymphoid progenitor expansion, then T-cell maturation. Data indicate approximately 40% of anti-CEA cells expressed CD5 and CD7 after undergoing lymphoid expansion (Figure.6.2B), and approximately 22% of these CD5+ CD7+ cells were double positive for CD4 and CD8. Within this subset, 98% of the cells were expressing anti-CEA. After T-cell maturation (Figure.6.2C), 32% of anti-CEA cells were CD8 single positive, and nearly 100% of cells within this subset were CD3 positive. 98% of CD8b+ CD3+ cells were expressing anti-CEA. The viability for anti-CEA cells was approximately 56% post-lymphoid expansion and 68% after T-cell maturation.

T-cell differentiation was also performed using the dTomato iPSC line developed in section 5.2. After T-cell maturation, 78% of cells were CD8 single positive and nearly all CD8+ cells were CD3+. Despite starting cultures out with 85% dTomato+ cells (Appendix.B.12), 1% of CD8+ cells were expressing dTomato after T-cell maturation (Figure.6.2D).

6.3 Discussion

Data in Figure.6.1 indicate that a stably established iPSC line expressing anti-CEA was not created; anti-CEA expression continuously dropped. HSPC differentiation of anti-CEA iPSCs was associated with 32% of CD34+ CD45+ cells expressing anti-CEA (20% less than the initial starting percentage). It is reported that differentiation diminishes cell transgene expression. Though, after T-cell differentiation, anti-CEA was expressed in nearly 100% of phenotypic T-cells. This suggests T-cells have an advantage retaining anti-CEA expression. This hypothesis is supported by data in Figure.6.2 showing lost dTomato expression after a stably established dTomato iPSC line underwent T-cell differentiation. This culture was initiated from cells that were approximately 85% positive for dTomato, which is an additional 60% relative to anti-CEA iPSCs. 1% of dTomato iPSCs retained dTomato expression after T-cell differentiation. It is important to create a stably established iPSC line expressing anti-CEA so expression isn't lost during long-term expansion. This would enable multiple patients to use the line over an extended time frame.

The T-cell differentiation performed in Figure.6.2 utilized HSPCs generated from a method other than method 2. Their marker expression was assessed and is present in Appendix.B.12.

Data in Figure.5.2 display an average transfection efficiency of 81% when using an optimized S/MAR DNA vector containing dTomato. The anti-CEA vector used in section 6.1 is associated with a lower transfection efficiency (3%). The anti-CEA S/MAR DNA vector contains the promoter sEF1+CI and S/MAR-3 while sEF1 and S/MAR-4 were determined as the most optimal vector features in section 3. Not utilizing these features could be responsible for the low transfection efficiency and lack of establishment obtained for the anti-CEA iPSC



line. Additionally, the usage of anti-CEA instead of dTomato could also affect these results.

6.4 Conclusion

iPSCs can be genetically engineered to express a CAR using an S/MAR DNA vector, and these modified cells can differentiate into phenotypic T-cells. Although a stable anti-CEA expressing iPSC line was not established, nearly all phenotypic iPSC-derived T-cells expressed anti-CEA.

6.5 Future Aims

Future aims pertaining to anti-CEA iPSC-derived T-cells include:

- Establishing an anti-CEA iPSC line using optimal vector features.
- Comparing alkaline phosphatase and the expression of pluripotency markers between S/MAR DNA vector-modified iPSCs and non-modified iPSCs.
- Assessing the activation and functionality of anti-CEA iPSC-derived T-cells.
- Karyotyping and genetic analysis of iPSC-derived T-cells to determine their oncolytic potential.

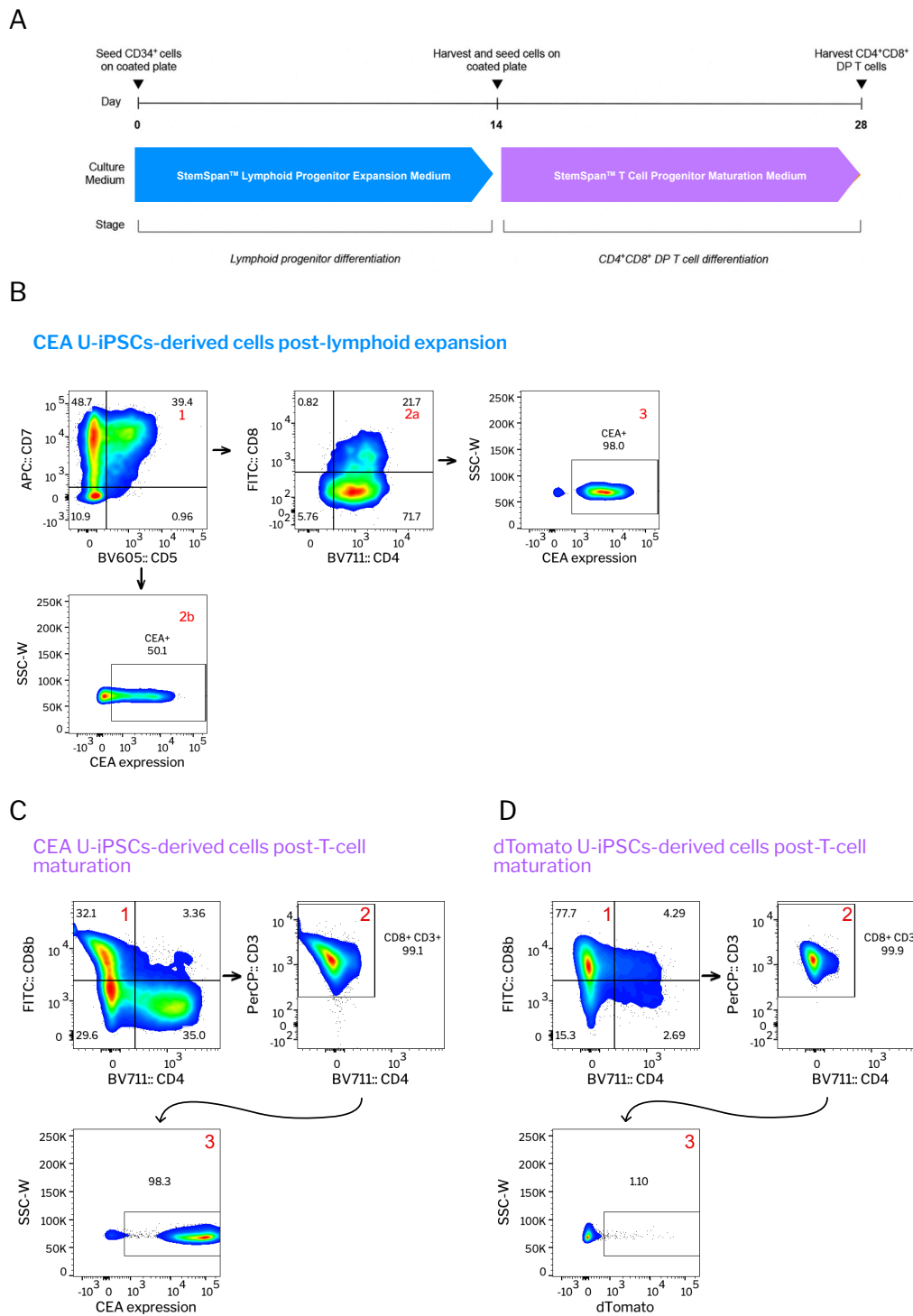


Figure 6.2: Anti-CEA CAR expressing iPSCs can differentiate into phenotypic T-cells from iPSC-derived CD34⁺ cells. A) A schematic representation of the T-cell differentiation process (method 2) when using iPSC-derived CD34⁺ cells. The image is obtained from [299]. B) FACS plots displaying CD5, CD7, CD8b, CD4, and anti-CEA expression in anti-CEA CAR iPSC-derived cells after undergoing lymphoid expansion. C) FACS plots displaying CD8b, CD4, CD3 and anti-CEA expression in anti-CEA iPSC-derived cells after undergoing T-cell maturation. D) FACS plots displaying CD8b, CD4, CD3 and dTomato expression in iPSC-derived cells after undergoing T-cell maturation.



Chapter 7

Conclusion

For the first time within our lab, S/MAR DNA vector features were screened in U-iPSCs. Data indicate S/MAR-4, RNA-out R6K production backbone, and sEF1 promoter to be the most optimal features (Chapter 3). U-iPSCs modified with a vector containing such features resulted in a high transfection efficiency (81%). Additionally, a genetically modified iPSC line was generated using this S/MAR DNA vector (Chapter 5). This iPSC line could differentiate into HSPC-like cells primed for the myeloid or lymphoid lineage, and subsequently phenotypic T-cells. Furthermore, an iPSC line expressing anti-CEA CAR could differentiate into phenotypic T-cells and nearly 100% of phenotypic T-cells, after maturation, were expressing anti-CEA (Chapter 6).

I developed a clean S/MAR DNA vector with simple cloning capacities as a single restriction cut site is present between each feature. Additionally, I have established a protocol for expanding mouse HSPCs to high cell counts suitable for the electroporation of multiple samples (Chapter 4).



Chapter 8

Methods

8.1 Human Cell Culture

This section provides a clarification of the cell cultures methods used to culture human cells. Within this section, one can find materials pertaining to the maintenance, thawing, validation, transfection, stable cell line generation, and flow cytometry analysis of human cell lines used. All techniques were performed aseptically.

8.1.1 Jurkat76 Cell Line

8.1.1.1 Thawing Jurkat76

15 mL of RPMI 10%FBS 1%P/S was prepared. 5 mL of this prepared medium was transferred to a T25 culture flask and placed into an incubator at 37°C with 5% CO². Another 5 mL of this prepared medium was transferred to a 15 mL Falcon tube. A vial of Jurkat76 cells were then removed from the cryostorage system and thawed in a 37°C water bath. This cell suspension was immediately and gently transferred into the 15 mL Falcon tube containing 5 mL of media, and centrifugation was applied at 250 g for 5 minutes to pellet the cells. The supernatant was aspirated using a vacuum pump. Cells were resuspended with 5 mL of the prepared media and transferred into the T25 culture flask contain media. The flask was stored vertically at 37°C with 5% CO². Cell line validation was performed following steps listed in section 8.3.4. For cell freezing, see section 8.3.6.

8.1.1.2 Routine Maintenance of Jurkat76

The Jurkat76 cell line was kept between $5(10)^5$ - $4(10)^6$ cells/mL. 20 mL of RPMI 10%FBS 1% P/S was transferred to a T175 flask. 5 mL of the cell suspension ($4(10)^6$ /mL) was transferred to each T175 flask prepared. Jurkat76 clump while proliferating. When splitting, larger clumps were gently broken-up so cells could receive equal access to nutrients. Cells were assessed under the microscope, then placed in an incubator at 37°C with 5% CO². This procedure resulted in a split every 2-3 days. If cell viability was below 70%, dead cell removal was performed, following methods in section 8.3.5.



8.1.1.3 Transfection of Jurkat76

Four days prior to the transfection, 1.5 mL and 2.0 mL eppendorf tubes were autoclaved. I checked that there were enough SE Strips, non-supplemented Nucleofector Solution, and SE Supplement Solution, which are a part of the Amaxa™ SE Cell Line 4D-Nucleofector™ X Kit S. I checked to make sure there were enough cells and medium (4 mL of medium per a sample is required) to perform the experiment.

The day of the experiment, a large beaker was obtained and used for disposing of pipette tips. Vectors were thawed on ice. The appropriate number of wells from a non-treated 48-well plate was filled with 1.5 mL of RPMI 10% FBS. 1x PBS was applied to the rest of the empty wells. This plate was placed into an incubator and incubated at 37°C with 5% CO². A 50 mL Falcon tube was filled with 30 mL of pre-warmed medium. Jurkat76 cells were removed from the incubator, and the cell density was calculated. The total number of cells needed for the experiment were transferred to a 15 mL tube—2(10)⁶ cells per a sample are required. Centrifugation was applied at 150 g for 10 minutes with an acceleration of 5 g and a deceleration of 5 g. The supernatant was aspirated, and 15 mL of PBS was gently applied to the cell pellet. Centrifugation was repeated at 150 g for 10 minutes with an acceleration of 5 g and a deceleration of 5 g.

While cells were in the centrifuge, the 4D-Nucleofector™ Core unit was turned on. The "x" unit was selected, and, subsequently, the appropriate well locations were defined.¹ The solution type "SE" was selected, and manually the pulse code "CL120" was typed in.² The SE cell line solution was supplemented by transferring the SE supplement into the SE solution. I allowed the solution to reach room temperature. An Amaxa™ SE cell line 4D-Nucleofector™ strip was appropriately labeled, and the volume of DNA corresponding to 1 μg was added to the base of the appropriate well of the Nucleofector™ strip.

Once centrifugation was complete. The supernatant was aspirated until 200 μL remained. Using a 200 μL pipette, the remaining of PBS was removed. The cell pellet was very gently resuspended with the appropriate amount of supplemented SE cell line solution—20 μL per sample. 20 μL of the cell suspension was then gently transferred to each appropriate well of the labelled Nucleofector™ strip. I then checked each well for bubbles. If any bubbles persisted, they were removed by gently tapping the Nucleofector™ strip on a table. The Nucleofector™ strip was positioned properly into the 4D-Nucleofector™ Core Unit. Then, electroporation was initiated. Once the nucleofection program was completed, the nucleofector™ strip was placed inside the cell culture hood for 10 minutes to allow for the cells to recover. 120 μL of RPMI 10%FBS 1% P/S was added to each well, and the cell suspension was gently transferred into the appropriate well of the prepared 48-well plate. Cells incubated for 4 hours at 37°C 5% CO². Supernatant was carefully removed—being mindful to not remove any cells—and pre-warmed medium was added gently down the side of the well. Cells incubated overnight at 37°C with 5% CO², and a FACS analysis was performed 24 hours or 48 hours post-transfection (section 8.1.1.4)

¹NOTE: the 4D-Nucleofector™ strip can only insert into the apparatus in one position.

²NOTE: selecting a program from the Lonza Database may lead to an incorrect pulse.



8.1.1.4 Flow Cytometry Analysis of Jurkat76

A 96-well round bottom plate was obtained and properly labeled. 200 μL of each Jurkat76 cell sample was transferred to the appropriate well of the 96-well plate. Centrifugation was then applied at 300 g for 5 minutes at 4°C, and the supernatant was discarded by flicking the plate over a sink. Cells pellets were resuspended in 200 μL of FACS Buffer (1%FBS in PBS). Centrifugation was applied at 300 g for 5 minutes at 4°C, and the supernatant was discarded by flicking the plate over a sink. This washing step was repeated. Then, cells were resuspended in 200 μL of FACS buffer containing 2 $\mu\text{g}/\text{mL}$ DAPI. Cells incubated for 10 minutes in the dark; then were transferred into a FACS tube containing a strainer. FACS analysis was then performed.

8.1.1.5 Using FACS to Collect a Specific Jurkat76 Population

Cell samples were transferred into a properly labeled tube—the type of tube is dependent of the total sample volume. Centrifugation was applied at 300 g for 5 minutes at 4°C. Then, the supernatant was aspirated. Cell pellets were resuspended in 1 mL of FACS Buffer (1%FBS in PBS), and centrifugation was applied again at 300 g for 5 minutes. Supernatant was aspirated, and cells were resuspended in 500 μL of FACS buffer containing 0.2 $\mu\text{g}/\text{mL}$ DAPI. Samples incubated for 10 minutes in the dark. Then they were filtered into a sterile FAC tube containing a strainer. 10,000 alive dTomato+ cells were sorted into a properly labeled well of 96-well plate containing 200 μL of RPMI 10%FBS 1%P/S. A full medium change was performed the following day by gently removing the supernatant—being mindful of not disrupting cells—and carefully replacing the medium by applying fresh medium down the side of the well. This method was used to establish stable cell lines expressing dTomato.

8.1.2 Primary Human T-Cells

8.1.2.1 Collecting and Expanding T-Cells From a Human Buffy Coat

A buffy coat from a human donor was collected from the DRK Blutspendedienst. The external tube from the blood bag was sterilize using 70% ethanol. A pair of scissors were also sterilized using 70% ethanol. A cell culture plate was used to lay the scissors and the external tube from the blood bag on. The top of the external tube from the blood bag was very carefully cut using the sterilized scissors. Carefully the blood was poured into the 1 L autoclaved bottle. Dilute the buffy coat 1:1 using 1x PBS (approximately 50 mL of 1x PBS was added). 15 mL of Ficoll-Plaque was transferred into four 50 mL Falcon tubes. Then, 25 mL of the diluted buffy coat was extremely carefully layered on top of the Ficoll-Plaque present in the 50 mL Falcons. Centrifugation was applied at 350 g for 30 minutes at room temperature using an acceleration of 5 g and a deceleration of 0 g. The plasma layer was carefully aspirated and discarded. The interphase layer (PBMCs) was then collected using a 1 mL pipette and transferred to a new 50 mL Falcon. Two interphases were collected and pooled into one 50 mL Falcon. 1x PBS was then added until a total volume of 50 mL was reached within each 50 mL Falcon. Centrifugation was applied at 350 g for 8 minutes with an acceleration of 9g and deceleration of 9g. The supernatant was aspirated, and each cell pellet



was resuspended in 25 mL of 1x RBC lysis buffer, then pooled together into one 50 mL Falcon. Samples incubated for 10 minutes at 37°C. Then, centrifugation was applied at 350 g for 8 minutes with an acceleration of 9 g and deceleration of 9 g. The supernatant was aspirated, and cells were resuspended in 50 mL of 1x PBS. Centrifugation was applied again at 350 g for 8 minutes with an acceleration of 9g and deceleration of 9g. This washing step was repeated twice. Cells were resuspended in 40 mL of TexMACS medium, and the cell density was calculated following methods from 8.3.1. 20 mL of cells were distributed into two T175 flasks and left overnight in the incubator 37°C with 5% CO².

T-cells were isolated using the Pan T-cell Isolation Kit. PBMCs were filtered twice using a 30 μm pre-separation filter. The cell density was calculated following methods from section 8.3.1, and the total volume of cells corresponding to 3x the cell number of interest was collected into an appropriate tube. Centrifugation was applied at 350g for 5 minutes. Then methods from the Pan T-cell Isolation Kit were followed. Purified T-cells should be activated at an optimal surface density of 1(10)⁶ cells per cm². Growing area and reagent volumes used should be kept proportional. IL-15 and IL-7 were added at a final concentration of 0.001 μg/mL (1:10,000 dilution from the stock) and TransAct was diluted to a 1:100 ratio. Cells incubated in these medium conditions for 3 days at 37°C with 5% CO². Then, a transfection was performed following methods described in section 8.1.2.3. The remainder of cells, not used for T-cell isolation, were frozen following methods from section 8.3.6.

8.1.2.2 Thawing Primary Human PBMCs

12.5 mL of TaxMACS was added to a 15 mL Falcon tube. A vial of Jurkat76 cells was then removed from the cryostorage system and thawed in a 37°C water bath. PBMCs were transferred into the 12.5 mL of TexMACS medium. Centrifugation was applied at 300 g for 5 minutes. Cells were resuspended in 30 mL of TexMACS medium and transferred to at T75 flask. Cells incubated at 37°C with 5% CO² overnight. Then, the following day, T-cells were isolated using the Pan T-cell Isolation Kit.

8.1.2.3 Transfection of Primary Human T-Cells

Four days prior to the transfection, 1.5 mL and 2.0 mL eppendorf tubes were autoclaved. I checked that there was an available P3 Primary cell line 4D-Nucleofector™ X kit S, and that there was enough medium to perform the experiment.

The day of the experiment, a large beaker was obtained and used for disposing of pipette tips. Vectors were thawed on ice. The appropriate number of wells from a nuclondelta 48-well plate was filled with 1 mL of 0.001 μg/mL IL-15 and 0.001 μg/mL IL-7 TexMACS solution. The remaining wells were filled with 1x PBS. This plate was placed in an incubator and incubated at 37°C with 5% CO² for at least 30 minutes. A 50 mL Falcon tube was filled with 30 mL of pre-warmed TexMACS medium. Primary T-cells were removed from the incubator, and the cell density was calculated. The appropriate number of cells were transferred to a 50 mL Falcon tube—need 2(10)⁶ cells per a sample. Centrifugation was applied at 100 g for 10 minutes with an acceleration of 5 g and a deceleration of 5 g. The supernatant was aspirated, and 10 mL of TexMACS was gently added to the cell pellet. Centrifugation was again applied



at 100 g for 10 minutes with an acceleration of 5 g and a deceleration of 5 g.

While cells were in the centrifuge, the 4D-Nucleofector™ Core unit was turned on. The "x" unit was selected, and, subsequently, the appropriate well locations were defined.³ The solution type "P3" was selected, and manually the pulse code "FI-115" was typed in.⁴ The P3 primary cell solution was supplemented by transferring the P3 supplement into the P3 solution. I allowed the solution to reach room temperature. A P3 cell 4D-Nucleofector™ strip was appropriately labeled, and the volume of DNA corresponding to 2 μg was added to the base of the appropriate well of the Nucleofector™ strip.

Once centrifugation was completed, the cell pellet was very gently resuspended with the supplemented P3 nucleofection solution at a volume corresponding to 20 μL per sample. 20 μL of the cell suspension was then transferred into each well of the strip. I then checked each well for bubbles. If any bubbles persisted, they were removed by gently tapping the Nucleofector™ strip on a table. The Nucleofector™ strip was positioned properly into the 4D-Nucleofector™ Core Unit. Then, electroporation was initiated. Once the nucleofection program was completed, cells recovered for 10 minutes at room temperature. 180 μL of 1 ng/mL IL-15 and 1 ng/mL IL-7 TexsMACS was added to each well, and the cells were gently transferred into an appropriately labeled well of pre-incubated 48-well plate. Cells incubated at 37°C with 5% CO₂. 6 hours post-electroporation, TexMACS medium was gently replaced with 1 ng/mL IL-15 and 1 ng/mL IL-7 TexsMACS containing 1:100 of TransAct. If a cell population was going to be collected via FACS after transfection, half medium changes were performed daily until three days post-electroporation. Then, three days post-electroporation, 20,000 cells were collected into a 96-well plate.

8.1.2.4 Flow Cytometry Analysis of Primary T-Cells

A 96-well round bottom plate was obtained and properly labeled. 200 μL of each sample was transferred to the appropriately labeled well of a 96-well plate. Centrifugation was then applied at 300 g for 5 minutes at 4°C. Supernatant was discarded into the sink by flicking the plate over the sink. The cell pellet was then resuspended in 200 μL of FACS Buffer. Centrifugation was applied again at 300g for 5 minutes, and the supernatant was discarded into the sink by flicking the plate over the sink. This washing step was repeated. Cells were then resuspended in 100 μL of FAC buffer containing 1:50 of APC anti-human CD3. Samples incubated for 30 minutes at 4°C in the dark. Centrifugation was then applied at 300 g for 5 minutes. Cell pellets were then resuspended in 200 μL of FACS Buffer. Centrifugation was applied at 300 g for 5 minutes. The supernatant was discarded into the sink by flicking the plate over the sink. 200 μL of 0.2 $\mu\text{g}/\text{mL}$ DAPI FACS buffer was then used to resuspend the cells. Cells incubated for 10 minutes in the dark. Then, were transferred into filter FACS tubes. FACS analysis was then performed.

³NOTE: the 4D-Nucleofector™ strip can only insert into the apparatus in one position.

⁴NOTE: selecting a program from the Lonza Database may lead to an incorrect pulse.



8.1.2.5 General Maintenance of Primary Human T-Cells

Primary human T-cells can remain in culture for a maximum of 28 days. After T-cells have been in culture for 18 days, the amount of TransAct used was reduced to 1:500. After T-cells have been in culture for 20 days, TransAct was removed. If a cell population was collected via FACS, a full gently medium change was performed the following day. Five days post-sort, a half medium change was performed. Additional medium changes and splits that point forward were dependent on the cell density.

8.1.3 Immortalized Normal Human Dermal Fibroblasts (iNHDFs)

8.1.3.1 Thawing iNHDFs

1% NEAA 1% GlutaMAX 10% FBS DMEM was prepared, and 35 mL was transferred into a 50 mL Falcon and pre-warmed. A T75 flask was coated with 10 mL of 0.1% gelatin and placed into a 37°C 5% CO² incubator for 20 minutes. The gelatin was then aspirated from the flask. 10 mL of pre-warmed medium was added to the flask, being mindful of not disturbing the coated base. The flask was placed back into the 37°C 5% CO² incubator. A vial of cells was obtained from the cryostorage system, and the cells were thawed in a 37°C water bath. The cells were carefully transferred to a 15 mL Falcon using a 1 mL pipette, and 10 mL of pre-warmed media was slowly added to the Falcon containing the fibroblasts. Centrifugation was applied at 300 g for 5 minutes with an acceleration of 5 g and a deceleration of 5 g. The supernatant was aspirated, and cells were resuspended in 10 mL of pre-warmed medium. This cell suspension was transferred to the flask containing pre-warmed media, and the cells incubated at 37°C with 5%CO².

8.1.3.2 Routine Maintenance of iNHDFs

Passaging of iNHDFs was performed every three days at a 1:3 split ratio. Medium was aspirated from a T75 flask containing cells. Cells were gently washed with 10 mL of PBS, PBS was aspirated. Then, 5 mL of prewarmed trypsin was added on top of the cells and incubated for 1-2 minutes at 37°C with 5%CO². 10 mL of 1% NEAA 1% GlutaMAX 10% FBS DMEM was added into the flask to deactivate the trypsin, and the cell suspension was transferred to a 50 mL Falcon. Centrifugation was applied at 300 g for 5 minutes. Then, the supernatant was aspirated. Cells were resuspended in 12 mL of 1% NEAA 1% GlutaMAX 10% FBS DMEM. A new T175 flask was coated with 10 mL of 0.1% gelatin and incubated for 20 minutes in a 37°C 5% CO² incubator. The gelatin was aspirated, and 15 mL of 1% NEAA 1% GlutaMAX 10% FBS DMEM was added into the flask. Then, 1/3 of the prepared cell suspension was transferred into this T175 flask. Cells incubated at 37°C with 5% CO².

8.1.3.3 Transfection of iNHDFs

Vectors were thawed on ice. Then, the appropriate number of wells of a 48-well nuclodelta plate were prepared with 1 mL of 1% NEAA 1% GlutaMAX 10% FBS DMEM, and 1x PBS was added to the remaining wells. This plate incubated at 37°C with 5% CO² for at least 30 minutes. A 50 mL Falcon tube was filled with 30 mL of warm medium. The flask(s) of



iNHDFs was removed from the incubator. Medium was aspirated from the flask(s) containing cells. Cells were gently washed with PBS, PBS was aspirated. Then, 5 mL of prewarmed trypsin was added on top of the cells and incubated for 1-2 minutes at 37°C with 5% CO². 10 mL of 1% NEAA 1% GlutaMAX 10% FBS DMEM was added into the flask to deactivate the trypsin, and the cell suspension was transferred to a 50 mL Falcon. Centrifugation was applied at 300 g for 5 minutes. The supernatant was aspirated, and cells were resuspended in 1x PBS. The cell density was calculated, and the appropriate volume of cells was removed and transferred to a 50 mL Falcon tube—1(10)⁵ cells per a sample needed. Centrifugation was applied at 100 g for 10 minutes with an acceleration of 5 g and a deceleration of 5 g. The supernatant was aspirated. A washing step with 1x PBS was repeated.

While centrifugation was applied to the cells, the 4D-Nucleofector™ Core unit was turned on. The "x" unit was selected, and, subsequently, the appropriate well locations were defined.⁵ The solution type "P2" was selected, and manually the pulse code "DT130" was typed in.⁶ The P2 primary cell solution was supplemented by transferring the P2 supplement into the P2 solution. I allowed the solution to reach room temperature. A P2 primary cell 4D-Nucleofector™ strip was appropriately labeled, and the volume of DNA corresponding to 1 μg was added to the base of the appropriate well of the Nucleofector™ strip.

Once the washing steps for the cells was completed. Supernatant was aspirated, and cells were resuspended very gently with supplemented P2 Primary cell nucleofection solution—20 μL per sample. 20 μL of the cell suspension was transferred into each well of a Nucleofector™ strip. I then checked each well for bubbles. If any bubbles persisted, they were removed by gently tapping the Nucleofector™ strip on a table. The Nucleofector™ strip was positioned properly into the 4D-Nucleofector™ Core Unit. Then, electroporation was initiated. Once the nucleofection program was completed, cells recovered for 10 minutes at room temperature. 180 μL of 1% NEAA 1% GlutaMAX 10% FBS DMEM was added to each well and the cell suspension was transferred to an appropriate well of pre-incubated 48 well plate. Cells then incubated at 37°C 5% CO².

8.1.3.4 Supernatant Collection for ELISA: iNHDFs

Different volumes of supernatant were collected at various time points. 1.5 hours post-pulse, 99 μL of supernatant was removed. 3 hours post-pulse, 93.06 μL of supernatant was removed. 6 hours post-pulse, 87.45 μL of supernatant was removed. 12 hours post-pulse, 82.17 μL of supernatant was removed. 24 hours post-pulse, 77.3 μL of supernatant was removed. 48 hours post-pulse, 72.7 μL of supernatant was removed. Collected supernatant was transferred to a 1.5 mL Eppendorf tube, and samples were brought to a total volume of 99 μL using 10% FBS, 1% NEAA DMEM. Centrifugation was applied to remove cellular debris. Samples were then stored at -20°C. Proceed to section 8.3.8 for ELISA analysis.

⁵NOTE: the 4D-Nucleofector™ strip can only insert into the apparatus in one position.

⁶NOTE: selecting a program from the Lonza Database may lead to an incorrect pulse.

8.1.4 HEK293T Cell Line

8.1.4.1 Thawing HEK293T

1% P/S 10% FBS DMEM was prepared, and 10 mL was transferred into a 15 mL Falcon tube. A vial of cells was obtained from the cryostorage system, and the cells were thawed in a 37°C water bath. The cells were carefully transferred to the 15 mL Falcon containing 10 mL of medium. Centrifugation was then applied at 300 g for 5 minutes with an acceleration of 5 g and a deceleration of 5 g. The supernatant was aspirated, and cells were resuspended in 10 mL of pre-warmed medium. This cell suspension was transferred into a 15 cm dish. The cells were evenly distributed within the dish, and the cells incubated at 37°C with 5% CO².

8.1.4.2 Routine Maintenance of HEK293T

Passaging was conducted when cells reached a confluency of 90% or higher. For passaging, medium was very gently aspirated from the dish. Then 1 mL of trypsin was added to each 15 cm dish. Cells incubated with trypsin for a few minutes. Then, 4 mL of 1% P/S 10% FBS DMEM was used to dislodge the cells, and cells were collected into a 15 mL Falcon. Centrifugation was then applied at 300 g for 5 minutes. Cells were resuspended in 3 mL of 1% P/S 10% FBS DMEM, and 1 mL was added to a new 15 cm dish containing 10 mL of 1% P/S 10% FBS DMEM. At this point, remaining cells could be processed for cryopreservation.

8.1.5 Human Induced Pluripotent Stem Cells (iPSCs)

8.1.5.1 Generating Human iPSCs From Urinary-Derived Cells

Human iPSCs were generated from urinary-derived cells. Methods pertaining to their development are described in the thesis of Manuela Urban [319].

8.1.5.2 Thawing Human iPSCs

An aliquot of 1% P/S Basic04 medium was thawed, and 10 μM ROCK 1%P/S Basic04 medium was prepared. 10 μM ROCK Basic04 medium was always used when cells were plated as single cells. A 6-well plate was obtained and 2 mL of 1x PBS was added into each well. 9.6 μL of iMatrix Laminin-511 was added into each well, and evenly distributed. This 6-well plate incubated for 1 hour at 37°C with 5% CO². iMatrix Laminin-511 solution was aspirated, and 500 μL of 10 μM ROCK 1% P/S Basic04 medium was added to each well.

A 15 mL Falcon and a 5 mL stripette were obtained. A vial of cells was collected from the cryostorage system and thawed in a 37°C water bath. The vial was then sterilized using 70% ethanol. Cells were gently transferred to a 15 mL Falcon. The collection of bubbles was avoided when cells were being collected and dispensed. Dropwise, 5 mL of 10 μM ROCK 1% P/S Basic04 medium was added to the cell suspension, and while medium was added, the tube was periodically shaken. Centrifugation was applied at 100 g for 5 minutes. Then, supernatant was aspirated until 200 μL of medium was left. The bottom of the tube was flicked to resuspend the cells, and 1 mL of 10 μM ROCK 1% P/S Basic04 was added. The cell suspension was collected starting from the bottom of the tube using a 5 mL stripette. Then



the cells were gently transferred into the iMatrix Laminin-511 coated well containing 500 μL of 10 μM ROCK 1% P/S Basic04. The following day, a full medium change was performed with 1% P/S Basic04 (ROCK was removed).

8.1.5.3 Routine Maintenance of Human iPSCs

The splitting of iPSCs followed a 5-day pattern. Passaging occurred on day 0, and a full medium change was performed on days 1 and 4. A 6-well plate was obtained and 2 mL of 1x PBS was added into each well. 9.6 μL of iMatrix Laminin-511 was added into each well, and evenly distributed. This 6-well plate incubated for 1 hour at 37°C with 5% CO². After 1 hour, the Laminin solution was aspirated and 1.5 mL of 10 μM ROCK 1%P/S Basic04 was added into each well. For each sample, a 1.5 mL Eppendorf tube was properly labeled. Medium was then aspirated from each well containing cells. Cells were washed using 1x PBS. 1x PBS was aspirated, and 5 drops of ACCUTASE™ was added into each well containing cells. Cells incubated at 37°C with 5% CO² for 5 minutes. Cell detachment was assessed using a microscope. 500 μL of 10 μM ROCK 1%P/S Basic04 was added to each well, and cells were collected and transferred to the appropriately labeled 1.5 mL Eppendorf tube. The cell density was then calculated, and the appropriate volume of cell suspension, corresponding to 4(10)⁵ cells was transferred to each well of the 6-well plate. The following day (within 24 hours) a medium change was performed by aspirating medium and adding 1.5 mL of 1% P/S Basic04 (ROCK was removed) to each well.

8.1.5.4 Validating iPSC Phenotype: AP Staining

An aliquot of Basic04 medium was thawed, and 10 μM ROCK 1%P/S Basic04 medium was prepared at the appropriate volume—requires 1.2 mL per a sample if performing AP and IF staining in parallel. 1.175 μL of laminin was added to 300 μL of 1x PBS into the well of a μ -Plate 96-Well. The Laminin solution was evenly distributed within the well of the μ -Plate 96-Well. Plate incubated at 37°C with 5% CO² for 1 hour. Then the laminin solution was aspirated, and 100 μL of 10 μM ROCK 1%P/S Basic04 medium was added to each well. iPSCs expanded for this experiment were collected utilizing ACCUTASE™. The cell density was calculated following methods described in section 8.3.1. The appropriate number of cells was collected—24,000 cells per a sample when both AP and IF staining are performed in parallel. Centrifugation was applied at 200 g for 5 minutes, and cells were resuspended at a density of 4,000 cells per 100 μL of 10 μM ROCK 1%P/S Basic04 medium. 100 μL of the cell suspension was added to each prepared well of the μ -Plate 96-Well; this brings the total volume to 200 μL per a well. If only AP staining is performed, only two wells containing 4,000 cells in 200 μL of medium is required per a sample (including non-treated). The following day, a full medium change is performed using 1%P/S Basic04 medium (remove ROCK).

Four days post-seeding, AP staining was performed using the Stemgent® AP Staining Kit II. Methods described in the Stemgent® AP Staining Kit II protocol were followed [301]. PBST was prepared, and 40 μL of Solution A, Solution B, and Solution C were used per a well of a 96-well plate for preparing the AP substrate solution. 100 μL of Fix Solution and 120 μL of freshly prepared AP substrate solution were used per one well of a 96-well plate. Microscope



images were than taken at 4x, 10x, and 20x using the Keyence microscope. Images can be taken within a day of sample preparation.

8.1.5.5 Validating iPSC Phenotype: IF Staining

For plating cells, follow methods described in paragraph 1 of section 8.1.5.4. If AP and IF staining are performed in parallel, IF staining should be performed after AP staining. If only IF staining is performed, only 5 well containing 4,000 cells in 200 μL of medium is required per a sample (including non-treated control).

Four days post-seeding, 4% PFA in 1x PBS, 1x PBS, permeabilization buffer, PBST, blocking solution, and 1 $\mu\text{g}/\text{mL}$ DAPI solution were obtained. IF staining was performed in the dark to keep fluorescent protein stable. Medium was discarded from the plate containing cells by flicking the plate over a sink. Cells were washed with 1x PBS. Then, 100 μL of 4% PFA 1x PBS was added to each well and incubated for 10 minutes at room temperature in the dark. 4% PFA was then discarded into the appropriate container, and cells were washed 3 times with 1x PBS. During each washing step, cells incubated for 5 minutes in the 1x PBS. 1x PBS was aspirated, and 100 μL of permeabilization buffer was added to each well. Cells incubated in permeabilization buffer for 5 minutes at room temperature. Cells were washed 3 times with 1x PBST. During each washing step, cells incubated for 5 minutes in the 1x PBST. PBST was aspirated, and 100 μL of blocking solution was added to each well. Cells incubated for 1 hour at room temperature in blocking solution. Each well was labeled appropriately with sample name and antibody used. Individual primary antibody solutions were than prepared in blocking solution—100 μL per a sample was prepared—following guidelines described in Table.8.1. 100 μL of each primary antibody solution was then added into the appropriately labeled well. Plates were sealed, wrapped in aluminum foil, and incubated overnight at 4°C.

Table 8.1: Primary antibodies used for IF staining of iPSCs.

Antibody	Dilution	Reference #	Host	Reactivity
aLin28	1:50	SC374460	mouse	human
aTra180	1:50	SC21705	mouse	human
aNanog	1:50	SC2931211E6C4	mouse	human
aOct3/4	1:100	SC8628n-19	goat	human, mouse

The primary antibody solution was discarded by flicking the plate over a sink. Wells were washed 3 times using 1x PBS. During each washing step, cells incubated for 5 minutes in the 1x PBS. Secondary antibody solutions were than prepared using 1 $\mu\text{g}/\text{mL}$ DAPI within blocking solution—100 μL per a sample was prepared—following guidelines described in Table.8.2. 1x PBS was aspirated from each well, and 100 μL of the appropriate secondary antibody solution was added into the appropriate well. Samples incubated for 1 hour at room temperature in the dark. The secondary antibody solution was discarded, and cells were washed 3 times with 1x PBS. During each washing step, cells incubated for 5 minutes in the 1x PBS. 200 μL of 1x PBS was added to each well, and the plate was sealed. Images were taken at 10x and 20x using the Nikon microscope. Images can be taken within a day of sample preparation.

**Table 8.2:** Secondary antibodies used for IF staining of iPSCs.

Antibody	Dilution	Reference #	Reactivity
aGoat-647, cy5	1:1000	ab150131	goat
Alpha mouse-488, FITC	1:1000	Ab150105	mouse

8.1.5.6 Transfection of iPSCs

Replicates of two were used for each sample genetically modified. A treated 24-well plate was coated with iMatrix Laminin-511 by adding 500 μL of PBS and 2.4 μL iMatrix Laminin-511 into a well. It was ensured that the iMatrix Laminin-511 was distributed evenly within the well by vigorous pipetting. After an 1-hour incubation, the laminin solution was aspirated, and 1 mL of 10 μM ROCK 1%P/S Basic04 medium was added to each well. A 1.5 mL Eppendorf tube was properly labeled. Medium was aspirated from wells containing cells that will be used for this experiment. Cells were washed using 1x PBS. 1x PBS was aspirated, and 5 drops of ACCUTASE™ was added into each well containing cells. Cells incubated at 37°C with 5% CO² for 5 minutes. Cell detachment was assessed using a microscope. 500 μL of 10 μM ROCK 1%P/S Basic04 was added to each well, and cells were collected and transferred to the 1.5 mL Eppendorf tube. The cell density was then calculated, and the appropriate volume of cell suspension, corresponding to 4(10)⁵ cells was transferred to each well of the prepared laminin-coated 24-well plate. The following day (within 24 hours) a medium change was performed by aspirating medium and adding 2 mL of Basic04 each well. No antibiotics were used during the transfection process.

The appropriate number of 1.5 mL Eppendorf tubes was obtained—one tube per a vector used and one for the lipofectamine stock solution. Volume A of Optimem was added to a 1.5 mL Eppendorf tube. Volume B of Lipofectamine stem was added into the Optimem (1:25 dilution), and the solution was vigorously vortexed.

$$25 \text{ uL } (\# \text{ of samples})(\# \text{ of repliates} + 0.5) = \text{Volume A}$$

$$\text{Volume A} \div 25 = \text{Volume B}$$

DNA solutions were than prepared. 1.5 mL Eppendorf tubes were appropriately labeled, and volume C of Optimem was added into each tube. A volume corresponding to Mass A of DNA was added into each appropriately labeled tube containing volume C of Optimem. The solution was mixed well by vortexing.

$$25 \text{ uL } (\# \text{ of replicates} + 0.5) = \text{Volume C}$$

$$600 \text{ ng } (\# \text{ of replicates} + 0.5) = \text{Mass A}$$

The DNA solution was added to the diluted Lipofectamine Stem. Each solution was vortexed for 5 seconds. Then incubated at room temperature for 10 minutes in the dark. 50 μL of each DNA/lipofectamine solution was added to the appropriately labeled well(s).

3-days post-transfection, transfection efficiency was accessed using the Nikon microscope. Images were taken at 4x, 10x, and 20x in BF and TRITC channels. FACS analysis was then



performed following steps described in section 8.1.5.9 after passaging was completed following steps described in section 8.1.5.3. For general maintenance, see section 8.1.5.3.

8.1.5.7 Lentiviral Vector Transduction of iPSCs

Cells were prepared following steps described in paragraph 1 of section 8.1.5.6. Then, 1 μL of 8 mg/mL polybrene was added to each well. 100 μL of lentiviral vector generated following steps described in section 8.5.1 was added to each appropriate well. Samples incubated with virus for 16 hours at 37°C with 5% CO_2 . Medium was then aspirated, and 1 mL of Basic04 medium was added to each well.

3-days post-transduction, passaging and FACS analysis were conducted. After passaging was performed following steps described in section 8.1.5.3, a FACS analysis was conducted following steps described in section 8.1.5.9. Images were taken five days post-transduction using the Nikon microscope. To prepare an established cell line, steps described in section 8.1.5.8 were followed.

8.1.5.8 Developing Vector-Maintained iPSC Lines

A laminin coated 24-well plate was prepared following steps described in section 8.1.5.6. 1.5 mL of 10 μM ROCK 1%P/S Basic04 medium was added to each well. Plate incubated at 37°C with 5% CO_2 . A DAPI PBS solution was prepared by transferring 12.5 μL of 0.1 mg/mL DAPI into 5 mL of 1x PBS. Medium was aspirated from wells containing cells that would be sorted. Wells were washed using 1x PBS. PBS was aspirated, and 5 drops of ACCUTASE™ was added to each well. Plate incubated at 37°C with 5% CO_2 for 5 minutes. Then 300-500 μL of DAPI PBS solution (prepared above) was used to resuspend cells. Cells were filtered into a FACS tube containing a filter. 10,000-30,000 positive cells were sorted into one well of a 24-well plate. Centrifugation was applied to the plate at 50 g for 3 minutes. 1 mL of medium was aspirated from each well and replaced with fresh 10 μM ROCK 1%P/S Basic04 medium. A full medium change was then performed the following day with 1%P/S Basic04 medium. Methods for routine maintenance—described in section 8.1.5.3—were followed until the next sorting day. Sorts were generally performed 1 week, 2 weeks, 3 weeks, and 5 weeks post-transfection, and 1 week and 2 weeks post-transduction. After the final sort, vials of cells were cryopreserved. Between weeks 3 and 5, more than 50% of cells retaining vector should be present. If not, perform another sort 7 weeks post-modification. If vectors are not established by then, repeat genetic modification with fresh cells.

8.1.5.9 Flow Cytometry Analysis of iPSCs

Cells were collected following methods described in section 8.1.5.8. Centrifugation was applied at 150 g for 5 minutes, and supernatant was aspirated. If a secondary antibody was used (Table.8.3), 100 μL of secondary antibody solution was added to each sample. Samples incubated at 4°C for 60 minutes in the dark. Then, centrifugation was applied at 200 g for 5 minutes. Supernatant was aspirated, and cells were resuspended in 200 μL of 0.2 $\mu\text{g}/\text{mL}$ DAPI PBS or 200 μL of 0.2 $\mu\text{g}/\text{mL}$ DAPI PBS containing absolute count beads. Samples were then filtered into a FACS tube, and FACS analysis was performed using an LSRFortessa. Data

analysis was conducted using FlowJo software. For calculations regarding absolute count beads, refer to section 8.3.9.

Table 8.3: FACS antibodies used to assess iPSCs phenotype.

Channel	Marker	Fluorophore	Clone	Catalog #	Company	Dilution	
BL525	TRA-160-R	-	AF488	TRA-160-R	330614	Biolegend	1:50

8.1.6 Differentiation: iPSCs Into HSPCs

8.1.6.1 Method 1

This method is based off [298]. A laminin coated 24-well plate was prepared as described in section 8.1.5.6 and 1 mL of 1%P/S Basic04 was added to each well. Medium was aspirated from plates containing cells that will be used for this experiment. Cells were washed using 1x PBS. PBS was aspirated, and 500 μL of ACCUTASE™ was added to each well. Within 1 minute, ACCUTASE™ was aspirated using a 1 mL pipette. This exposed cells to a thin layer of ACCUTASE™. Cells incubated at 37°C with 5% CO² for 3 minutes (not any longer). 500 μL of 1%P/S Basic04 was added to each well, and cells were gently detached by scrapping the bottom of the well with the tip of a 1 mL pipette tip. Cell clumps were transferred to a 1.5 mL Eppendorf tube using a 5 mL stripette. A 5 mL stripette was used as it has a larger opening; this prevented cell clumps from breaking into smaller pieces. Duplicate aggregate counts were performed to determine the average number of cell aggregates $\geq 50 \mu\text{m}$ in diameter [298]. A “+” was drawn centered on the bottom of 2 wells—per a sample—of a treated 96-well flat-bottom plate, which served as a counting grid [298]. 40 μL of basic04 was aliquoted into each well, and 5 μL of aggregate mixture was added to each well. The total number of cell clumps $\geq 50 \mu\text{m}$ within each well was counted and was averaged between the two wells used for one sample. This was the average number of cell aggregates (NA). The concentration of cell aggregates (C) was calculated following Equation.8.1, and the total number of cell aggregates in the mixture (NT) was calculated based on the total volume of the mixture (VT) (Equation.8.2) [296]. The volume of cell aggregate suspension to seed per a sample (VP) was calculated following Equation.8.3.

$$C = (NA \times 10) \div (5 \mu\text{L}) \quad (8.1)$$

$$NT = C \times VT \quad (8.2)$$

$$VP = NP \div C \quad (8.3)$$

$NP = \text{plating density (ex. 40)}$



The cell aggregate mixture was gently resuspended prior to plating to ensure a uniform cell clump suspension, and volume VP was added to the appropriate well of the laminin coated 24-well plate. The plate was moved in several quick, short, back-and-forth and side-to-side motions to distribute the cell aggregates evenly. This plate was placed into a 37°C incubator with 5% CO².

The following day, the STEMdiff™ Hematopoietic Kit was used for hematopoietic differentiation, and methods described in its protocol were followed [298]. On day 10, some cells were removed during the medium change and were used for a MethoCult assay following methods described in section 8.1.6.4. On day 12, microscope images were taken at 10x and 20x using the Nikon microscope. Cells were harvested by vigorously pipetting cells up and down to break-up cell clumps. This cell suspension was transferred to an appropriately labeled container, and 1 mL of supplemented Ham's F12 was added. Centrifugation was applied at 300g for 5 minutes. Supernatant was aspirated, and cells were resuspended in 1 mL of 1x PBS. Cells were then transferred to an appropriately labeled 1.5 mL Eppendorf tube, if not already in one. FACS analysis was then performed following methods described in section 8.1.5.9.

8.1.6.2 Method 2

This method is based off [300]. For method 2, the STEMdiff™ T Cell Kit was used. 3.3 mL aliquots of EB Basal medium were prepared, 7.5 μL aliquots of Supplement A were prepared, and 200 μL aliquots of Supplement B were prepared.

Table 8.4: Composition of the medium used for method 2 HSPC differentiation.

EB Medium A	
EB Basal Medium	1.5 mL
Supplement A	7.5 μL
EB Formation Medium	
EB Medium A	1 mL
10 μM Y-27632	1 μL of 10 mM stock
EB Medium B	
EB Basal Medium	1.8 mL
Supplement B	200 μL

An aliquot of supplement A and EB Basal medium were thawed, and mixed thoroughly. EB Medium A and EB Formation Medium were prepared following methods described in Table.8.4. The appropriate number of wells of an Aggrewell400 24-well plate were rinsed with 500 μL of anti-adherence rinsing solution. Centrifugation was applied at 1300 g for 5 minutes in a swinging-rotor centrifuge. The plate was observed under a microscope to assess if bubbles have been removed from each microwell [300]. If bubbles remained, centrifugation was applied again at 1300 g for 5 minutes [300]. The anti-adherence rinsing solution was aspirated from each well, and 2 mL of pre-warmed DMEM/F-12 with 15 mM HEPES was added to each well. Centrifugation was applied at 1300g for 5 minutes in a swinging-rotor centrifuge. Medium was aspirated from each well, and 500 μL of EB Formation medium was applied to each well.

Culture medium was aspirated from wells containing iPSCs that would be used for this experiment. Wells were washed with 1x PBS. PBS was aspirated and 5 drops of ACCUTASE™



was added to each well. Plate(s) incubated at 37°C with 5% CO² for 5 minutes. 1 mL of DMEM/F-12 with 15 mM HEPES was used to collect the cell suspension, and cell aggregates were carefully dissociated using a 1 mL pipette. Cells were transferred to a 15 mL conical tube, and the cell density was calculated following methods described in section 8.3.1.

1.4(10)⁶ cells were collected per a sample (2 replicates of 700,000 cells). Centrifugation was applied at 300 g for 5-10 minutes. The supernatant was aspirated, and cells were resuspended in 1 mL of EB Formation Medium. 500 μL of each cell suspension was added to the appropriately labeled well. It was ensured that cells were evenly distributed within each well. Centrifugation was then applied at 100 g for 3 minutes. The distribution of cells was examined using a microscope. Plate incubated at 37°C with 5% CO² for 2 days.

The STEMdiff™ T Cell Kit was used for hematopoietic differentiation, and methods described in its protocol were followed [300]. On day 12, FACS analysis was performed and CD34+ cells were collected into Lymphoid progenitor expansion medium.

8.1.6.3 Validating iPSC-Derived HSPC Phenotype Using FACS

1x PBS was aliquoted into a 50 mL Falcon and stored at 4°C. Collected cells were washed using 2 mL 1x PBS. Centrifugation was applied at 290 g for 5 minutes, and the supernatant was aspirated. Zombie yellow viability dye solution was prepared at a 1:250 dilution of zombie yellow solution in 1x PBS. Samples were resuspended in 100 μL of zombie yellow viability dye solution. Samples incubated for 20 minutes at room temperature in the dark. During this time, the secondary antibody solution and compensation beads were prepared. 100 μL of 1x PBS was added to each sample. Centrifugation was applied at 200 g for 5 minutes at 4°C. The supernatant was aspirated using a pipette tip. Unstained zombie yellow control sample was resuspended in 300 μL of 1x PBS and transferred to an appropriate tube and stored on ice. The rest of the samples were resuspended in 80 μL of 2mM EDTA FBS 1x PBS. Then 20 μL of FcR blocking was added to each sample. Samples incubated for 15 minutes at 4°C. Centrifugation was applied at 200 g for 5 minutes at 4°C. The supernatant was aspirated using a pipette tip. Cells of each sample were resuspended in 100 μL of secondary antibody solution. Samples incubated at 4°C for 60 minutes in the dark. Then centrifugation was applied at 200 g for 5 minutes at 4°C. Samples were then resuspended in 200 μL of FBS 1x PBS.

One drop of UltraComp or Comp beads were added to the appropriate wells of a 96-well U-bottom plate (Table.8.6). Centrifugation was applied at 200 g for 5 minutes. Supernatant was discarded by flicking the plate over a sink. Beads were resuspended in 100 μL of 1x PBS, and the appropriate volume of secondary antibody was added to each well. Samples incubated for 1 hour at room temperature. Then were stored at 4°C and used within 30 minutes.

8.1.6.4 Validating iPSC-Derived HSPC Functionality Using MethoCult

This method is based off [295]. 3 mL of MethoCult medium was aliquoted by thawing 100 mL MethoCult overnight at 4°C. Once thawed, the bottom was vigorously shaken for 1-2 minutes. The bottle stood for 5 minutes for air bubbles to dissipate. Using a 3cc syringe attached to a 16 G blunt-end needle, the needle was placed into the MethoCult medium and approximately 1 mL was drawn-up. The medium was expelled by gently pressing the plunger, and this was



Table 8.5: FACS antibodies used for the FACS analysis of iPSCs-derived HSPCs.

Channel	Marker		Fluorophore	Clone	Catalog #	Company	Dilution
VL710	CD45	+	Brilliant Violet 711	HI30	304050	Biolegend	1:50
VL450	CD34	+	Pacific Blue	581	343610	Biolegend	1:100
RL780	CD33	N/A	APC/fire750	P67.6	366632	Biolegend	1:50
RL700	CD38	-	AF700	HB-7	356623	Biolegend	1:50
RL670	CD43	+	APC	CD43-10G7	343206	Biolegend	1:50
VL785	CD90	+	BV785	5E10	328141	Biolegend	1:50
BL525	TRA-160-R	-	AF488	TRA-160-R	330614	Biolegend	1:50

Table 8.6: FACS compensation beads used to phenotype iPSCs-derived HSPCs.

Color	UltraBeads (x $\mu\text{L}/100 \mu\text{L}$)	CompBeads (x $\mu\text{L}/100 \mu\text{L}$)
BV711-CD45		1
PacBlue-CD34		1
APC-CD43		1
AF700-CD38	1	
BV785-CD90		1
AF488-TRA		1
APC-fire-CD33		1

repeated until no more air bubbles were visible. 3.5 mL of MethoCult was collected, and 3 mL of MethoCult was dispensed into a 15 mL Falcon tube. The remaining 500 μL was left in the syringe and 3.5 mL of MethoCult, in total, was collected again. This was repeated until the entire stock container was aliquoted. Aliquots were then stored at -20°C . Aliquots were prepared for 1.1 mL sample duplicates.

One aliquot of MethoCult was thawed at 4°C overnight per a sample. The following day, 30 μL of 10,000 U Pen/Strep was added, and tubes were vortexed for approximately 4 seconds. Aliquot stood for 5 minutes. 4-8 mL of sterile water was added to the empty spaces between a 6-well SmartDish [295]. 6-well SmartDish was placed into a large square dish that contained uncovered 3 cm culture dishes filled with 3 mL of sterile water. 25 mM HEPES 1% P/S IMDM medium was then prepared.

On Day 10, of the protocol described in section 8.1.6.1, a half medium change was performed. During this medium change, some of the cells were collected. Cell density was then calculated following methods described in section 8.3.1. 25,000 alive cells were transferred to an appropriately labeled 1.5 mL Eppendorf tube. Centrifugation was applied at 100 g for 7 minutes at 4°C . Supernatant was carefully aspirated, and cells were resuspended in 500 μL of 25 mM HEPES 1% P/S IMDM. 150 μL of the cell suspension was added into an appropriately labeled MethoCult aliquot. The tube was vigorously vortexed for at least 4 seconds and aliquots stood for approximately 5 minutes. A sterile 16 G blunt-end needle was attached to a sterile 3cc syringe. The air was expelled from the syringe by place the needle into the



MethoCult medium and drawing up 1 mL of medium [295]. The medium was expelled by gently pressing the plunger, and this was repeated until no more air bubbles were visible [295]. 3 mL of the MethoCult cell suspension was drawn-up and 1.1 mL was dispensed into the appropriately labeled 35 mm wells as follows: the tip of the syringe's needle was positioned over the center of a well without touching the base of the well, and 1.1 mL was dispensed. The medium was evenly distributed across the surface of each 35 mm well by gently tilting and rotating the dish [295]. The 6-well SmartDish was placed back into the large square dish that contained uncovered 3 cm culture dishes, and a rectangular dish was placed over top, I made sure it was loosely fitted [295]. The dish incubated at 37°C in 5% CO² with > 95% humidity for 14-16 days. On day 14, 15, or 16, the STEMgrid-6 was carefully attached to the bottom of the SmartDish 6-well plate, and CFU colonies were counted at 4x and 10x using the Evos microscope.

8.1.7 Differentiation: iPSC-Derived HSPCs Into T-Cells

8.1.7.1 Method 2: A Continuation From Section 8.1.6.2

Kit components a part of the STEMdiff™ T Cell Kit were used [300]. A bottle of STEMspan SFEM II thawed overnight at 4°C. The next day it was mixed thoroughly. StemSpan Lymphoid Progenitor Expansion Supplement (10x) was thawed and mixed thoroughly. Centrifugation was applied for 30 seconds to remove liquid from lid. StemSpan T-cell Progenitor Maturation Supplement (10x) was thawed and mixed thoroughly. Centrifugation was applied for 30 seconds to remove liquid from lid. Solutions were aliquoted with the volume listed in Table.8.7.

Table 8.7: Aliquots prepared of method 2 T-cell differentiation medium.

Lymphoid Differentiation Coating Material	10 μ L
StemSpan SFEM II	3.6 mL
StemSpan Lymphoid Progenitor Expansion Supplement	200 μ L
StemSpan T-cell Progenitor Maturation Supplement	200 μ L

A non-treated 96-well plate was coated with lymphoid differentiation coating material—one well per a sample. 10 μ L of lymphoid differentiation coating material was diluted in 990 μ L of 1x PBS for a total of 6 wells—this was scaled-up appropriately when necessary. This solution was mixed, and 150 μ L was distributed into six 96-wells. Plates incubated for 2 hours at 37°C. This solution was aspirated, and 1x PBS was added to each coated well. 1x PBS was aspirated prior to use. The appropriate number of StemSpan SFEM II aliquots were thawed—900 μ L of medium is required per a sample. A 3.6 mL StemSpan SFEM II aliquot was supplemented with 400 μ L of StemSpan Lymphoid Progenitor Expansion Supplement. This was called Lymphoid Progenitor Expansion Medium (Table.8.8). 200 μ L of this Lymphoid Progenitor Expansion Medium was added to each coated 96-well.

7,500 CD34+ cells from section 8.1.6.2 were collected into a lymphoid differentiation coated 96-well containing 200 μ L of Lymphoid Progenitor Expansion medium. Cells settled for 1



Table 8.8: Composition of the medium used for method 2 T-cell differentiation.

Medium Name	Components	Volume
StemSpan Lymphoid Progenitor Expansion Medium	StemSpan SFEM II	3.6 mL
	StemSpan Lymphoid Progenitor Expansion Supplement	400 μ L
StemSpan T Cell Progenitor Maturation Medium	StemSpan SFEM II	3.6 mL
	StemSpan T Cell Progenitor Maturation Supplement	400 μ L

hour in an incubator at 37°C with 5% CO². 100 μ L was very carefully removed, and 100 μ L of Lymphoid Progenitor Expansion medium was very gently added back into the well. Centrifugation was applied at 50 g for 3 minutes. This medium exchange was repeated three more times. 100 μ L of medium was removed and cells incubated at 37°C with 5% CO². Additional steps were performed following details described in it's protocol [300]. On day 14, cells were transferred to a 24-well or 96-well depending on the total number of alive cells available. On day 28, cells were harvested, and transferred to an appropriately labeled tube. FACS analysis was performed for phenotype assessment.

8.1.7.2 Validating iPSC-Derived T-Cell Phenotype Using FACS

The primary antibody solution was prepared in 1x PBS following details described in Table 8.9. iPSC-derived T-cell samples were collected. A portion of non-modified iPSC-derived T-cells and dTomato expressing iPSC-derived T-cells were transferred to separate tubes; these tubes will be used as controls. Centrifugation was applied to the samples at 300 g for 5 minutes at 4°C. Supernatant was aspirated using pipette. Control samples were resuspended in 200 μ L of 0.1 μ g/mL DAPI 1x PBS solution and stored at 4°C. Samples to be analyzed were resuspended in 50 μ L of primary antibody solution, and incubated at 4°C for 30 minutes in the dark. Centrifugation was applied at 300 g for 5 minutes. Supernatant was aspirated using a pipette, and 100 μ L of secondary antibody solution was added to each well (Table.8.9). Samples incubated at 4°C for 45 minutes in the dark. Centrifugation was applied at 200 g for 5 minutes at 4°C. Samples were resuspended in 200 μ L of 0.1 μ g/mL DAPI 1x PBS. FACS analysis was performed using an LSR Fortessa.

**Table 8.9:** FACS antibodies used to assess the phenotype of iPSCs-derived T-cells.

Channel	Marker	Fluorophore	Clone	Catalog #	Company	Dilution	
NA	Biotin CD8b	NA	NA	REA715	130-110-508	Miltenyi Bio	1:50
VL710	CD45	+	BV711	HI30	304050	Biolegend	1:50
BL530	CD4	+	FITC	RP4-T4	300506	Biolegend	1:50
VL780	Strept- avidin (CD8b)	+	BV786	-	405249	Biolegend	1:50
BL695	CD3	+	PerCP	UCHT1	300427	Biolegend	1:50
VL610	CD5	+	BV605	L17F12	364019	Biolegend	1:50
RD670	CD7	+	APC	CD7-6B7	343107	Biolegend	1:50

8.2 Mouse Cell Culture

8.2.1 Mouse HSPCs

Within this section, I describe the *ex vivo* expansion and maintenance of mouse HSPCs.⁷ For mouse bone marrow transplantations, see section 8.6.

8.2.1.1 Extracting Bone Marrow Cells From Mouse Femurs and Tibias

Methods described here are based off previously described methods [330, 331]. 1.5 mL and 2.0 mL Eppendorf tubes were autoclaved. 10% PVA solution, TPO, and SCF aliquots were prepared.

1x PBS was added to the appropriate number of 50 mL Falcons, which were stored on ice. 5-week-old C57BL/6J male mice were obtained and euthanized by cervical dislocation. The epidermis, dermis, and hypodermis were removed around the caudal part of the body. The legs were collected, placed on paper towel, and sterilized using 70% ethanol. The femur and tibia were dislocated at the knee by cutting the knee tendons and ligaments, and by gently placing pressure at the knee joint using scissors. Once dislocated, muscles around the femur were removed by peeling muscles towards the hip bone. The head of the femur was dislocated from the acetabulum. Femur(s) was then placed in the appropriately labeled 50 mL Falcon. To obtain the tibia, the foot was dislocated from the tibia by severing a couple tendons and ligaments, then by using the scissors to create pressure at the ankle and moving the foot back and forth until dislocated. Once dislocated, muscles were removed around the tibia. The tibia(s) was then place in the appropriately labeled 50 mL Falcon tube.

For the following steps, aseptic techniques were used by extracting cells from the bone marrow inside a laminar flow hood. 1x PBS was aspirated from the tube(s) containing femur(s) and tibia(s) and 10 mL of 70% ethanol was applied and immediately aspirated. Bones were washed twice with 1x PBS and stored in 1 mL of 1x PBS. 2 mL of 1 mM EDTA 1x PBS was added to the appropriate number of wells of a 6-well plate. Then bones were transferred into the appropriate well. Bones were crushed using the opening of an uncapped 15 mL Falcon tube by

⁷Techniques were performed aseptically.

crushing bones near the side of well. A 30 μm strainer was placed on top of a 15 mL Falcon tube. The cell suspension from a single well was transferred into the 15 mL Falcon tube through the strainer. 2 mL of 1 mM EDTA 1x PBS was added to the well, and bones were crushed even further. This cell suspension was transferred to the same 15 mL Falcon. This washing step was repeated two more times. Centrifugation was applied at 150 g for 7 minutes. Supernatant was carefully aspirated and 1x PBS was applied to each cell pellet. Centrifugation was applied at 150 g for 7 minutes, and supernatant was carefully aspirated, and 1x PBS was applied. The cell density was calculated following methods described in section 8.3.1.

8.2.1.2 Culturing Mouse Bone Marrow Cells Depleted of Mature Hematopoietic Cells

Steps described in section 8.2.1.1 were first performed. Mature hematopoietic cells were then removed from the bone marrow cells by using the Direct Lineage Cell Depletion Kit (Mouse) [204]. After lineage depleted cells were collected, the cell density was calculated following steps described in section 8.3.1. Centrifugation was applied at 200 g for 7 minutes. Supernatant was aspirated, and cells were resuspended in supplemented Ham's F-12 medium at $5(10)^5$ cells/mL. 1 mL or 1.5 mL of medium was transferred to the appropriate wells of a fibronectin coated 24-well plate, and cells incubated at 37°C with 5% CO².

Gently medium changes were performed daily following methods described in Wilkinson [330]. For medium changes performed \geq day 2, a small portion of cells are generally collected during a medium change. To prevent loss of cells, 3-5 drops of the collected supernatant were transferred to a new well—containing fresh medium—and pooled together with leftover cells from 3 other wells.

4 days post-cell extraction, cells were collected and washing with 1 mM EDTA PBS. Centrifugation was applied at 200 g for 7 minutes and another washing step was performed using 1x PBS. Lineage depletion was performed again using the Direct Lineage Cell Depletion Kit (Mouse) [204]. Cells were applied to the column in 1 mM EDTA PBS. After hematopoietic stem and progenitor cells (HSPCs) were collected, the cell density was calculated following steps described in section 8.3.1. Centrifugation was applied at 200 g for 7 minutes. Supernatant was aspirated, and cells were resuspended in supplemented Ham's F-12 medium at $5(10)^5$ cells/mL. 1 mL of medium was transferred to the appropriate wells of a fibronectin coated 24-well plate, and cells incubated at 37°C with 5% CO². Gentle medium changes were performed following the steps described above. If cells were to be used for an electroporation experiment, viable cells were isolated using the Dead Cell Removal Kit 1 day prior to electroporation, and cells were seeded at $5(10)^5$ cells/mL in supplemented Ham's F-12 medium. Medium changes were not performed within 24 hours of a sample analysis as SCF expression is affected by medium changes performed within 24 hours [330]. At the end of every experiment, a microplasma analysis was performed following methods described in section 8.3.3.

8.2.1.3 Culturing Mouse Bone Marrow Cells Enriched With Rare HSPC



Populations

For the initial part of this protocol, methods described in paragraph 1 of section 8.2.1.2 were followed. Except after lineage depleted cells were collected, centrifugation was applied, and cells were resuspended in 1 mL of PBS. 10 μL of a sample's cell suspension was removed and transferred to a 1.5 mL Eppendorf tube. This sample will be used as a zombie yellow single stained control. Centrifugation was applied at 290 g for 7 minutes at 4°C to all the samples. Zombie yellow viability dye solution was prepared at a 1:250 dilution of zombie yellow solution in 1 mM EDTA 1x PBS. Samples were resuspended in 100 μL of zombie yellow viability dye solution. Samples incubated for 20 minutes at room temperature in the dark. During this time, the primary antibody solution, secondary antibody solution, and compensation beads were prepared. 100 μL of 1x PBS was added to each sample. Centrifugation was applied at 290 g for 5 minutes at 4°C. The supernatant was aspirated using a pipette tip. The zombie yellow control sample was resuspended in 300 μL of 1 mM EDTA 1x PBS and transferred to an appropriate tube and stored on ice. The rest of the samples were resuspended in 100 μL of 2 mM EDTA 1x PBS. Then, 8 μL of FcR blocking was added to each sample. Samples incubated for 15 minutes at 4°C. 100 μL of the primary antibody solution was added to each sample, and samples incubated at 4°C for 30 minutes in the dark. Centrifugation was applied at 290 g for 7 minutes, and the supernatant was aspirated using a pipette. Cells from each sample were resuspended in 200 μL of the secondary antibody solution. Samples incubated at 4°C for 60 minutes in the dark (or 90 minutes when CD34 was used). Centrifugation was applied at 290 g for 5 minutes at 4°C. The supernatant was aspirated, and cells were resuspended in the appropriate amount of 1 mM EDTA 1x PBS, and filtered into a sterile 5 mL Polystyrene Round-Bottom Tube with Cell-Strainer Cap.

One drop of OneComp eBeads and UltraComp eBeads was added to the appropriate well of a U-bottom 96-well plate. Centrifugation was applied at 300 g for 5 minutes. Supernatant was discarded by flicking the plate over a sink. 100 μL of primary antibody solution was added to the well labeled for APC-eFluor780-Lineage. All other wells were resuspended in 1x PBS. Samples incubated for 30 minutes at room temperature in the dark. Then centrifugation was applied at 300 g for 5 minutes. The supernatant was discarded by flicking the plate over a sink. Beads were resuspended in 100 μL of 1x PBS, and the appropriate amount of secondary antibody was added to each well. Samples incubated for 30 minutes at room temperature in the dark. Centrifugation was applied at 300 g for 5 minutes. Samples were resuspended in 300 μL of 1x PBS. Beads were stored on ice.

A fibronectin coated 24-well plate had an appropriate number of wells filled with 1.5 mL of supplemented Ham's F-12 medium. Sorting was performed using a BD FACSAria™ Fusion. Voltages were set using the zombie yellow control sample. Compensation beads were recorded, and the proper compensation parameters were set-up. Experimental samples were ran using 4-way purity, and 3,000 alive cells were sorted into each well containing 1.5 mL of medium. Cells incubated at 37°C with 5% CO₂ for 5 days. Then a gentle medium change was performed every three days [330]. The day prior to electroporation, viable cells were isolated using the Dead Cell Removal Kit (section 8.3.5). At the end of every experiment, a microplasma analysis was performed as described in section 8.3.3.



Table 8.10: FACS antibodies used to assess the phenotype of mHSPCs.

Channel	Marker		Fluorophore	Clone	Catalog #	Company	Dilution
NA	CD4	NA	Biotin		13-0042-85	eBioscience	1:2800
NA	CD8	NA	Biotin		12-0081-86	eBioscience	1:2800
NA	CD45R (B220)	NA	Biotin		13-0452-85	eBioscience	1:1400
NA	TER119	NA	Biotin		13-5921-85	eBioscience	1:700
NA	Ly6G	NA	Biotin		13-5931-85	eBioscience	1:700
NA	CD127	NA	Biotin		13-1271-85	eBioscience	1:1400
VL450	Sca1	+	BV421	D7	108127	Biologend	1:200
RL780	Lineage	-	Strept- avidin APC- eFluor780	-	47-4317-82	Invitrogen	1:400
RL670	c-Kit	+	APC	2B8	105811	Biologend	1:100
VL710	CD150	+	BV711	TC15- 12F12.2	115941	Biologend	1:150
BL530	CD34	-	FITC	Ram34	11-0341-81	Invitrogen	1:100
YG561	CD135	-	PE	A2F10	12-1351-82	Invitrogen	1:50
VL780	CD48	-	BV785	HM48-1	103449	Biologend	1:100

Table 8.11: FACS compensation bead used to phenotype mHSPCs.

Color	UltraBeads (x $\mu\text{L}/100 \mu\text{L}$)	CompBeads (x $\mu\text{L}/100 \mu\text{L}$)
BV421	1 μL	-
APC	-	4 μL
APC-eFluor780	-	0.5 μL
BV711	-	0.5 μL
FITC	-	4 μL
PE	-	0.7 μL
BV785	2 μL	-

8.2.1.4 Gentle Medium Changes for Mouse HSPCs

Medium changes were performed holding the plate at a 45° angle. The tip of a 1 mL pipette was placed at the level of the meniscus at the side of the well containing the collected medium. While following the level of the meniscus, the medium was slowly collected. When performing medium changes on wells that reached a confluency $\geq 50\%$ (always the case with BM cells only depleted of mature hematopoietic cells, section 8.2.1.2), many cells were usually collected in the final 200 μL of medium aspirated. Directly transfer this 200 μL (between 3-5 drops) into a fibronectin coated 24-well plate containing fresh medium. Depending on the concentration of cells, 3-4 well that had a medium change performed on them, had their aspirated cells pooled together.

8.2.1.5 Transfecting Mouse HSPCs

Cells were collected, after following the expansion protocol described in section 8.2.1. S/MAR DNA vectors were obtained and thawed on ice. The appropriate number of 1.5 mL Eppendorf tubes was obtained and appropriately labeled—the total number of 1.5 mL Eppendorf tubes corresponded to the total number of pulsed samples and S/MAR DNA vector used. S/MAR



DNA vector solutions were prepared in EP Buffer at a concentration of 72 $\mu\text{g}/\text{mL}$ (final concentration will be 36 $\mu\text{g}/\text{mL}$). 13 μL of each S/MAR DNA solution was transferred to the appropriately labeled sample 1.5 Eppendorf tube. For pulsed controls (no S/MAR DNA vector) 13 μL of EP buffer was transferred to the appropriately labeled sample 1.5 Eppendorf tube. The appropriate number of OC25x3 electroporator strips were obtained, and properly labeled. A fibronectin coated 96-well plate was obtained and the appropriate number of well—corresponding to the number of samples—was filled with 200 μL of supplemented Ham's F-12 medium without antibiotics nor cytokines (supplemented Ham's F-12 medium (electroporation)).

The appropriate number of cells were collected— $3(10)^5$ per a sample—and transferred to a 15 mL Falcon tube. Remaining cells were kept in culture and a microplasma analysis was performed following steps described in section 8.3.3. Centrifugation was applied at 100 g for 10 minutes with an acceleration of 5 g and a deceleration of 5 g. Supernatant was aspirated, and 5 mL of EP buffer was slowly applied to the cell pellet without disrupting it. Centrifugation was applied at 100 g for 10 minutes with an acceleration of 5 g and a deceleration of 5 g. Supernatant was aspirated, and 5 mL of EP buffer was slowly applied to the cell pellet without disrupting it. Centrifugation was applied at 100 g for 4 minutes with an acceleration of 5 g and a deceleration of 5 g. Supernatant was aspirated until 200 μL remained. Samples were moved to a fixed angle rotor centrifuge, and centrifugation was applied at 100 g for 1 minute. supernatant was carefully aspirated, and the appropriate volume of EP buffer was applied to the cell pellet—13 μL per a sample. Samples were resuspended by flicking the base of the tube. 13 μL of cell suspension was transferred to the appropriate labeled 1.5 mL Eppendorf tube containing DNA. 26 μL of cell suspension in DNA was transferred to an appropriate well of an electroporator strip using a 200 μL pipette containing a 20 μL tip. Samples were loaded by placing the tip into the center of the electroporation strip well with little space from the bottom. Quickly 5 μL was loaded, and then the rest of the cell suspension was slowly added while lifting the pipette tip out of the well. The electroporator strip was inserted into the appropriate location of the MaxCyte GT, and the pulse code Opt-8 was applied. Samples recovered for 20 minutes in an incubator at 37°C with 5% CO². Then were transferred to an appropriately labelled well of the prepared fibronectin coated 96-well plate. The well of the electroporator strip was rinsed with supplemented Ham's F-12 medium (electroporation) and this solution was transferred to the appropriate well of the fibronectin coated 96-well plate. 3 hours post-electroporation, a full gentle medium change (section 8.2.1.4) was performed using pre-warmed supplemented Ham's F-12 medium containing cytokines and without antibiotics. 24 hours post-electroporation, microscope images were taken, supernatant was collected and stored at -80°C, and cells were analyzed via FACS following methods described in section 8.2.1.7.⁸⁹

⁸NOTE: An extra set of non-modified cells was necessary for setting laser voltages for the FACS analysis. This was kept in mind for each experiment requiring FACS analysis.

⁹NOTE: Very minimal pipetting of cells occurred prior to electroporation. Shear forces (caused by pipetting) combined with electroporation can be detrimental for cells.



8.2.1.6 Transducing Mouse HSPCs Using AAVs

Supplemented Ham's F-12 medium was prepared. Cells were obtained, and the cell density was calculated (section 8.3.1). The appropriate number of cells from each donor was collected— $1(10)^5$ cells per sample. Centrifugation was applied at 200 g for 8 minutes. Supernatant was aspirated, and each sample was resuspended in 500 μL of supplemented Ham's F-12 medium and plated into a fibronectin coated 24-well plate. AAV virus was added to the cells at an MOI of $5(10)^4$. Samples incubated at 37°C with 5% CO_2 for three days. A full gentle medium change was performed (section 8.2.1.4). The transduction efficiency was assessed using microscopy (Nikon microscope) and FACS (section 8.2.1.7). At the end of every experiment, a microplasma analysis was performed following methods described in section 8.3.3

8.2.1.7 Flow Cytometry Analysis of Mouse HSPCs

Medium changes were performed 24 hours or more prior to FACS analysis. Cells were transferred to a 96-well V-bottom plate. Centrifugation was applied at 200 g for 7 minutes at 4°C . Supernatant was aspirated using a pipette, and cells were resuspended in 100 μL of 1x PBS. Centrifugation was applied at 200 g for 7 minutes at 4°C . Supernatant was aspirated using a pipette, and cells were resuspended in 70 μL of zombie yellow solution diluted in 1x PBS at a 1:87.5 ratio. Samples incubated for 20 minutes at room temperature in the dark. During this time, primary antibody solution and secondary antibody solution (Table 8.10) were prepared. Cells were resuspended in 50 μL of 1x PBS, and 4 μL of FcR blocking was added to each sample. Samples incubated for 15 minutes at 4°C . 50 μL of the primary antibody solution was added, and samples incubated at 4°C for 30 minutes in the dark. Centrifugation was applied at 200 g for 7 minutes, and the supernatant was aspirated using a pipette. Cells were resuspended in 100 μL of the secondary antibody solution. Samples incubated at 4°C for 60 minutes in the dark (or 90 minutes when CD34 was used). Centrifugation was applied at 200 g for 5 minutes at 4°C . The supernatant was aspirated, and cells were resuspended in 200 μL of 1x PBS or ACB solution (section 8.3.9), and filtered into a sterile 5 mL Polystyrene Round-Bottom Tube with Cell-Strainer Cap. Compensation beads were prepared following steps described in paragraph 2 of section 8.1.6.3. FACS analysis was performed using an LSR Fortessa. Data was analyzed using FlowJo software, R, and Gephi.

8.2.1.8 FLOWMAP Code

Code 1

```
mode ← 'one-special' minimum ← 2 maximum ← 8 distance.metric ← 'manhattan'
cluster.numbers ← 300 var.annotate ← list('FJComp-FITC-A' = 'CD34', 'FJComp-APC-Fire
750-A' = 'Lineage', 'FJComp-BV421-A' = "Sca-1", 'FJComp-BV711-A' = "CD150",
'FJComp-APC-A' = "c-kit") var.remove ← c() clustering.var ← c("Sca-1", "CD150", "c-kit",
"Lineage", "CD34") seed.X ← 1 set.seed(seed.X) subsamples ← 300 name.sort ← FALSE
downsample ← FALSE savePDFs ← TRUE which.palette ← 'bluered'
```

```
FLOWMAPR::FLOWMAP(mode = mode, files = files, var.remove= var.remove, var.annotate
```



```
= var.annotate, clustering.var = clustering.var, cluster.numbers = cluster.numbers,
distance.metric = distance.metric, minimum = minimum, maximum = maximum, save.folder
= save.folder, subsamples = subsamples, name.sort = name.sort, downsample = downsample,
seed.X = seed.X, savePDFs = savePDFs, which.palette = which.palette)
```

Code 2

```
mode ← 'single' minimum ← 2 maximum ← 5 distance.metric ← 'manhattan'
cluster.numbers ← 300 var.annotate ← list('FJComp-BL-525_50-A' = 'CD34',
'FJComp-RL-780_60-A' = 'Lineage', 'FJComp-VL-450_50-A' = "Sca-1",
'FJComp-VL-710_50-A' = "CD150", 'FJComp-RL-670_30-A' = "c-kit",
'FJComp-VL-610_20-A'="viability") var.remove ← c("viability") clustering.var ← c("Sca-1",
"CD150", "c-kit", "CD34", "Lineage") seed.X ← 1 k←5 set.seed(seed.X) subsamples ← 600
name.sort ← FALSE downsample ← FALSE savePDFs ← TRUE which.palette ← 'bluered'

FLOWMAPR::FLOWMAP(mode = mode, files = files, var.remove= var.remove, var.annotate
= var.annotate, clustering.var = clustering.var, cluster.numbers = cluster.numbers,
distance.metric = distance.metric, minimum = minimum, maximum = maximum, save.folder
= save.folder, subsamples = subsamples, name.sort = name.sort, downsample = downsample,
seed.X = seed.X,k=k, savePDFs = savePDFs, which.palette = which.palette)
```

Code 1= [section 4.1.1](#) Code 2= [section 4.1.2](#)

8.3 Cell Culture: Routine Procedures

8.3.1 Cell Counting

The Cell Counter Luna™ FL Auto was used to calculate cell densities. 10 μL of trypan blue was transferred to a 1.5 mL Eppendorf tube, and 10 μL of cell suspension was added and resuspended. 10 μL of the trypan blue cell suspension solution was transferred to a Luna Chamber. The Luna chamber was inserted into the Cell Counter Luna™ FL Auto. The protocol “cell counting” was ran with standard settings and a 1:1 dilution. Cell densities are most reliably measured between $0.5(10)^6$ and $3(10)^6$ cells/mL. If count is above this range, perform an appropriate dilution.

8.3.2 Preparing FBS Aliquots

FBS was thawed in a water bath at 37°C. Once thawed, FBS incubated at 56°C for 30-60 minutes to inactivate it. FBS was then cooled to 4°C, and 25 mL aliquots were prepared following aseptic technique. These aliquots were then stored at -20°C.

8.3.3 Microplasma Testing

Cells were kept in culture for three days in the absence of antibiotics. 500 μL of supernatant was collected and microplasma analysis was performed following methods described by Eurofins Genomics [91].

8.3.4 Cell Line Validation

$1(10)^6 - 5(10)^6$ of cells were obtained—for primary cells, aim for $5(10)^6$. Centrifugation was applied at 300 g for 5 minutes. DNA extraction was performed following steps described by QIAGEN using the DNeasy Blood & Tissue Kit for cultured cells [262]. DNA concentration and quality was measure and recorded. The purified genomic DNA concentration was adjusted to 15-30 ng/ μ L. DNA was stored at 4°C (short-term) or -20°C (long-term). An e.biss submission form was completed (relevant for DKFZ internals). Sample tubes were labeled with “MCA” and the specific sample name corresponding to the name provided in the e.biss submission form. $\geq 15 \mu$ L of each sample was added to the appropriately labeled tube, and shipped for Multiplexion genomics analysis.

8.3.5 Dead Cell Removal

Dead cell removal was performed using the Dead Cell Removal Kit from Miltenyi Biotec B.V. Methods description by Miltenyi Biotec B.V were followed [203].

8.3.6 Cell Cryopreservation

The appropriate number of cells were collected for cryopreservation. Centrifugation was applied at 200 g for 5 minutes. Supernatant was aspirated and cells were gently resuspended in the appropriate volume of freezing medium (Table.8.12). The appropriate volume of cell suspension was transferred to a CryoTube™ vial. Vials were place in a CoolCell® container, and this container incubated at -80°C overnight. CryoTube™ vials were removed from the CoolCell® container by transferring onto dry ice. These vials were then transferred to a nitrogen freeze tank (-180°C) for long-term storage.

Table 8.12: Cell cryopreservation medium.

Cell Type	Standard Freezing Medium	Cell Count	Freezing Volume	Plate Format for Thawing
Jurkat76	RPMI 10% DMSO 10%FBS 1% AA 1% P/S	$2(10)^6$	1 mL	T25
Human PBMCs	FBS 10% DMSO	$5(10)^6$	1 mL	T75 flask
iNHDFs	DMEM 10% DMSO 10% FBS 1% NEAA 1% GlutaMAX	1/2 of a 95% confluent T75 flask	1 mL	T75 flask
HEK293T	DMEM 10%DMSO 10% FBS	1/6 of a 90% confluent T175 flask	1 mL	T175 flask
Human iPSCs	Basic04 10% DMSO	75,000	500 μ L	one well of a 6-well plate

8.3.7 ELISA Legendplex

Samples were thawed and warmed to 21°C. Centrifugation was applied at 300 g for 5 minutes in order to remove cellular debris. 15 μ L of sample supernatant was applied to the



appropriate wells of the LegendPlex V-bottom plate. Methods described by BioLegend were then followed using the LEGENDplex™ Mouse Anti-Virus Response Panel with V-bottom Plate [27]. Reagents were scaled appropriately to 15 μL of seeded sample supernatant. Data were acquired using an LSR Foressa with HTS. 3,000 total bead events per sample were acquired—500 beads events per a bead type used [28]. Data analysis was performed using the Legendplex software [26].

8.3.8 ELISA InvivoGen

The LumiKine™ Xpress hIFN- β 2.0 Kit was used and methods described by InvivoGen were followed [145]. Solutions, reagents, and the hIFN- β coated plate (requires an overnight incubation) were prepared the day prior to analysis. If aliquots of reagents were already prepared from a previous experiment, the appropriate number of aliquots were thawed the day of analysis. The VICTOR Nivo™ luminometer was used to measure relative light units for 0.1-0.5 seconds immediately after QUANT-Luc Plus solution was added. A calibration curve was prepared using a dose response four parameter logistic curve fit (Equation. 8.4) using R.

$$y = \frac{d + (a - d)}{1 + (x/c)^b} \quad (8.4)$$

b= slope c= point of inflection a= minimum value d= maximum value

8.3.9 Absolute Count Beads

Absolute count bead (ACB) solution was prepared by adding 2 mL of 1x PBS to an appropriate tube. CountBright™ Absolute Counting Beads were vigorously vortexed for 1 minute. 70 μL of CountBright™ Absolute Counting Beads was added to the 2 mL of 1x PBS, and the solution was well mixed. The volume of ACB solution used to resuspend cells was recorded (generally 200 μL).

Absolute cell counts were calculated following methods described by Invitrogen [144].

8.4 Plasmids

8.4.1 DNA Vectors With a Bacterial Backbone

Ligations were performed using In-Fusion® cloning. In-Fusion® clones were designed using SnapGene. Once the design was determined, the proper vectors, enzymes, and primers were collected. First, the DNA fragment for insertion was generated via PCR amplification using the composition described in Table.8.13 and the PCR settings described in Table.8.14.

DNA fragment used as a backbone was then digested. 4 μg of DNA vector was added to an autoclaved 1.5 mL Eppendorf tube. 2 μL of 10x FD Green Buffer, 1.5 μL of each restriction enzyme, and the appropriate amount of nuclease free water to reach a total volume of 20 μL was added (Table. 8.15). This solution incubated at 37°C for 1 hour.



Table 8.13: The required reagents to PCR amplify a ligation insert.

Clone Amp HiFi PCR preMix	12.5 μL
Forward primer (10 μM)	0.75 μL
Reverse primer (10 μM)	0.75 μL
Template DNA	500 pg
Water (nuclease free)	x
Total	25 μL

Table 8.14: PCR cycle settings to amplify a ligation insert.

1. Heat lid to 110°C
2. 95°C for 2 minutes
3. Open 35x cycles
4. 98°C 10 seconds
5. 55°C 10 seconds
6. 72°C 10 seconds (5 seconds per 1 kb)
7. Close cycles
8. 72°C 10 minutes
9. Store forever 4°C

Table 8.15: The required reagents to digest a backbone.

DNA Vector	4 μg
Enzyme 1	1.5 μL
Enzyme 2	1.5 μL
10x FD Green Buffer	2 μL
Water (nuclease free)	x
Total	20μL

The amplified DNA fragment for insert and the DNA fragment used as a backbone were purified using a 1% agarose gel. A 1% agarose gel was prepared by adding 0.5 g of agarose into a flask, and adding 50 mL of EP Buffer. This solution was gently heated in a microwave. As soon as bubbling appeared, the microwave was turned off, and the flask was carefully swiveled wearing the proper protective gear—be mindful of bumping. This was repeated until no solid agarose particles are present. Sample cooled for 5 minutes. Then, 1 μL of pegGREEN was added, and poured into a gel cast that was properly positioned in a gel chamber with a 10-well or 12-well comb. If bubbles were present in the gel, they were popped using a pipette tip. Gel set for 20 minutes. The comb was removed, and the gel cast was properly positioned in the gel chamber for running DNA (negative to positive). EP buffer was used to fill the gel chamber until the gel was covered. 6 μL of a 1 kb gene ruler ladder was loaded into a well formed within the gel. Samples were also loaded into the appropriate wells. However, prior to loading PCR samples, 4 μL of Gel Loading Dye was added to the PCR amplified DNA fragment for insert. The gel had 80 V applied for 45-60 minutes—until the DNA ladder marker ran to the bottom of the gel. The gel within the cast was carefully removed and placed into a Fusion SL VILBER Lourmat PEQlab chamber. "Fl zoom" was selected within its computer program settings, and manual exposure was applied for the appropriate amount of time. Image was recorded and examined. The appropriate DNA bands



were extracted from the gel using a scalpel by placing the gel on a UV imager, applying exposure—while wearing the appropriate protective gear—and quickly cut around band. Tweezers were used to remove each band, and bands were transferred to individual 2.0 mL Eppendorf tubes. The weight of each band was approximated, and DNA was extracted from the gel using the GenElute™ Gel Extraction Kit [286]. The concentration and purity of the DNA was calculated using the Nanodrop.

An In-Fusion® cloning was then performed in a 1.5 mL Eppendorf tube by mixing the proper reagents together. 100 ng of backbone DNA fragment, 50 ng of insert DNA fragment, 2 μL of 5x In-Fusion Mix, and the appropriate amount of nuclease free water was added to reach a total volume of 10 μL . This solution incubated at 50°C for 15 minutes, then was immediately placed on ice.

Transformation of the In-Fusion® cloning was then performed. An ampicillin agar plate was prepared by gently heating a pre-aliquoted LB agar in a microwave. Once LB agar was liquidized, it was placed into a 55°C water bath, and periodically shaken. After 10 minutes, 15 μL of 100 mg/mL ampicillin stock was applied to each aliquot. Tubes were shaken, and the solution was poured into a bacteria culture plate in the presence of a bunsen burner. Agar set within the plate while resting on the bench for 7 minutes. Then, plates were transferred into a bacterial cell culture hood, and rested there with the lids slightly off for 90 minutes. This was performed to dry the agar, and to prevent sweating from occurring during storage. 50 μL of stellar competent cells was obtained. If 50 μL of stellar competent cells was left, they were snap frozen in dry ice and ethanol, then stored at -80°C. 2.5 μL of the In-Fusion reaction was added to the obtained 50 μL of stellar competent cells. Solution incubated on ice for 30 minutes. Samples were transferred to a heat block set to 42°C and incubated there for 45 seconds. 500 μL of SOC medium was gently applied to the bacteria, and samples incubated at 37°C for 1 hour with shaking. Centrifugation was applied at 4,000 rpm for 5 minutes. Supernatant was aspirated, and cells were resuspended in 50 μL of SOC medium. Bacteria solution was transferred onto the prepared ampicillin plate, and evenly distributed over the surface using a spreader. Plates incubated, up-side-down, at 37°C overnight.

5-10 colonies that formed were picked and transferred to individual test tubes containing 5 mL of LB medium with 5 μL of 100 mg/mL ampicillin. Tubes incubated at 37°C with shaking. The following day, a 1:1 mixture of bacteria suspension and 50% glycerol solution was added to a 2 mL Eppendorf tube, then stored at -80°C. Plasmid DNA was then extracted from the remain bacteria using the QIAprep Spin Miniprep Kit [261]. The DNA concentration and purity was then calculated. A control digestion and sanger sequencing was performed on selected colonies following methods described in sections 8.4.3.2 and 8.4.3.3, respectively. A selected colony was then expanded for mass production of DNA plasmid using an Endotoxin free Maxiprep Kit.

8.4.2 DNA Vectors With an RNA-out R6K Backbone

RNA-out R6K DNA vectors were produced following methods from Nature Technology Cloning.



8.4.3 Plasmid: Routine Procedures

8.4.3.1 DNA Precipitation

3 M sodium acetate (pH 5.2) was added at a 1:10 ratio to DNA solution. 100% ethanol was added at a 3:1 ratio to DNA solution. This solution incubated at -20°C overnight.

Centrifugation was applied at max speed for 10 minutes at 4°C. Supernatant was aspired using a pipette, and 500 μ L of cold 75% ethanol was added. This solution incubated for 2 minutes at 21°C. Centrifugation was applied at max speed for 1 minute. Supernatant was carefully aspired using a pipette, and the pellet dried in a cell culture hood for 45-60 minutes, until no liquid persisted. Nuclease free water was applied to the DNA pellet with no pipetting and incubated overnight at 4°C in order to allow the DNA to dissolve. The DNA concentration and purity were then measured using the Nanodrop 2000c.

8.4.3.2 Quality Control: Restriction Digest Test

200 ng of DNA vector, 1.5 μ L of each restriction enzyme, and 2 μ L of 10x FD green buffer was added to a 1.5 mL Eppendorf tube. The remaining volume was filled with nuclease free water until the total solution volume reached 20 μ L. Solution incubated at 37°C for 2 hours. While digestion was occurring, a 1% agarose gel was prepared. A 1 kb gene ruler ladder was loaded into a well. Samples were loaded into the appropriate wells. The gel had 80 V applied for 10 minutes, then 100 V until the DNA ladder marker ran to the bottom of the gel. The gel with the cast was carefully removed and placed into a Fusion SL VILBER Lourmat PEQlab chamber. "Fl zoom" was selected within its computer program settings, and manual exposure was applied for the appropriate amount of time. Image was recorded and examined.

8.4.3.3 Quality Control: Sanger Sequencing

Primers were designed through Primer3Plus [257]. When designing the primers, I took into consideration that sanger sequences can read about 1,000 bp and that the first 100 bp reading is poor. Sequencing was performed using Eurofins Genomics [92]. Sequences were aligned within the appropriate Snappene file, and assessed.

8.4.3.4 Glycerol Stocks

A 1:1 mixture of bacteria suspension and 50% glycerol solution were added to a 2 mL Eppendorf tube, then stored at -80°C.

8.5 Viral Vector Production

8.5.1 Lentiviral Vector Production

HEK293T cells at passages less than 15 were utilized. Methods described in this section are based off methods from Aga Sekretny and Francesco Baccianti. HEK293T were grown to near 100% confluency in a 15 cm dish. 25 mL of 1% P/S 10% FBS DMEM was added to two 15 cm dishes. Medium was aspired from cultured HEK293T cells. 1 mL of trypsin was added to



the cells, and cells incubated with trypsin for a few minutes. 4 mL of medium was used to deactivate trypsin and dislodge the cells. This cell suspension was then transferred to a 15 mL Falcon. Centrifugation was applied at 300 g for 5 minutes. Supernatant was aspirated, and cells were vigorously resuspended in 3 mL of DMEM. 1 mL of cell suspension was added to each 15 cm dish. Remaining cells were cryopreserved following methods described in section 8.3.6.

The following day, medium was gently aspirated from the 15 cm dishes containing HEK293T cells, and 10 mL of 10% FBS DMEM (no antibiotics) was added gently down the side of the dish. In the evening, a transfection mixture was prepared. Solution 1 was composed of 1200 μ L DMEM, 12 μ g of transfer plasmid (based off B1284), 6 μ g of B653 packaging plasmid, 6 μ g of B654 packaging plasmid. Kindly provided by the Henri-Jacques Delecluse lab. This solution was vortexed. Solution 2 consisted of 1200 μ L of DMEM and 72 μ L of Metafectene—3 μ L of metafectene per 1 μ g of DNA. This solution was gently mixed. Dropwise, solution 1 (DNA solution) was transferred into solution 2 (Metafectene solution). This solution was gently mixed, and incubated for 20 minutes at 21°C. Dropwise, 1200 μ L of this mixture was applied to each 15 cm dish containing HEK293T cells. Medium was gently swirled around the plate, and cells incubated at 37°C with 5% CO².

In the morning of the following day, a full medium change was performed by aspirating the medium and applying 10 mL of 10% FBS DMEM (no antibiotics) gently down the side of the dish. Cells incubated at 37°C with 5% CO².

In the morning of the following day, cell supernatant was collected into a 50 mL Falcon. This supernatant was filtered through a 0.45 μ m PVDF filter and stored at 4°C. 5 mL of Basic04, was gently applied down the side of the dish, and cells incubated at 37°C with 5% CO².

In the morning of the following day, supernatant was collected into a 50 mL Falcon tube. This supernatant was filtered through a 0.45 μ m PVDF filter and stored at 4°C. A 50,000 MWCO PES Vivaspin 20 column was pre-equilibrated by applying 20 mL of PBS to the column and applying centrifugation at 2,000 g for 5 minutes. Flow-through was discarded. 20 mL of PBS was applying to the column and centrifugation was initiated at 2,000 g for 5 minutes. Flow-through was discarded. The 20 mL of DMEM viral vector supernatant was applied to the pre-equilibrated column, and centrifugation was applied at 1500 g for 10 minutes. Then, 20 minutes at 2,000 g. Flow-through was discarded. The 10 mL of Basic04 viral vector supernatant was then applied to the column. Centrifugation was applied for 25 minutes at 2,000 g, until about 2.5 mL was left. Flow-through was discarded, and 10 mL of Basic04 was applied to the column, resuspending solution at the bottom. Centrifugation was applied at 2,000 g for 25 minutes—until about 2 mL remained. Then, flow-through was discarded. Columns were vigorously vortexed to dislodge viral vector from the column filter. 1 mL of the viral vector supernatant was collected into a 15 mL Falcon. The remaining 1 mL of viral vector supernatant was used to dislodge particles from the column filter by vigorously pipetting against the filter. Then, were pooled together with the other viral particles in the 15 mL Falcon. 100 μ L aliquots were prepared in 1.5 mL Eppendorf tubes and stored at -80°C.



8.5.2 AAV Vector Production

HEK293T cells at passages less than 15 were utilized. Methods described in this section are based off methods from Anna Hartley. Three confluent T-175 culture flasks were used to seed twenty 15 cm dishes. Ten 15 cm dishes per a construct were used for AAV production. 22 mL of DMEM 10% FBS 1% L-Glutamine 1% PenStrep was used for one 15 cm dish.

Three confluent T-175 flasks containing HEK293T were harvested in parallel. Medium was aspirated, and 15 mL of 1x PBS was gently applied to each flask—be mindful that HEK293T cells detach easily. PBS was aspirated, then 2 mL of Trypsin was gently applied to each dish. Cells incubated with Trypsin for 2 minutes, the flask was tapped to detach cells, and cells were resuspended in 16 mL of DMEM 10% FBS 1% L-Glutamine 1% PenStrep. This cell suspension was transferred to a 50 mL Falcon, and all three T-175 flasks were pooled together. The cell density was calculated following methods described in section 8.3.1. The appropriate number of cells was obtained— $8(10)^7$ to $4(10)^6$ cells per a 15 cm dish—and transferred to a separate 50 mL Falcon. Centrifugation was applied at 300 g for 5 minutes. Supernatant was aspirated, and cells were resuspended at a density of $2(10)^6$ cells/mL. 20 mL of DMEM 10% FBS 1% L-Glutamine 1% PenStrep was applied to twenty 15 cm dishes. 2 mL of the cell suspension was transferred to each 15 cm dish. Dishes were placed in an incubator at 37°C with 5% CO².

Transfection reagent using 25k PEI was prepared. 250 μ g of transfer plasmid and helper plasmid combined was required per ten 15 cm dishes. The exact amount of transfer plasmid and helper plasmid was determined based off a 1:1 molar ratio of transfer plasmid to helper plasmid. 3.2 mL of ready to use 25k PEI was required per ten 15 cm dishes. This was determined based off 25 μ g of total DNA per a dish, an NP ratio of 3.93:1 (25k PEI to DNA), and a concentration of 323 μ g/mL for 25k PEI. 17.8 mL of 0.35 M NaCl was required per ten 15 cm dishes. This was determined based on a desired 0.3 M NaCl final concentration and a total volume of 21 mL per ten 15 cm dishes. Prior to use, PEI and 0.3M NaCl were pre-warmed in a water bath to 37°C. 17.8 mL of 0.35 M NaCl was added to a 50 mL Falcon, for each viral vector construct. The appropriate amount of helper plasmid was added to each 50 mL Falcon. The appropriate amount of transfer plasmid was added to each 50 mL Falcon. The appropriate amount of 25k PEI was added to each 50 mL Falcon. This solution was vigorously vortexed and incubated at 21°C for 10 minutes. 2 mL of this transfection solution was evenly dispersed dropwise into each 15 cm dish—ten 15 cm dishes in total. Plates were gently moved around to evenly distribute PEI/DNA particle complexes. Plates incubated at 37°C with 5% CO² for three days.

Cells were then harvested. 8 mL of supernatant was aspirated from each dish. Using a cell scraper, cells were detached from the dish. Cells around the rim of the dish were first detached, then the remaining were detached. This cell suspension was collected and pooled into four 50 mL Falcon. The harvested dishes were rinsed with 5 mL PBS and this cell suspension was transferred into the four 50 mL Falcons. Centrifugation was applied to this cell suspension at 800 g for 15 minutes. The supernatant was aspirated. Each cell pellet was resuspended in 10 mL 1x PBS and pooled into one 50 mL Falcon. Centrifugation was applied



at 800 g for 15 minutes. Supernatant was aspirated, and cell pellets were frozen at -80°C .

Viral particles were then removed from cells. Cell pellets were resuspended in 5 mL of virus lysis solution, and this cell suspension underwent snap freezing by storing samples at -196°C for 5 minutes, then thawing samples at 37°C . This process was repeated 5 times. At this point, samples can be stored at -80°C or can be continued for processing. Samples were sonicated for 1 minute and 20 seconds. $1.5\ \mu\text{L}$ of 250 u/ μL benzonase (100,000 u) was added to each sample to reach a final concentration of 75 u/mL. Benzonase was added to get rid of RNA and DNA. Samples were vortexed, then incubated at 37°C for 1 hour. Samples were inverted every 10 minutes. Centrifugation was applied at 4,000 g at 4°C for 15 minutes. Supernatant was transferred to a 50 mL Falcon. Centrifugation was applied at 4,000 g at 4°C for 15 minutes.

An Iodixanol gradient was performed to extract viral vectors from other impurities. PBS-MK, PBS-MK-NaCl, 60% Iodixanol, 40% Iodixanol, 25% Iodixanol, 15% Iodixanol solutions were prepared for Iodixanol gradient. A 16x 76 mm Beckman Ultracentrifuge tube was obtained. A Pasteur pipette was placed through the opening of the centrifuge tube and the tip of the Pasteur pipette rested at the base of the centrifuge tube. The viral vector supernatant was collected using a 10 mL serological pipette. The tip of the 10 mL serological pipette had a 1 mL pipette tip added to it. The viral vector supernatant was carefully transferred into the centrifuge tube through the Pasteur pipette. Avoid bubbles as this will disrupt the centrifuge tube during centrifugation. 1.5 mL of 15% Iodixanol solution was transferred into the centrifuge tube following the same method—a slow steady stream is required for layering the solutions, disrupted layers may affect the efficacy of the viral vector collection. This was also performed for 1.5 mL of 25% Iodixanol solution, 1.5 mL of 40% Iodixanol solution, and 1.5 mL of 60% Iodixanol solution. The Pasteur pipette was carefully removed while blocking the opening of the Pasteur pipette with a finger—while wearing the appropriate safety equipment. Using a 1 mL syringe, virus lysis solution was slowly added until the entire tube was filled with solution. If any bubbles are present, carefully tap the tube. Tubes were sealed using a tube sealer instrument. Tubes were balanced using red plugs, a maximum difference of 0.01 g is possible. Ultracentrifugation was applied at 50,000 rpm for 2 hours at 4°C .

The 40% Iodixanol phase was collected as viral vector particles persist there. An ultracentrifuge tube was fixed in the brackets of a stand. A 20G x 1.5 Nr.1, 0.8x 40 mm needle was stuck into the top of the tube. A 1 mL syringe had a 20G x 1.5 Nr.2, 0.8x 40 mm needle attached to it, and the needle was stuck into the ultracentrifuge tube at an angle through the 60% iodixanol phase into the 40% iodixanol phase. A maximum of 1.2 mL is generally collected. Avoid the 25% iodixanol phase as this phase contains empty viral capsids.

Viral vector particles were concentrated and had iodixanol removed using a Vivaspin6 100 kDa column. Column were filled with 6 mL of cold 1x PBS, and centrifugation was applied at 2,000 g for 5 minutes. Flow-through was discarded, and this washing step was repeated. 5 mL of 1x PBS was added to the column. The viral vector solution was then added.

Centrifugation was applied at 1,500 for 5 minutes. Flow-through was discarded. 6 mL of 1x PBS was applied to each column. Centrifugation was applied at 2,000 g until about 400 μL of solution was left—do not want membrane to dry. Flow-through was discarded. Washing was



performed three more times. Columns were vortexed to dislodge viral particles stuck on membrane. This viral vector solution was removed using a 200 μL pipette tip. Then, the column membrane was vigorously washed using 100 μL of 1x PBS. This was pooled with the collected viral vector particles. Aliquots were prepared, and store at -80°C .



8.6 Mouse Bone Marrow Transplantations

5 to 6-week-old C57BL/6J male mice from Janvier labs (expanded following methods described in section 8.2.1 and 11-week-old C57BL/6J Ly5.1 female mice bred in-house were utilized.

8.6.1 Preparing Recipient Mice for Transplantations

The day prior to irradiation, mice were weighted and ear punched. Lethal irradiation of the recipients was performed with 2x 500 Rad in a cesium irradiator by the authorized animal caretakers. Within 24 hours of irradiation, bone marrow transplantation was performed (section 8.6.4).

8.6.2 Preparing Donor Cells for Primary Engraftment

8.6.2.1 Preparing Bone Marrow Protection Cells (Ly5.1)

Bone marrow cells were harvested from 11-week-old C57BL/6J Ly5.1 female mice following methods described in section 8.2.1. The cell density was calculated following methods in section 8.3.1. 1.5 mL Eppendorf tubes were labeled appropriately. 500,000 C57BL/6J Ly5.1 bone marrow cells were transferred into each tube. Centrifugation was applied at 200 g for 5 minutes. Supernatant was aspirated, and cells were resuspended in 500 μL of 1x PBS.

8.6.2.2 Preparing Expanded HSPCs (Ly5.2) With Bone Marrow Protection Cells

The cell density was calculated for each donor following methods in section 8.3.1. 120,000 expanded cells from each donor was transferred into an appropriately labeled 1.5 mL Eppendorf tube. Centrifugation was applied at 200 g for 10 minutes. Supernatant was carefully aspirated, and cells were resuspended in 1 mL of 1x PBS. The appropriate volume of cell suspension (Table. 8.16) was transferred into the appropriately labeled tubes containing bone marrow protection cells (Section 8.6.2.1).

Table 8.16: Cell counts used for mouse bone marrow engraftments.

Total number of expanded HSPCs to be engrafted into mice	Volume of expanded HSPCs stock (120,000 cells/mL) added to 1 mL PBS
control	0 μL
200	8.3 μL
2,000	83.3 μL
20,000	833.3 μL

500 μL of 1x PBS was added to control samples, 491.7 μL of 1x PBS was added to samples containing 200 expanded HSPCs, and 416.7 μL of 1x PBS was added to samples containing 2,000 expanded HSPCs. For samples containing 20,000 expanded HSPCs, centrifugation was applied at 200 g for 5 minutes. Supernatant was aspirated, and cells were resuspended in 1000 μL of 1x PBS. Cells were stored on ice. 200 μL of cell suspension was transplanted into an irradiated 11-week-old C57BL/6J Ly5.1 female mouse (Section 8.6.4).

8.6.3 Preparing Donor Cells for Secondary Engraftment

Bone marrow cells were harvested from recipient mice that underwent a primary transplantation (4-months post-engraftment). Cells were harvested following methods described in section 8.2.1. 500,000 cells were collected from each donor and transferred to an appropriately labeled 1.5 mL Eppendorf tube. The remaining cells were stored on ice, and were used for FACS analysis described in section 8.6.5. For the 500,000 cells collected, centrifugation was applied at 150 g for 7 minutes. The supernatant was aspirated, and cells were resuspended in 500 μ L of 1x PBS. Cells were stored on ice. 200 μ L of cell suspension was transplanted into an irradiated 11-week-old C57BL/6J Ly5.1 female mouse.

8.6.4 Performing Bone Marrow Transplantations

Engraftments were performed by Michael Bonadonna.

8.6.5 Peripheral Blood FACS Analysis

Blood collections from the cheek were performed to assess the current engraftment efficiency of expanded mouse HSPCs. Blood was collected into EDTA coated tubes from recipient mice 2-months post-primary engraftment, 4-months post-primary engraftment, and 4-months post-secondary engraftment. Samples were placed on ice. 1.5 mL Eppendorf tubes were appropriately labeled, and 200 μ L of 2% FBS 1x PBS solution was added to each tube. 50 μ L of blood was transferred into the appropriately labeled 1.5 mL Eppendorf tube containing 2% FBS 1x PBS. Samples incubated on ice for 20 minutes. Then, 1 mL of ACK lysing buffer was added to each sample. Samples incubated at 21°C for 10 minutes with gentle mixing. Centrifugation was applied at 1,500 rpm for 5 minutes at 4°C. The supernatant was aspirated, and cells were resuspended in 1 mL of 2% FBS 1x PBS. Centrifugation was applied at 1,500 rpm for 5 minutes at 4°C. Supernatant was aspirated, and samples were resuspended in 200 μ L of 2% FBS 1x PBS containing the appropriate antibodies (Table. 8.17). Samples incubated at 4°C for 20 minutes. Centrifugation was applied at 1,500 rpm for 5 minutes at 4°C. Supernatant was aspirated, and cells were resuspended in 0.1 μ g/mL DAPI PBS. FACS analysis was performed using an LSR Fortessa. Compensation beads were prepared using OneComp beads resuspended in 100 μ L of 2% FBS 1x PBS and 2 μ L of antibody.

Table 8.17: FACS antibodies used to phenotype mouse peripheral blood cells after engraftment.

Marker	Fluorophore	Clone	Catalog #	Company	Dilution
CD4	PE	GK1.5	12-0041-81	eBioscience	1:2000
CD8a	PE	53-6.7	12-0081-81	eBioscience	1:1000
CD11b	APC	M1/70	17-0112-81	eBioscience	1:3000
CD45R (B220)	PE	RA3-6B2	12-0452-81	eBioscience	1:1000
CD45R (B220)	APC	RA3-6B2	17-0452-81	eBioscience	1:1000
Ly6G	APC-Cy7	1A8	127624	Biolegend	1:500
Ly6C	FITC	HK1.4	128005	Biolegend	1:200
CD45.1	BV605	A20	110738	Biolegend	1:100
CD45.2	BV711	104	109847	Biolegend	1:200



8.6.6 Bone Marrow FACS Analysis

Bone marrow cells 4-months post-primary engraftment and 4-months post-secondary engraftments were collected. Viability dye was prepared using 70 μL of 1x PBS and 0.8 μL of zombie yellow per a sample. FcR blocking solution was prepared at a 1:9 ratio of mouse FcR blocking to 1x PBS. The primary antibody solution was prepared in 1x PBS following ratios described in Table.8.18. The secondary antibody solution was prepared in 1x PBS following ratios also described in Table.8.18.

Cells were transferred to an appropriately labeled well of a 96-well v-bottom plate. Centrifugation was applied at 200 g for 7 minutes at 4°C. Supernatant was aspirated, and 100 μL of 1x PBS was added to each well. Centrifugation was applied again, supernatant was aspirated, and samples were resuspended in 70 μL of viability dye. Samples incubated for 20 minutes at 21°C in the dark. Centrifugation was applied at 200 g for 5 minutes at 4°C. Supernatant was aspirated, and samples were resuspended in 50 μL of FcR blocking solution. Samples incubated for 15 minutes at 4°C. 50 μL of primary antibody solution was applied to each sample. Samples incubated for 30 minutes at 4°C in the dark. Centrifugation was applied, and supernatant was aspirated. Cells were resuspended in 100 μL of secondary antibody solution. Samples incubated for 90 minutes at 4°C in the dark. Centrifugation was applied at 290 g for 5 minutes at 4°C, supernatant was aspirated, and samples were resuspended in 200 μL of 1x PBS as a washing step. Centrifugation was applied again. Supernatant was aspirated, and samples were resuspended in 200 μL of 1x PBS.

Compensation beads were then prepared. One drop of OneComp beads was applied to 6 wells, and one drops of UltraComp beads was applied to 2 wells of a 96-well plate. 100 μL of 1x PBS was applied to each well containing beads. Centrifugation was applied at 300 g for 5 minutes. Supernatant was discarded following the flicking method. 100 μL of primary antibody solution was added to the well for APC-eFluor780. Other samples were resuspended in 1x PBS. Samples incubated for 30 minutes at 21°C in the dark. Centrifugation was applied at 300 g for 5 minutes. Supernatant was discarded, and beads were resuspended in 200 μL of 1x PBS. The appropriate amount of secondary antibody (Table. 8.19) was applied to each well. Samples incubated at 21°C for 30 minutes in the dark. Centrifugation was applied at 300 g for 5 minutes. Bead pellets were resuspended in 200 μL of 1x PBS, and were stored on ice until analysis.



Table 8.18: FACS antibodies used to phenotype mouse bone marrow cells after engraftment.

Channel	Marker	Fluorophore	Clone	Catalog #	Company	Dilution	
NA	CD4	NA	Biotin	13-0042-85	eBioscience	1:2800	
NA	CD8	NA	Biotin	12-0081-86	eBioscience	1:2800	
NA	CD45R (B220)	NA	Biotin	13-0452-85	eBioscience	1:1400	
NA	TER119	NA	Biotin	13-5921-85	eBioscience	1:700	
NA	Ly6G	NA	Biotin	13-5931-85	eBioscience	1:700	
NA	CD127	NA	Biotin	13-1271-85	eBioscience	1:1400	
VL450	Sca1	+	BV421	D7	108127	Biolegend	1:200
RL780	Lineage	-	Strept APC- eFluor780	-	47-4317-82	Invitrogen	1:400
RL670	c-Kit	+	APC	2B8	105811	Biolegend	1:100
BL530	CD34	-	FITC	Ram34	11-0341-81	Invitrogen	1:100
YG561	CD135	-	PE	A2F10	12-1351-82	Invitrogen	1:50
VL780	CD48	-	BV785	HM48- 1	103449	Biolegend	1:100
VL710	CD45.2		BV711	104	109847	biolegend	1:200
BL695/40	CD45.1		PerCP	A20	110725	biolegend	1:100

Table 8.19: FACS compensation beads used to phenotype mouse cells after engraftment.

Color	Ultra beads ($\mu\text{L}/200 \mu\text{L}$)	Comp beads ($\mu\text{L}/200 \mu\text{L}$)
BV421	1	x
BV711	x	0.5
FITC	x	4
APC	x	4
APC-eFluor780	x	0.5
PE	x	0.7
BV785	2	x
PerCP	x	2



Chapter A

Materials

A.1 Cells

A.1.1 Human Cells

Cell Type	Obtained from
Jurkat76	Matthias Bozza
Human PBMCs	Francesco Baccianti
Human Buffy Coat	DRK Blutspendedienst
iNHDFs	Manuela Urban
HEK293T	Aga Sekretny
Human iPSCs	Manuela Urban

A.1.2 Murine Cells

Cell Type	Obtained from
Murine HSPCs	Obtained from the bone marrow of C57bl/6J

A.1.3 Bacteria

Cell Type	Catalog #	Company
Stellar Competent Cells	636766	Takara Bio
NTC1050811-HF [dem-]	NTC-NP-CC11	Nature Technology Corp



A.2 Mammalian Cell Culture

A.2.1 Plasticware

Item	Catalog #	Company
μ -Plate 96 Well Black	89626	ibibi
Human Fibronectin Cellware 96-Well Plate	354409	Corning Incorporated
Human Fibronectin Cellware 24-Well Plate	354411	Corning Incorporated
Ultra-low attachment Cellware 96-Well Plate U-bottom	781900	BRAND GmbH
Non-treated Cellware 96-Well Plate F-bottom	655101	Greiner bio-one
Non-treated Cellware 48-Well Plate	CC7672-7548	CytoOne
Non-treated Cellware 24-Well Plate	3527	Corning Incorporated costar
Non-treated Cellware 6-Well Plate	3506	Corning Incorporated costar
Treated Cellware 96-Well Plate flat bottom	655180	Greiner Bio-One
Treated Cellware 96-Well Plate U-bottom	650180	Greiner Bio-One
Treated Cellware 96-Well Plate V-bottom	249952	ThermoFisher Scientific
Treated Cellware 48-Well NUNCLON Delta Plate	150687	ThermoFisher Scientific
Treated Cellware 24-Well NUNCLON Delta Plate	142475	ThermoFisher Scientific
Treated Cellware 6-Well Cellstar® Plate	657 160	Greiner bio-one
SmartDish™ (6-Well Plates)	27370	Stemcell Technologies
STEMgrid-6	27000	Stemcell Technologies
T-25 Cellstar® culture flask	690175	Greiner bio-one
T-75 Cellstar® culture flask	658175	Greiner bio-one
T-175 Cellstar® culture flask	660175	Greiner bio-one
6 cm culture dishes	628160	Greiner bio-one
15 cm dish	93150	TPP
2 mL Serological Pipet	357507	Corning Incorporated Falcon
5 mL Stripette	4487	Corning Incorporated costar
10 mL Stripette	4488	Corning Incorporated costar
Continued on next page		



Table A.0 – continued from previous page

Item	Catalog #	Company
25 mL Stripette	4489	Corning Incorporated costar
50 mL Stripette	4490	Corning Incorporated costar
Safe-Lock Tubes 0.5 mL	0030 121.023	Eppendorf
Safe-Lock Tubes 1.5 mL	0030 120.086	Eppendorf
Safe-Lock Tubes 2.0 mL	0030 120.094	Eppendorf
15 mL tube	188271-N	Greiner bio-one
50 mL tube	352070	Corning Incorporated Falcon
Pre-Separation Filters (30 μ m)	130-041-407	Miltenyi Biotec
LS Columns	130-042-401	Miltenyi Biotec
AggreWell™ 400 24-well plate	34411	Stemcell Technologies
EASYstrainer™ 40 μ m	542040	greiner
Blunt-End Needles (16 G)	28110	Stemcell Technologies
3cc Syringes	28240	Stemcell Technologies
CryoTube™ Vials	366656	Thermo Scientific nunc
50 mL Pipetting Reservoir	04395-27	Cole-Parmer

A.2.2 Cell Culture Components

Application	Item	Catalog #	Company	Preparation Notes
Cell collection kits	Dead Cell Removal Kit	130-090-101	Miltenyi Biotec B.V	-
Cell collection kits	Pan T Cell Isolation Kit (Human)	130-096-535	Miltenyi Biotec B.V	-
Cell collection kits	Direct Lineage Cell Depletion Kit (Mouse)	130-110-470	Miltenyi Biotec B.V	-
Cell collection solutions	1x PBS pH 7.4	10010-023	Gibco	-
Cell collection solutions	0.5 M EDTA pH 8.0	AM9260G	Invitrogen	-
Medium kit	STEMdiff™ Hematopoietic Kit	05310	STEMCELL Technologies	-
Medium kit	STEMdiff™ T Cell Kit	100-0194	STEMCELL Technologies	-
Basal medium	RPMI-1640 Medium	21875-034	Gibco	-
Basal medium	DMEM	41965-039	Gibco	-

Continued on next page



Table A.0 – continued from previous page

Application	Item	Catalog #	Company	Preparation Notes
Basal medium	TexMACS™ medium	130-097-196	Miltenyi Biotec B.V	-
Basal medium	Basic04	SFB-500	Amsbio	-
Basal medium	MethoCult	04636	STEMCELL Technologies	-
Basal medium	F12 medium	11-765-054	Thermo Fisher Scientific	-
Basal medium	DMEM (1x)	41965-039	Gibco	-
supplement	FBS	10270	Gibco	-
supplement	Pen Strep (PS)	15140-122	Gibco	-
supplement	Pen Strep Glut (PSG)	10378016	Thermo Fisher Scientific	-
supplement	TransAct™	130-111-160	Miltenyi Biotec	-
supplement	glutaMAX 100x	35050	Gibco	-
supplement	Non-essential amino acids (NEAA)	M7145	Sigma Aldrich	-
supplement	10 μ M Y-27632 (ROCK)	1293823-10 mg	BioGems	10 mg resuspended into 3.12 mL of PBS. 60 μ L aliquots are prepared and stored at -20°C. (Makes 52 aliquots). 1/1000 dilution into medium. Refreeze aliquot after use.
supplement	100x ITSX	51-500-056	Thermo Fisher Scientific	-
supplement	1 M HEPES	15-630-106	Thermo Fisher Scientific	-

Continued on next page



Table A.0 – continued from previous page

Application	Item	Catalog #	Company	Preparation Notes
supplement	10% PVA (87% hydrolyzed) 1mg/mL	P8136-250G	Sigma Aldrich	Prepare a 10% PVA solution by adding 5 g to 50 mL of cell culture grade water (100mg/mL). Send to for steam autoclaving. Make 1 mL aliquots of 10% PVA and store at 4°C for up to 3 months.
cytokine	human IL-7 research grade	130-093-937	Miltenyi Biotec	When there is a new stock, allow tube to reach room temperature. Then resuspend with 100 μ L of sterile water.
cytokine	human IL-15 research grade	130-093-955	Miltenyi Biotec	When there is a new stock, allow tube to reach room temperature. Then resuspend with 100 μ L of sterile water.

Continued on next page



Table A.0 – continued from previous page

Application	Item	Catalog #	Company	Preparation Notes
cytokine	TPO	AF-315-14-50 μ g	PeprTech	Apply centrifugation to vial and reconstitute material in 50 μ L of cell culture grade water. Do not vortex. Add 450 μ L of F-12 medium. Make aliquots of 10 μ L. Store at -20°C for 1 year. Store at 4°C for 1 week.
cytokine	SCF	AF-250-03-10 μ g	PeprTech	Apply centrifugation to vial and reconstitute material in 100 μ L of cell culture grade water. Do not vortex. Add 900 μ L of F-12 medium. Make aliquots of 20 μ L. Store at -20°C for 1 year. Store at 4°C for 1 week.
Coating material	iMatrix Laminin-511	AMS.892 021	Amsbio	-
Coating material	Anti-Adherence Rinsing Solution	07010	STEMCELL Technologies	-
Dissociation reagent	Trypsin-EDTA Solution	T4049-100 mL	Sigma-Aldrich	-
Dissociation reagent	ACCUTASE™	07922	STEMCELL Technologies	-
Dissociation reagent	TrypLE Express	12604-013	Thermo Fischer Scientific	-

Continued on next page



Table A.0 – continued from previous page

Application	Item	Catalog #	Company	Preparation Notes
Dissociation reagent	Collagenase Type II	07418	STEMCELL Technologies	If activity is 125 CDU/mL. Supplement with 5 mL of DMEM/F-12 with HEPES. Then, filter sterilize via 0.2 μ M filter.
Inhibitor	ODN2088	130-105-815	Miltenyi Biotec	Material was reconstituted in 10 μ L of distilled water. A quick spin was applied to the tube. The material incubated at 4°C overnight. 195 μ L of F-12 was added to the tube. 10 μ L aliquots were prepared and stored at -20°C.
Inhibitor	Ac-YVAD-cmk	SML0429-1MG	Sigma-Aldrich	Container was placed into a 50 mL falcon tube. Centrifugation was performed at 250 g for 30 seconds. Material was reconstituted in 50 μ L of DMSO. Centrifugation was performed at 250 g for 30 seconds. 10 μ L aliquots were prepared and stored at -20°C.

Continued on next page



Table A.0 – continued from previous page

Application	Item	Catalog #	Company	Preparation Notes
Inhibitor	C-176	SML2559-10MG	Sigma-Aldrich	Container was placed into a 50 mL falcon tube. Centrifugation was performed at 250 g for 30 seconds. 10 mg of material was reconstituted in 500 μ L of DMSO. Centrifugation was performed at 250 g for 30 seconds. Then a 1/5 dilutions was performed into DMSO. 25 μ L aliquots were prepared and stored at -20°C.



A.2.3 Cell Medium Composition

Cell Type	Medium Name	Medium Composition
Jurkat76	-	RPMI 10% FBS 1% P/S
PBMCs	-	TexMACS medium
Primary Human T-cells	-	TexMACS medium 1 ng/ml IL-15, 1 ng/ml IL-7, and 1:100 TransAct™
iNHDFs	-	DMEM 10% FBS 1% NEAA 1% GlutaMAX
HEK293T	-	DMEM 10% FBS
Human iPSCs	-	Basic04 1% P/S
iPSC-derived HSPCs	STEMdiff™ Hematopoietic kit	Follow product instructions.
iPSC-derived HSPCs	STEMdiff™ T Cell Kit EB medium A	Transfer 1.5 mL of EB Basal medium to a separate tube labeled EB Medium A. Supplement this new tube with 7.5 μ L of Supplement A. The remain EB Basal Medium is stored at 4°C.
iPSC-derived HSPCs	STEMdiff™ T Cell Kit EB Medium B	The remaining 1.8 mL of EB Basal medium was supplemented with 200 μ L of Supplement B.
iPSC-derived HSPCs	STEMdiff™ T Cell Kit EB Formation Medium	1 μ L of 10 mM Y-276321 was added to 1 mL of EB Medium A.
iPSC-derived T-cells	StemSpan Lymphoid Progenitor Expansion Medium	3.6 mL of StemSpan SFEM II supplemented with 400 μ L of StemSpan Lymphoid Progenitor Expansion Supplement.
iPSC-derived T-cells	StemSpan T Cell Progenitor Maturation Medium	3.6 mL of StemSpan SFEM II supplemented with 400 μ L of StemSpan T Cell Progenitor Maturation Supplement.
Mouse HSPCs	Supplemented Ham's F-12 medium	19.2 mL of F-12 medium. 200 μ L of 100x ITS-x. 200 μ L of 1 M HEPES. 200 μ L of 10% PVA solution 1 mg/mL PVA (87% hydrdolyzed). 200 μ L of 100x PSG. 20 μ L 100 μ g/mL TPO mouse. 20 μ L 10 μ g/mL SCF.
Continued on next page		



Table A.0 – continued from previous page

Cell Type	Medium Name	Medium Composition
Mouse HSPCs	Supplemented Ham's F-12 medium (Electroporation)	19.2 mL of F-12 medium. 200 μ L of 100x ITS-x 200 μ L of 1 M HEPES. 200 μ L of 10% PVA solution 1 mg/mL PVA (87% Hydrdolyzed). 200 μ l of 100x PSG.

A.2.4 Transfection/Transduction Reagents

Item	Catalog #	Company
SE cell line 4D-Nucleofector™ X Kit S	V4XC-1032	Lonza
P3 Primary Cell 4D-Nucleofector™ X Kit S	V4XP-3032	Lonza
P2 Primary Cell 4D-Nucleofector™ X Kit S	V4XP-2032	Lonza
Stem Lipofectamine	STEM00003	Invitrogen
Metafectamine®	T020-0.2	Biontex
25k PEI	-	Obtained from Anna Hartley
1.5 M NaCl	-	Produced In-House
Aqua	0123	Aqua B. Braun
OPTI-MEM® 1 (1x)	31985-062	Gibco
8 mg/mL Polybrene	-	Obtained from Francesco Baccianti
Electroporation (EP) Buffer	301-944-1700	MaxCyte®
OC-25x3 Processing Assembly	TSP-180	MaxCyte®



A.3 Mammalian Cell Analysis

This section contains a list of materials used for the analysis of mammalian cells.

A.3.1 Plasticware

Item	Catalog #	Company
5 mL Polystyrene Round-Bottom Tube with Cell-Strainer Cap	352235	Corning Incorporated Falcon
V-bottom Plate for LEGENDplex™	740379	Biolegend
Luna Cell Counting Slide	L12001	logos

A.3.2 Kits

Item	Catalog #	Company
Stemgent® AP Staining Kit II	00-0055	Stemgent
DNeasy Blood Tissue Kit	69504	QIAGEN
LEGENDplex™ Mouse Anti-Virus Response Panel (13-plex) with V-bottom Plate	740622	BioLegend®
LumiKine™ Xpress hIFN- β 2.0 kit	luex-hifnbv2	InvivoGen

A.3.3 Commercial Reagents

Item	Catalog #	Company
1x PBS pH 7.4	10010-023	Gibco
Cell Culture Grade Water	15230-147	Gibco
1x DMEM/F-12	11320033	Gibco
1x IMDM	21980032	Life Technologies
Pen Strep (PS)	15140-122	Gibco
1 M HEPES	15-630-106	Thermo Fisher Scientific
0.5 M EDTA pH 8.0	AM9260G	Invitrogen
RBC Lysis Buffer (10X) 100 mL	42030	BioLegend
ACK lysing buffer	882090	Biozym
4% PFA in PBS	TCL119-100 mL	HIMEDIA
Triton X-100	A4975,1000	AppliChem
Tween20	A4974,0250	AppliChem PanReac
Continued on next page		



Table A.0 – continued from previous page

Item	Catalog #	Company
Albumin bovine Fraction V (BSA)	11930.03	SERVA

A.3.4 Prepared Solutions

Application	Name	Reagent
Cell culture	DMEM/F-12 with 15 mM HEPES	50 mL of DMEM/F-12 medium. 750 μ L of 1M HEPES
Cell culture	25 mM HEPES 1% P/S IMDM medium	5 mL of IMDM. 50 μ L of 10,000 U Pen/Strep. 200 μ L of 1M HEPES. For Methylcult assay.
FACS	Viability Dye Buffer: 2mM EDTA PBS	50 mL of 1x PBS. 200 μ L of EDTA 0.5 M. For FACS analysis.
FACS	FACS buffer	1x PBS with 0.5% BSA and 2 mM EDTA. For FACS analysis.
AP staining	PBST	10 mL of 1x PBS. 5 μ L of Tween 20. Final conc of 0.05%. Mix well and store at room temperature. For AP staining.
IF staining	Permeabilization Buffer	0.1% Triton X-100 in 1x PBS
IF staining	PBST	0.1% Tween20 in 1x PBS
IF staining	Blocking Solution	3% BSA in PBST
IF staining	1 μ g/mL DAPI in blocking solution	1:1000 dilution of 1 mg/mL DAPI into blocking solution.

A.3.5 Pre-Defined Chemical Reagents

Application	Item	Catalog #	Company
FACS analysis	Mosue FcR Blocking Reagent	130-092-575	Miltenyi Biotec B.V
FACS analysis	Human FcR Blocking Reagent	130-059-901	Miltenyi Biotec B.V
Viability dye	1.0 mg/ml DAPI	564907	BD Pharmingen™
Viability dye	Zombie Yellow Solution	423103	BioLegend
Cell counting	Trypan blue stain 0.4%	T10282	Invitrogen



A.3.6 FACS

A.3.6.1 FACS Beads

Item	Catalog #	Company
OneComp eBeads™	01-1111-42	Life Technologies
UltraComp eBeads™	01-2222-42	Life Technologies
CountBright™ Absolute Counting Beads	C36950	Invitrogen™

A.3.6.2 FACS Antibodies

Table A.0: FACS primary antibodies

Antibody	Specificity	Clone	Origin	Dilution	Company	Catalog #
CD4 Monoclonal Antibody, Biotin	Mouse	RM4-5	Rat	1:2800	eBioscience™	13-0042-85
CD8a Monoclonal Antibody, Biotin	Mouse	53-6.7	Rat	1:2800	eBioscience™	12-0081-86
CD45R (B220) Monoclonal Antibody, Biotin	Human, Mouse	RA3-6B2	Rat	1:4000	eBioscience™	13-0452-85
TER-119 Monoclonal Antibody, Biotin	Mouse	TER-119	Rat	1:700	eBioscience™	13-5921-85
Ly-6G/Ly-6C Monoclonal Antibody, Biotin	Mouse	RB6-8C5	Rat	1:700	eBioscience™	13-5931-85
CD127 Monoclonal Antibody, Biotin	Mouse	A7R34	Rat	1:1400	eBioscience™	13-1271-85
Biotin CD8b	Human	REA715	Human cell line	1:50	Miltenyi Biotec B.V	130-110-508



Table A.0: FACS secondary antibodies

Antibody		Specificity	Clone	Dilution	Company	Catalog #
APC	CD3	human	sk7	1:50	Biologend	344812
AF488	Tra-1-60	human	TRA-160-R	1:50	Biologend	330614
BV711	CD45	human	HI30	1:50	Biologend	304050
Pacific Blue	CD34	human	581	1:100	Biologend	343610
APC/fire750	CD33	human	P67.6	1:50	Biologend	366632
AF700	CD38	human	HB-7	1:50	Biologend	356623
APC	CD43	human	CD43-10G7	1:50	Biologend	343206
BV785	CD90	human	5E10	1:50	Biologend	328141
FITC	CD4	human	RP4-T4	1:50	Biologend	300506
BV786	Streptavidin	-	-	1:50	Biologend	405249
PerCP	CD3	human	UCHT1	1:50	Biologend	300427
BV605	CD5	human	L17F12	1:50	Biologend	364019
APC	CD7	human	CD7-6B7	1:50	Biologend	343107
BV421	Ly-6A/E (Sca-1)	mouse	D7	1:200	Biologend	108127
APC-eFluor780	Streptavidin	-	-	1:400	Invitrogen	47-4317-82
APC	CD117 (c-Kit)	mouse	2B8	1:100	Biologend	105811
BV711	CD150	mouse	TC15-12F12.2	1:150	Biologend	115941
FITC	CD34	mouse	Ram34	1:100	Invitrogen	11-0341-81
PE	CD135	mouse	A2F10	1:50	Invitrogen	12-1351-82
BV785	CD48	mouse	HM48-1	1:100	Biologend	103449
BV711	CD45.2	mouse	104	1:400	Biologend	109847
PerCP	CD45.1	mouse	A20	1:200	Biologend	110725
PE	CD4	mouse	GK1.5	1:2000	eBioscience	12-0041-81
PE	CD8a	mouse	53-6.7	1:1000	eBioscience	12-0081-81
APC	CD11b	mouse	M1/70	1:3000	eBioscience	17-0112-81
PE	CD45R (B220)	mouse	RA3-6B2	1:1000	eBioscience	12-0452-81
APC	CD45R (B220)	mouse	RA3-6B2	1:1000	eBioscience	17-0452-81
APC-Cy7	Ly6G	mouse	1A8	1:500	Biologend	127624
FITC	Ly6C	mouse	HK1.4	1:200	Biologend	128005
BV605	CD45.1	mouse	A20	1:100	Biologend	110738

Continued on next page



Table A.0 – continued from previous page

Antibody		Specificity	Clone	Dilution	Company	Catalog #
BV711	CD45.2	mouse	104	1:200	Biologend	109847

A.3.7 IF Staining Antibodies

A.3.7.1 Primary IF Antibodies

Antibody	Specificity	Species	Dilution	Company	Catalog #
aLin28	human	mouse	1:50	Santa Cruz Biotechnology, Inc.	sc374460
aTra180	human	mouse	1:50	Santa Cruz Biotechnology, Inc.	SC21705
aNanog	human	mouse	1:50	Santa Cruz Biotechnology, Inc.	SC2931211E6C4
aOct3/4	human, mouse	goat	1:100	Santa Cruz Biotechnology, Inc.	sc8628 n-19

A.3.7.2 Secondary IF Antibodies

Antibody	Specificity	Species	Dilution	Company	Catalog #
aGoat-647, cy5	goat	mouse	1:1000	Abcam	ab150131
Alpha mouse-488, FITC	mouse	mouse	1:1000	Abcam	Ab150105



A.4 Virus Production

For transfection reagents, see Table.A.2.4.

A.4.1 Plasticware

Item	Catalog #	Company
15 cm Dishes	93150	TPP
50 mL Falcons	352070	Falcon
0.45 nm PVDF Filter	P667.1	Carl Roth GmbH Co.
30 mL Syringe	SS+30L1MP	Terumo
50,000 MWCO PES Vivaspin 20 column	ST-2724	Neolab
Ultracentrifuge tubes 16x76 mm with seal	342413	Beckmann
Cell scrapers	SIAL0010	SIGMA-ALDRICH
21Gx1,5, 0,8x40mm	CH21112	CHIRANA T. Injecta
T-175 Cellstar® Culture Flask	660175	Greiner bio-one
Pasteur pipette	-	DKFZ In-House
1 mL Syringe	SS+01T1	TERUMO®
Vivaspin6 100 kDa MWCO	28-9323-1-1	Sartorius
Safe-Lock Tubes 1.5 mL	0030 120.086	Eppendorf

A.4.2 Commercial Solutions

Solution Name	Catalog #	Company
OptiPrep	STEMCELL	07820
250u/uL benzonase	E8263-5ku	Sigma Aldrich
Phenol Red solution (0.5%)	P0290-100mL	Sigma Aldrich
1x PBS (pH 7.4)	10010-023	Gibco
1M Tris-HCl (pH: 8.5)	-	Obtained from Manuela Urban



A.4.3 Prepared Solutions

Solution Name	Reagents
Virus Lysis Solution	50 mL of 1 M Tris-HCl (pH 8.5), 8.8 g of NaCl, and 8.8 g MgCl ₂ . Dilute in 900 mL Aqua Braun. Adjust pH to 8.5. If necessary, fill up with Aqua Braun to 1 L. Autoclave the solution.
PBS-MK	1xPBS with 1 mM MgCl ₂ and 2.5 mM KCl. Sterilization via filtration.
PBS-MK-NaCl	PBS-MK with 1 M NaCl. Sterilization via filtration.
60% Iodixanol	48 mL of Optiprep with 2.5 μ L/mL Phenolred. Prepare aseptically.
40% Iodixanol	30 mL Optiprep with 15 mL PBS-MK. Prepare aseptically.
25% Iodixanol	20 mL Optiprep with 28 mL PBS-MK and 120 μ L Phenolred. Prepare aseptically.
15% Iodixanol	12 mL Optiprep with 36 mL PBS-MK-NaCl. Prepare aseptically.



A.5 Bacterial Cell Culture

A.5.1 Plasticware and Glassware

Item	Catalog #	Company
Petri Dish	82.1473.001	Sarstedt
Plate Spreader	SPR-L-S01	Lazy-L-Spreaders™
Scalpel	02.001.30.021	Feather safety razor co., LTD
Test Tubes for Colony Picking	-	DKFZ In-House
Safe-Lock Tubes 1.5 mL	0030 120.086	Eppendorf
Safe-Lock Tubes 2.0 mL	0030 120.094	Eppendorf
Flask (for gel prep)	-	DKFZ In-House
Colony Pickers	VWR1612-2498	VWR

A.5.2 Commercial Culture Components

Item	Catalog #	Company
Agarose	A9539-500G	Sigma Aldrich
Ampicilin, Sodium Salt BioChemica	A0839,0010	PanReac AppliChem
Glycerol 87%	A3561,1000	AppliChem
SOC Medium	636763	Takara
1x PBS	10010-023	Gibco

A.5.3 Prepared Culture Compositions

Solution Name	Reagents
LB Medium	Obtained from DKFZ In-House
LB Agar Plates	15 g of agar was added to LB medium and send for autoclaving. After autoclaving is complete, allow the container and its components to cool homogeneously in a 65°C water bath. In the presence of a bunsen burner, transfer 30 mL of the solution into 16 50 mL Falcon tube using a graduated pipette. Store aliquots at 4°C.
100 mg/mL Ampicillin Stock Solution	100 mg of Ampicillin was added to a 1.5 mL Eppendorf tube. 1 mL of sterile 1x PBS was added.
50% Glycerol Solution	25 mL of glycerol and 25 mL of 1x PBS were added to a 100 mL container and autoclaved.



A.6 Plasmid Production

This section contains a list of materials used for vector production. Materials pertaining to the usage of bacteria are found in section A.5.

A.6.1 Kits

Item	Catalog #	Company
GenElute™ Gel Extraction Kit	NA1111	Sigma Aldrich
QIAprep Spin Miniprep Kit	27106	QIAGEN
Endotoxin-Free Plasmid Maxi Kit	12362	QIAGEN

A.6.2 Commercial Solutions

Item	Catalog #	Company
Chloroform	32211-1L	Sigma Aldrich
Isopropanol	33539-2.5L-M	Sigma Aldrich
Tween20	A4974,0250	AppliChem PanReac
Nuclease Free Water	T143	Carl Roth GmbH
Ethanol	32205-2.5L-M	Sigma Aldrich
3 M Sodiumacetate (pH 5.2)	R1181	Thermo Scientific
EP Buffer	-	Obtained DKFZ In-House

A.6.3 Pre-Defined Chemical Reagents

Item	Catalog #	Company	Notes
6x Gel Loading Dye	B7024A	NEB labs	
Clone Amp HiFi PCR preMix	STO506	Takara	
10xFastDigest Green Buffer	LT-02241	Thermo Fisher	
pegGREEN	37-5010	peglab	
Ladder Gene Ruler 1 kb	N3232S	NEB	Ladder:Dye:Water 1:1:3
5x Infusion Mix	ST0345	Takara	



A.7 Cloning Primers

Primer Name	Sequence (5' to 3')
JP4.3 ori/amp/ampP.FWD	AAAATGAATGCAATTGTTTCCATAGGCTCCG CCCCC
JP4.3 ori/amp/ampP.REV	TGGCCAATATTGACATGCATCGCGGAACCCC TATTTGTTTATTTTTCT
JP4.3 seq ori/amp/ampP .REV	TCGCTGAGATAGGTGCCTC
JP4.3 seq ori/amp/ampP.FWD1	AGTTCTTGAAGTGGTGGCCT
JP4.4 polyA. FWD	CGCGGGCCCCGGGATCCAACCTGTTTATTGCA GCTTATAATGGTTACAAA
JP4.4 polyA. REV	CCTATGGAAACAATTGTAAGATACATTGATGA GTTTGGACAAACCACA
JP4.7 Ele40 seq.FWD	GGTTAGCTCCTTCGGTCCTC
JP4.7 Ele40 seq.FWD2	AGGTTTTGTTCTTCGTTTCTTCA
JP4.7 Ele40.Fwd	ATAGGGGTCCGCGAAGCTTGATCAAGAAAG CACTCCGGGC
JP4.7 Ele40.Rev	TGGCCAATATTGACAATCGATGATCTAATGTA CATCATGAGGGCTATAGTTAATAAAAATG- TATTGT
JP4.8 CMarPCR.F	GCCTGAAGATCTCGAGTCGACATGCATGCAG AAGTTGGTTCG
JP4.8 CMarPCR.R	AACAAGTTGGATCCCGGGGAGTGGACACCTG TGGAGAGAAAG
JP4.8 scmars.FWD	GTGTCCACTCGGATCCAACCTGTTTATTGCA GCTTATAATGG
JP4.8 scmars.FWD	GCCTGAAGATCTCGAGTCGACATGCATGCAG AAGTTGGTTCG
JP4.8 test	TCGGAAGTGAAGATCTAAAGCTTTGCATGCA GAAGTTGGT
JP4.9 sEF1 cI.FWD	AACACAGGTAAGTATCAAGTTACAAGACAG
JP4.9 sEF1 cI.REV	AACATACCGGTAGCGCTAGCCTGTGGAGAGA AAG
JP4.9 sEF1.FWD	TACATTAGATCATCGATGAGGCTCCGGTGCCC G
JP4.9 sEF1.REV	ATACTTACCTGTGTTCTGGCGG
JP4.10 CAG.FWD	TACATTAGATCATCGATGCTAGTTATTAATAG TAATCAATTACGGGGTCATTAGTTCA
JP4.12 dtomato.F	CTTTCTCTCCACAGGCTAGCATGGTGAGCAA GGGCGAGGA
JP4.12 dtomato.R	CTGCATGCATGTCGACTTACTTGTACAGCTC GTCCATGCC

Continued on next page

Table A.0 – continued from previous page

Primer Name	Sequence (5' to 3')
JP4.13 CAG dtom.F	GGGGTACCGAAGCCGCTAGCATGGTGAGCAA GGGCGAGGA
ori/amp/ampP seqJP4.3 .FWD2	TCAGCAATAAACCAGCCAGC
JP4.17 sEF1 dtom.REV	TGCTCACCATGCTAGCCTGTGTTCTGGCGG
JP4.17 Lenti .REV1	CCTTCCAGGGATCCGAGTGGACACCTG
JP4.17 Lenti. FWD1	CGAGACTAGCCTCGAGGAGGCTCCGGTGCCC
JP4.17 NTX seq.REV	CACCTTGTAGATCAGCGTGC
JP4.17 NTX.FWD	ACTATAGCCCTCATGATGTACAATTCTTCC
JP4.17 NTX.REV	CCCTTGCTCACCATGCTAGCCTGTGTTCTGG CGGCA
JP4.17 NTX.seq1	CTTCTCTAGGCACCGTTCA
JP4.17 Lenti . FWD2	CGGATCCCTGGAAGGGCTAATTCACCTCCCAAC
JP4.17 Lenti .REV1	CCTTCCAGGGATCCGAGTGGACACCTG
JP4.17 Lenti. FWD1	CGAGACTAGCCTCGAGGAGGCTCCGGTGCCC
JP4.17 Lenti. REV2	AATTAGTCAGCCATGCCATGGGGCGGAGAAT GG
JP4.AAVF217. FWD	CTGCGGCCGCGCTAGGAGGCTCCGGTGCCC
JP4.AAVF217.REV	GCCCACGCGTGGATCTAAGATACATTGATGA GTTTGGACAAACCACAAC
JP4.18 CP dtom.F	TACATTAGATCATCGATAACAAGCAGATTTGCA GGGAGC
JP4.18 CP dtom.R	TGCTCACCATGCTAGCGTCGTAGCTTCCGGT GGAAAGA
JP4.18 CP.F	TACATTAGATCATCGATAACAAGCAGATTTGCA GGGAGC
JP4.19 CI .F	CTACGACGTAAGTATCAAGGTTACAAGACAGG TTTAAGGAG
JP4.19 CP.REV	ATACTTACGTCGTAGCTTCCGGTGGAAAGA
JP4.19 CI IL2RG.REV	GTTTCAACATGCTAGCCTGTGGAGAGAAAGG CAAAGTGGA
JP4.19 CP Cl.F	TACATTAGATCATCGATAACAAGCAGATTTGCA GGGAGC
JP4.19 CP Cl.REV	TGCTCACCATGCTAGCCTGTGGAGAGAAAGG CAAAGTGGA
JP4.21 hs IL2RG CP.FWD	TACATTAGATCATCGATTATTATAAGTCACAC TTCTCGCCAGTCT
JP4.21 hs IL2RG CP.REV	TGCTCACCATGCTAGCGTCATAGCTTCCGGT GGAAAGAAC
JP4.22 Cl.FWD	CTATGACGTAAGTATCAAGGTTACAAGACAG GTTTAAGG

Continued on next page



Table A.0 – continued from previous page

Primer Name	Sequence (5' to 3')
JP4.22 CI.REV	TGCTCACCATGCTAGCCTGTGGAGAGAAAGG
JP4.22 hsCP.REV	ATACTTACGTCATAGCTTCCGGTGGAAAGAAC



A.8 Vectors

A.8.1 DNA Vectors

Vector Name	Vector Size (bp)	Conc (ng/ μ L)
JP4.22 CP CI hs dtom	4898	790.6
JP4.21 CP hs dtom	4765	712.4
Jp4.20 CAG dtom	6100	1519.7
JP4.19 CP CI dtom	4898	738
JP4.18 CP dtom	4765	781.1
JP4.17 sEF1 dtom	4497	1595.6
JP4.13 sEF1 CI dtom	4630	598.2
NJP4.13 SMAR 1	4911	1000
NJP4.13 SMAR 2	3753	1000
NJP4.13 SMAR 3	3479	1000
NJP4.13 SMAR 4	3202	1000
NJP4.17 SMAR 4	3069	1126.8

A.8.2 Viral Vectors

Vector Name	Obtained From	Vector Size (bp)	Conc. (ng/ μ L)
JP4.L1 SMAR 4 (Lentiviral Transfer Plasmid)	Based off B1284 from Francesco Baccianti	6,623	3495
B653 pCMV-Gag.Pol (Lentiviral Helper)	Francesco Baccianti	12,051	1036
B654 pCMV-VSV-G (Lentiviral Packaging)	Francesco Baccianti	6,246	4429
JP4.AAVF217 (AAV Transfer Plasmid)	Based off pAAVMCS2[48]	4475	807.5
pDGM6 (Helper Plasmid AAV) ¹	Addgene[116]	21829	3334.5

¹pDGM6 was a gift from David Russell. Addgene plasmid # 110660.



A.9 Mice

A.9.1 Mouse Lines

Line Name	Obtained from
C57bl/6J	Javier Labs
C57BL/6J Ly5.1	Obtained from DKFZ In-House

A.9.2 Materials for Mouse Handling

Item	Catalog #	Company
EDTA Coated Tubes	363706	BD
1 mL Syringe	SS+01T1	TERUMO®
Solofix	ATK9.1	Braun
Papertowels	66424	Essity Hygiene and Health AB SE
1x PBS	10010-023	Gibco
Needles	-	-
Scissors	-	-
Twizzors	-	-



A.10 Equipment

Item	Catalog #	Company
Bacterial Cell Culture Hood	46752	Holten LaminAir
Cell Culture Hood Safe 2020	41557902	Thermo Fisher Scientific
Cell Culture Incubator	NU-5810E	Nuaire
Cryostorage system	24k	Tec-lab
Water bath	UC-8A	julabo
Swing-rotor Centrifuge	5810	Eppendorf
Centrifuge 5424 R	5404DO216436	Eppendorf
Optima LE-80k Ultracentrifuge	Col99CO9	Beckman
Vacuum Pump	Vacunsafe	Integra
Microscope	Evos XL Core	Invitrogen
Microscope	CK40	Olympus
Microscope	BZ-9000	Keyence
Microscope	Eclipse Ti	Nikon
Cell Counter Luna™ vFL Auto	LUF-13-00-196	logos
4D-Nucleofector™ Core Unit with X and Y Units	AAF-1002B, AAF-1002X, AAF-1002Y	Lonza
MaxCyte GTx™	-	MaxCyte
QuadroMACS™ Starting Kit (LS) and MACS® MultiStand	130-091-051 and 130-042-303	Miltenyi Biotec
Nanodrop 2000c	G814	Thermo Fisher Scientific
BD LSR Fortessa™ HTS	-	BD
BD FACSAria™ Fusion	-	BD
CoolCell® Container	432138	Corning®
VICTOR Nivo tm	-	PerkinElmer
Electrophoresis Chamber	-	BioRad
Gel Cast	-	BioRad
Fixed Height Comb	-	BioRad
PowerPac™ Basic	-	BioRad
Microwave	-	Siemens
Fusion SL VILBER Lourmat PEQlab Chamber	-	VILBER
UV Imager	7001298	Konrad Benda
Thermomixer Comfort	5355 YN 195	Eppendorf
-20 Freezer	MediLine	Liebherr
Ultra-low Temperature Freezer	U725/ U725-G	New Brunswick
Tube Sealer Instrument	342428	Beckman
PCR Cycler	26672-01Y00312	Peqlab
Bunset Burner	Emb69204	CampingAZ



A.11 Software

FlowJo
SnapGene
R
Gephi
Affinity Designer
BioRender
LaTeX

Some images displayed within this report were created using [BioRender.com](https://www.biorender.com).



Chapter B

Supplemental Results

B.1 Chapter 3

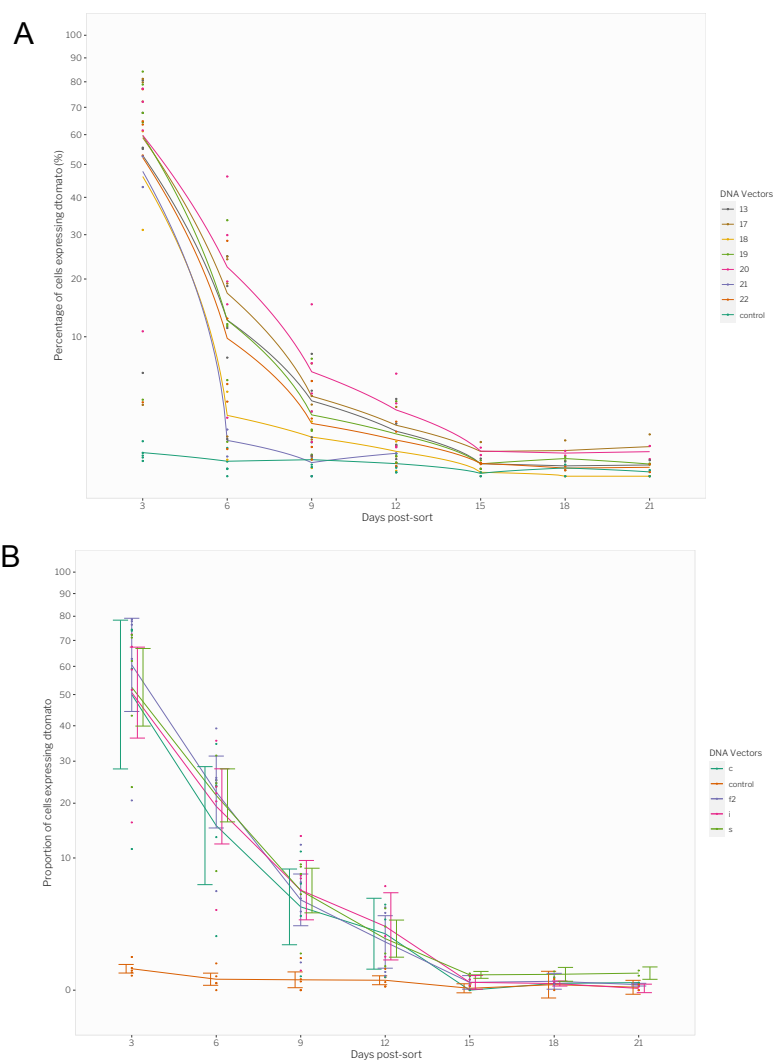


Figure B.1: Establishing S/MAR DNA vectors in primary human T-cells. Three days post-electroporation, alive cells expressing dTomato were sorted into a well of a 96-well plate. The proportion of cells expressing dTomato was then monitored every three days. 21 days post-sort, T-cells began to die. A) Comparing promoters. B) Comparing S/MARS.

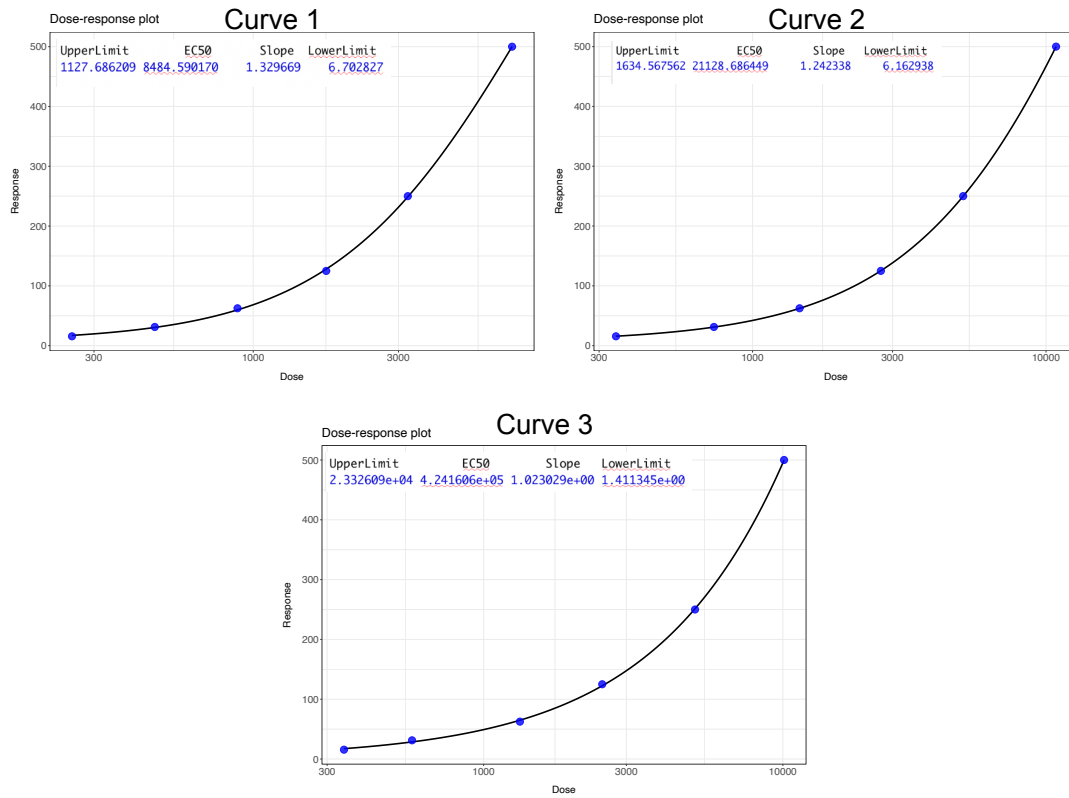


Figure B.2: Calibration curves used for Invivogen IFN-beta ELISA. More details pertaining to this ELISA can be found in methods 8.3.8.

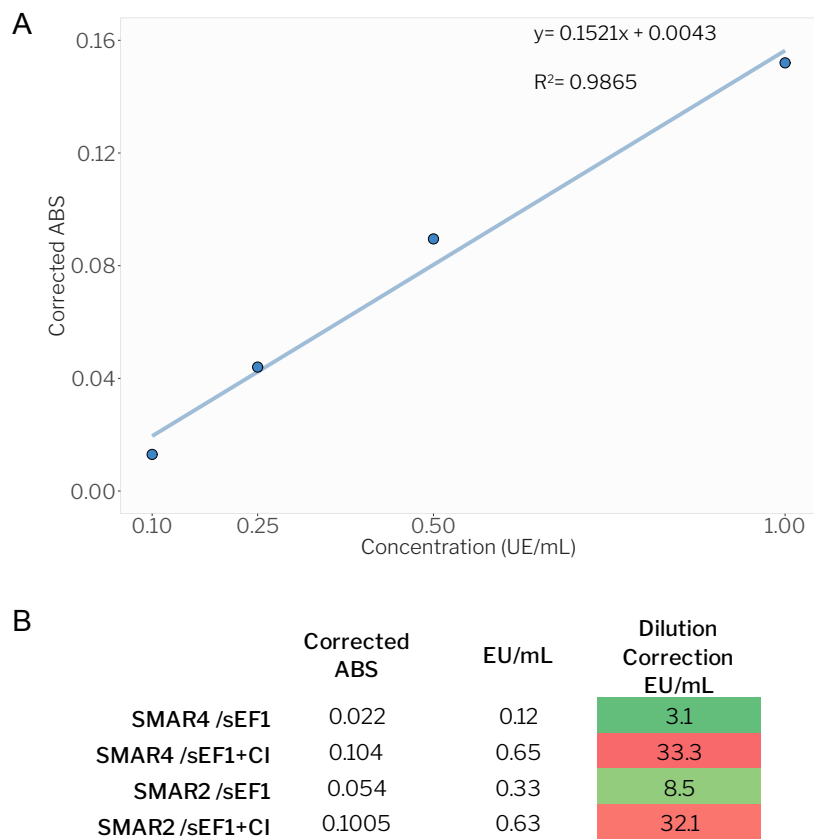


Figure B.3: Calculating the concentration of endotoxins present in S/MAR DNA Vectors. The Pierce™ Chromogenic Endotoxin Quantification Kit was used to calculate the concentration of endotoxins present in S/MAR DNA vectors. A) Displays the calibration curve used. B) Displays the calculated endotoxin concentrations present in S/MAR DNA vectors produced in-house (S/MAR4/sEF1 and S/MAR2/sEF1) and external (SMAR4/sEF1+CI and SMAR2/sEF1+CI). Differences could also be due to the CI, rather than the production entity. This would further need to be verified.



B.2 Chapter 4

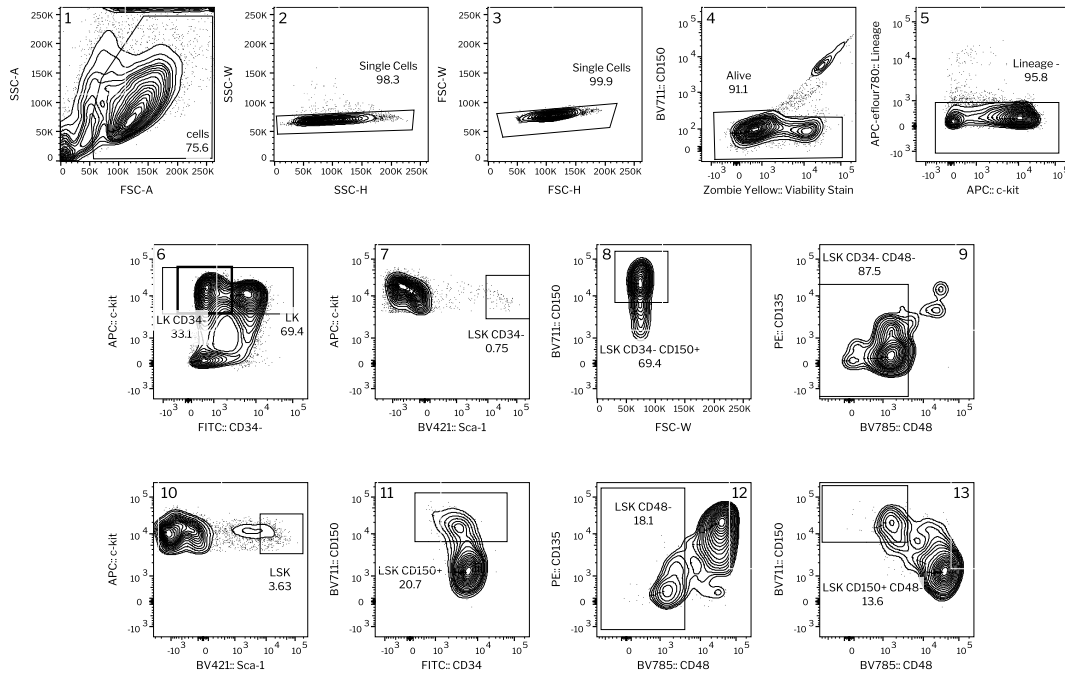


Figure B.4: FACS gating scheme used to collect various mouse HSPC populations. 100 cells from gates 7- 13 were sorted into three wells of a fibronectin coated 96-welled plate containing supplemented Ham's F-12 medium. 5 days post-sort, all 300 cells were combined into the same well. Prior to sorting, mouse bone marrow cells were lineage cell depleted. FSC-A, forward scatter area; FSC-H, forward scatter height; FSC-W, forward scatter width; SSC-A, side scatter area; SSC-H, side scatter height; SSC-W, side scatter width; LSK, lineage negative sca-1 positive c-kit positive cells.

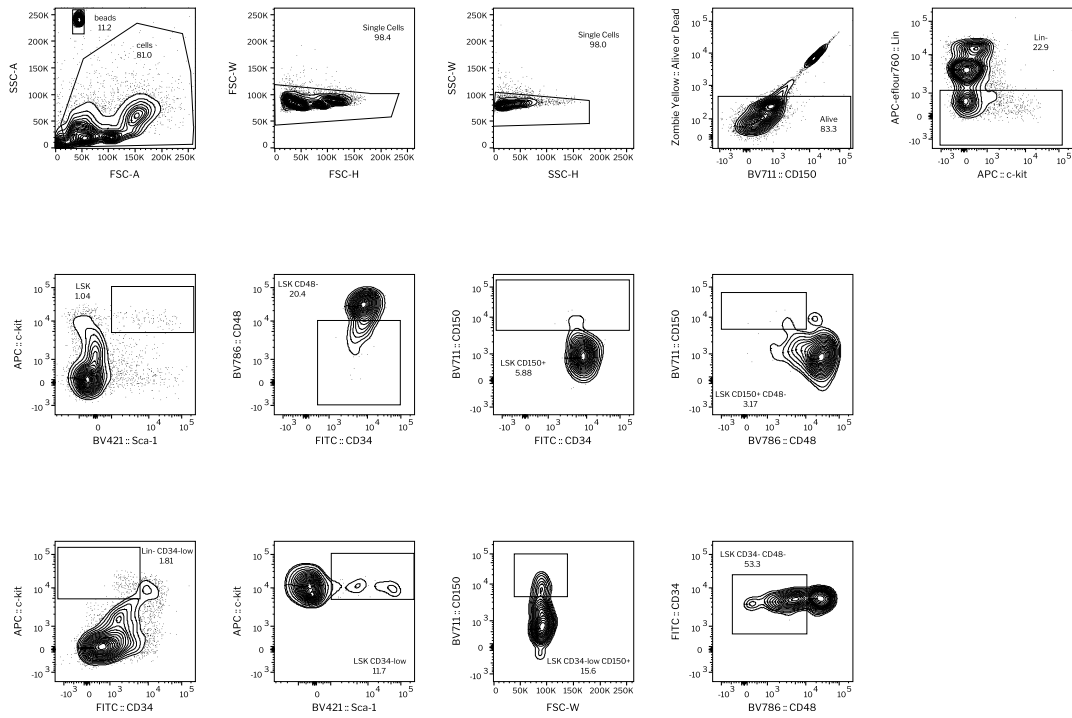


Figure B.5: FACS gating used to calculate BM composition. Absolute count beads were used to obtain cell counts of various populations present in collected mouse bone marrow. Data is representative of 3 donors.

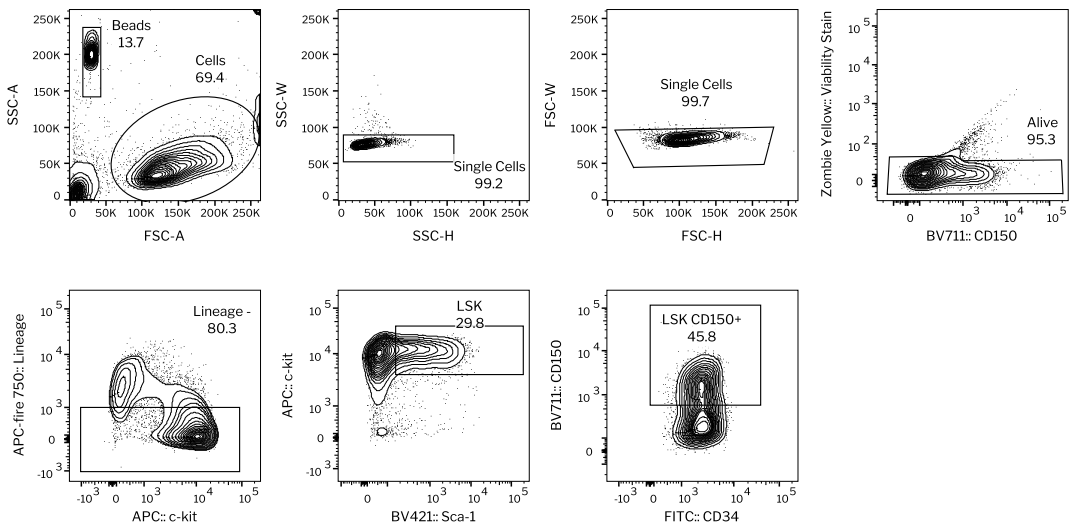


Figure B.6: Representative flow cytometry gating scheme for sample analysis of expanded mHSPCs. Samples were analyzed on a BD LSR Fortessa to assess cell counts and expression of lineage markers, c-kit, sca-1, and CD150. FSC-A, forward scatter area; FSC-H, forward scatter height; FSC-W, forward scatter width; SSC-A, side scatter area; SSC-H, side scatter height; SSC-W, side scatter width; LSK, lineage negative sca-1 positive c-kit positive cells.



Expanded LSK CD150+ cells transfected with Lipofectamine Stem

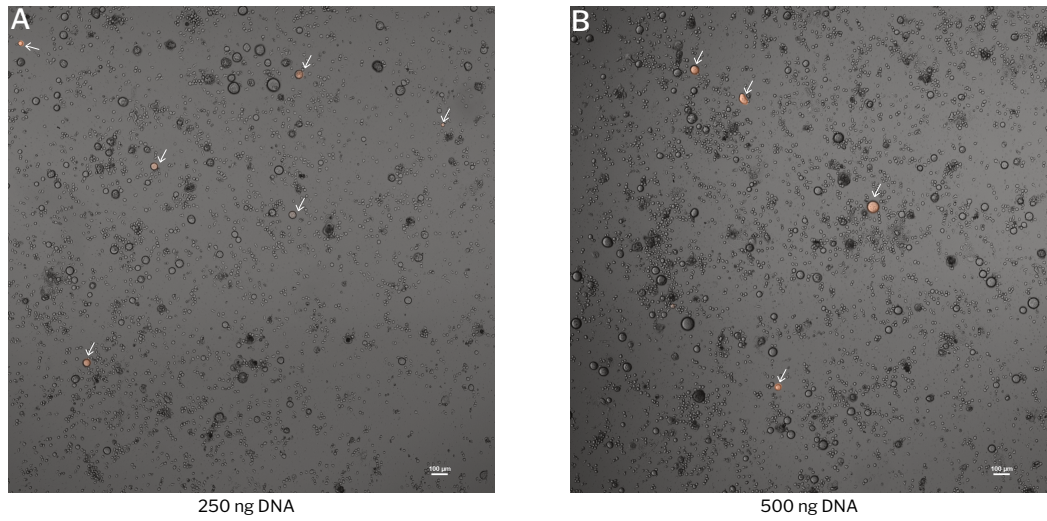


Figure B.7: The genetic modification of mHSPCs using lipofection. Lipofection was associated with a low viability and a low percentage of cells that were genetically modified.

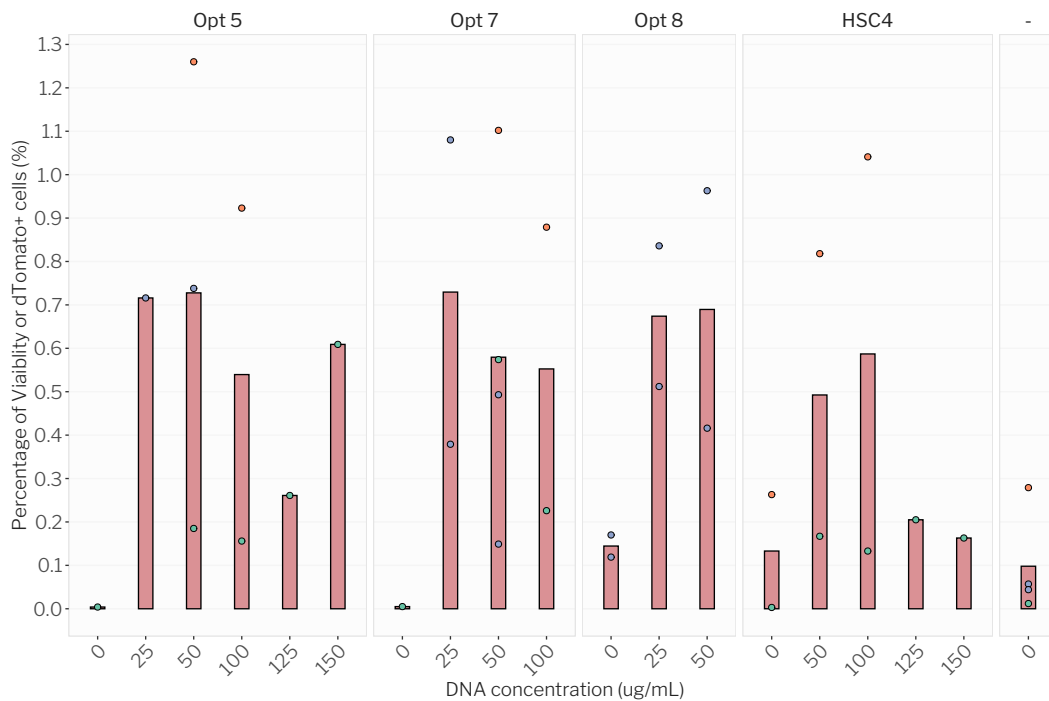


Figure B.8: Pre-screening of MaxCyte GT electroporation protocols for mouse HSPCs. DNA concentrations ranging between 0 and 150 $\mu\text{g}/\text{mL}$ were screened. Pulse protocols Opt5, Opt7, Opt8, and HSC4 were examined.

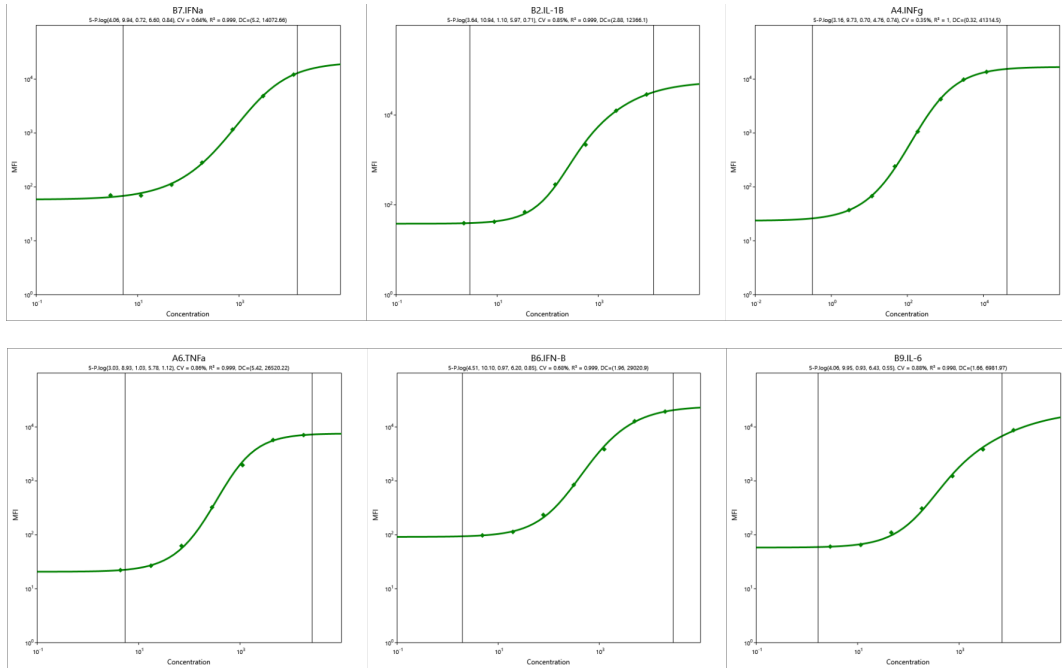


Figure B.9: Calibration curves for LEGENDplex™ analysis. Calibration curves were generated using the LEGENDplex™ Data Analysis Software.

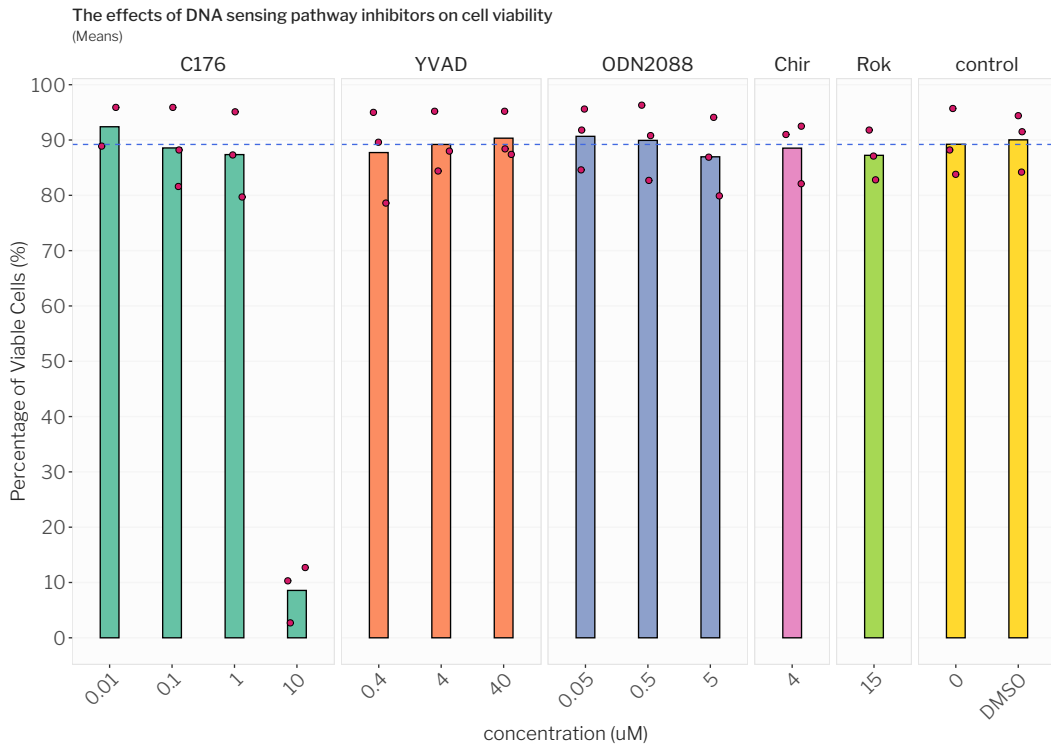


Figure B.10: The effects of DNA sensing pathway inhibitors on mHSPC viability. 3×10^5 cells incubated with inhibitors for 24 hours in a 24-well plate. Then, viability was assessed via FACS.

B.3 Chapter 5

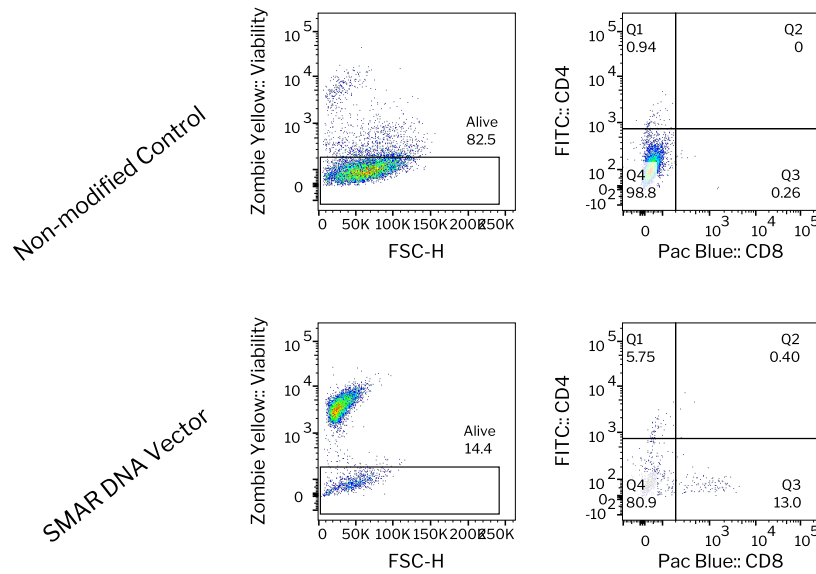


Figure B.11: Assessing the T-cell phenotype of CD34⁺ suspension cells that underwent T-cell differentiation. iPSCs that underwent HSPC differentiation using the STEMdiff™ Hematopoietic Kit were differentiated into T-cells. This is the assessment of their T-cell phenotype.

B.4 Chapter 6

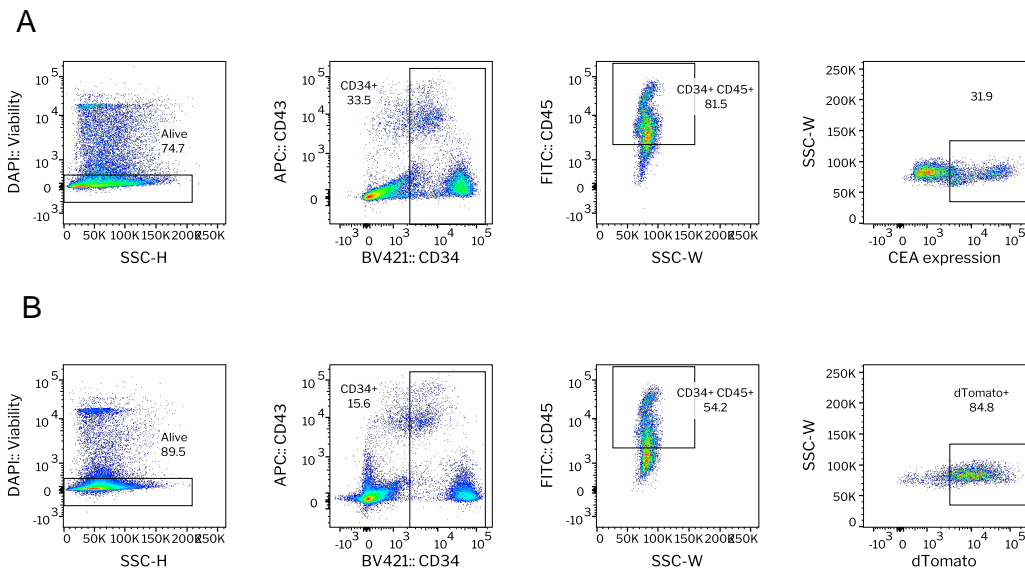


Figure B.12: Assessing the phenotype of iPSC lines that underwent HSPC differentiation. The HSPC differentiation utilized here is different from methods 1 and 2. These cells were used for T-cell differentiation of the CEA iPSC line.



Bibliography

- [1] *AddGene. Adeno-associated Virus (AAV) Guide*. URL: <https://www.addgene.org/guides/aav/>.
- [2] *AddGene. gamma-Retroviral Plasmids*. URL: <https://www.addgene.org/viral-vectors/retrovirus/>.
- [3] *AddGene. gamma-Retrovirus Guide*. URL: <https://www.addgene.org/guides/retrovirus/>.
- [4] *AddGene. Lentiviral Guide*. URL: <https://www.addgene.org/guides/lentivirus/>.
- [5] *AddGene. Lentiviral Plasmids*. URL: <https://www.addgene.org/viral-vectors/lentivirus/>.
- [6] *Adverum Biotechnologies, Inc. ADVM-022 Intravitreal Gene Therapy for Wet AMD (OPTIC). ClinicalTrials.gov identifier: NCT03748784. Updated March 22, 2022. Accessed December 14, 2022.* <https://clinicaltrials.gov/ct2/show/NCT03748784>.
- [7] N A Alhakamy, D T Curiel, and C J Berkland. “The era of gene therapy: From preclinical development to clinical application”. In: *Drug Discov Today* 26.7 (2021), pp. 1602–1619. DOI: 10.1016/j.drudis.2021.03.021. URL: <https://www.ncbi.nlm.nih.gov/pubmed/33781953>.
- [8] Hajaj M Alhomaidan and Ali M Alhomaidan. “The impact of religion on human embryonic stem cell regulations: comparison between the UK, Germany and the US”. In: *Generics and Biosimilars Initiative Journal* 7.1 (2018), pp. 22–25. DOI: 10.5639/gabij.2018.0701.005.
- [9] M Aljurf et al. “"Worldwide Network for Blood & Marrow Transplantation (WBMT) special article, challenges facing emerging alternate donor registries"”. In: *Bone Marrow Transplant* 54.8 (2019), pp. 1179–1188. DOI: 10.1038/s41409-019-0476-6. URL: <https://www.ncbi.nlm.nih.gov/pubmed/30778127>.
- [10] *Amgen Europe B.V. Imlygic (talimogene laherparepvec) [assessment report]. European Medicines Agency. Revised March 2019. Assessed October 10, 2022*. URL: https://www.ema.europa.eu/en/documents/assessment-report/imlygic-epar-public-assessment-report_en.pdf.
- [11] A M Ansari et al. “Cellular GFP Toxicity and Immunogenicity: Potential Confounders in in Vivo Cell Tracking Experiments”. eng. In: *Stem Cell Rev Rep* 12.5 (2016), pp. 553–559. DOI: 10.1007/s12015-016-9670-8.
- [12] A V Anzalone, L W Koblan, and D R Liu. “Genome editing with CRISPR-Cas nucleases, base editors, transposases and prime editors”. In: *Nat Biotechnol* 38.7 (2020), pp. 824–844. DOI: 10.1038/s41587-020-0561-9. URL: <https://www.ncbi.nlm.nih.gov/pubmed/32572269>.

- [13] A V Anzalone et al. “Search-and-replace genome editing without double-strand breaks or donor DNA”. In: *Nature* 576.7785 (2019), pp. 149–157. DOI: 10.1038/s41586-019-1711-4. URL: <https://www.ncbi.nlm.nih.gov/pubmed/31634902>.
- [14] A Artero Castro et al. “Generation of a human iPSC line by mRNA reprogramming”. In: *Stem Cell Res* 28 (2018), pp. 157–160. DOI: 10.1016/j.scr.2018.02.011. URL: <https://www.ncbi.nlm.nih.gov/pubmed/29499498>.
- [15] M B Atkins et al. “High-dose recombinant interleukin 2 therapy for patients with metastatic melanoma: analysis of 270 patients treated between 1985 and 1993”. In: *J Clin Oncol* 17.7 (1999), pp. 2105–2116. DOI: 10.1200/JCO.1999.17.7.2105. URL: <https://www.ncbi.nlm.nih.gov/pubmed/10561265>.
- [16] L Aurelian. “Oncolytic virotherapy: the questions and the promise”. In: *Oncolytic Virother* 2 (2013), pp. 19–29. DOI: 10.2147/OV.S39609. URL: <https://www.ncbi.nlm.nih.gov/pubmed/27512655>.
- [17] Susanna Bachle. *Popular Retroviral Vectors and Their Uses in Scientific Research*. 2018. URL: [https://blog.addgene.org/popular-retroviral-vectors-and-their-uses-in-scientific-research#:~:text=Gamma-retroviral%20vectors%20are%20derived,immunodeficiency%20virus%20\(HIV\)%20genome..](https://blog.addgene.org/popular-retroviral-vectors-and-their-uses-in-scientific-research#:~:text=Gamma-retroviral%20vectors%20are%20derived,immunodeficiency%20virus%20(HIV)%20genome..)
- [18] A. Baiker et al. “Mitotic stability of an episomal vector containing a human scaffold/matrix-attached region is provided by association with nuclear matrix”. In: *Nature Cell Biology* 2.3 (Mar. 2000), pp. 182–184. DOI: 10.1038/35004061. URL: http://www.nature.com/articles/ncb0300_182.
- [19] A Barahona. “Barbara McClintock and the transposition concept”. eng. In: *Arch Int Hist Sci (Paris)* 46.137 (1997), pp. 309–329.
- [20] R Barrangou and P Horvath. “CRISPR: new horizons in phage resistance and strain identification”. In: *Annu Rev Food Sci Technol* 3 (2012), pp. 143–162. DOI: 10.1146/annurev-food-022811-101134. URL: <https://www.ncbi.nlm.nih.gov/pubmed/22224556>.
- [21] D E Bauer et al. “An erythroid enhancer of BCL11A subject to genetic variation determines fetal hemoglobin level”. In: *Science* 342.6155 (2013), pp. 253–257. DOI: 10.1126/science.1242088. URL: <https://www.ncbi.nlm.nih.gov/pubmed/24115442>.
- [22] *Beijing Tongren Hospital. Safety and Efficacy of Autologous Transplantation of iPSC-RPE in the Treatment of Macular Degeneration. ClinicalTrials.gov identifier: NCT05445063. Updated July 6, 2022. Accessed October 16, 2022.* URL: <https://clinicaltrials.gov/ct2/show/NCT05445063>.
- [23] J C Bell, B Lichty, and D Stojdl. “Getting oncolytic virus therapies off the ground”. In: *Cancer Cell* 4.1 (2003), pp. 7–11. DOI: 10.1016/s1535-6108(03)00170-3. URL: <https://www.ncbi.nlm.nih.gov/pubmed/12892708>.
- [24] M J Berendt, R J North, and D P Kirsstein. “The immunological basis of endotoxin-induced tumor regression. Requirement for T-cell-mediated immunity”. In: *The Journal of experimental medicine* 148.6 (1978), pp. 1550–1559. DOI: 10.1084/jem.148.6.1550. URL: <https://www.ncbi.nlm.nih.gov/pubmed/309921>.



- [25] A Bhardwaj and V Nain. “TALENs-an indispensable tool in the era of CRISPR: a mini review”. In: *J Genet Eng Biotechnol* 19.1 (2021), p. 125. DOI: 10.1186/s43141-021-00225-z. URL: <https://www.ncbi.nlm.nih.gov/pubmed/34420096>.
- [26] BioLegend. *LEGENDplex™ Data Analysis Software V8.0 User Guide*. URL: https://www.biolegend.com/Files/Images/BioLegend/legendplex/manuals/LEGENDplex_Data_Analysis_Software_v8.0_User_Guide.pdf.
- [27] BioLegend. *LEGENDplex™ Multi-Analyte Flow Assay Kit*. URL: https://d1spbj2x7qk4bg.cloudfront.net/Files/Images/media_assets/pro_detail/datasheets/75354_Mu_Anti-Virus_Resp_FINAL_R2.pdf?v=20221013063042.
- [28] BioLegend. *Setup Procedure for BD FACSAria™, FACSCanto™, and LSR Series*. URL: <https://www.biolegend.com/Files/Images/BioLegend/legendplex/instructions/Setup31-34.pdf>.
- [29] Bioray Laboratories. *Safety and Efficacy Evaluation of BRL-101 in Subjects With Transfusion-Dependent β -Thalassemia*. *ClinicalTrials.gov* identifier: NCT05577312. Updated November 10, 2022. Accessed December 15, 2022. URL: <https://clinicaltrials.gov/ct2/show/NCT05577312>.
- [30] C Anthony Blau. “E. Donnall Thomas, M.D. (1920–2012)”. In: *Stem Cells Translational Medicine* 2.2 (2013), pp. 81–82. DOI: 10.5966/sctm.2013-0008.
- [31] bluebird bio Inc. *SKYSONA (elivaldogene autotemcell) [package insert]*. U.S. Food and Drug Administration website. Revised September 2022. Assessed December 15, 2022. URL: <https://www.fda.gov/media/161640/download>.
- [32] bluebird bio Inc. *ZYNTEGLO (betibeglogene autotemcel) [package insert]*. U.S. Food and Drug Administration website. <https://www.fda.gov/media/160991/download> Revised August 2022. Assessed December 15, 2022. URL: <https://www.fda.gov/media/160991/download>.
- [33] J Boch and U Bonas. “Xanthomonas AvrBs3 family-type III effectors: discovery and function”. In: *Annu Rev Phytopathol* 48 (2010), pp. 419–436. DOI: 10.1146/annurev-phyto-080508-081936. URL: <https://www.ncbi.nlm.nih.gov/pubmed/19400638>.
- [34] J Boch et al. “Breaking the code of DNA binding specificity of TAL-type III effectors”. In: *Science* 326.5959 (2009), pp. 1509–1512. DOI: 10.1126/science.1178811. URL: <https://www.ncbi.nlm.nih.gov/pubmed/19933107>.
- [35] D E Bowles et al. “Phase 1 gene therapy for Duchenne muscular dystrophy using a translational optimized AAV vector”. In: *Mol Ther* 20.2 (2012), pp. 443–455. DOI: 10.1038/mt.2011.237. URL: <https://www.ncbi.nlm.nih.gov/pubmed/22068425>.
- [36] M Bozza et al. “A nonviral, nonintegrating DNA nanovector platform for the safe, rapid, and persistent manufacture of recombinant T cells”. In: *Sci Adv* 7.16 (2021). DOI: 10.1126/sciadv.abf1333. URL: <https://www.ncbi.nlm.nih.gov/pubmed/33853779>.
- [37] Matthias Bozza. “The development of a novel S/MAR DNA vector platform for the stable, persistent and safe Genetic Engineering of Dividing Cells”. PhD thesis. 2017.

- [38] Matthias Bozza et al. “Novel Non-integrating DNA Nano-S/MAR Vectors Restore Gene Function in Isogenic Patient-Derived Pancreatic Tumor Models”. In: *Molecular Therapy - Methods & Clinical Development* 17 (June 2020), pp. 957–968. DOI: 10.1016/j.omtm.2020.04.017. URL: <https://linkinghub.elsevier.com/retrieve/pii/S2329050120300772>.
- [39] J R Brahmer et al. “Phase I study of single-agent anti-programmed death-1 (MDX-1106) in refractory solid tumors: safety, clinical activity, pharmacodynamics, and immunologic correlates”. In: *J Clin Oncol* 28.19 (2010), pp. 3167–3175. DOI: 10.1200/JCO.2009.26.7609. URL: <https://www.ncbi.nlm.nih.gov/pubmed/20516446>.
- [40] M Brameshuber et al. “Monomeric TCRs drive T cell antigen recognition”. In: *Nat Immunol* 19.5 (2018), pp. 487–496. DOI: 10.1038/s41590-018-0092-4. URL: <https://www.ncbi.nlm.nih.gov/pubmed/29662172>.
- [41] C J Braun et al. “Gene therapy for Wiskott-Aldrich syndrome—long-term efficacy and genotoxicity”. In: *Sci Transl Med* 6.227 (2014), 227ra33. DOI: 10.1126/scitranslmed.3007280. URL: <https://www.ncbi.nlm.nih.gov/pubmed/24622513>.
- [42] Bristol-Myers Squibb Co. *Opdivo and Yervoy (nivolumab and ipilimumab)*. U.S. Food and Drug Administration website. Revised May 2020. Accessed October 9, 2022. URL: <https://www.fda.gov/drugs/resources-information-approved-drugs/fda-approves-nivolumab-plus-ipilimumab-first-line-mnscclc-pd-11-tumor-expression-1>.
- [43] Bristol-Myers Squibb Co. *Opdualag (nivolumab and relatlimab) [package insert]*. U.S. Food and Drug Administration website. Revised March 2022. Accessed October 9, 2022. URL: https://www.accessdata.fda.gov/drugsatfda_docs/label/2022/761234s0001b1.pdf.
- [44] Bristol-Myers Squibb Co. *Yervoy (ipilimumab) [Assessment Report]*. European Medicines Agency website. Revised May 2011. Accessed October 9, 2022. URL: https://www.ema.europa.eu/en/documents/assessment-report/yervoy-epar-public-assessment-report_en.pdf.
- [45] Bristol-Myers Squibb Co. *Yervoy (ipilimumab) [Highlights of Prescribing Information]*. U.S. Food and Drug Administration website. Revised October 2020. Accessed October 9, 2022. URL: https://www.accessdata.fda.gov/drugsatfda_docs/label/2020/125377s1151b1.pdf.
- [46] Bristol-Myers Squibb. *Opdivo (nivolumab) [medicine overview]*. European Medicines Agency. Revised April 2022. Accessed October 9, 2022. URL: https://www.ema.europa.eu/en/documents/overview/opdivo-epar-medicine-overview_en.pdf.
- [47] Bristol-Myers Squibb. *Opdivo (nivolumab) [package insert]*. U.S. Food and Drug Administration website. Revised May 2016. Accessed October 9, 2022. URL: https://www.accessdata.fda.gov/drugsatfda_docs/label/2016/125554s0191b1.pdf.
- [48] S Britton, J Coates, and S P Jackson. “A new method for high-resolution imaging of Ku foci to decipher mechanisms of DNA double-strand break repair”. In: *J Cell Biol*



- 202.3 (2013), pp. 579–595. DOI: 10.1083/jcb.201303073. URL: <https://www.ncbi.nlm.nih.gov/pubmed/23897892>.
- [49] C Burger et al. “Recombinant AAV viral vectors pseudotyped with viral capsids from serotypes 1, 2, and 5 display differential efficiency and cell tropism after delivery to different regions of the central nervous system”. In: *Mol Ther* 10.2 (2004), pp. 302–317. DOI: 10.1016/j.ymthe.2004.05.024. URL: <https://www.ncbi.nlm.nih.gov/pubmed/15294177>.
- [50] *Business Wire. Century Therapeutics and Bristol Myers Squibb Enter into a Strategic Collaboration to Develop iPSC-derived Allogeneic Cell Therapies*. Philadelphia & New York, 2022. URL: <https://www.businesswire.com/news/home/20220110005266/en/>.
- [51] Roberto Calcedo and James M. Wilson. “Humoral Immune Response to AAV”. In: *Frontiers in Immunology* 4 (2013). DOI: 10.3389/fimmu.2013.00341. URL: <http://journal.frontiersin.org/article/10.3389/fimmu.2013.00341/abstract>.
- [52] *California’s stem cell agency. Induced Pluripotent Stem Cell Repository*. URL: <https://www.cirm.ca.gov/researchers/ipsc-repository/about>.
- [53] Emmanuelle Cameau, Andreia Pedregal, and Clive Glover. “Cost modelling comparison of adherent multi-trays with suspension and fixed-bed bioreactors for the manufacturing of gene therapy products”. In: *Cell and Gene Therapy Insights* 5.11 (2019), pp. 1663–1674. DOI: 10.18609/cgti.2019.175.
- [54] Emily Capra et al. *Viral-vector therapies at scale: Today’s challenges and future opportunities*. 2022. URL: <https://www.mckinsey.com/industries/life-sciences/our-insights/viral-vector-therapies-at-scale-todays-challenges-and-future-opportunities>.
- [55] *Caribou Biosciences, Inc. CRISPR-Edited Allogeneic Anti-CD19 CAR-T Cell Therapy for Relapsed/Refractory B Cell Non-Hodgkin Lymphoma ClinicalTrials.gov identifier: NCT04637763. Updated November 2, 2022. Accessed December 15, 2022*. URL: <https://clinicaltrials.gov/ct2/show/NCT04637763>.
- [56] *Celgene Corporation, a Bristol-Myers Squibb Company. ABECMA (idecabtagene vicleucel). [Package Insert]. U.S. Food and Drug Administration website. Revised March 2021. Accessed December 11, 2022*. URL: <https://www.fda.gov/media/147055/download>.
- [57] *Cellectis S.A. Study Evaluating Safety and Efficacy of UCART123 in Patients With Relapsed/ Refractory Acute Myeloid Leukemia (AMELI-01). ClinicalTrials.gov identifier: NCT03190278. Updated June 7, 2022. Accessed December 15, 2022*. URL: <https://clinicaltrials.gov/ct2/show/NCT03190278>.
- [58] *Cellectis S.A. Study Evaluating UCART20x22 in B-Cell Non-Hodgkin Lymphoma (NatHaLi-01). ClinicalTrials.gov identifier: NCT05607420. Updated December 12, 2022. Accessed December 15, 2022*. URL: <https://clinicaltrials.gov/ct2/show/NCT05607420>.
- [59] *Cellectis S.A.. Study Evaluating Safety and Efficacy of UCART Targeting CS1 in Patients With Relapsed/Refractory Multiple Myeloma (MELANI-01)*.

- ClinicalTrials.gov* identifier: NCT04142619. Updated August 31, 2022. Accessed December 15, 2022. URL: <https://clinicaltrials.gov/ct2/show/NCT04142619>.
- [60] Center for International Blood and Marrow Transplant Research. Generation of an Induced Pluripotent Stem (iPS) Cell Bank Immune Matched to a Majority of the US Population. *ClinicalTrials.org* identifier: NCT03434808. Updated July 15, 2020. Accessed Dec 3, 2022. URL: <https://clinicaltrials.gov/ct2/show/NCT03434808>.
- [61] CENTOGENE GmbH Rostock. Induced Pluripotent Stem Cells for the Development of Novel Drug Therapies for Inborn Errors of Metabolism (iPSC-IEM) (iPSC-IEM). *ClinicalTrials.org* identifier: NCT04097275. Updated May 17, 2021. Accessed October 16, 2022. URL: <https://clinicaltrials.gov/ct2/show/NCT04097275>.
- [62] Randy J Chandler et al. “Genotoxicity in Mice Following AAV Gene Delivery: A Safety Concern for Human Gene Therapy?” In: *Molecular Therapy* 24.2 (2016), pp. 198–201. DOI: 10.1038/mt.2016.17.
- [63] Smita S. Chandran and Christopher A. Klebanoff. “T cell receptor-based cancer immunotherapy: Emerging efficacy and pathways of resistance”. In: *Immunological Reviews* 290.1 (July 2019), pp. 127–147. DOI: 10.1111/imr.12772. URL: <https://onlinelibrary.wiley.com/doi/10.1111/imr.12772>.
- [64] C Chen et al. “Comparative analysis of the transduction efficiency of five adeno associated virus serotypes and VSV-G pseudotype lentiviral vector in lung cancer cells”. In: *Virology* 10 (2013), p. 86. DOI: 10.1186/1743-422X-10-86. URL: <https://www.ncbi.nlm.nih.gov/pubmed/23497017>.
- [65] I. P. Chernov, S. B. Akopov, and L. G. Nikolaev. “Structure and functions of nuclear matrix associated regions (S/MARs)”. In: *Russian Journal of Bioorganic Chemistry* 30.1 (2004), pp. 1–11. DOI: 10.1023/B:RUBI.0000015767.28683.69.
- [66] N Chirmule et al. “Immune responses to adenovirus and adeno-associated virus in humans”. In: *Gene Ther* 6.9 (1999), pp. 1574–1583. DOI: 10.1038/sj.gt.3300994. URL: <https://www.ncbi.nlm.nih.gov/pubmed/10490767>.
- [67] Markus Chmielewski and Hinrich Abken. “CAR T cells transform to trucks: chimeric antigen receptor–redirected T cells engineered to deliver inducible IL-12 modulate the tumour stroma to combat cancer”. In: *Cancer Immunology, Immunotherapy* 61.8 (Aug. 2012), pp. 1269–1277. DOI: 10.1007/s00262-012-1202-z. URL: <https://www.nature.com/articles/s41467-020-20599-x>.
- [68] T M Clay et al. “Efficient transfer of a tumor antigen-reactive TCR to human peripheral blood lymphocytes confers anti-tumor reactivity.” In: *Journal of immunology (Baltimore, Md. : 1950)* 163.1 (July 1999), pp. 507–13. URL: <http://www.ncbi.nlm.nih.gov/pubmed/10384155>.
- [69] William B Coley. “I. The Treatment of Malignant Tumors by Repeated Inoculations of Erysipelas”. In: *Annals of Surgery* 18 (1893). DOI: 10.1097/00000658-189307000-00009.
- [70] A Colman. “Profile of John Gurdon and Shinya Yamanaka, 2012 Nobel laureates in medicine or physiology”. In: *Proc Natl Acad Sci U S A* 110.15 (2013), pp. 5740–5741. DOI: 10.1073/pnas.1221823110. URL: <https://www.ncbi.nlm.nih.gov/pubmed/23538305>.



- [71] Chari Cortez. *CRISPR 101: Homology Directed Repair*. Ed. by AddGene Blog. 2015. URL: https://blog.addgene.org/crispr-101-homology-directed-repair?gclid=Cj0KCQiAqOucBhDrARIsAPCQL1Y0j3C2XaTt_Ld7TlXgPBFgKDPSeTCvnuaQ7ZbYxqt98BJLdxJ7EkcaAt79EALw_wcB.
- [72] B J Crenshaw et al. “Perspective on Adenoviruses: Epidemiology, Pathogenicity, and Gene Therapy”. In: *Biomedicines* 7.3 (2019). DOI: 10.3390/biomedicines7030061. URL: <https://www.ncbi.nlm.nih.gov/pubmed/31430920>.
- [73] P Cruz-Tapias, J Castiblanco, and JM Anaya. “Major histocompatibility complex: Antigen processing and presentation.” In: *Autoimmunity: From Bench to Bedside*. Ed. by JM Anaya, Y Shoenfeld, and A Rojas-Villarraga. Bogota (Colombia): El Rosario University Press, 2013. Chap. 10.
- [74] Z Cui et al. “The comparison of ZFNs, TALENs, and SpCas9 by GUIDE-seq in HPV-targeted gene therapy”. In: *Mol Ther Nucleic Acids* 26 (2021), pp. 1466–1478. DOI: 10.1016/j.omtn.2021.08.008. URL: <https://www.ncbi.nlm.nih.gov/pubmed/34938601>.
- [75] A Cumano, F Dieterlen-Lievre, and I Godin. “Lymphoid potential, probed before circulation in mouse, is restricted to caudal intraembryonic splanchnopleura”. In: *Cell* 86.6 (1996), pp. 907–916. DOI: 10.1016/s0092-8674(00)80166-x. URL: <https://www.ncbi.nlm.nih.gov/pubmed/8808626>.
- [76] D A Dalwadi et al. “Liver Injury Increases the Incidence of HCC following AAV Gene Therapy in Mice”. In: *Mol Ther* 29.2 (2021), pp. 680–690. DOI: 10.1016/j.ymthe.2020.10.018. URL: <https://www.ncbi.nlm.nih.gov/pubmed/33554867>.
- [77] Rajat K. Das et al. “Naïve T-cell Deficits at Diagnosis and after Chemotherapy Impair Cell Therapy Potential in Pediatric Cancers”. In: *Cancer Discovery* 9.4 (Apr. 2019), pp. 492–499. DOI: 10.1158/2159-8290.CD-18-1314. URL: <https://aacrjournals.org/cancerdiscovery/article/9/4/492/10709/Naive-T-cell-Deficits-at-Diagnosis-and-after>.
- [78] S S De Ravin et al. “CRISPR-Cas9 gene repair of hematopoietic stem cells from patients with X-linked chronic granulomatous disease”. In: *Sci Transl Med* 9.372 (2017). DOI: 10.1126/scitranslmed.aah3480. URL: <https://www.ncbi.nlm.nih.gov/pubmed/28077679>.
- [79] Ella De Trizio and Christopher S Brennan. “The business of human embryonic stem cell research and an international analysis of relevant laws”. eng. In: *The journal of biolaw & business* 7.4 (2004), pp. 14–22. URL: <http://europepmc.org/abstract/MED/15675095>.
- [80] Melvin L. DePamphilis. “Replication origins in metazoan chromosomes: Fact or fiction?” In: *BioEssays* 21.1 (1999), pp. 5–16. DOI: 10.1002/(SICI)1521-1878(199901)21:1<5::AID-BIES2>3.0.CO;2-6.
- [81] J G Doench et al. “Rational design of highly active sgRNAs for CRISPR-Cas9-mediated gene inactivation”. In: *Nat Biotechnol* 32.12 (2014), pp. 1262–1267. DOI: 10.1038/nbt.3026. URL: <https://www.ncbi.nlm.nih.gov/pubmed/25184501>.



- [82] J A Doudna and E Charpentier. “Genome editing. The new frontier of genome engineering with CRISPR-Cas9”. In: *Science* 346.6213 (2014), p. 1258096. DOI: 10.1126/science.1258096. URL: <https://www.ncbi.nlm.nih.gov/pubmed/25430774>.
- [83] D Duan, Y Yue, and J F Engelhardt. “Expanding AAV packaging capacity with trans-splicing or overlapping vectors: a quantitative comparison”. In: *Mol Ther* 4.4 (2001), pp. 383–391. DOI: 10.1006/mthe.2001.0456. URL: <https://www.ncbi.nlm.nih.gov/pubmed/11592843>.
- [84] M E Dudley et al. “Cancer regression and autoimmunity in patients after clonal repopulation with antitumor lymphocytes”. In: *Science* 298.5594 (2002), pp. 850–854. DOI: 10.1126/science.1076514. URL: <https://www.ncbi.nlm.nih.gov/pubmed/12242449>.
- [85] Tom Dull et al. “A Third-Generation Lentivirus Vector with a Conditional Packaging System”. In: *Journal of Virology* 72.11 (1998), pp. 8463–8471. DOI: doi:10.1128/JVI.72.11.8463-8471.1998. URL: <https://journals.asm.org/doi/abs/10.1128/JVI.72.11.8463-8471.1998>.
- [86] C P Duong et al. “Cancer immunotherapy utilizing gene-modified T cells: From the bench to the clinic”. In: *Mol Immunol* 67.2 Pt A (2015), pp. 46–57. DOI: 10.1016/j.molimm.2014.12.009. URL: <https://www.ncbi.nlm.nih.gov/pubmed/25595028>.
- [87] T J Eberlein, M Rosenstein, and S A Rosenberg. “Regression of a disseminated syngeneic solid tumor by systemic transfer of lymphoid cells expanded in interleukin 2”. eng. In: *The Journal of experimental medicine* 156.2 (1982), pp. 385–397. DOI: 10.1084/jem.156.2.385. URL: <http://europepmc.org/abstract/MED/6980254>.
- [88] A Ehrhardt et al. “Episomal vectors for gene therapy”. In: *Curr Gene Ther* 8.3 (2008), pp. 147–161. DOI: 10.2174/156652308784746440. URL: <https://www.ncbi.nlm.nih.gov/pubmed/18537590>.
- [89] Paul Ehrlich. “Über den jetzigen stand der karzinomforschung.” In: *Ned Tijdschr Geneeskde* 5 (1909), pp. 273–290.
- [90] Alan Engelman. “Reverse Transcription and Integration”. In: *Retroviruses Molecular Biology, Genomics and Pathogenesis*. Ed. by Reinhard Kurth and Norbert Bannert. Norfolk, UK: Caister Academic Press, 2010. Chap. 5, pp. 129–159.
- [91] *euofins Genomics*. *Product details & sample submission: Sample preparation*. 2022. URL: <https://euofinsgenomics.eu/en/genotyping-gene-expression/applied-genomics-services/mycoplasmacheck/>.
- [92] *euofins Genomics*. *TubeSeq: Sample Submission Guide for the TubeSeq Sequencing Service*. 2021. URL: https://euofinsgenomics.eu/media/1587670/euofins-flyer-tubeseq_20210406_online.pdf.
- [93] *European Medicines Agency*. *Glybera. Assessed 13 Dec 2022*. URL: <https://www.ema.europa.eu/en/medicines/human/EPAR/glybera>.
- [94] *European Medicines Agency*. *Strimvelis. Assessed 13 Dec 2022*. URL: <https://www.ema.europa.eu/en/medicines/human/EPAR/strimvelis>.



- [95] *Expression Therapeutics, LLC. Hematopoietic Stem Cell Transplantation Gene Therapy for Treatment of Severe Hemophilia A. ClinicalTrials.gov identifier: NCT04418414. Updated May 23, 2022. Accessed 13 December 2022. URL: <https://clinicaltrials.gov/ct2/show/NCT04418414>.*
- [96] *Fate Therapeutics. FT500 as Monotherapy and in Combination With Immune Checkpoint Inhibitors in Subjects With Advanced Solid Tumors. ClinicalTrials.gov identifier: NCT03841110. Updated September 29, 2022. Accessed October 16, 2022. URL: <https://clinicaltrials.gov/ct2/show/NCT03841110>.*
- [97] James L.M. Ferrara and H. Joachim Deeg. “Graft-versus-Host Disease”. In: *New England Journal of Medicine* 324.10 (Mar. 1991). Ed. by Franklin H. Epstein, pp. 667–674. DOI: 10.1056/NEJM199103073241005. URL: <http://www.nejm.org/doi/10.1056/NEJM199103073241005>.
- [98] G Ferrari, A J Thrasher, and A Aiuti. “Gene therapy using haematopoietic stem and progenitor cells”. In: *Nat Rev Genet* 22.4 (2021), pp. 216–234. DOI: 10.1038/s41576-020-00298-5. URL: <https://www.ncbi.nlm.nih.gov/pubmed/33303992>.
- [99] L Fong and E J Small. “Anti-cytotoxic T-lymphocyte antigen-4 antibody: the first in an emerging class of immunomodulatory antibodies for cancer treatment”. In: *J Clin Oncol* 26.32 (2008), pp. 5275–5283. DOI: 10.1200/JCO.2008.17.8954. URL: <https://www.ncbi.nlm.nih.gov/pubmed/18838703>.
- [100] O. Forostyak, G. Dayanithi, and S. Forostyak. “CNS Regenerative Medicine and Stem Cells”. In: *Opera Med Physiol* 2.1 (2016), pp. 55–62. DOI: 20388/OMP2016.001.0023.
- [101] *Fraunhofer-Gesellschaft. The EBiSC – European Bank for induced pluripotent Stem Cells. 2022. URL: <https://ebisc.org/>.*
- [102] T Friedmann. “A brief history of gene therapy”. In: *Nat Genet* 2.2 (1992), pp. 93–98. DOI: 10.1038/ng1092-93. URL: <https://www.ncbi.nlm.nih.gov/pubmed/1303270>.
- [103] T Friedmann and R Roblin. “Gene therapy for human genetic disease?” In: *Science* 175.4025 (1972), pp. 949–955. DOI: 10.1126/science.175.4025.949. URL: <https://www.ncbi.nlm.nih.gov/pubmed/5061866>.
- [104] Y Fu et al. “High-frequency off-target mutagenesis induced by CRISPR-Cas nucleases in human cells”. In: *Nat Biotechnol* 31.9 (2013), pp. 822–826. DOI: 10.1038/nbt.2623. URL: <https://www.ncbi.nlm.nih.gov/pubmed/23792628>.
- [105] *FUJIFILM Cellular Dynamics, Inc. FUJIFILM Cellular Dynamics Announces the Appointment of Dr. Ilyas Singeç as Chief Scientific Officer. Madison, Wis., 2022. URL: https://www.fujifilm.com/us/en/news/FCDI_CS0_Ilyas_Singec.*
- [106] C Gandara, V Affleck, and E A Stoll. “Manufacture of Third-Generation Lentivirus for Preclinical Use, with Process Development Considerations for Translation to Good Manufacturing Practice”. In: *Hum Gene Ther Methods* 29.1 (2018), pp. 1–15. DOI: 10.1089/hgtb.2017.098. URL: <https://www.ncbi.nlm.nih.gov/pubmed/29212357>.
- [107] Daniel Gaudet, Julie Méthot, and John Kastelein. “Gene therapy for lipoprotein lipase deficiency”. In: *Current Opinion in Lipidology* 23.4 (Aug. 2012), pp. 310–320. DOI: 10.1097/MOL.0b013e3283555a7e. URL: <https://journals.lww.com/00041433-201208000-00007>.



- [108] Karsten Gavenis. *Safety and Efficacy of Induced Pluripotent Stem Cell-derived Engineered Human Myocardium as Biological Ventricular Assist Tissue in Terminal Heart Failure (BioVAT-HF)*. *ClinicalTrials.gov identifier: NCT04396899*. Updated May 27, 2022. Accessed Oct 16, 2022. URL: <https://clinicaltrials.gov/ct2/show/NCT04396899>.
- [109] Genentech, Inc. *Rituxan (Rituximab) [Approval Letter]*. U.S. Food and Drug Administration website. November 1997. Accessed October 9, 2022. URL: <https://web.archive.org/web/20170222172426/https://www.fda.gov/downloads/Drugs/DevelopmentApprovalProcess/HowDrugsareDevelopedandApproved/ApprovalApplications/TherapeuticBiologicApplications/ucm107740.pdf>.
- [110] A M Geurts et al. “Gene transfer into genomes of human cells by the sleeping beauty transposon system”. In: *Mol Ther* 8.1 (2003), pp. 108–117. DOI: 10.1016/s1525-0016(03)00099-6. URL: <https://www.ncbi.nlm.nih.gov/pubmed/12842434>.
- [111] Roger D. Gingrich et al. “The use of partially matched, unrelated donors in clinical bone marrow transplantation”. In: *Transplantation* 39.5 (May 1985), pp. 526–531. DOI: 10.1097/00007890-198505000-00014. URL: <http://journals.lww.com/00007890-198505000-00014>.
- [112] S L Ginn et al. “Gene therapy clinical trials worldwide to 2017: An update”. In: *J Gene Med* 20.5 (2018), e3015. DOI: 10.1002/jgm.3015. URL: <https://www.ncbi.nlm.nih.gov/pubmed/29575374>.
- [113] A Gogol-Doring et al. “Genome-wide Profiling Reveals Remarkable Parallels Between Insertion Site Selection Properties of the MLV Retrovirus and the piggyBac Transposon in Primary Human CD4(+) T Cells”. In: *Mol Ther* 24.3 (2016), pp. 592–606. DOI: 10.1038/mt.2016.11. URL: <https://www.ncbi.nlm.nih.gov/pubmed/26755332>.
- [114] N Gomez-Ospina et al. “Human genome-edited hematopoietic stem cells phenotypically correct Mucopolysaccharidosis type I”. In: *Nat Commun* 10.1 (2019), p. 4045. DOI: 10.1038/s41467-019-11962-8. URL: <https://www.ncbi.nlm.nih.gov/pubmed/31492863>.
- [115] F F Gonzalez-Galarza et al. “Allele frequency net database (AFND) 2020 update: gold-standard data classification, open access genotype data and new query tools”. In: *Nucleic Acids Res* 48.D1 (2020), pp. D783–D788. DOI: 10.1093/nar/gkz1029. URL: <https://www.ncbi.nlm.nih.gov/pubmed/31722398>.
- [116] P Gregorevic et al. “Systemic delivery of genes to striated muscles using adeno-associated viral vectors”. In: *Nat Med* 10.8 (2004), pp. 828–834. DOI: 10.1038/nm1085. URL: <https://www.ncbi.nlm.nih.gov/pubmed/15273747>.
- [117] I Gresser et al. “Increased survival in mice inoculated with tumor cells and treated with interferon preparations”. In: *Proc Natl Acad Sci U S A* 63.1 (1969), pp. 51–57. DOI: 10.1073/pnas.63.1.51. URL: <https://www.ncbi.nlm.nih.gov/pubmed/5257966>.
- [118] G Gross, T Waks, and Z Eshhar. “Expression of immunoglobulin-T-cell receptor chimeric molecules as functional receptors with antibody-type specificity”. In: *Proc*



- Natl Acad Sci U S A* 86.24 (1989), pp. 10024–10028. DOI: 10.1073/pnas.86.24.10024. URL: <https://www.ncbi.nlm.nih.gov/pubmed/2513569>.
- [119] GSK. *GSK signs strategic agreement to transfer rare disease gene therapy portfolio to Orchard Therapeutics*. London, UK, 2018. URL: <https://www.gsk.com/en-gb/media/press-releases/gsk-signs-strategic-agreement-to-transfer-rare-disease-gene-therapy-portfolio-to-orchard-therapeutics/>.
- [120] Jordan U Gutterman. *Letter to Helen Coley Nauts*. 1978.
- [121] J B Haanen. “Immunotherapy of melanoma”. In: *EJC Suppl* 11.2 (2013), pp. 97–105. DOI: 10.1016/j.ejcsup.2013.07.013. URL: <https://www.ncbi.nlm.nih.gov/pubmed/26217118>.
- [122] Rudolf Haase et al. “PEPito: A significantly improved non-viral episomal expression vector for mammalian cells”. In: *BMC Biotechnology* 10 (2010), pp. 1–14. DOI: 10.1186/1472-6750-10-20.
- [123] S Hacein-Bey-Abina et al. “A serious adverse event after successful gene therapy for X-linked severe combined immunodeficiency”. In: *N Engl J Med* 348.3 (2003), pp. 255–256. DOI: 10.1056/NEJM200301163480314. URL: <https://www.ncbi.nlm.nih.gov/pubmed/12529469>.
- [124] S Hacein-Bey-Abina et al. “LMO2-associated clonal T cell proliferation in two patients after gene therapy for SCID-X1”. In: *Science* 302.5644 (2003), pp. 415–419. DOI: 10.1126/science.1088547. URL: <https://www.ncbi.nlm.nih.gov/pubmed/14564000>.
- [125] G Hampson et al. “Gene therapy: evidence, value and affordability in the US health care system”. In: *J Comp Eff Res* 7.1 (2018), pp. 15–28. DOI: 10.2217/cer-2017-0068. URL: <https://www.ncbi.nlm.nih.gov/pubmed/29144165>.
- [126] M Han et al. “Polybrene: Observations on cochlear hair cell necrosis and minimal lentiviral transduction of cochlear hair cells”. In: *Neurosci Lett* 600 (2015), pp. 164–170. DOI: 10.1016/j.neulet.2015.06.011. URL: <https://www.ncbi.nlm.nih.gov/pubmed/26071903>.
- [127] Claudia Hagedorn Hans J Lipps. “pEPI for Gene Therapy Non viral episomes and their Application in Somatic Gene Therapy”. In: *Journal of Cell Science & Therapy* 04.02 (2013). DOI: 10.4172/2157-7013.S6-001. URL: <https://www.omicsonline.org/pepi-for-gene-therapy-non-viral-episomes-and-their-application-in-somatic-gene-therapy-2157-7013.S6-001.php?aid=2824>.
- [128] D T Harris and D M Kranz. “Adoptive T Cell Therapies: A Comparison of T Cell Receptors and Chimeric Antigen Receptors”. In: *Trends Pharmacol Sci* 37.3 (2016), pp. 220–230. DOI: 10.1016/j.tips.2015.11.004. URL: <https://www.ncbi.nlm.nih.gov/pubmed/26705086>.
- [129] R P Harrison et al. “Chimeric antigen receptor-T cell therapy manufacturing: modelling the effect of offshore production on aggregate cost of goods”. In: *Cytotherapy* 21.2 (2019), pp. 224–233. DOI: 10.1016/j.jcyt.2019.01.003. URL: <https://www.ncbi.nlm.nih.gov/pubmed/30770285>.



- [130] R P Harrison et al. “Decentralized manufacturing of cell and gene therapies: Overcoming challenges and identifying opportunities”. In: *Cytotherapy* 19.10 (2017), pp. 1140–1151. DOI: 10.1016/j.jcyt.2017.07.005. URL: <https://www.ncbi.nlm.nih.gov/pubmed/28797612>.
- [131] G C Heffner et al. “Prostaglandin E(2) Increases Lentiviral Vector Transduction Efficiency of Adult Human Hematopoietic Stem and Progenitor Cells”. In: *Mol Ther* 26.1 (2018), pp. 320–328. DOI: 10.1016/j.ymthe.2017.09.025. URL: <https://www.ncbi.nlm.nih.gov/pubmed/29102562>.
- [132] *Help Therapeutics. Allogeneic iPSC-derived Cardiomyocyte Therapy in Patients With Worsening Ischemic Heart Failure. ClinicalTrials.org identifier: NCT05566600. Updated October 4, 2022. Accessed October 16, 2022.* URL: <https://clinicaltrials.gov/ct2/show/NCT05566600>.
- [133] *Help Therapeutics. Treating Congestive HF With hiPSC-CMs Through Endocardial Injection. ClinicalTrials.gov identifier: NCT04982081. Updated September 23, 2022. Accessed October 16, 2022.* URL: <https://clinicaltrials.gov/ct2/show/NCT04982081>.
- [134] *HEMACORD® (HPC, Cord Blood) Patient Overview.* URL: <https://hemacord.info/patients/>.
- [135] A G Henssen et al. “Genomic DNA transposition induced by human PGBD5”. In: *Elife* 4 (2015). DOI: 10.7554/eLife.10565. URL: <https://www.ncbi.nlm.nih.gov/pubmed/26406119>.
- [136] D J Hicklin, F M Marincola, and S Ferrone. “HLA class I antigen downregulation in human cancers: T-cell immunotherapy revives an old story”. In: *Mol Med Today* 5.4 (1999), pp. 178–186. DOI: 10.1016/s1357-4310(99)01451-3. URL: <https://www.ncbi.nlm.nih.gov/pubmed/10203751>.
- [137] B M Hiller et al. “Optimizing maturity and dose of iPSC-derived dopamine progenitor cell therapy for Parkinson’s disease”. In: *NPJ Regen Med* 7.1 (2022), p. 24. DOI: 10.1038/s41536-022-00221-y. URL: <https://www.ncbi.nlm.nih.gov/pubmed/35449132>.
- [138] Ben Hirschler. *GSK slims portfolio with sale of rare disease gene therapy drugs*. Ed. by Keith Weir David Goodman. 2018. URL: <https://www.reuters.com/article/us-gsk-orchard-idUSKBN1HJ0V5>.
- [139] F S Hodi et al. “Improved survival with ipilimumab in patients with metastatic melanoma”. In: *N Engl J Med* 363.8 (2010), pp. 711–723. DOI: 10.1056/NEJMoa1003466. URL: <https://www.ncbi.nlm.nih.gov/pubmed/20525992>.
- [140] P D Holler, L K Chlewicki, and D M Kranz. “TCRs with high affinity for foreign pMHC show self-reactivity”. In: *Nat Immunol* 4.1 (2003), pp. 55–62. DOI: 10.1038/ni863. URL: <https://www.ncbi.nlm.nih.gov/pubmed/12469116>.
- [141] J Huang et al. “A single peptide-major histocompatibility complex ligand triggers digital cytokine secretion in CD4(+) T cells”. In: *Immunity* 39.5 (2013), pp. 846–857. DOI: 10.1016/j.immuni.2013.08.036. URL: <https://www.ncbi.nlm.nih.gov/pubmed/24120362>.



- [142] K Hubner et al. “Derivation of oocytes from mouse embryonic stem cells”. In: *Science* 300.5623 (2003), pp. 1251–1256. DOI: 10.1126/science.1083452. URL: <https://www.ncbi.nlm.nih.gov/pubmed/12730498>.
- [143] Intima Bioscience Inc. *A Study of Metastatic Gastrointestinal Cancers Treated With Tumor Infiltrating Lymphocytes in Which the Gene Encoding the Intracellular Immune Checkpoint CISH Is Inhibited Using CRISPR Genetic Engineering*. *ClinicalTrials.gov identifier: NCT04426669*. 2022. URL: <https://clinicaltrials.gov/ct2/show/NCT04426669>.
- [144] invitrogen. *CountBright™ and CountBright™ Plus Absolute Counting Beads User Guide*. 2019. URL: https://www.thermofisher.com/document-connect/document-connect.html?url=https://assets.thermofisher.com/TFS-Assets%2FMSG%2Fmanuals%2FMAN0018850_CountBrightPlus_UG.pdf.
- [145] InvivoGen. *LumiKine™ Xpress hIFN- β 2.0. Version 19E14-ED*. URL: https://www.invivogen.com/sites/default/files/invivogen/products/files/lumikine_xpress_hifnb_tds.pdf.
- [146] Z Ivics et al. “Molecular reconstruction of Sleeping Beauty, a Tc1-like transposon from fish, and its transposition in human cells”. In: *Cell* 91.4 (1997), pp. 501–510. DOI: 10.1016/S0092-8674(00)80436-5. URL: <https://www.ncbi.nlm.nih.gov/pubmed/9390559>.
- [147] Andreas C.W. Jenke et al. “Nuclear scaffold/matrix attached region modules linked to a transcription unit are sufficient for replication and maintenance of a mammalian episome”. In: *Proceedings of the National Academy of Sciences of the United States of America* 101.31 (2004), pp. 11322–11327. DOI: 10.1073/pnas.0401355101.
- [148] Bok Hee C Jenke et al. “An episomally replicating vector binds to the nuclear matrix protein SAF-A in vivo”. In: *EMBO Reports* 3.4 (2002), pp. 349–354. DOI: 10.1093/embo-reports/kvf070.
- [149] S Jenks. “Gene therapy death—everyone has to share in the guilt”. In: *J Natl Cancer Inst* 92.2 (2000), pp. 98–100. DOI: 10.1093/jnci/92.2.98. URL: <https://www.ncbi.nlm.nih.gov/pubmed/10639505>.
- [150] M Jinek et al. “A programmable dual-RNA-guided DNA endonuclease in adaptive bacterial immunity”. In: *Science* 337.6096 (2012), pp. 816–821. DOI: 10.1126/science.1225829. URL: <https://www.ncbi.nlm.nih.gov/pubmed/22745249>.
- [151] *Johns Hopkins University. Cell-Based Approaches For Modeling and Treating Ataxia-Telangiectasia*. *ClinicalTrials.gov identifier: NCT02246491*. Updated March 19, 2019. Accessed October 16, 2022. URL: <https://clinicaltrials.gov/ct2/show/NCT02246491>.
- [152] J K Joung and J D Sander. “TALENs: a widely applicable technology for targeted genome editing”. In: *Nat Rev Mol Cell Biol* 14.1 (2013), pp. 49–55. DOI: 10.1038/nrm3486. URL: <https://www.ncbi.nlm.nih.gov/pubmed/23169466>.
- [153] C H June et al. “CAR T cell immunotherapy for human cancer”. In: *Science* 359.6382 (2018), pp. 1361–1365. DOI: 10.1126/science.aar6711. URL: <https://www.ncbi.nlm.nih.gov/pubmed/29567707>.

- [154] *Juno Therapeutics, Inc., a Bristol-Myers Squibb Company. BREYANZI (lisocabtagene maraleucel). [Package Insert]. U.S. Food and Drug Administration website. Revised June 2022. Accessed December 11, 2022.* URL: <https://www.fda.gov/media/145711/download>.
- [155] W F Kaemmerer. “How will the field of gene therapy survive its success?” In: *Bioeng Transl Med* 3.2 (2018), pp. 166–177. DOI: 10.1002/btm2.10090. URL: <https://www.ncbi.nlm.nih.gov/pubmed/30065971>.
- [156] M Kalos et al. “T cells with chimeric antigen receptors have potent antitumor effects and can establish memory in patients with advanced leukemia”. In: *Sci Transl Med* 3.95 (2011), 95ra73. DOI: 10.1126/scitranslmed.3002842. URL: <https://www.ncbi.nlm.nih.gov/pubmed/21832238>.
- [157] Batool Kazmi, Christopher J Inglefield, and Mark P Lewis. “Autologous cell therapy: current treatments and future prospects”. In: *Wounds* 21.9 (2009), pp. 234–242.
- [158] P Kebriaei et al. “Gene Therapy with the Sleeping Beauty Transposon System”. In: *Trends Genet* 33.11 (2017), pp. 852–870. DOI: 10.1016/j.tig.2017.08.008. URL: <https://www.ncbi.nlm.nih.gov/pubmed/28964527>.
- [159] *Kite Pharma Inc. YESCARTA (axicabtagene ciloleucel) [Assessment Report]. European Medicines Agency website. April 2022. Accessed December 11, 2022.* URL: https://www.ema.europa.eu/en/documents/variation-report/yescarta-h-c-004480-ii-0042-epar-assessment-report-variation_en.pdf.
- [160] *Kite Pharma Inc. YESCARTA (axicabtagene ciloleucel) [Package Insert]. U.S. Food and Drug Administration website. Revised November 2022. Accessed December 11, 2022.* URL: <https://www.fda.gov/media/108377/download>.
- [161] *Kite Pharma, Inc. TECARTUS (brexucabtagene autoleucel). [Package Insert]. U.S. Food and Drug Administration website. Revised October 2021. Accessed December 11, 2022.* URL: <https://www.fda.gov/media/140409/download>.
- [162] D A Knorr et al. “Clinical-scale derivation of natural killer cells from human pluripotent stem cells for cancer therapy”. In: *Stem Cells Transl Med* 2.4 (2013), pp. 274–283. DOI: 10.5966/sctm.2012-0084. URL: <https://www.ncbi.nlm.nih.gov/pubmed/23515118>.
- [163] A Knuth et al. “T-cell-mediated cytotoxicity against autologous malignant melanoma: analysis with interleukin 2-dependent T-cell cultures”. In: *Proc Natl Acad Sci U S A* 81.11 (1984), pp. 3511–3515. DOI: 10.1073/pnas.81.11.3511. URL: <https://www.ncbi.nlm.nih.gov/pubmed/6610177>.
- [164] K A Koelsch et al. “GFP affects human T cell activation and cytokine production following in vitro stimulation”. In: *PLoS One* 8.4 (2013), e50068. DOI: 10.1371/journal.pone.0050068. URL: <https://www.ncbi.nlm.nih.gov/pubmed/23577054>.
- [165] *Koichi Toda. Clinical Trial of Human (Allogeneic) iPS Cell-derived Cardiomyocytes Sheet for Ischemic Cardiomyopathy. ClinicalTrials.gov identifier: NCT04696328. Updated April 20, 2021. Accessed October 16, 2022.* URL: <https://clinicaltrials.gov/ct2/show/NCT04696328>.



- [166] Adrian Kovač and Zoltán Ivics. “Specifically integrating vectors for targeted gene delivery: progress and prospects”. In: *Cell and Gene Therapy Insights* 3.2 (2017), pp. 103–123. DOI: 10.18609/cgti.2017.013.
- [167] J Kraunus et al. “Self-inactivating retroviral vectors with improved RNA processing”. In: *Gene Ther* 11.21 (2004), pp. 1568–1578. DOI: 10.1038/sj.gt.3302309. URL: <https://www.ncbi.nlm.nih.gov/pubmed/15372067>.
- [168] J Kurtzberg et al. “Results of the Cord Blood Transplantation Study (COBLT): clinical outcomes of unrelated donor umbilical cord blood transplantation in pediatric patients with hematologic malignancies”. In: *Blood* 112.10 (2008), pp. 4318–4327. DOI: 10.1182/blood-2007-06-098020. URL: <https://www.ncbi.nlm.nih.gov/pubmed/18723429>.
- [169] Chee Keong Kwok et al. “Scalable expansion of iPSC and their derivatives across multiple lineages”. In: *Reproductive Toxicology* 112 (Sept. 2022), pp. 23–35. DOI: 10.1016/j.reprotox.2022.05.007. URL: <https://linkinghub.elsevier.com/retrieve/pii/S0890623822000685>.
- [170] R Lansford. “Engineering Viruses for CNS studies”. In: *Encyclopedia of Neuroscience*. Ed. by Larry R Squire. Oxford: Academic Press, 2009, pp. 1059–1068. DOI: <https://doi.org/10.1016/B978-008045046-9.02006-4>. URL: <https://www.sciencedirect.com/science/article/pii/B9780080450469020064>.
- [171] L Lapteva et al. “Clinical Development of Gene Therapies: The First Three Decades and Counting”. In: *Mol Ther Methods Clin Dev* 19 (2020), pp. 387–397. DOI: 10.1016/j.omtm.2020.10.004. URL: <https://www.ncbi.nlm.nih.gov/pubmed/33209964>.
- [172] D W Lee et al. “Current concepts in the diagnosis and management of cytokine release syndrome”. In: *Blood* 124.2 (2014), pp. 188–195. DOI: 10.1182/blood-2014-05-552729. URL: <https://www.ncbi.nlm.nih.gov/pubmed/24876563>.
- [173] C Li and R J Samulski. “Engineering adeno-associated virus vectors for gene therapy”. In: *Nat Rev Genet* 21.4 (2020), pp. 255–272. DOI: 10.1038/s41576-019-0205-4. URL: <https://www.ncbi.nlm.nih.gov/pubmed/32042148>.
- [174] W Li et al. “Ligandomics: a paradigm shift in biological drug discovery”. In: *Drug Discov Today* 23.3 (2018), pp. 636–643. DOI: 10.1016/j.drudis.2018.01.013. URL: <https://www.ncbi.nlm.nih.gov/pubmed/29326083>.
- [175] J J Luke and G K Schwartz. “Chemotherapy in the management of advanced cutaneous malignant melanoma”. In: *Clin Dermatol* 31.3 (2013), pp. 290–297. DOI: 10.1016/j.clindermatol.2012.08.016. URL: <https://www.ncbi.nlm.nih.gov/pubmed/23608448>.
- [176] J J Luke et al. “Targeted agents and immunotherapies: optimizing outcomes in melanoma”. In: *Nat Rev Clin Oncol* 14.8 (2017), pp. 463–482. DOI: 10.1038/nrclinonc.2017.43. URL: <https://www.ncbi.nlm.nih.gov/pubmed/28374786>.

- [177] H Main et al. “Karolinska Institutet Human Embryonic Stem Cell Bank”. In: *Stem Cell Res* 45 (2020), p. 101810. DOI: 10.1016/j.scr.2020.101810. URL: <https://www.ncbi.nlm.nih.gov/pubmed/32339905>.
- [178] K S Makarova et al. “A putative RNA-interference-based immune system in prokaryotes: computational analysis of the predicted enzymatic machinery, functional analogies with eukaryotic RNAi, and hypothetical mechanisms of action”. In: *Biol Direct* 1 (2006), p. 7. DOI: 10.1186/1745-6150-1-7. URL: <https://www.ncbi.nlm.nih.gov/pubmed/16545108>.
- [179] K S Makarova et al. “An updated evolutionary classification of CRISPR-Cas systems”. In: *Nat Rev Microbiol* 13.11 (2015), pp. 722–736. DOI: 10.1038/nrmicro3569. URL: <https://www.ncbi.nlm.nih.gov/pubmed/26411297>.
- [180] R Maldonado, S Jalil, and K Wartiovaara. “Curative gene therapies for rare diseases”. In: *J Community Genet* 12.2 (2021), pp. 267–276. DOI: 10.1007/s12687-020-00480-6. URL: <https://www.ncbi.nlm.nih.gov/pubmed/32803721>.
- [181] M Marchand et al. “Tumor regression responses in melanoma patients treated with a peptide encoded by gene MAGE-3”. In: *Int J Cancer* 63.6 (1995), pp. 883–885. DOI: 10.1002/ijc.2910630622. URL: <https://www.ncbi.nlm.nih.gov/pubmed/8847150>.
- [182] Marie Marchand et al. “Tumor regressions observed in patients with metastatic melanoma treated with an antigenic peptide encoded by gene MAGE-3 and presented by HLA-A1”. In: *International Journal of Cancer* 80.2 (1999), pp. 219–230. DOI: 10.1002/(sici)1097-0215(19990118)80:2<219::Aid-ijc10>3.0.Co;2-s.
- [183] Maria Grant. *Human iPSC for Repair of Vasodegenerative Vessels in Diabetic Retinopathy (iPSC)*. *ClinicalTrials.org identifier: NCT03403699*. Updated May 18, 2022. Accessed October 16, 2022. URL: <https://clinicaltrials.gov/ct2/show/NCT03403699>.
- [184] José Marín-García. “Chapter 23 - Gene- and Cell-Based Therapy for Cardiovascular Disease”. In: *Post-Genomic Cardiology (Second Edition)*. Ed. by José Marín-García. Boston: Academic Press, 2014, pp. 783–833. DOI: <https://doi.org/10.1016/B978-0-12-404599-6.00023-8>. URL: <https://www.sciencedirect.com/science/article/pii/B9780124045996000238>.
- [185] Philippa Marrack and John Kappler. “The T Cell Receptor”. In: *Science* 238.4830 (Nov. 1987), pp. 1073–1079. DOI: 10.1126/science.3317824. URL: <https://www.science.org/doi/10.1126/science.3317824>.
- [186] D J Mathews et al. “Pluripotent stem cell-derived gametes: truth and (potential) consequences”. In: *Cell Stem Cell* 5.1 (2009), pp. 11–14. DOI: 10.1016/j.stem.2009.06.005. URL: <https://www.ncbi.nlm.nih.gov/pubmed/19570509>.
- [187] K R Matthews and D Morali. “National human embryo and embryoid research policies: a survey of 22 top research-intensive countries”. In: *Regen Med* 15.7 (2020), pp. 1905–1917. DOI: 10.2217/rme-2019-0138. URL: <https://www.ncbi.nlm.nih.gov/pubmed/32799737>.



- [188] K R W Matthews and D Morali. “Can we do that here? An analysis of US federal and state policies guiding human embryo and embryoid research”. In: *J Law Biosci* 9.1 (2022), lsac014. DOI: 10.1093/jlb/lsac014. URL: <https://www.ncbi.nlm.nih.gov/pubmed/35692936>.
- [189] S Maurya, P Sarangi, and G R Jayandharan. “Safety of Adeno-associated virus-based vector-mediated gene therapy-impact of vector dose”. In: *Cancer Gene Ther* 29.10 (2022), pp. 1305–1306. DOI: 10.1038/s41417-021-00413-6. URL: <https://www.ncbi.nlm.nih.gov/pubmed/35027711>.
- [190] Edward F McCarthy. “The toxins of William B. Coley and the treatment of bone and soft-tissue sarcomas”. In: *Iowa Orthop J* 26 (2006), pp. 154–158.
- [191] D M McCarty. “Self-complementary AAV vectors; advances and applications”. In: *Mol Ther* 16.10 (2008), pp. 1648–1656. DOI: 10.1038/mt.2008.171. URL: <https://www.ncbi.nlm.nih.gov/pubmed/18682697>.
- [192] D M McCarty, P E Monahan, and R J Samulski. “Self-complementary recombinant adeno-associated virus (scAAV) vectors promote efficient transduction independently of DNA synthesis”. In: *Gene Ther* 8.16 (2001), pp. 1248–1254. DOI: 10.1038/sj.gt.3301514. URL: <https://www.ncbi.nlm.nih.gov/pubmed/11509958>.
- [193] B McClintock. “The origin and behavior of mutable loci in maize”. In: *Proc Natl Acad Sci U S A* 36.6 (1950), pp. 344–355. DOI: 10.1073/pnas.36.6.344. URL: <https://www.ncbi.nlm.nih.gov/pubmed/15430309>.
- [194] K E McGrath, J M Frame, and J Palis. “Early hematopoiesis and macrophage development”. In: *Semin Immunol* 27.6 (2015), pp. 379–387. DOI: 10.1016/j.smim.2016.03.013. URL: <https://www.ncbi.nlm.nih.gov/pubmed/27021646>.
- [195] K E McGrath et al. “Distinct Sources of Hematopoietic Progenitors Emerge before HSCs and Provide Functional Blood Cells in the Mammalian Embryo”. In: *Cell Rep* 11.12 (2015), pp. 1892–1904. DOI: 10.1016/j.celrep.2015.05.036. URL: <https://www.ncbi.nlm.nih.gov/pubmed/26095363>.
- [196] Merck & Co., Inc. *MUSTARGEN® Mechlorethamine HCl for injection*. [package insert]. U.S. Food & Drug Administration website. Assessed December 13, 2022. URL: https://www.accessdata.fda.gov/drugsatfda_docs/label/2004/06695s1r031_mustargen_lbl.pdf.
- [197] Merck & Co., Inc. *VALCHLOR (mechlorethamine)*. [Package Insert]. U.S. Food and Drug Administration website. Revised August 2013. Accessed December 13, 2022. URL: https://www.accessdata.fda.gov/drugsatfda_docs/label/2013/2023171bl.pdf.
- [198] Merck Sharp & Dohme Corp. *Keytruda (pembrolizumab)* [package insert]. U.S. Food and Drug Administration website. Revised August 2016. Accessed October 9, 2022. URL: https://www.accessdata.fda.gov/drugsatfda_docs/label/2016/125514s0091bl.pdf.
- [199] J A Metcalf et al. “A self-inactivating gamma-retroviral vector reduces manifestations of mucopolysaccharidosis I in mice”. In: *Mol Ther* 18.2 (2010), pp. 334–342. DOI: 10.1038/mt.2009.236. URL: <https://www.ncbi.nlm.nih.gov/pubmed/19844196>.



- [200] D G Miller, L M Petek, and D W Russell. “Adeno-associated virus vectors integrate at chromosome breakage sites”. In: *Nat Genet* 36.7 (2004), pp. 767–773. DOI: 10.1038/ng1380. URL: <https://www.ncbi.nlm.nih.gov/pubmed/15208627>.
- [201] J Miller, A D McLachlan, and A Klug. “Repetitive zinc-binding domains in the protein transcription factor IIIA from *Xenopus* oocytes”. In: *EMBO J* 4.6 (1985), pp. 1609–1614. DOI: 10.1002/j.1460-2075.1985.tb03825.x. URL: <https://www.ncbi.nlm.nih.gov/pubmed/4040853>.
- [202] R A Miller et al. “Treatment of B-cell lymphoma with monoclonal anti-idiotypic antibody”. In: *N Engl J Med* 306.9 (1982), pp. 517–522. DOI: 10.1056/NEJM198203043060906. URL: <https://www.ncbi.nlm.nih.gov/pubmed/6173751>.
- [203] Miltenyi Biotec. *Dead Cell Removal Kit*. 2020. URL: <https://www.miltenyibiotec.com/upload/assets/IM0001218.PDF>.
- [204] Miltenyi Biotec. *Direct Lineage Cell Depletion Kit mouse Protocol*. 2020. URL: <https://www.miltenyibiotec.com/upload/assets/IM0016259.PDF>.
- [205] L M Minasian et al. “Hemorrhagic tumor necrosis during a pilot trial of tumor necrosis factor-alpha and anti-GD3 ganglioside monoclonal antibody in patients with metastatic melanoma”. In: *Blood* 83.1 (1994), pp. 56–64. DOI: 10.1182/blood.V83.1.56.56.
- [206] Mingtao Zhao. *iPSC Repository of Pediatric Cardiovascular Disease*. *ClinicalTrials.org* identifier: NCT05550324. Updated September 22, 2022. Accessed October 16, 2022. URL: <https://clinicaltrials.gov/ct2/show/NCT05550324>.
- [207] Jovan Mirkovitch, Marc Edouard Mirault, and Ulrich K. Laemmli. “Organization of the higher-order chromatin loop: specific DNA attachment sites on nuclear scaffold”. In: *Cell* 39.1 (1984), pp. 223–232. DOI: 10.1016/0092-8674(84)90208-3.
- [208] Alvaro Morales. “Treatment of carcinoma in situ of the bladder with BCG”. In: *Cancer Immunology Immunotherapy* 9.1-2 (1980). DOI: 10.1007/bf00199531.
- [209] R A Morgan et al. “Cancer regression in patients after transfer of genetically engineered lymphocytes”. In: *Science* 314.5796 (2006), pp. 126–129. DOI: 10.1126/science.1129003. URL: <https://www.ncbi.nlm.nih.gov/pubmed/16946036>.
- [210] C Morrison. “\$1-million price tag set for Glybera gene therapy”. In: *Nat Biotechnol* 33.3 (2015), pp. 217–218. DOI: 10.1038/nbt0315-217. URL: <https://www.ncbi.nlm.nih.gov/pubmed/25748892>.
- [211] D L Morton et al. “Immunological factors in human sarcomas and melanomas: a rational basis for immunotherapy”. In: *Ann Surg* 172.4 (1970), pp. 740–749. DOI: 10.1097/0000658-197010000-00018. URL: <https://www.ncbi.nlm.nih.gov/pubmed/5272336>.
- [212] Mona Motwani, Scott Pesiridis, and Katherine A. Fitzgerald. “DNA sensing by the cGAS–STING pathway in health and disease”. In: *Nature Reviews Genetics* 20.11 (Nov. 2019), pp. 657–674. DOI: 10.1038/s41576-019-0151-1. URL: <https://www.nature.com/articles/s41576-019-0151-1>.
- [213] Michael Muehlebach et al. “Gamma Retroviral and Lentiviral Vectors for Gene Delivery”. In: *Retroviruses Molecular Biology, Genomics and Pathogenesis*. Ed. by



- Reinhard Kurth and Norbert Bannert. Norfolk, UK: Caister Academic Press, 2010. Chap. 13, pp. 347–370.
- [214] M Nafria et al. “Protocol for the Generation of Definitive Hematopoietic Progenitors from Human Pluripotent Stem Cells”. In: *STAR Protoc* 1.3 (2020), p. 100130. DOI: 10.1016/j.xpro.2020.100130. URL: <https://www.ncbi.nlm.nih.gov/pubmed/33377024>.
- [215] M Nakagawa et al. “Generation of induced pluripotent stem cells without Myc from mouse and human fibroblasts”. In: *Nat Biotechnol* 26.1 (2008), pp. 101–106. DOI: 10.1038/nbt1374. URL: <https://www.ncbi.nlm.nih.gov/pubmed/18059259>.
- [216] H Nakai et al. “Extrachromosomal recombinant adeno-associated virus vector genomes are primarily responsible for stable liver transduction in vivo”. In: *J Virol* 75.15 (2001), pp. 6969–6976. DOI: 10.1128/JVI.75.15.6969-6976.2001. URL: <https://www.ncbi.nlm.nih.gov/pubmed/11435577>.
- [217] N Nakatsuji, F Nakajima, and K Tokunaga. “HLA-haplotype banking and iPS cells”. In: *Nat Biotechnol* 26.7 (2008), pp. 739–740. DOI: 10.1038/nbt0708-739. URL: <https://www.ncbi.nlm.nih.gov/pubmed/18612291>.
- [218] Sarah Nam, Jeff Smith, and Guang Yang. *Driving the next wave of innovation in CAR T-cell therapies*. 2019. URL: <https://www.mckinsey.com/industries/life-sciences/our-insights/driving-the-next-wave-of-innovation-in-car-t-cell-therapies>.
- [219] T S Nambiar et al. “Stimulation of CRISPR-mediated homology-directed repair by an engineered RAD18 variant”. In: *Nat Commun* 10.1 (2019), p. 3395. DOI: 10.1038/s41467-019-11105-z. URL: <https://www.ncbi.nlm.nih.gov/pubmed/31363085>.
- [220] National Cancer Institute. *Dictionary of Cancer Terms*. URL: <https://www.cancer.gov/publications/dictionaries/cancer-terms/def/tumor-infiltrating-lymphocyte>.
- [221] National Eye Institute NEI. *Autologous Transplantation of Induced Pluripotent Stem Cell-Derived Retinal Pigment Epithelium for Geographic Atrophy Associated With Age-Related Macular Degeneration*. *ClinicalTrials.org* identifier: NCT04339764. Updated August 16, 2022. Accessed Oct 16, 2022. URL: <https://clinicaltrials.gov/ct2/show/NCT04339764>.
- [222] National Institute of Neurological Disorders and Stroke (NINDS). *Gene Therapy for Gaucher’s and Fabry Disease Using Viruses and Blood-Forming Cells*. *ClinicalTrials.org* identifier: NCT00001234. Updated March 4, 2008. Accessed October 23, 2022. URL: <https://clinicaltrials.gov/ct2/show/NCT00001234>.
- [223] National Institutes of Health Clinical Center (CC). *Blood Collection From Healthy Volunteers and Patients for the Production of Clinical Grade Induced Pluripotent Stem Cell (iPSC) Products*. *ClinicalTrials.gov* identifier: NCT02056613. Updated Nov 5, 2022. URL: <https://clinicaltrials.gov/ct2/show/NCT02056613>.
- [224] National Institutes of Health Clinical Center CC. *Cyclophosphamide and Fludarabine Followed by Vaccine Therapy, Gene-Modified White Blood Cell Infusions, and Aldesleukin in Treating Patients With Metastatic Melanoma*. *ClinicalTrials.gov*



- identifier: NCT00091104. Updated March 15, 2012. URL:
<https://clinicaltrials.gov/ct2/show/NCT00091104>.
- [225] National Institutes of Health Clinical Center CC. *Gene-Modified White Blood Cells Followed By Interleukin-2 and Vaccine Therapy in Treating Patients With Metastatic Melanoma*. *ClinicalTrials.gov* identifier: NCT00085462. Updated June 22, 2012. Accessed December 5, 2022. URL:
<https://clinicaltrials.gov/ct2/show/NCT00085462>.
- [226] S Nayak and R W Herzog. “Progress and prospects: immune responses to viral vectors”. In: *Gene Ther* 17.3 (2010), pp. 295–304. DOI: 10.1038/gt.2009.148. URL:
<https://www.ncbi.nlm.nih.gov/pubmed/19907498>.
- [227] *New York Blood Center, Inc. HEMACORD (HPC, Cord Blood)*. [Package Insert]. U.S. Food and Drug Administration website. Revised April 2013. Accessed December 12, 2022. URL: <https://www.fda.gov/media/82016/download>.
- [228] G N Nguyen et al. “A long-term study of AAV gene therapy in dogs with hemophilia A identifies clonal expansions of transduced liver cells”. In: *Nat Biotechnol* 39.1 (2021), pp. 47–55. DOI: 10.1038/s41587-020-0741-7. URL:
<https://www.ncbi.nlm.nih.gov/pubmed/33199875>.
- [229] Natalie F. Nidetz et al. “Adeno-associated viral vector-mediated immune responses: Understanding barriers to gene delivery”. In: *Pharmacology & Therapeutics* 207 (Mar. 2020), p. 107453. DOI: 10.1016/j.pharmthera.2019.107453. URL:
<https://linkinghub.elsevier.com/retrieve/pii/S0163725819302050>.
- [230] H Nishimura et al. “Autoimmune dilated cardiomyopathy in PD-1 receptor-deficient mice”. In: *Science* 291.5502 (2001), pp. 319–322. DOI:
10.1126/science.291.5502.319. URL:
<https://www.ncbi.nlm.nih.gov/pubmed/11209085>.
- [231] Hiroyuki Nishimura et al. “Development of Lupus-like Autoimmune Diseases by Disruption of the PD-1 Gene Encoding an ITIM Motif-Carrying Immunoreceptor”. In: *Immunity* 11.2 (1999), pp. 141–151. DOI: 10.1016/s1074-7613(00)80089-8.
- [232] *Novartis Pharmaceuticals Corporation. KYMRIAH (tisagenlecleucel)* [Assessment Report]. European Medicines Agency website. Revised September 2022. Accessed December 11, 2022. URL: https://www.ema.europa.eu/en/documents/variation-report/kymriah-h-c-4090-ii-56-epar-assessment-report-variation_en.pdf.
- [233] *Novartis Pharmaceuticals Corporation. KYMRIAH (tisagenlecleucel)* [Package Insert]. U.S. Food and Drug Administration website. Revised May 2022. Accessed December 11, 2022. URL: <https://www.fda.gov/media/107296/download>.
- [234] Naoki Okumura et al. “Enhancement on Primate Corneal Endothelial Cell Survival In Vitro by a ROCK Inhibitor”. In: *Investigative Ophthalmology & Visual Science* 50.8 (Aug. 2009), p. 3680. DOI: 10.1167/iovs.08-2634. URL:
<http://iovs.arvojournals.org/article.aspx?doi=10.1167/iovs.08-2634>.
- [235] G Opelz and B Dohler. “Pediatric kidney transplantation: analysis of donor age, HLA match, and posttransplant non-Hodgkin lymphoma: a collaborative transplant study report”. In: *Transplantation* 90.3 (2010), pp. 292–297. DOI:

- 10.1097/TP.0b013e3181e46a22. URL:
<https://www.ncbi.nlm.nih.gov/pubmed/20548266>.
- [236] Orchard Therapeutics. *Gene Therapy for Metachromatic Leukodystrophy (MLD)*. *ClinicalTrials.gov* identifier: NCT01560182. Updated November 9, 2022. Accessed 13 December 2022. URL: <https://clinicaltrials.gov/ct2/show/NCT01560182>.
- [237] Orchard Therapeutics. *Orchard Statement on Strimvelis®, a Gammaretroviral Vector-Based Gene Therapy for ADA-SCID*. 2020. URL:
<https://ir.orchard-tx.com/news-releases/news-release-details/orchard-statement-strimvelisr-gammaretroviral-vector-based-gene>.
- [238] Orchard Therapeutics. *Strimvelis [assessment report]*. European Medicines Agency website. Revised April 2016. Assessed October 23, 2022. URL:
https://www.ema.europa.eu/en/documents/assessment-report/strimvelis-epar-public-assessment-report_en.pdf.
- [239] Organon Teknika Corp., LLC. *TICE BCG (BCG Live) [Summary for Basis of Approval]*. U.S Food and Drug Administration website. August 1998. Accessed Oct 9, 2022. URL: <http://wayback.archive-it.org/7993/20170723144330/https://www.fda.gov/downloads/BiologicsBloodVaccines/Vaccines/ApprovedProducts/UCM101490.pdf>.
- [240] J Palis et al. “Development of erythroid and myeloid progenitors in the yolk sac and embryo proper of the mouse”. In: *Development* 126.22 (1999), pp. 5073–5084. DOI: 10.1242/dev.126.22.5073. URL:
<https://www.ncbi.nlm.nih.gov/pubmed/10529424>.
- [241] E Papanikolaou and A Bosio. “The Promise and the Hope of Gene Therapy”. In: *Front Genome Ed* 3 (2021), p. 618346. DOI: 10.3389/fgeed.2021.618346. URL:
<https://www.ncbi.nlm.nih.gov/pubmed/34713249>.
- [242] E Papanikolaou et al. “Cell cycle status of CD34(+) hemopoietic stem cells determines lentiviral integration in actively transcribed and development-related genes”. In: *Mol Ther* 23.4 (2015), pp. 683–696. DOI: 10.1038/mt.2014.246. URL:
<https://www.ncbi.nlm.nih.gov/pubmed/25523760>.
- [243] E P Papapetrou et al. “Genomic safe harbors permit high beta-globin transgene expression in thalassemia induced pluripotent stem cells”. In: *Nat Biotechnol* 29.1 (2011), pp. 73–78. DOI: 10.1038/nbt.1717. URL:
<https://www.ncbi.nlm.nih.gov/pubmed/21151124>.
- [244] M Papworth, P Kolasinska, and M Minczuk. “Designer zinc-finger proteins and their applications”. In: *Gene* 366.1 (2006), pp. 27–38. DOI: 10.1016/j.gene.2005.09.011. URL: <https://www.ncbi.nlm.nih.gov/pubmed/16298089>.
- [245] T S Park et al. “Derivation of primordial germ cells from human embryonic and induced pluripotent stem cells is significantly improved by coculture with human fetal gonadal cells”. In: *Stem Cells* 27.4 (2009), pp. 783–795. DOI: 10.1002/stem.13. URL:
<https://www.ncbi.nlm.nih.gov/pubmed/19350678>.
- [246] Deepa H Patel and Ambikanandan Misra. “5 - Gene Delivery Using Viral Vectors”. In: *Challenges in Delivery of Therapeutic Genomics and Proteomics*. Ed. by Ambikanandan Misra. London: Elsevier, 2011, pp. 207–270. DOI:

- <https://doi.org/10.1016/B978-0-12-384964-9.00005-0>. URL:
<https://www.sciencedirect.com/science/article/pii/B9780123849649000050>.
- [247] Paul-Ehrlich-Institut. *Gene Therapy Medicinal Products*. 2022. URL:
<https://www.pei.de/EN/medicinal-products/atmp/gene-therapy-medicinal-products/gene-therapy-node.html>.
- [248] M Pavel-Dinu et al. “Gene correction for SCID-X1 in long-term hematopoietic stem cells”. In: *Nat Commun* 10.1 (2019), p. 1634. DOI: 10.1038/s41467-019-09614-y. URL: <https://www.ncbi.nlm.nih.gov/pubmed/30967552>.
- [249] E E Perez et al. “Establishment of HIV-1 resistance in CD4+ T cells by genome editing using zinc-finger nucleases”. In: *Nat Biotechnol* 26.7 (2008), pp. 808–816. DOI: 10.1038/nbt1410. URL: <https://www.ncbi.nlm.nih.gov/pubmed/18587387>.
- [250] Justine Perrin et al. “Cell Tracking in Cancer Immunotherapy”. In: *Frontiers in Medicine* 7 (Feb. 2020). DOI: 10.3389/fmed.2020.00034. URL: <https://www.frontiersin.org/article/10.3389/fmed.2020.00034/full>.
- [251] Julia Peterson et al. “A Protocol for Expanding Mouse HSPCs to High Cell Yields for Pre-Clinical Screenings of Gene Therapy Vector Constructs”. In: *Molecular Therapy* 30.4S1 (2022), p. 182. URL: [https://www.cell.com/molecular-therapy-family/molecular-therapy/pdf/S1525-0016\(22\)00246-5.pdf?_returnURL=https%3A%2F%2Flinkinghub.elsevier.com%2Fretrieve%2Fpii%2FS1525001622002465%3Fshowall%3Dtrue](https://www.cell.com/molecular-therapy-family/molecular-therapy/pdf/S1525-0016(22)00246-5.pdf?_returnURL=https%3A%2F%2Flinkinghub.elsevier.com%2Fretrieve%2Fpii%2FS1525001622002465%3Fshowall%3Dtrue).
- [252] Julia Denise Peterson et al. “Utilizing Urinary-Derived iPSCs to Generate SMAR DNA Vector Modified CD34+ Cells”. In: *Molecular Therapy* 30.4S1 (2022), p. 349.
- [253] A Pickar-Oliver and C A Gersbach. “The next generation of CRISPR-Cas technologies and applications”. In: *Nat Rev Mol Cell Biol* 20.8 (2019), pp. 490–507. DOI: 10.1038/s41580-019-0131-5. URL: <https://www.ncbi.nlm.nih.gov/pubmed/31147612>.
- [254] F Piras et al. “Lentiviral vectors escape innate sensing but trigger p53 in human hematopoietic stem and progenitor cells”. In: *EMBO Mol Med* 9.9 (2017), pp. 1198–1211. DOI: 10.15252/emmm.201707922. URL: <https://www.ncbi.nlm.nih.gov/pubmed/28667090>.
- [255] D L Porter et al. “Chimeric antigen receptor-modified T cells in chronic lymphoid leukemia”. In: *N Engl J Med* 365.8 (2011), pp. 725–733. DOI: 10.1056/NEJMoa1103849. URL: <https://www.ncbi.nlm.nih.gov/pubmed/21830940>.
- [256] R T Prehn and J M Main. “Immunity to methylcholanthrene-induced sarcomas.” In: *J Natl Cancer Inst* (1957), pp. 769–778.
- [257] *Primer3Plus pick primers from a DNA sequence*. URL: <https://www.primer3plus.com/>.
- [258] M A Purbhoo et al. “T cell killing does not require the formation of a stable mature immunological synapse”. In: *Nat Immunol* 5.5 (2004), pp. 524–530. DOI: 10.1038/ni1058. URL: <https://www.ncbi.nlm.nih.gov/pubmed/15048111>.
- [259] M C Puri and A Nagy. “Concise review: Embryonic stem cells versus induced pluripotent stem cells: the game is on”. In: *Stem Cells* 30.1 (2012), pp. 10–14. DOI: 10.1002/stem.788. URL: <https://www.ncbi.nlm.nih.gov/pubmed/22102565>.



- [260] Wm Allen Pusey. “Lupus Healed with Roentgen Rays”. In: *Journal of the American Medical Association* XXXV.23 (1900). DOI: 10.1001/jama.1900.246204900340011.
- [261] QIAGEN. (EN) - *QIAprep Spin Miniprep Kit (2015) - Contains QIAprep 2.0 Spin Column*. 2015. URL:
<https://www.qiagen.com/us/resources/resourcedetail?id=56b0162c-23b0-473c-9229-12e8b5c8d590&lang=en>.
- [262] QIAGEN. *Quick-Start Protocol DNeasy Blood & Tissue Kit*. 2016. URL:
<https://www.qiagen.com/us/resources/resourcedetail?id=63e22fd7-6eed-4bcb-8097-7ec77bcd4de6&lang=en>.
- [263] R Rai et al. “Targeted gene correction of human hematopoietic stem cells for the treatment of Wiskott - Aldrich Syndrome”. In: *Nat Commun* 11.1 (2020), p. 4034. DOI: 10.1038/s41467-020-17626-2. URL:
<https://www.ncbi.nlm.nih.gov/pubmed/32788576>.
- [264] H A Rees and D R Liu. “Base editing: precision chemistry on the genome and transcriptome of living cells”. In: *Nat Rev Genet* 19.12 (2018), pp. 770–788. DOI: 10.1038/s41576-018-0059-1. URL:
<https://www.ncbi.nlm.nih.gov/pubmed/30323312>.
- [265] P F Robbins et al. “Cutting edge: persistence of transferred lymphocyte clonotypes correlates with cancer regression in patients receiving cell transfer therapy”. In: *J Immunol* 173.12 (2004), pp. 7125–7130. DOI: 10.4049/jimmunol.173.12.7125. URL:
<https://www.ncbi.nlm.nih.gov/pubmed/15585832>.
- [266] A Roig-Merino. “Genetic Modification of Stem Cells Utilizing S/MAR DNA Vectors”. PhD thesis. 2018.
- [267] A Roig-Merino et al. “An episomal DNA vector platform for the persistent genetic modification of pluripotent stem cells and their differentiated progeny”. In: *Stem Cell Reports* 17.1 (2022), pp. 143–158. DOI: 10.1016/j.stemcr.2021.11.011. URL:
<https://www.ncbi.nlm.nih.gov/pubmed/34942088>.
- [268] S A Rosenberg et al. “Gene transfer into humans—immunotherapy of patients with advanced melanoma, using tumor-infiltrating lymphocytes modified by retroviral gene transduction”. In: *N Engl J Med* 323.9 (1990), pp. 570–578. DOI: 10.1056/NEJM199008303230904. URL:
<https://www.ncbi.nlm.nih.gov/pubmed/2381442>.
- [269] S A Rosenberg et al. “The development of gene therapy for the treatment of cancer”. In: *Ann Surg* 218.4 (1993), pp. 454–455. DOI: 10.1097/00000658-199310000-00006. URL: <https://www.ncbi.nlm.nih.gov/pubmed/8215637>.
- [270] S A Rosenberg et al. “Use of tumor-infiltrating lymphocytes and interleukin-2 in the immunotherapy of patients with metastatic melanoma. A preliminary report”. In: *N Engl J Med* 319.25 (1988), pp. 1676–1680. DOI: 10.1056/NEJM198812223192527. URL:
<https://www.ncbi.nlm.nih.gov/pubmed/3264384>.
- [271] Steven Rosenberg. *National Cancer Institute (NCI). Immunotherapy Using Tumor Infiltrating Lymphocytes for Patients With Metastatic Human Papillomavirus-Associated Cancers. ClinicalTrials.gov identifier: NCT01585428*.



- Updated March 7, 2018. Accessed December 4, 2022. URL:
<https://clinicaltrials.gov/ct2/show/NCT01585428>.
- [272] Steven Rosenberg. *National Institutes of Health Clinical Center (CC). Immunotherapy Using 41BB Selected Tumor Infiltrating Lymphocytes for Patients With Metastatic Melanoma*. *ClinicalTrials.gov identifier: NCT02111863*. Updated September 19, 2017. Accessed December 4, 2022. URL:
<https://clinicaltrials.gov/ct2/show/NCT02111863>.
- [273] Steven Rosenberg. *National Institutes of Health Clinical Center (CC). Immunotherapy Using Tumor Infiltrating Lymphocytes for Patients With Metastatic Ocular Melanoma*. *ClinicalTrials.gov identifier: NCT01814046*. Updated October 11, 2018. Accessed December 4, 2022. URL: <https://clinicaltrials.gov/ct2/show/NCT01814046>.
- [274] Steven Rosenberg. *National Institutes of Health Clinical Center (CC). Lymphocyte Re-infusion During Immune Suppression to Treat Metastatic Melanoma*. *ClinicalTrials.gov identifier: NCT00001832*. Updated December 21, 2012. Accessed December 4, 2022. URL: <https://clinicaltrials.gov/ct2/show/NCT00001832>.
- [275] Paula Salmikangas, Niamh Kinsella, and Paul Chamberlain. “Chimeric Antigen Receptor T-Cells (CAR T-Cells) for Cancer Immunotherapy – Moving Target for Industry?” In: *Pharmaceutical Research* 35.8 (Aug. 2018), p. 152. DOI: 10.1007/s11095-018-2436-z. URL:
<http://link.springer.com/10.1007/s11095-018-2436-z>.
- [276] Sangamo Therapeutics. *Study of Autologous T-cells Genetically Modified at the CCR5 Gene by Zinc Finger Nucleases in HIV-Infected Subjects*. *ClinicalTrials.gov identifier: NCT01252641*. Updated September 20, 2019. Accessed December 15, 2022. URL:
<https://clinicaltrials.gov/ct2/show/NCT01252641>.
- [277] Daniel Schaarschmidt et al. “An episomal mammalian replicon: Sequence-independent binding of the origin recognition complex”. In: *EMBO Journal* 23.1 (2004), pp. 191–201. DOI: 10.1038/sj.emboj.7600029.
- [278] G Schirotti et al. “Preclinical modeling highlights the therapeutic potential of hematopoietic stem cell gene editing for correction of SCID-X1”. In: *Sci Transl Med* 9.411 (2017). DOI: 10.1126/scitranslmed.aan0820. URL:
<https://www.ncbi.nlm.nih.gov/pubmed/29021165>.
- [279] T N Schumacher. “T-cell-receptor gene therapy”. In: *Nat Rev Immunol* 2.7 (2002), pp. 512–519. DOI: 10.1038/nri841. URL:
<https://www.ncbi.nlm.nih.gov/pubmed/12094225>.
- [280] *Scripps Translational Science Institute. Evaluating Cardiovascular Phenotypes Using Induced Pluripotent Stem Cells (iPSC)*. *ClinicalTrials.org identifier: NCT01517425*. Updated March 17, 2021. Accessed October 16, 2022. URL:
<https://clinicaltrials.gov/ct2/show/NCT01517425>.
- [281] V Shankaran et al. “IFN γ and lymphocytes prevent primary tumour development and shape tumour immunogenicity”. In: *Nature* 410.6832 (2001), pp. 1107–1111. DOI: 10.1038/35074122. URL:
<https://www.ncbi.nlm.nih.gov/pubmed/11323675>.



- [282] K L Shaw et al. “Clinical efficacy of gene-modified stem cells in adenosine deaminase-deficient immunodeficiency”. In: *J Clin Invest* 127.5 (2017), pp. 1689–1699. DOI: 10.1172/JCI90367. URL: <https://www.ncbi.nlm.nih.gov/pubmed/28346229>.
- [283] P L Sheridan et al. “Generation of retroviral packaging and producer cell lines for large-scale vector production and clinical application: improved safety and high titer”. In: *Mol Ther* 2.3 (2000), pp. 262–275. DOI: 10.1006/mthe.2000.0123. URL: <https://www.ncbi.nlm.nih.gov/pubmed/10985957>.
- [284] Juhyun Shin and Jae-Wook Oh. “Development of CRISPR/Cas9 system for targeted DNA modifications and recent improvements in modification efficiency and specificity”. In: *BMB Reports* 53.7 (2020), pp. 341–348. DOI: 10.5483/BMBRep.2020.53.7.070.
- [285] Chang Shu, Xin Li, and Pingwei Li. “The mechanism of double-stranded DNA sensing through the cGAS-STING pathway”. In: *Cytokine & Growth Factor Reviews* 25.6 (Dec. 2014), pp. 641–648. DOI: 10.1016/j.cytogfr.2014.06.006. URL: <https://linkinghub.elsevier.com/retrieve/pii/S1359610114000604>.
- [286] SIGMA-ALDRICH. *Product Information GenElute™ Gel Extraction Kit*. URL: <https://www.sigmaaldrich.com/deepweb/assets/sigmaaldrich/product/documents/144/866/na1111bul.pdf>.
- [287] D Simmons and B Seed. “Isolation of a cDNA encoding CD33, a differentiation antigen of myeloid progenitor cells”. In: *The Journal of Immunology* 141.8 (1988), pp. 2797–2800. DOI: 10.4049/jimmunol.141.8.2797. URL: <https://doi.org/10.4049/jimmunol.141.8.2797>.
- [288] P L Sinn, S L Sauter, and P B McCray Jr. “Gene therapy progress and prospects: development of improved lentiviral and retroviral vectors—design, biosafety, and production”. In: *Gene Ther* 12.14 (2005), pp. 1089–1098. DOI: 10.1038/sj.gt.3302570. URL: <https://www.ncbi.nlm.nih.gov/pubmed/16003340>.
- [289] M J Smyth et al. “Differential tumor surveillance by natural killer (NK) and NKT cells”. In: *The Journal of experimental medicine* 191.4 (2000), pp. 661–668. DOI: 10.1084/jem.191.4.661. URL: <https://www.ncbi.nlm.nih.gov/pubmed/10684858>.
- [290] M J Smyth et al. “Perforin-mediated cytotoxicity is critical for surveillance of spontaneous lymphoma”. In: *The Journal of experimental medicine* 192.5 (2000), pp. 755–760. DOI: 10.1084/jem.192.5.755. URL: <https://www.ncbi.nlm.nih.gov/pubmed/10974040>.
- [291] F Soares-da-Silva et al. “Yolk sac, but not hematopoietic stem cell-derived progenitors, sustain erythropoiesis throughout murine embryonic life”. In: *The Journal of experimental medicine* 218.4 (2021). DOI: 10.1084/jem.20201729. URL: <https://www.ncbi.nlm.nih.gov/pubmed/33566111>.
- [292] Francisca Soares-da-Silva et al. “Crosstalk Between the Hepatic and Hematopoietic Systems During Embryonic Development”. In: *Frontiers in Cell and Developmental Biology* 8 (July 2020). DOI: 10.3389/fcell.2020.00612. URL: <https://www.frontiersin.org/article/10.3389/fcell.2020.00612/full>.
- [293] Paul J Spiess, James C Yang, and Steven A Rosenberg. “In Vivo Antitumor Activity of Tumor-Infiltrating Lymphocytes Expanded in Recombinant Interleukin-2”. In: *JNCI: Journal of the National Cancer Institute* (1987). DOI: 10.1093/jnci/79.5.1067.



- [294] S Stein et al. “Genomic instability and myelodysplasia with monosomy 7 consequent to EVI1 activation after gene therapy for chronic granulomatous disease”. In: *Nat Med* 16.2 (2010), pp. 198–204. DOI: 10.1038/nm.2088. URL: <https://www.ncbi.nlm.nih.gov/pubmed/20098431>.
- [295] StemCell. *Human Colony-Forming Unit (CFU) Assays Using MethoCult*. URL: https://cdn.stemcell.com/media/files/manual/MA28404-Human_Colony_Forming_Unit_Assays_Using_MethoCult.pdf.
- [296] StemCell. “Maintenance of Human Pluripotent Stem Cells in TeSR2”. In: (). URL: https://cdn.stemcell.com/media/files/manual/10000005573-Maintenance_Human_Pluripotent_Stem_Cells_TeSR2.pdf.
- [297] *STEMCELL Technologies TM. Hematopoietic Stem and Progenitor Cells (HSPCs): Isolation, Culture, and Assays. Version 6.0.0. Document # 29068*. 2015. URL: <https://www.stemcell.com/hematopoietic-stem-and-progenitor-cells-lp.html>.
- [298] *STEMCELL Technologies. STEMdiff™ Hematopoietic Kit*. 2020. URL: https://cdn.stemcell.com/media/files/pis/10000003456-PIS_01.pdf?_ga=2.16123518.914795903.1667472699-1177694203.1666965632.
- [299] *STEMCELL Technologies. STEMdiff™ T Cell Kit*. URL: <https://www.stemcell.com/products/stemdiff-t-cell-kit.html>.
- [300] *STEMCELL Technologies. Technical Manual for the Generation of T Cells Using STEMdiff™ or StemSpan™ T Cell Kits. 10000007541*. 2021. URL: https://cdn.stemcell.com/media/files/manual/10000007541-Generation_of_T_Cells_Using_STEMdiff_or_StemSpan_T_Cell_Kit.pdf?_ga=2.164090682.44900934.1667579160-1177694203.1666965632.
- [301] Stemgent. *Protocol, Detection of AP using the Alkaline Phosphatase Staining Kit II*. URL: <https://resources.reprocell.com/hubfs/website/resources/protocols-stemgent/P000055.pdf?hsLang=en>.
- [302] O Stutman. “Tumor development after 3-methylcholanthrene in immunologically deficient athymic-nude mice”. In: *Science* 183.4124 (1974), pp. 534–536. DOI: 10.1126/science.183.4124.534. URL: <https://www.ncbi.nlm.nih.gov/pubmed/4588620>.
- [303] C Summerford, J S Johnson, and R J Samulski. “AAVR: A Multi-Serotype Receptor for AAV”. In: *Mol Ther* 24.4 (2016), pp. 663–666. DOI: 10.1038/mt.2016.49. URL: <https://www.ncbi.nlm.nih.gov/pubmed/27081719>.
- [304] Y Sykulev et al. “Evidence that a single peptide-MHC complex on a target cell can elicit a cytolytic T cell response”. In: *Immunity* 4.6 (1996), pp. 565–571. DOI: 10.1016/S1074-7613(00)80483-5. URL: <https://www.ncbi.nlm.nih.gov/pubmed/8673703>.
- [305] K Takahashi et al. “Induction of pluripotent stem cells from adult human fibroblasts by defined factors”. In: *Cell* 131.5 (2007), pp. 861–872. DOI: 10.1016/j.cell.2007.11.019. URL: <https://www.ncbi.nlm.nih.gov/pubmed/18035408>.
- [306] D C Taussig et al. “Hematopoietic stem cells express multiple myeloid markers: implications for the origin and targeted therapy of acute myeloid leukemia”. In: *Blood*

- 106.13 (2005), pp. 4086–4092. DOI: 10.1182/blood-2005-03-1072. URL: <https://www.ncbi.nlm.nih.gov/pubmed/16131573>.
- [307] C J Taylor et al. “Banking on human embryonic stem cells: estimating the number of donor cell lines needed for HLA matching”. In: *Lancet* 366.9502 (2005), pp. 2019–2025. DOI: 10.1016/S0140-6736(05)67813-0. URL: <https://www.ncbi.nlm.nih.gov/pubmed/16338451>.
- [308] C J Taylor et al. “Clinical and socioeconomic benefits of serological HLA-DR matching for renal transplantation over three eras of immunosuppression regimens at a single unit.” In: *Clinical transplants* (1993), pp. 233–41. URL: <http://www.ncbi.nlm.nih.gov/pubmed/7918156>.
- [309] E D Thomas et al. “Intravenous infusion of bone marrow in patients receiving radiation and chemotherapy”. In: *N Engl J Med* 257.11 (1957), pp. 491–496. DOI: 10.1056/NEJM195709122571102. URL: <https://www.ncbi.nlm.nih.gov/pubmed/13464965>.
- [310] B G Till et al. “Adoptive immunotherapy for indolent non-Hodgkin lymphoma and mantle cell lymphoma using genetically modified autologous CD20-specific T cells”. In: *Blood* 112.6 (2008), pp. 2261–2271. DOI: 10.1182/blood-2007-12-128843. URL: <https://www.ncbi.nlm.nih.gov/pubmed/18509084>.
- [311] *Timeline of Progress in Immunotherapy*. 2022. URL: <https://www.cancerresearch.org/en-us/immunotherapy/timeline-of-progress>.
- [312] F Tucci et al. “Update on Clinical Ex Vivo Hematopoietic Stem Cell Gene Therapy for Inherited Monogenic Diseases”. In: *Mol Ther* 29.2 (2021), pp. 489–504. DOI: 10.1016/j.ymthe.2020.11.020. URL: <https://www.ncbi.nlm.nih.gov/pubmed/33221437>.
- [313] *U.S. Food & Drug Administration. Approved Cellular and Gene Therapy Products*. 2022. URL: <https://www.fda.gov/vaccines-blood-biologics/cellular-gene-therapy-products/approved-cellular-and-gene-therapy-products>.
- [314] *uniQure biopharma B.V. Glybera (alipogene tiparvovec) [assessment report]. European Medicines Agency website. Revised July 2012. Assessed 23 Oct 2022*. URL: https://www.ema.europa.eu/en/documents/assessment-report/glybera-epar-public-assessment-report_en.pdf.
- [315] *University College, London. Lentiviral Gene Therapy for Epilepsy. ClinicalTrials.gov identifier: NCT04601974. Updated May 24, 2022. Accessed 13 December 2022*. URL: <https://clinicaltrials.gov/ct2/show/NCT04601974>.
- [316] *University Hospital, Angers. Multi-Omics and iPSCs to Improve Diagnosis of Rare Intellectual Disabilities (MIDRID). ClinicalTrials.gov identifier: NCT03635294. Updated January 3, 2020. Accessed October 16, 2022*. URL: <https://clinicaltrials.gov/ct2/show/NCT03635294>.
- [317] *University Hospital, Grenoble. Development of the Tool " iPSC " for the Functional Study of Mutations Responsible for Mental Retardation (Rementips). ClinicalTrials.org identifier: NCT02980302. Updated October 12, 2018. Accessed October 16, 2022*. URL: <https://clinicaltrials.gov/ct2/show/NCT02980302>.

- [318] University of Pennsylvania. *Autologous T-Cells Genetically Modified at the CCR5 Gene by Zinc Finger Nucleases SB-728 for HIV (Zinc-Finger)*. *ClinicalTrials.gov identifier: NCT00842634*. Updated February 8, 2019. Accessed December 15, 2022. URL: <https://clinicaltrials.gov/ct2/show/NCT00842634>.
- [319] Manuela Urban and Dr. Richard P Harbottle. “Utilising S/MAR DNA vectors for the genetic modification of human induced pluripotent stem cells for cell and gene therapy”. PhD thesis. Heidelberg, 2021. DOI: 10.11588/heidok.00030872.
- [320] F Urbinati et al. “Mechanism of reduction in titers from lentivirus vectors carrying large inserts in the 3’LTR”. In: *Mol Ther* 17.9 (2009), pp. 1527–1536. DOI: 10.1038/mt.2009.89. URL: <https://www.ncbi.nlm.nih.gov/pubmed/19384292>.
- [321] H Uyama et al. “Competency of iPSC-derived retinas in MHC-mismatched transplantation in non-human primates”. In: *Stem Cell Reports* 17.11 (2022), pp. 2392–2408. DOI: 10.1016/j.stemcr.2022.09.014. URL: <https://www.ncbi.nlm.nih.gov/pubmed/36306783>.
- [322] C Uyttenhove, J Maryanski, and T Boon. “Escape of mouse mastocytoma P815 after nearly complete rejection is due to antigen-loss variants rather than immunosuppression”. In: *The Journal of experimental medicine* 157.3 (1983), pp. 1040–1052. DOI: 10.1084/jem.157.3.1040. URL: <https://www.ncbi.nlm.nih.gov/pubmed/6187879>.
- [323] Charles P. Venditti. “Safety questions for AAV gene therapy”. In: *Nature Biotechnology* 39.1 (Jan. 2021), pp. 24–26. DOI: 10.1038/s41587-020-00756-9. URL: <http://www.nature.com/articles/s41587-020-00756-9>.
- [324] Santhosh Chakkaramakkil Verghese et al. “S/MAR sequence confers long-term mitotic stability on non-integrating lentiviral vector episomes without selection”. In: *Nucleic Acids Research* 42.7 (Apr. 2014), e53–e53. DOI: 10.1093/nar/gku082. URL: <https://academic.oup.com/nar/article-lookup/doi/10.1093/nar/gku082>.
- [325] Vertex Pharmaceuticals Incorporated. *Evaluation of Safety and Efficacy of CTX001 in Pediatric Participants With Transfusion-Dependent β -Thalassemia (TDT)*. *ClinicalTrials.gov identifier: NCT05356195*. Updated November 1, 2022. Accessed December 15, 2022. URL: <https://clinicaltrials.gov/ct2/show/NCT05356195>.
- [326] M A Vodyanik, J A Thomson, and Slukvin II. “Leukosialin (CD43) defines hematopoietic progenitors in human embryonic stem cell differentiation cultures”. In: *Blood* 108.6 (2006), pp. 2095–2105. DOI: 10.1182/blood-2006-02-003327. URL: <https://www.ncbi.nlm.nih.gov/pubmed/16757688>.
- [327] V Volarevic et al. “Ethical and Safety Issues of Stem Cell-Based Therapy”. In: *Int J Med Sci* 15.1 (2018), pp. 36–45. DOI: 10.7150/ijms.21666. URL: <https://www.ncbi.nlm.nih.gov/pubmed/29333086>.
- [328] Mark Walters. *Transplantation of Clustered Regularly Interspaced Short Palindromic Repeats Modified Hematopoietic Progenitor Stem Cells (CRISPR_SCD001) in Patients With Severe Sickle Cell Disease*. *ClinicalTrials.gov identifier: NCT04774536*. Updated April 27, 2022. URL: <https://clinicaltrials.gov/ct2/show/NCT04774536>.
- [329] X Wang et al. “The EF-1alpha promoter maintains high-level transgene expression from episomal vectors in transfected CHO-K1 cells”. In: *J Cell Mol Med* 21.11 (2017),



- pp. 3044–3054. DOI: 10.1111/jcmm.13216. URL:
<https://www.ncbi.nlm.nih.gov/pubmed/28557288>.
- [330] A C Wilkinson et al. “Long-term ex vivo expansion of mouse hematopoietic stem cells”. In: *Nat Protoc* 15.2 (2020), pp. 628–648. DOI: 10.1038/s41596-019-0263-2. URL: <https://www.ncbi.nlm.nih.gov/pubmed/31915389>.
- [331] Adam C. Wilkinson et al. “Long-term ex vivo haematopoietic-stem-cell expansion allows nonconditioned transplantation”. In: *Nature* 571.7763 (2019), pp. 117–121. DOI: 10.1038/s41586-019-1244-x. URL: <http://dx.doi.org/10.1038/s41586-019-1244-x>.
- [332] Yongyan Wu et al. “CHIR99021 promotes self-renewal of mouse embryonic stem cells by modulation of protein-encoding gene and long intergenic non-coding RNA expression”. In: *Experimental Cell Research* 319.17 (Oct. 2013), pp. 2684–2699. DOI: 10.1016/j.yexcr.2013.08.027. URL: <https://linkinghub.elsevier.com/retrieve/pii/S0014482713003832>.
- [333] *Wuhan Neurophth Biotechnology Limited Company. Gene Therapy Clinical Trial for the Treatment Of Leber’s Hereditary Optic Neuropathy (GOLD). ClinicalTrials.gov identifier: NCT04912843. Updated November 14, 2022. Accessed 13 December 2022.* URL: <https://clinicaltrials.gov/ct2/show/NCT04912843>.
- [334] *Xijing Hospital. CRISPR (HPK1) Edited CD19-specific CAR-T Cells (XYF19 CAR-T Cells) for CD19+ Leukemia or Lymphoma. ClinicalTrials.gov identifier: NCT04037566. Updated July 30, 2019. Accessed December 15, 2022.* URL: <https://clinicaltrials.gov/ct2/show/NCT04037566>.
- [335] C Yang et al. “DNMT 1 maintains hypermethylation of CAG promoter specific region and prevents expression of exogenous gene in fat-1 transgenic sheep”. In: *PLoS One* 12.2 (2017), e0171442. DOI: 10.1371/journal.pone.0171442. URL: <https://www.ncbi.nlm.nih.gov/pubmed/28158319>.
- [336] C Yee et al. “Adoptive T cell therapy using antigen-specific CD8+ T cell clones for the treatment of patients with metastatic melanoma: in vivo persistence, migration, and antitumor effect of transferred T cells”. In: *Proc Natl Acad Sci U S A* 99.25 (2002), pp. 16168–16173. DOI: 10.1073/pnas.242600099. URL: <https://www.ncbi.nlm.nih.gov/pubmed/12427970>.
- [337] Q Zhao et al. “Engineered TCR-T Cell Immunotherapy in Anticancer Precision Medicine: Pros and Cons”. In: *Front Immunol* 12 (2021), p. 658753. DOI: 10.3389/fimmu.2021.658753. URL: <https://www.ncbi.nlm.nih.gov/pubmed/33859650>.
- [338] Y Zhou et al. “Unstable expression of transgene is associated with the methylation of CAG promoter in the offspring from the same litter of homozygous transgenic mice”. In: *Mol Biol Rep* 41.8 (2014), pp. 5177–5186. DOI: 10.1007/s11033-014-3385-1. URL: <https://www.ncbi.nlm.nih.gov/pubmed/24804614>.
- [339] D Zychlinski et al. “Physiological promoters reduce the genotoxic risk of integrating gene vectors”. In: *Mol Ther* 16.4 (2008), pp. 718–725. DOI: 10.1038/mt.2008.5. URL: <https://www.ncbi.nlm.nih.gov/pubmed/18334985>.